UNIVERSIDAD AUTÓNOMA DE MADRID

FACULTAD DE MEDICINA

Instituto Teófilo Hernando de I+D del Medicamento

Departamento de Farmacología y Terapéutica

EXOCITOSIS Y ENDOCITOSIS REGULADAS POR DOS MODOS DIFERENTES DE ENTRADA DE CALCIO

Memoria de tesis para optar al grado de Doctor presentada por

Juliana Martins da Rosa

Directores:

Antonio G. Garcia

Luis Gandia

Madrid, 2010

Instituto Teófilo Hernando del I+D del Medicamento
Facultad de Medicina
UAM

D. ANTONIO GARCÍA GARCÍA, Catedrático del Departamento de Farmacología y Terapéutica y Director del Instituto Teófilo Hernando de I+D del Medicamento de la Facultad de Medicina de la Universidad Autónoma de Madrid,

y D. LUIS GANDIA JUAN, Profesor Titular del Departamento de Farmacología y Terapéutica y del Instituto Teófilo Hernando de I+D del Medicamento de la Universidad Autónoma de Madrid,

CERTIFICAN, que Doña JULIANA MARTINS DA ROSA ha realizado bajo su dirección el presente trabajo titulado: **"EXOCITOSIS Y ENDOCITOSIS REGULADAS POR DOS MODOS DIFERENTES DE ENTRADA DE CALCIO"**, como Tesis para alcanzar el grado de Doctor.

Para que conste a efectos oportunos, expiden y firman la presente en Madrid a 7 de septiembre de 2010.

D. Antonio García García
Catedrático de Farmacología

D. Luis Gandía Juan
Profesor Titular de Farmacología

ABREVIATURAS Y ACRÓNIMOS

$[Ca^{2+}]_c$	Concentración de Ca^{2+} citosólico
ACh	Acetilcolina
AgaIVA	ω-agatoxina IVA
ATP	Trifosfato de adenosina
CCDV	Canales de calcio dependientes de voltaje
CDI	Inactivación dependiente de calcio
DHP	Dihidropiridinas
DMEM	Medio Dulbecco modificado por Eagle
EGTA	Ácido etilenoglicos-bis(beta-aminoetil eter)-N,N,N´,N´-tetraacético
Endo/Exo	Relación endocitosis/exocitosis
GVIA	ω-conotoxina GVIA
GTP	Trifosfato de guanina
HEPES	(N-[2-hidroxietil]-piperacino-N´-[2-ácido etanosulfónico])
HVA	Canales de alto humbral de activación
I	Corriente
LVA	Canales de bajo humbral de activación
MVIIC	ω-conotoxina MVIIC
Nife	Nifedipino
RE	Retículo endoplasmático
S1P	Esfingosina-1-fosfato
SpD	Esfingosina dializada
SMase	Esfingomielinasa
SNC	Sistema nervioso central
SNARE	soluble N-ethylmaleimide-sensitive factor attachment protein receptor
TEA	Cloruro de tetraetilamonio
TTX	Tetrodoxina
V	Voltaje
Vm	Potencial de membrana

INDICE

I. MARCO DE LA TESIS

El trabajo presentado en esta Tesis Doctoral ha sido desarrollado en el Instituto Teófilo Hernando de I+D del Medicamento (ITH) de la Universidad Autónoma de Madrid. A lo largo de más de tres décadas, el ITH ha cultivado una amplia y sólida línea de investigación relacionada con la caracterización de los principales mecanismos celulares en los que está implicado el catión calcio (Ca^{2+}). Entre ellos, hacemos hincapié en la comunicación interneuronal y en los mecanismos de muerte neuronal por apoptosis y necrosis.

El Ca^{2+} es uno de los mediadores intracelulares más versátiles de todo el organismo. Interviene en procesos tan diversos como la contracción muscular, la secreción hormonal y de neurotransmisores, la coagulación de la sangre, el metabolismo celular, la expresión de genes, la fecundación, la inmunidad, el envejecimiento, la muerte celular...

Una importante característica del Ca^{2+} es que la célula no puede producirlo ni destruirlo, sino únicamente controlar sus concentraciones intracelulares. El nivel citosólico de Ca^{2+} libre ($[Ca^{2+}]_c$) en una célula en reposo suele permanecer alrededor de 10-100 nM, pero tras una estimulación, la concentración intracelular de este ión puede incrementarse hasta alcanzar niveles iguales o incluso superiores a 1 µM. Para regular estas variaciones, la célula se sirve de mecanismos capaces de controlar el aumento y/o la disminución de la concentración de la $[Ca^{2+}]_c$. Entre los mecanismos que controlan el aumento de Ca^{2+} se incluyen diversos subtipos de canales de Ca^{2+}dependientes de voltaje (CCDV) y receptores presentes en la membrana plasmática, que permiten la entrada de Ca^{2+} extracelular, y receptores presentes en el retículo endoplásmico (RE), que movilizan Ca^{2+} desde estes depósito. Respecto a los mecanismos que contribuyen a disminuir los niveles citosólicos de Ca^{2+}, cabe destacar que la célula cuenta con diversas proteínas que unen Ca^{2+} y con una serie de bombas y transportadores de membrana que movilizan el Ca^{2+} desde el citosol hacia depósitos intracelulares o hacia el medio extracelular.

En los últimos 30 años, nuestro grupo ha realizado diversos estudios encaminados al esclarecimiento del papel del Ca^{2+} como mediador de los procesos de neurotransmisión. Para una revisión reciente, ver Garcia et al. (2006). También el ITH ha cultivado durante la última década una línea de investigación relacionada con el Ca^{2+} y su implicación en los procesos de muerte neuronal (Cano-Abad *et al.*, 2000; Cano-Abad *et al.*, 2001; Cano-Abad *et al.*, 2002; Sobrado *et al.*, 2003; Egea *et al.*, 2007),

intentado establecer un posible vínculo con enfermedades neurodegenerativas como la Enfermedad de Alzheimer.

Nuestro modelo experimental por excelencia es la célula cromafín de la médula suprarrenal. En este tipo celular se realizaron los primeros registros electrofisiológicos de canal único y se descubrieron las primeras proteínas implicadas en la exocitosis y en la endocitosis. Como las neuronas, la célula cromafín posee diferentes subtipos de CCDV. Hace años que en nuestro grupo trabajamos en la búsqueda de nuevas estrategias experimentales para confirmar nuestra hipótesis de que el Ca^{2+} que entra en la célula a través de los distintos subtipos de CCDV (L, N, PQ y R), ejerce funciones diferentes.

La presente Tesis está relacionada con dos de las líneas de investigación que se desarrollan actualmente en el ITH, a saber, (1) la implicación del Ca^{2+} y esfingolípidos de membrana en los procesos de neurotransmisión: exocitosis y endocitosis; y (2) la caracterización funcional de los distintos subtipos de CCDV. Además, intentamos hacer una correlación de todos estos aspectos a procesos fisiopatológicos como la Enfermedad de Alzheimer.

Para el desarrollo de los experimentos de esta Tesis, nos hemos servido de uno de los principales avances tecnológicos para el estudio del Ca^{2+}, la técnica de p*atch-clamp* desarrollada por Bert Sakmann y Erwin Neher (Hamill *et al.*, 1981). Esta técnica nos permite estudiar las corrientes de entrada de Ca^{2+} por los diferentes subtipos de CCDV y su implicación en los procesos exo- y endocitóticos mediante el registro de la capacidad de la membrana a tiempo real (Korn & Horn, 1989; Gillis *et al.*, 1991). Así como técnicas fotométricas para corroborar los datos eletrofisiológicos, marcaje con anticuerpos para estudiar la colocalización de las proteínas endocitóticas y CCDV y técnicas de fotoliberación de calcio intracelular.

Parte de los resultados que presento en esta Tesis han aparecido en las publicaciones siguientes:

1. Rosa J.M., Orozco A., Colmena I, de Pascual R, García AG and Gandía L. **Ca^{2+} entry during calcium channel deactivation matters for the control of exocytosis and endocytosis**. *Journal of Neurochemistry* 2010 (enviado a plubicación).
2. Rosa J.M., Torregrosa-Hetland, C.J., Colmena, I., Gutiérrez, L.M., García, A.G. and Gandía, L. **Preferential functional coupling between L-type of calcium**

channels and endocytosis in chromaffin cells. *Cell Calcium* 2010 (enviado a publicación).

3. Rosa, J.M., Gandía, L. and García, A.G. **Permissive role of sphingosine on calcium-dependent endocytosis in chromaffin cells**. *Pflugers Arch*. 2010 Jul 17 [Epub ahead of print].
4. Darios, F., Wasser, C., Shakirzyanova, A., Giniatullin, A., Goodman, K., Bravo, J.L.M., Raingo, J., Jorgačevski, J., Kreft, M., Zorec, R., Rosa, J.M., Gandía, L., Gutiérrez, L.M., Giniatullin, R., Binz, T., Kavalali, E.T. and Davletov, B. **Sphingosine targets synaptobrevin and activates synaptic vesicle exocytosis**. *Neuron* 62: 683–694, 2009.
5. Rosa, J.M., Gandía, L. and García, A.G. **Inhibition of N and PQ calcium channels by calcium entry through L channels in chromaffin cells**. *Pflugers Arch*. 458: 795-807, 2009.
6. Rosa, J.M., de Diego, A.M.G., Gandía, L. and García, A.G. **L-type calcium channels are preferentially coupled to endocytosis in bovine chromaffin cells**. *Biochemical and Biophysical Research Communications* 357: 834–839, 2007.

II. INTRODUCCIÓN

Esta Tesis Doctoral presenta un estudio sobre cómo la entrada de Ca^{2+} por los CCDV del subtipo L regula el proceso endocitótico en la célula cromafín y modula la actividad de los canales de los subtipos N y PQ. Además, aportamos evidencias sobre la participación del metabolismo de los esfingolípidos de membrana en la endocitosis. En la discusión final de esta Tesis intentamos hacer una correlación de los aspectos mencionados a una posible perspectiva clínica en la Enfermedad de Alzheimer.

A continuación describiré los protagonistas que intervienen en este estudio, esto es los canales de Ca^{2+} dependientes de voltaje, los procesos de exocitosis y endocitosiss; así como el papel de los esfingolípidos de membrana en la endocitosis.

1. LOS CANALES DE CALCIO DEPENDIENTES DE VOLTAJE

Los cambios en la concentración del Ca^{2+} citosólico ($[Ca^{2+}]_c$) regulan una variedad de importantes funciones celulares como la neurotransmisión, la contracción muscular, la secreción hormonal, la liberación de Ca^{2+} desde depósitos intracelulares, la expresión génica y participan también como una señal en la fecundación y en la muerte celular por necrosis o apoptosis (Garcia *et al.*, 2006).

Los canales de Ca^{2+} activados por voltaje o canales de Ca^{2+} dependientes de voltaje (CCDV) se encuentran presentes en la membrana plasmática de células nerviosas, musculares, cardíacas, endocrinas, -pancreáticas e inmunológicas y constituyen una de las principales vías de entrada de Ca^{2+} a la célula en respuesta a una despolarización de la membrana plasmática.

Gracias al avance de las técnicas electrofisiológicas (principalmente la técnica de *patch-clamp*), al desarrollo de marcadores fluorescentes para Ca^{2+}, la identificación y purificación de diferentes neurotoxinas específicas para los CCDV y las técnicas de biología molecular, se ha logrado identificar y caracterizar diferentes subtipos de CCDV que coexisten en las células excitables. La clasificación de estos canales se puede realizar en base a sus propiedades biofísicas y farmacológicas, así como en base a aspectos de biología molecular.

Estructuralmente, los CCDV son proteínas oligoméricas formadas por la combinación de cuatro subunidades distintas (α_1, α_2-δ, β, γ) (**Figura 1**). La subunidad α_1 es la responsable de la formación del poro central, que confiere características específicas al canal tales como la permeabilidad y las cinéticas de activación e

inactivación, que presentan diferencias para cada subtipo de canal. Está constituida por cuatro dominios (I, II, III, IV), cada uno de ellos formado a su vez por seis segmentos transmembrana (S1-S6). El segmento S4 de cada dominio está altamente cargado y se considera que es el que actúa como sensor de los cambios de potencial de la membrana (Jarvis *et al.*, 2002; Doering & Zamponi, 2003). El asa P que une el quinto y sexto segmento, también forma parte del poro del canal y las demás subunidades son denominadas reguladoras o auxiliares. Las asas citoplasmáticas que unen los cuatro dominios son estructuralmente importantes para que ocurra la interacción entre las subunidades β y segundos mensajeros (Marcantoni *et al.*, 2008).

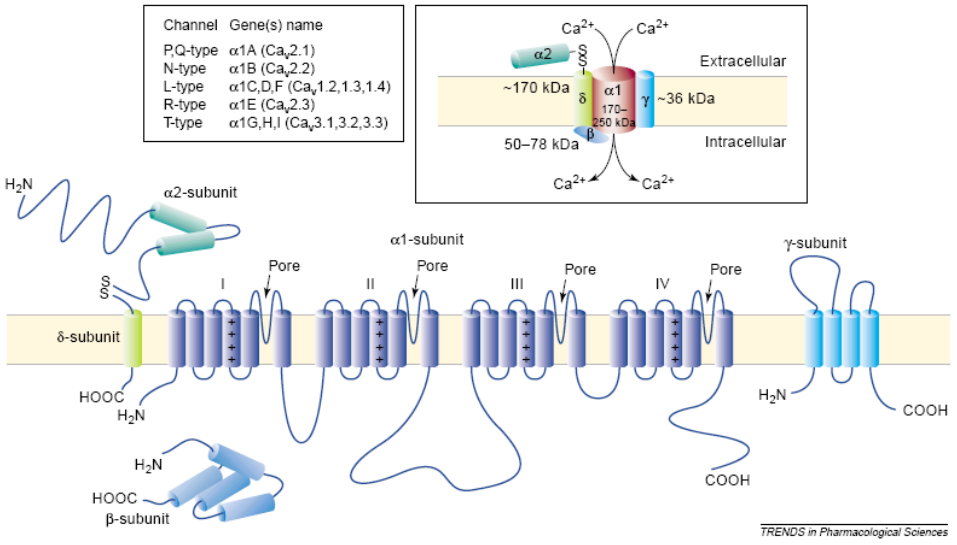

Figura 1: Estructura de un canal de calcio dependiente de voltaje con sus distintas subunidades (Adaptado de Jarvis et al. 2002).

1.1. Subtipos de canales de Ca^{2+} dependientes de voltaje

Los CCDV se pueden clasificar atendiendo al rango de voltaje necesario para su activación, agrupándose así en dos categorías: canales de bajo umbral de activación (LVA: *low voltage-activated*; que comprenden los canales de tipo T) y canales de alto umbral de activación (HVA: *high voltage-activated*, que comprenden los canales de tipo L, N, PQ). Algunos autores clasifican el canal tipo R como activado por un voltaje intermedio, mientras que otros los clasifican como pertenecientes al grupo de alto umbral (Catterall, 2000; Garcia *et al.*, 2006).

Recientemente esta nomenclatura ha sido modificada para unificarla con la utilizada para otros tipos de canales iónicos, utilizando la terminología Ca_v (canal de Ca^{2+} dependiente de voltaje) seguido de un número asignado según la composición de la cadena peptídica del canal: Ca_v1 (canales L); $Ca_v2.1$ (canal PQ); $Ca_v2.2$ (canal N); $Ca_v2.3$ (canal R) y, Ca_v3 (canales T) (Garcia *et al.*, 2006).

A continuación, haré una breve descripción de los distintos subtipos de canales de Ca^{2+} dependientes de voltaje y de sus características biofísicas y farmacológicas.

Los **canales tipo T** empiezan a abrirse con una despolarización débil, mucho más negativa que la requerida por los demás CCDV y poseen la característica de presentar una apertura transitoria, controlando de esta forma la entrada de Ca^{2+} durante pequeñas despolarizaciones de la membrana. La máxima corriente se alcanza a un potencial cercano a los -30 mV, presentando una rápida inactivación dependiente de voltaje pero insensible a Ca^{2+} y una lenta desactivación (Marcantoni *et al.*, 2008). Los canales T han sido relacionados con la actividad marcapaso del corazón, la nocicepción, el control del tono vascular, la fertilización y la hipertrofia cardíaca. Se ha demostrado que los canales T se encuentran altamente expresados en las etapas embrionarias y perinatales en las células cromafínes, pero desaparecen durante la vida adulta. Las células cromafínes adultas poseen ARNm para este canal (Garcia-Palomero *et al.*, 2000), pero éstos no son funcionales (Cena *et al.*, 1983; Carabelli *et al.*, 1998). Sin embargo, se ha descrito que su función puede ser activada por la presencia intracelular de AMPc, la estimulación de receptores adrenérgicos β_1 o durante la hipoxia crónica. Las subunidades α_{1G} y α_{1H} presentes en los canales T tienen los motivos característicos de un CCDV, incluida la estructura tetramérica, el sensor de voltaje S4 y la región P; sin embargo, les faltan otros motivos conservados en el resto de las subunidades α_1, como el implicado en las interacciones con las subunidades δ_1 y el Ca^{2+}.

Los **canales tipo L** presentan un alto umbral de voltaje para su activación y se inactivan lentamente. Se han identificado hasta cuatro subtipos de canales L ($Ca_v1.1$, $Ca_v1.2$, $Ca_v1.3$ o $Ca_v1.4$), correspondientes a las subunidades α_{1S}, α_{1C}, α_{1D} o α_{1F}, cada uno de ellos presentando diferentes características. Los canales L participan en un gran

número de funciones dependientes de Ca^{2+} como la secreción hormonal, el desarrollo celular, la diferenciación y la apoptosis. Han sido descritos en la mayoría de las células excitables y son la principal vía de entrada de Ca^{2+} en el corazón y en el músculo esquelético. Farmacológicamente, se caracterizan por su sensibilidad dihidropiridinas (DHP) tanto agonistas (Bay K8644) como antagonistas (nifedipino, nitrendipino, nisoldipino, nimodipino, furnidipino). También actúan como antagonistas de este tipo de canal las fenilaquilaminas y las benzotiazepinas (Catterall *et al.*, 2005). Los agonistas DHP prolongan el tiempo de apertura del canal, retrasando el cierre del mismo tras la repolarización de la membrana.

Los **canales tipo N** se identificaron primeramente en neuronas y se caracterizan por ser bloqueados irreversiblemente por la toxina ω-conotoxina GVIA, aislada del caracol marino *Conus geographus* (Olivera *et al.*, 1984; McCleskey *et al.*, 1987; Plummer *et al.*, 1989). La purificación de los canales N ha permitido identificar la subunidad α_{1B} como la responsable de la formación del poro iónico, así como las subunidades α_2/δ y β como reguladoras (McEnery *et al.*, 1991; Witcher *et al.*, 1993). Los canales N necesitan grandes despolarizaciones para su activación y se inactivan rápidamente, aunque de forma incompleta, a potenciales positivos.

Los **canales tipo P** son corrientes resistentes a DHP y ω-conotoxina GVIA. Se denominan canales de tipo P porque se describieron por primera vez en las células de *Purkinje* del cerebelo (Llinas *et al.*, 1989; Hillman *et al.*, 1991). Los canales P se caracterizan sobre todo por dos aspectos: no se inactivan durante las despolarizaciones y son insensibles frente a los cambios de potenciales (Garcia *et al.*, 2006). Farmacológicamente, las corrientes del tipo P son sensibles a la ω-conotoxina AgaIVA (Gandía *et al.*, 2008).También pueden bloquearse de manera no específica por la ω-conotoxina MVIIC (Monje *et al.*, 1993), la ω-conotoxina MVIID y la ω-gramotoxina SVIA (Lampe *et al.*, 1993; Turner *et al.*, 1995). Los canales P parecen ser los más ampliamente distribuidos en el SNC de mamíferos y están relacionados con la generación de la actividad intrínseca, la modulación neuronal y liberación de neurotransmisores (Bertolino & Llinas, 1992).

Los **canales tipo Q** se identificaron gracias a la purificación y síntesis de la toxina del caracol marino *Conus magnus* ω-conotoxina MVIIC, que bloquea potentemente, pero no específicamente, este subtipo de CCDV. Este canal es resistente a DHPs, ω-conotoxina GVIA y bajas concentraciones de ω-agatoxina IVA (<100 nM). Altas concentraciones (> 1μM) de ω-AgaIVA sí que producen un bloqueo de los canales Q. Así como los canales P, los canales Q poseen la subunidad α_{1A} como la formadora del poro, generando controversias en relación a las corrientes P y Q. Tras la clonación de α_{1A} y estudios en ovocitos de *Xenopus laevis*, se propuso que esta subunidad era la base de la corriente tipo Q y, en menor grado la de tipo P (Stea *et al.*, 1994). Sin embargo, otros estudios demuestran que α_{1A} es la principal subunidad responsable de la corriente P (Berrow *et al.*, 1997; Moreno *et al.*, 1997). Las controversias generadas y la dificultad de separar las subunidades α_{1A} de los canales P y Q han llevado al consenso de clasificarlos como un único canal: canales de calcio tipo PQ.

Los **canales R** son definidos como la corriente de Ca^{2+} residual que se observa tras el bloqueo de todos los otros subtipos de CCDV. Estos canales muestran una rápida cinética de inactivación y son más sensibles al bloqueo por Ni^{2+} que por Cd^{2+}. Se ha descrito al SNX-482, un péptido síntetico derivado de una toxina de la tarántula *Hysterocrates gigas*, como el primer bloqueante selectivo de los canales R (Newcomb *et al.*, 1995); sin embargo, se ha demostrado que esta toxina también es capaz de bloquear las corrientes PQ en células cromafínes (Arroyo *et al.*, 2003). Las corrientes R se observan en la configuración de parche perforado, pero no en célula entera, sugiriendo una diálisis de factores citosólicos responsables de la inactivación de este subtipo de canal al romper la membrana. La subunidad α_{1E} ha sido propuesta como la formadora del poro para las corrientes tipo R (Pearson *et al.*, 1995); sin embargo, experimentos con ratones *knockout* para α_{1E} concluyen que la mayoría de la corriente tipo R no depende de la expresión de esta subunidad (Wilson *et al.*, 2000).

1.1.1.-Subtipos de canales de calcio en la célula cromafín

Un hecho interesante en cuanto a la naturaleza de los CCDV, es que estos pueden coexistir en una misma célula, y que además la expresión de cada subtipo de

canal varía de unas especies a otras **(Figura 2)**. En lo que respecta a las células cromafines, en las últimas décadas se ha podido observar que existen profundas diferencias en la proporción de los diferentes subtipos de CCDV entre células cromafines de diferentes especies (Garcia *et al.*, 2006; Gandía *et al.*, 2008). Estudios electrofisiológicos detallados han determinado que, por ejemplo, el canal del subtipo L representa aproximadamente un 20% del total de los canales de Ca^{2+} en la célula cromafin humana (Gandia *et al.*, 1998), bovina (Albillos *et al.*, 1993; Gandia *et al.*, 1993a) y en cerdo (Kitamura *et al.*, 1998); sin embargo, está en torno al 50% en células cromafines de gato (Albillos *et al.*, 1994), rata (Gandia *et al.*, 1995) y ratón (Hernandez-Guijo *et al.*, 1998).

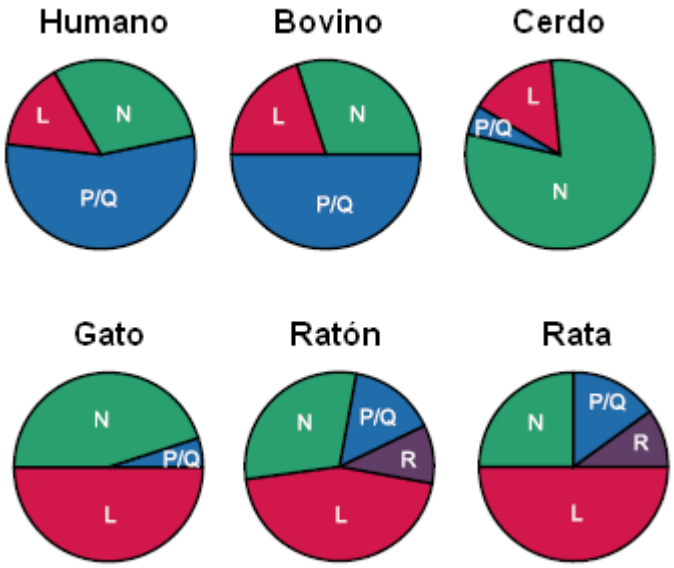

Figura 2: Distribución de los diferentes subtipos de canales de calcio en cultivos primarios de células cromafines de la médula adrenal de distintas especies (Garcia *et al.*, 2006)

El canal tipo N también muestra gran variabilidad entre especies. En el cerdo representa un 80% de la corriente (Kitamura *et al.*, 1998), en el gato un 45% (Albillos *et al.*, 1994); mientras que en bovina (Lopez *et al.*, 1994), rata (Gandia *et al.*, 1995), ratón (Hernandez-Guijo *et al.*, 1998) y humanas (Gandia *et al.*, 1998) la fracción de la corriente tipo N es un 30% de la corriente total.

Así como los anteriores subtipos de CCDV, el canal tipo P igualmente presenta diferencias entre las especies estudiadas. La fracción de corriente a través de los canales PQ es de 50% en células cromafines bovinas (Albillos *et al.*, 1996b) y 60% en células cromafines humanas (Gandia *et al.*, 1998); por cotnra, en cromafines de cerdo la proporción desciende a un 5% (Kitamura *et al.*, 1998) al igual que en gato (Albillos *et al.*, 1994). En cromafines de rata (Gandia *et al.*, 1995) y de ratón (Hernandez-Guijo *et al.*, 1998) el canal PQ representa un 20 y 30% respectivamente de la corriente total.

La similitud en cuanto a la proporción de los subtipos de canales entre la especie humana y bovina, con una presencia predominante de los canales PQ, favorece nuestros estudios en este modelo celular. La relevancia fisiológica de esta diferencia entre especies aún no se sabe, pero seguramente presenta consecuencias importantes en el control de los procesos secretores, así como de la entrada de calcio.

1.2. Mecanismos moduladores de la actividad de los CCDV

Como hemos comentado anteriormente, los CCDV representan un papel crucial en innumerables respuestas celulares y por ello necesitan ser modulados finamente para poder regular las señales citosólicas de Ca^{2+}, evitando así un aumento excesivo de la concentración de Ca^{2+} intracelular que podría llevar a una activación de los mecanismos de muerte presentes en la célula.

Dos factores controlan principalmente la actividad de los CCDV: el voltaje y el propio Ca^{2+}. Ambas formas de inactivación son reguladas por diversos dominios en las subunidades α y β (Wykes *et al.*, 2007). También se ha descrito la existencia de mecanismos moduladores autocrino/paracrinos producidos por diversos productos neurosecretores, mediados por proteínas G (Garcia *et al.*, 2006).

1.2.1. Modulación de los CCDV por Ca^{2+}

Las corrientes de Ca^{2+} pueden ser moduladas en mayor o menor grado dependiendo del tipo celular. Los CCDV se pueden modular por una acumulación de Ca^{2+} en la superfície interna de la membrana (Brehm & Eckert, 1978; Tillotson, 1979). Esta **inactivación dependiente de Ca^{2+}** (CDI, del inglés *"calcium-dependent inactivation"*) se describió por primera vez en la fibra muscular del *Balanus nubilus* por

Hagiwara y Nakajima (Hagiwara & Nakajima, 1966). Estos autores observaron que las contracciones musculares tras aplicar una fuerte despolarización, solamente se producían cuando la concentración de Ca^{2+} intracelular se encontraba disminuida por la presencia de quelantes como el EGTA, EDTA o K-citrato. Años más tarde, esta hipótesis fue corroborada con estudios en otras células excitables (Brehm & Eckert, 1978; Tillotson, 1979; Hagiwara & Byerly, 1981).

La CDI presenta una serie de características específicas entre las que cabe destacar las siguientes: (1) posee una típica curva en "U", donde el mayor efecto de inactivación se observa a voltajes intermedios; (2) otros cationes divalentes son menos efectivos que el Ca^{2+} en promover la inactivación del canal; (3) es activada en respuesta al aumento de Ca^{2+} tanto intracelular como extracelular; y (4) puede iniciarse, aún en ausencia de despolarizaciones, en respuesta a un aumento de Ca^{2+} intracelular de 1 µM (Eckert & Chad, 1984).

Es de destacar que los diferentes subtipos de CCDV se diferencian entre sí en cuanto a esta propiedad de inactivación por el propio Ca^{2+}. Así, los canales de calcio de tipo L presentes en el músculo esquelético se inactivan rápidamente tras un estímulo despolarizante, mientras que por otro lado los llamados canales de calcio neuronales (N, PQ) presentan una inactivación más lenta (Yue *et al.*, 1990; von Gersdorff & Matthews, 1996). Algunos autores han descrito que la sustitución por Ba^{2+} en el medio extracelular, así como la reducción de la concentración de Ca^{2+} extracelular y/o la adición de quelantes de Ca^{2+}, ejercen poco efecto sobre la inactivación de los canales N y PQ, lo que apoyaría la idea de que la modulación de los canales de los subtipos N y PQ se ejercería solamente por el voltaje (Jones & Marks, 1989; Patil *et al.*, 1998). Por el contrario, otros grupos han encontrado claras evidencias a favor de la modulación de estos subtipos de canales por el Ca^{2+} (Cox & Dunlap, 1994; Tareilus *et al.*, 1994; Lee *et al.*, 1999; Shirokov, 1999).

En lo que respecta a los canales de calcio existentes en la membrana de la celula cromafin, el canal de calcio tipo L presenta una inactivación dependiente de calcio más lenta que la presentada por los canales N y PQ (Hernandez-Guijo *et al.*, 2001).

Con respecto al posible mecanismo implicado en la inactivación por calcio de los CCDV, diversos autores han identificado a la calmodulina como el sensor de Ca^{2+}

responsable de este fenómeno. La calmodulina es una proteína de 17 KDa que presenta cuatro sitios de unión para Ca^{2+}. La ocupación por Ca^{2+} de estos cuatro sitios produce un cambio notable de la conformación, de modo que la mayor parte de la molécula asume una estructura de hélice alfa capaz de activar o inactivar sitios de fosforilación presentes en las subunidades α y β **(Figura 3)**. La calmodulina también puede actuar indirectamente a través de la regulación de la proteína calcineurina (Burley & Sihra, 2000; Meuth *et al.*, 2002; Wahl-Schott *et al.*, 2006).

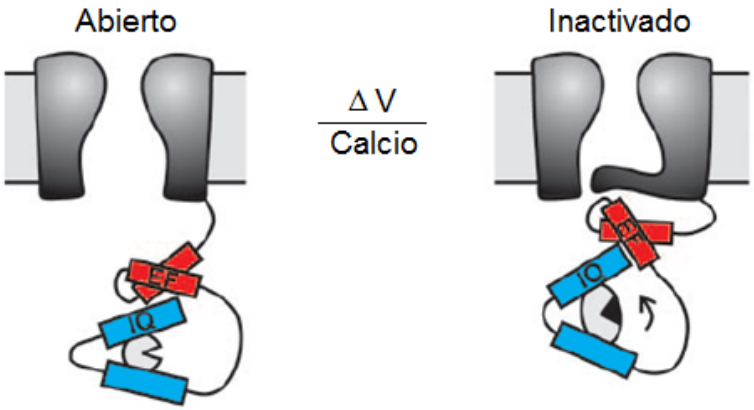

Figura 3: Esquema ilustrativo del mecanismo de inactivación por Ca^{2+} de los CCDV (calmodulina: círculo gris; calcio: triangulo negro) (Wahl-Schott *et al.*, 2006).

1.2.2. Modulación de los CCDV por voltaje

Poco se conoce del mecanismo por lo cual los canales de calcio se inactivan por voltaje. Sin embargo, este proceso de inactivación puede ser observado al compararse la corriente generada por una secuencia de dos pulsos de voltaje. Si el intervalo entre los dos pulsos es corto y no permite una recuperación del canal, la inactivación se evidencia como una disminución de la amplitud de la corriente durante el segundo pulso de voltaje (Gutnick *et al.*, 1989). Otra forma de observarse la inactivación por voltaje es cambiando el potencial de fijación de membrana a potenciales menos negativos (Villarroya *et al.*, 1999).

La inactivación por voltaje parece afectar de forma diferente a los distintos subtipos de CCDV y se podría decir que presenta dos fases o estados de inactivación:

una inactivación media, a bajos potenciales (en torno a -55 mV), que afecta fundamentalmente al componente sensible a ω-conotoxina GVIA (canales tipo N), y una segunda fase que afecta el componente mantenido de la corriente, inactivado a voltajes sobre -10 mV y que es sensible a dihidropiridinas (canal tipo L). También se ha descrito que los canales del tipo N no sufren inactivación por voltaje (Artalejo *et al.*, 1992). A nivel de la célula cromafín, se ha demostrado que los canales N y PQ son más susceptibles que los canales L a la inactivación por voltaje (Villarroya *et al.*, 1999).

1.2.3. Modulación de los CCDV por proteínas G

Este tipo de regulación de la entrada de Ca^{2+} asociado a proteínas G se caracteriza por presentar las corrientes de calcio una cinética de activación lenta y una menor inhibición a potenciales positivos. Por otro lado, la aplicación de un breve prepulso despolarizante es capaz de producir una pérdida parcial de la inhibición, lo que ha sido denominado por algunos autures como "facilitación" de la corriente de calcio (Bean, 1989; Ikeda, 1991; Ikeda & Dunlap, 1999; Garcia *et al.*, 2006).

En 1986, se propuso por vez primera que la inhibición de las corrientes de calcio producida por algunos neurotransmisores podría estar siendo modulada por voltaje. En estos experimentos, se observó un enlentecimiento de la activación de los canales de calcio a potenciales negativos en presencia de dopamina (Marchetti *et al.*, 1986). En las dos últimas décadas, se ha profundizado en el conocimiento de este tipo de mecanismo modulador de la actividad de los CCDV, habiéndose demostrado el papel de las subunidades $\beta\gamma$ de las proteínas G en la inhibición de los CCDV. Así, la unión de diversos neurotransmisores a sus receptores de membrana van a activar determinados subtipos de proteínas G. Las subunidades βγ de la proteína G se unen directamente a la subunidad α_1 del CCDV, haciendo el canal resistente a la apertura (Ikeda, 1996; Fox *et al.*, 2008).

La unión del ATP a su receptor es un ejemplo de la modulación de los CCDV por proteínas G (Gandia *et al.*, 1993b; Ulate *et al.*, 2000). Cuando el ATP se une a los receptores purinérgicos, se activa una proteína G que actúa enlenteciendo la activación de la corriente de calcio y disminuyendo su amplitud. En condiciones controles, la aplicación de un prepulso despolarizante no suele afectar ni a la cinética ni al tamaño de la corriente; sin embargo, en presencia de ATP, el prepulso despolarizante va a actuar

desacoplando la proteína G del canal, promoviendo así una aparente "facilitación" de la corriente de entrada (**Figura 4**).

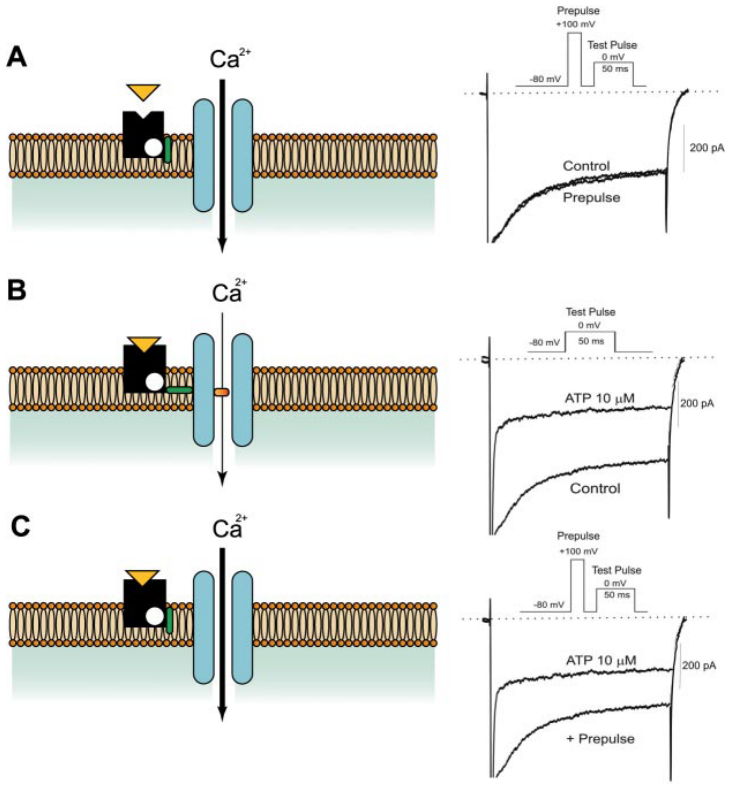

Figura 4: Mecanismo de inhibición de los canales de calcio por proteínas G. En condiciones controles, las proteínas G no están acopladas a los canales de calcio. La aplicación de un estímulo despolarizante, genera una corriente de entrada que no se modifica en caso de la aplicación de un prepulso despolarizante (A). Cuando el ATP se une a los receptores purinérgicos, la proteína G cambia de conformación modulando el canal disminuyendo el pico de la corriente (B). La aplicación de un prepulso despolarizante en estas condiciones desacopla la proteína G del canal de calcio, revertiendo la inactivación (C) (Garcia *et al.*, 2006).

Dos observaciones experimentales apoyan el papel de la proteína G en la modulación de los CCDV. Por un lado, tanto la diálisis celular con GDP-β-S como el pretratamiento con toxina *Pertussis*, ambos inhibidores de la actividad de las proteínas G, impiden la inactivación de los canales por neurotransmisores. Por otro lado, la adición a la solución intracelular de GTP-γ-S, un análogo no hidrolizable de GTP que actúa como activador de la proteína G, inhibe las corrientes de calcio (Diverse-Pierluissi *et al.*, 1991; Gandia *et al.*, 1993b; Garcia *et al.*, 2006; Fox *et al.*, 2008).

A nivel de la célula cromafín, también se ha demostrado que la activación de los receptores opioides μ y δ inhiben la corriente de calcio y disminuyen su activación

(Albillos *et al.*, 1996a) y que diversos componentes de las vesículas secretoras (catecolaminas, ATP, neuropéptidos y opióides) podrían estar modulando los CCDV a través de este mecanismo mediado por proteínas G, habiéndose descrito que se trataría de un mecanismo de modulación de tipo autocrino/paracrino de los CCDV (Albillos *et al.*, 1996a; Garcia *et al.*, 2006).

2. CANALES DE CALCIO Y NEUROTRANSMISIÓN

2.1- El acoplamiento estímulo-secreción

La secreción de catecolaminas por la célula cromafín se conoce desde las primeras décadas del siglo pasado. Ya en 1934, Feldberg y Minz demostraron que la estimulación del nervio esplácnico producía la liberación de ACh y que ésta era responsable de la secreción de adrenalina por la médula adrenal (Feldberg *et al.*, 1934).

Años después, surgió el concepto de "**acoplamiento estímulo-secreción**" de la mano de William Douglas y Donald Rubin. Al estudiar en la médula adrenal de gato el papel de la composición iónica del medio extracelular en la secreción de catecolaminas, demostraron que la acción secretagoga de la ACh era dependiente de la entrada de Ca^{2+} (Douglas & Rubin, 1961). En estos experimentos observaron que la eficacia de la ACh para iniciar el proceso secretor se encontraba reducida cuando el Ca^{2+} estaba disminuido y era prácticamente nula en ausencia de Ca^{2+}, mientras que a altas concentraciones de Ca^{2+} extracelular la respuesta secretora se veía incrementada. Douglas y Rubin también sugirieron por vez primera en este trabajo que el Ca^{2+} podría estar actuando en el anclaje de las vesículas en la membrana plasmática.

Un ejemplo de acoplamiento estimulo-secreción: El proceso fisiológico de liberación de catecolaminas adrenomedulares

En condiciones de reposo, se estima que las fibras nerviosas del nervio esplácnico disparan potenciales de acción a una frecuencia de 0,1 Hz (Brandt *et al.*, 1976). En situaciones de estrés, sin embargo, la frecuencia de descarga se incrementa hasta tres veces, lo cual se traduce en la liberación de gran cantidad de ACh, el

neurotransmisor fisiológico a nivel de la sinapsis esplácnico-cromafín (Feldberg *et al.*, 1934).

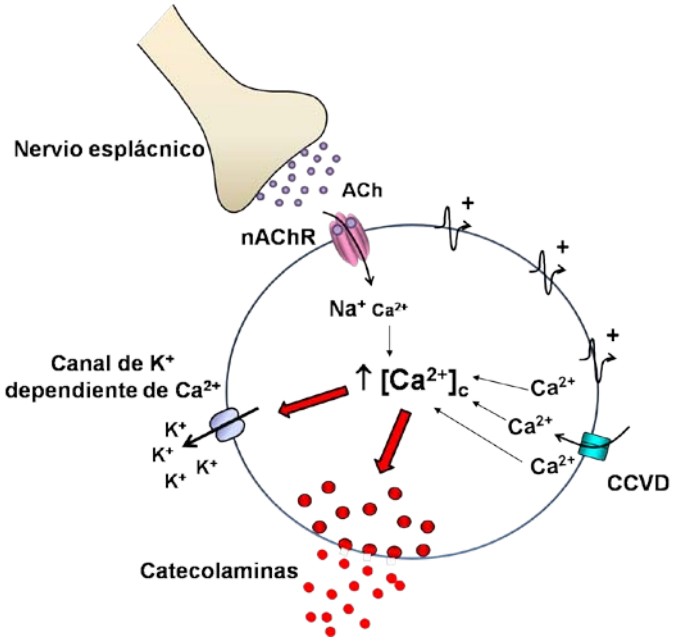

Figura 5. Esquema representativo del proceso de acoplamiento excitación-secreción en la célula cromafín.

Una vez en la sinapsis, la ACh actuará sobre receptores nicotínicos y/o muscarínicos presentes en la membrana de la célula cromafín. En la célula cromafín bovina, la activación del receptor nicotínico implica la apertura de su canal iónico, que en condiciones fisiológicas posibilita la entrada de Na^+ y, en menor medida, de Ca^{2+} al interior celular (Douglas *et al.*, 1967). Esta entrada de cationes en la célula provoca una despolarización de la membrana plasmática capaz de inducir la activación de los CCDV y, con ello se favorece la entrada de Ca^{2+} desde el espacio extracelular. El consecuente incremento de Ca^{2+} citosólico tendrá como consecuencia final la secreción de catecolaminas hacia el torrente sanguíneo (Garcia *et al.*, 1984) (**Figura 5**).

2.2- Exocitosis de neurotransmisores

Tras el proceso de entrada de Ca^{2+} al citosol, se ponen en marcha diversos mecanismos que conducen a la denominada exocitosis. La exocitosis del contenido

vesicular constitutuye la base de la comunicación intercelular en organismos multicelulares, a través de la liberación de una amplia gama de moléculas que van a actuar a nivel extracelular.

La fusión de la membrana vesicular con la plasmática es una reacción que requiere de la interacción de una serie de proteínas específicas que permitan a ambas membranas a mantenerse juntas, ya que la repulsión entre ambas membranas y el entorno acuoso no favorecería su fusión espontánea (Sudhof, 1995).

Algunas de estas proteínas, muy conservadas en la evolución y en los diferentes tipos de neuronas y células neuroendocrinas, constituyen el denominado **complejo SNARE** (s*oluble N-ethylmaleimide-sensitive factor attachment protein receptor*), y se localizan tanto en la membrana de las vesículas secretoras (v-SNAREs) como en la membrana plasmática (t-SNAREs). Se han identificado principalmente tres tipos (Sollner *et al.*, 1993; Roth & Burgoyne, 1994): sinaptobrevinas o VAMPs, sintaxinas y SNAP-25. Por sí mismas, estas proteínas son capaces de llevar a cabo el proceso de fusión *in vitro* (Weber *et al.*, 1998) pero *in vivo* la fusión de membranas requiere un gran número de otras proteínas reguladoras como la α-SNAP, el factor sensible a n-etilmaleimida (NSF) (Sudhof, 1995) o la sinaptotagmina (Voets *et al.*, 2001), entre otras. Todo este complejo entramado de proteínas constituye la denominada "**maquinaria de la exocitosis**".

Respecto a los requerimientos de Ca^{2+} para que se produzca exocitosis, hay trabajos que indican que el sensor de Ca^{2+} para la fusión de membranas en células neuroendocrinas tiene una afinidad por Ca^{2+} un orden de magnitud mayor que en células neuronales; así, en células cromafínes la concentración eficaz 50 (CE_{50}) de Ca^{2+} para la exocitosis es de 10-20 µM (Heinemann *et al.*, 1994) y la exocitosis se podría disparar a partir de concentraciones de Ca^{2+} citosólico cercanas a 5 µM, mientras que en neuronas es de aproximadamente 190 µM (Heidelberger *et al.*, 1994). No obstante, la relación entre Ca^{2+} y exocitosis en ambos tipos de células es muy controvertida en la literatura, con trabajos que postulan una relación lineal entre ellos y otros que postulan la cooperatividad entre iones calcio durante el proceso de exocitosis, lo que probablemente implicaría la unión del calcio a varios sitios de unión de una o más proteínas (Augustine & Neher, 1992; Meir *et al.*, 1999).

2.2.1.-Canales de calcio y exocitosis

Los CCDV representan la principal vía de entrada de Ca^{2+} a las células. La expresión de múltiples tipos de CCDV en neuronas (Olivera *et al.*, 1994) y células cromafínes de la médula adrenal (Garcia *et al.*, 2006) plantea la interesante cuestión de su especialización en el control de diferentes funciones celulares. Esto parece evidente en neuronas, donde la segregación geográfica de los diferentes subtipos de CCDV en dendritas, axones o soma facilita la especialización de sus funciones. Así, por ejemplo, los canales del subtipo N ($C_{aV}2.2$) y PQ ($C_{aV}2.1$) que se encuentran principalmente a lo largo de las dendritas (Westenbroek *et al.*, 1998), controlan la liberación de varios neurotransmisores (Wheeler *et al.*, 1994). Por otro lado, los canales de tipo L ($C_{aV}1.3$) situados en las dendritas proximales y soma de células neuronales (Ahlijanian *et al.*, 1990; Westenbroek *et al.*, 1990; Westenbroek *et al.*, 1998) se asocian a la regulación de la expresión génica y la actividad de enzimas en el hipocampo y neuronas corticales (Bading *et al.*, 1993; Deisseroth *et al.*, 1998).

Sin embargo, no resulta fácil de explicar una posible especialización de los CCDV en una célula como la cromafín, que se mantiene esférica en condiciones normales de cultivo. Como las neuronas, las células cromafínes de la médula adrenal expresan canales de Ca^{2+} de los subtipos L, N, R y PQ. Sin embargo, a diferencia de las neuronas, estas células carecen de dendritas y axones. Así, los estudios sobre la especialización de los subtipos de canales de Ca^{2+} en los cultivos de células cromafínes han proporcionado resultados poco claros (Garcia *et al.*, 2006).

Dependiendo del estímulo y patrón de estimulación aplicados, de la especie animal utilizada y de los métodos experimentales empleados para medir la exocitosis o liberación de catecolaminas, se han sugerido especializaciones diferentes de los diferentes CCDV en la modulación de la exocitosis (ver Garcia et al. 2006). Así, por ejemplo, los canales del tipo L se han asociado preferentemente a la secreción de catecolaminas en algunos estudios (Moro *et al.*, 1990; Jimenez *et al.*, 1993; Artalejo *et al.*, 1994). Otros estudios atribuyen más protagonismo a los canales del tipo N (O'Farrell *et al.*, 1997) o PQ (Lara *et al.*, 1998). Sin embargo, hay estudios que concluyen que la exocitosis de catecolaminas en células cromafines es proporcional a la entrada de Ca^{2+} inducida por cada subtipo de canal de Ca^{2+}, sin presentar ningún tipo de especialización (Engisch & Nowycky, 1996; Hernandez-Guijo *et al.*, 1999; Lukyanetz

& Neher, 1999; Carabelli *et al.*, 2003). Un resumen de las diferentes especializaciones de los subtipos de CCDV se puede ver en la **figura 6**.

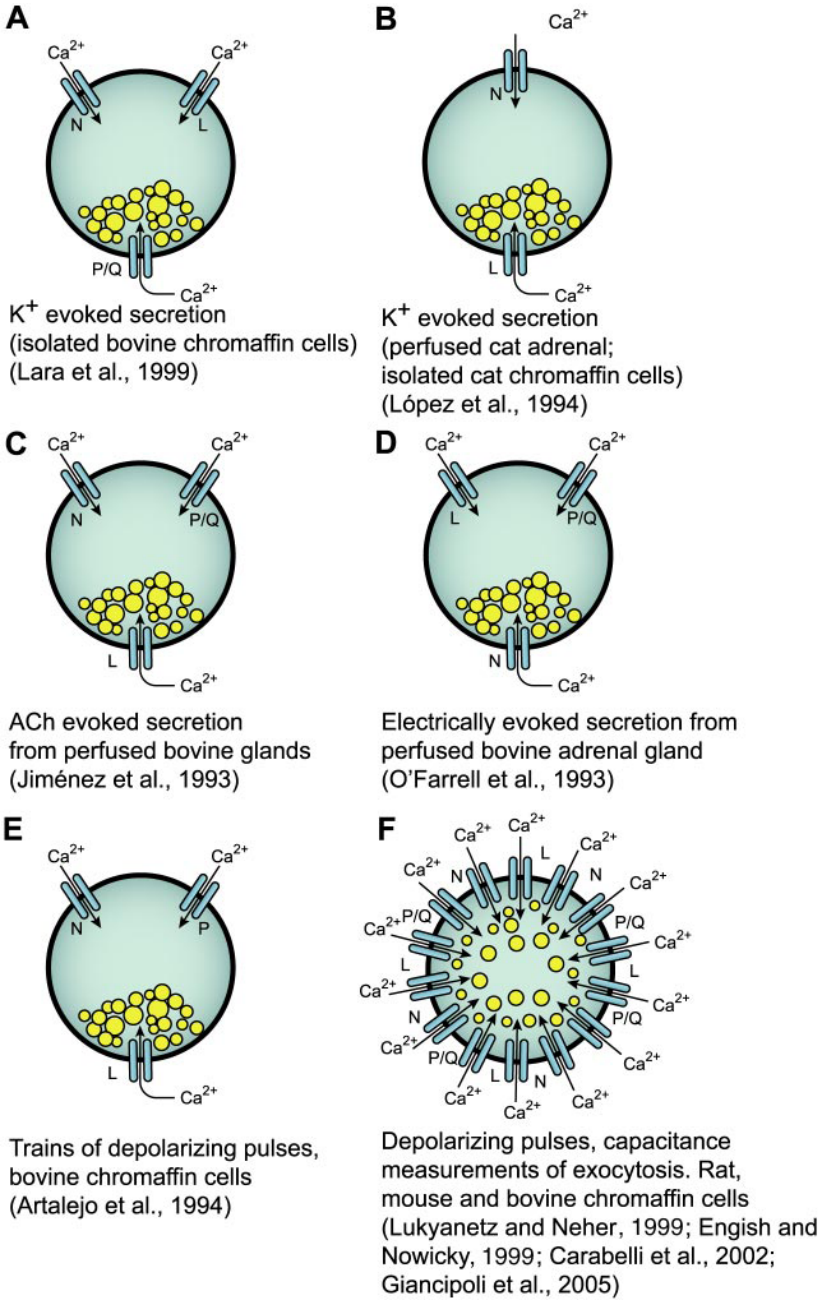

Figura 6: Subtipos de canales de calcio actúan de diferente forma en la exocitosis en la célula cromafín según el estímulo y las condiciones experimentales (Garcia *et al.*, 2006).

2.2.2.-Tipos de exocitosis

La exocitosis puede llevarse a cabo mediante dos mecanismos distintos. Durante la fusión, se forma un pequeño poro que une el espacio extracelular con el lumen vesicular y que permitirá la salida de los componentes vesiculares presentes en la

vesícula. Una vez que se ha formado el poro, la exocitosis puede producirse a través de una **fusión transitoria** (Ceccarelli *et al.*, 1973) o de una **fusión completa** (Heuser & Reese, 1973) de la vesícula con la membrana plasmática. Ambas formas de liberación vesicular se describieron por vez primera en la unión neuromuscular de rana, y posteriormente encontradas en sinapsis y células cromafines (Ales *et al.*, 1999; Sankaranarayanan *et al.*, 2000; Sankaranarayanan & Ryan, 2001).

En la fusión completa la membrana de la vesícula se fusiona con la membrana plasmática, de la cual terminará por formar parte, liberando todo el contenido vesicular. Por el contrario, mediante la fusión transitoria (denominada por algunos autores como *kiss-and-run* (Fesce *et al.*, 1994)), la vesícula no se fusiona completamente con la membrana sino que lo hace de una manera incompleta formando un pequeño poro que comunica el interior de la vesícula con el exterior celular por donde liberará su contenido. Posteriormente se cierra el poro quedando la vesícula en el citosol. Ambos tipos de fusión coexisten en las sinapsis nerviosas y desempeñan un importante papel en la neurotransmisión. El modo *kiss-and-run* presenta una función adicional en las terminaciones nerviosas del cerebro, permitiendo la conservación de los escasos recursos vesiculares y la habilidad de responder a estímulos de alta frecuencia (Harata *et al.*, 2006)

En relación a la implicación del calcio en el tipo de exocitosis, mediante la técnica de amperometria en célula única se ha demostrado que la entrada de Ca^{2+} a través de los canales L, N y PQ es responsable de la estabilidad del poro de fusión, controlando el tiempo y la cinética de la formación del poro y su expansión en la membrana (Ardiles *et al.*, 2007). Por otro lado, se ha visto que la elevación del calcio intracelular es capaz de cambiar de un estado de fusión completa a fusión transitoria de una manera dependiente de Ca^{2+} (Ales *et al.*, 1999).

2.3. Endocitosis

El proceso de neurotransmisión no se basa solamente en la fusión de las vesículas a la membrana plasmática con la consiguiente liberación de los neurotransmisores. Para mantener el tamaño celular de las terminaciones nerviosas y de las células neurosecretoras, es esencial mantener un equilibrio entre la cantidad de membrana vesicular incorporada al plasmalema durante la exocitosis y el tamaño

celular, que va a estar regulado mediante el proceso de recuperación o internalización de membrana plasmática conocido como **endocitosis**. Este proceso también garantiza que un determinado número de vesículas estén disponibles para participar en posteriores etapas de la exocitosis durante la activación de las células (Torri-Tarelli *et al.*, 1990; Smith & Neher, 1997; Royle & Lagnado, 2003).

2.3.1.-Tipos de endocitosis

En las células nerviosas coexisten tres tipos diferentes de endocitosis que actúan de forma simultánea o secuencial.

El primer tipo de endocitosis fue descubierto en la década de los 70 por Heuser y Reese a partir de estudios de microscopia electrónica (Heuser & Reese, 1973). Sus datos demostraban la presencia de un proceso endocitótico lento, dependiente de clatrina (**Figura 7**). Posteriormente, y gracias a las innovaciones técnicas, sobretodo electrofisiológicas, fue posible estimar en unos 15 minutos el tiempo aproximado que se rerquiere en células cromafínes bovinas para completar ese mecanismo lento de retirada de membrana (Henkel & Almers, 1996).

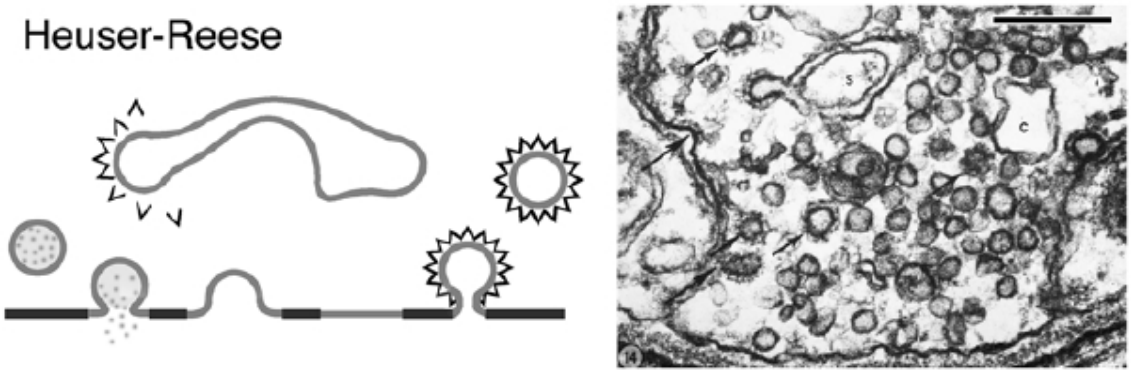

Figura 7: Modelo de endocitosis lenta propuesto por Heuser & Reese. Fotografía electrónica de una unión neuromuscular de rana donde se pueden observar vesículas acopladas a clatrina (flechas negras) y cisternas (C) (Royle & Lagnado, 2003).

El segundo modelo de endocitosis fue descrito por Cecarelli y colaboradores en 1973 en la unión neuromuscular de sapo (**Figura 8**), basándose en tres observaciones principales: (1) se apreciaban pocos cambios en la estructura de la terminación sináptica

tras la estimulación a 2 Hz utilizando microscopía electrónica; (2) las vesículas liberadas se reciclaban rápidamente y; (3) ausencia de clatrina (Ceccarelli *et al.*, 1973). Este modelo consiste en la existencia de una fusión transitoria de la membrana vesicular con la membrana plasmática durante la estimulación, sin llegar a producirse la fusión completa, liberándose parte del contenido vesicular. Este mecanismo ha sido denominado poéticamente como "*kiss-and-run*" por Fesce y colaboradores (Fesce *et al.*, 1994).

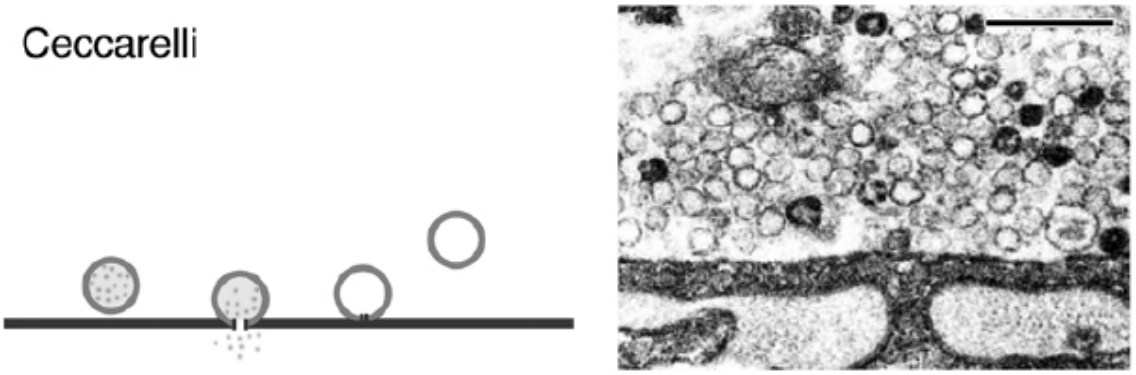

Figura 8: Modelo de endocitosis propuesto por Ceccarelli y colaboradores. Fotografía electrónica de una unión neuromuscular de sapo donde se observa la ausencia de puntos acoplados a clatrina y cisternas (Royle & Lagnado, 2003).

Se ha descrito un tercer mecanismo de endocitosis en varios modelos celulares que consiste en la formación de grandes invaginaciones o cisternas lejos de la zona exocitótica, tras la fusión completa de las vesículas sin la participación directa de clatrina (**Figura 9**) (Takei *et al.*, 1996; Gad *et al.*, 1998; Teng *et al.*, 1999; Richards *et al.*, 2000; Paillart *et al.*, 2003). Estas cisternas pueden estar localizadas en el citoplasma o permanecer adheridas a la membrana plasmática (Takei *et al.*, 1996; Teng & Wilkinson, 2000).

De estos tres mecanismos de endocitosis, el más claramente demostrado en diversos sistemas celulares es la endocitosis dependiente de clatrina.

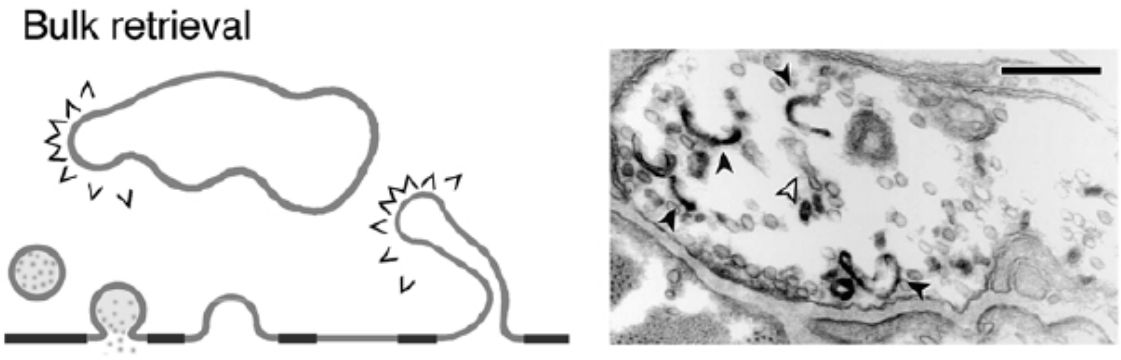

Figura 9 :. Modelo de endocitosis por retirada masiva de membrana. Fotografía electrónica donde se observa la formación de cisternas vacías (flechas blancas) o cisternas marcadas con FM1-43 (flechas negras) (Royle & Lagnado, 2003).

2.3.2.-Endocitosis en la célula cromafin

En la célula cromafín bovina se ha descrito la coexistencia los dos mecanismos propuestos por Heuser & Reeser y por Ceccarelli, presentando el proceso endocitótico, al menos, dos constantes de velocidad: una rápida y una lenta, que son activados por diferentes tipos de estimulación (Neher & Zucker, 1993; Thomas *et al.*, 1994; Engisch & Nowycky, 1998).

Smith y Neher (Smith & Neher, 1997) y Engisch y Nowycky (Engisch & Nowycky, 1998) encontraron dos formas de endocitosis rápida a las que denominaron **compensadora** (la cantidad de membrana recuperada es igual a la añadida durante el estímulo exocitótico) y **excesiva** (la cantidad de membrana recuperada con la endocitosis es mayor a la añadida durante la exocitosis). Algunos autores consideran la endocitosis excesiva como un cuarto mecanismo endocitótico presente en las células (Wu *et al.*, 2009).

La transición entre estos dos tipos de endocitosis se atribuye sobre todo a diferencias en la afinidad al Ca^{2+}, sugiriendo que la retirada de membrana excesiva y compensadora, tras la estimulación de las células cromafínes bovinas, representan dos mecanismos independientes de internalización de membrana regulados por Ca^{2+} (Engisch & Nowycky, 1998; Chan & Smith, 2001). Smith y Neher sugieren que la

endocitosis compensadora puede explicar la mayor parte de la recuperación de la membrana en condiciones fisiológicas (Smith & Neher, 1997).

Al igual que ocurría con la exocitosis, los mecanismos endocitóticos de también requieren interacciones entre proteínas de la vesícula sináptica y proteínas de membrana (De Camilli & Takei, 1996; Cousin & Robinson, 1999; Takei & Haucke, 2001). La fosforilación de diversas proteínas sinápticas tiene un importante papel en el reciclado vesicular. Sin embargo, ha sido la desfosforilación de proteínas del grupo de las desfosfinas (incluyendo dinamina-1 y ampifisina-1) lo que se ha considerado esencial en la endocitosis (Robinson *et al.*, 1993; Marks & McMahon, 1998; Cousin & Robinson, 2001; Cousin *et al.*, 2001). Así, se ha descrito que la endocitosis compensadora requiere dinamina-1, pero no clatrina (Artalejo *et al.*, 2002; Graham *et al.*, 2002), mientras que la endocitosis excesiva requeriría dinamina-2 y clatrina.

En la tabla 1, adaptada de una revisión publicada por Barg & Machado, podemos observar las diferencias entre los dos tipos de endocitosis (Barg & Machado, 2008).

Tabla 1: Datos comparativos entre los dos mecanismos de endocitosis en la CCB.

Propiedades	***Compensatoria***	***Excesiva***
Efecto de diálisis [a,b]	Se pierde la endocitosis	La endocitosis persiste
Cantidad de membrana retirada [a,c]	60-10% de la membrana exocitada	Cerca de ~10% de la superficie de la célula
Estímulo requerido [a,c]	Exocitosis (aumento de la entrada de Ca^{2+})	Umbral > 70-90 pC de entrada de Ca^{2+}, $[Ca^{2+}]_i$ >50 μM
Relación con la cantidad exocitada [a,c]	Directamente proporcional	NO
Velocidad inicial [a]	6 fF/s	240 fF/s
Constante τ tiempo τ [c]	Mono-exponencial	Doble-exponencial
	τ ≅ 3-6s	τ1 ≅ 600 ms; τ1 ≅ 6-7 s
Efecto de ciclosporina A [c]	Inhibición	No efecto
Efecto de calmidazolina [d]	No efecto	
Efecto del Ba^{2+}	No efecto [d]	No efecto
	Inhibidor [e]	
Efecto de estaurosporina [f]	Inhibidor	

[a] (Smith & Neher, 1997); [b] (Burgoyne, 1995); [c] (Engisch & Nowycky, 1998); [d] (Nucifora & Fox, 1998); [e] (Artalejo *et al.*, 1996); [f] (Chan & Smith, 2003).

2.3.3.-Calcio y endocitosis

Está claramente establecido que la exocitosis puede ser activada por el aumento de la concentración citoplasmática de diversos cationes divalentes, como Ca^{2+}, Sr^{2+} o Ba^{2+} (Douglas & Rubin, 1964; Neher & Zucker, 1993). Por el contrario, el papel del Ca^{2+} y otros iones divalentes en el proceso endocitótico se encuentra todavía confuso.

En los primeros estudios realizados en células cromafínes, se ha sugerido que la endocitosis rápida es dependiente de Ca^{2+}, GTP y dinamina pero no de clatrina (Neher & Zucker, 1993; Artalejo *et al.*, 1995). La dependencia al Ca^{2+} es ilustrada por los datos de Artalejo y colaboradores en 1995 que mostraron que la endocitosis rápida es activada por Ca^{2+}, pero no por Sr^{2+} o iones Ba^{2+} (Artalejo *et al.*, 1995); sin embargo, en un estudio posterior realizado por Nucifora y Fox, tanto el Ca^{2+} como el Ba^{2+} fueron capaces de activar la endocitosis en células cromafínes bovinas (Nucifora & Fox, 1998).

Por otro lado, algunos estudios han sugerido que el Ca^{2+} no afecta la endocitosis en sinapsis (Ryan *et al.*, 1996; Wu & Betz, 1996), mientras que otros indican que el Ca^{2+} es inhibidor (Rouze & Schwartz, 1998) o que, conjuntamente con la calmodulina, es capaz de activar todos los tipos de endocitosis (Wu *et al.*, 2009). Estas diferencias en cuanto al papel del Ca^{2+} en los procesos de endocitosis podrían deberse a diferentes tipos de células y/o preparaciones, y tal vez reflejan las diferentes vías endocitóticas utilizadas por las células.

3. ESFINGOLÍPIDOS DE MEMBRANA

En general, los lípidos de las membranas celulares ejercen importantes funciones por su capacidad de regular numerosos procesos cruciales para la vida de las células.

Dentro de éstos encontramos los denominados **esfingolípidos,** que son lípidos de membrana que incluyen en su estructura las denominadas esfingoides conocidas también como *bases de cadena larga* ó *esfingosinas*. Además de contener en su estructura la esfingosina, los esfingolípidos presentan un acido graso de longitud variable unido al carbono-2 de la cadena base y diversas cabezas polares unidas al carbono-1 **(Figura 10).** En el caso de la esfingomielina el grupo hidrofílico es la fosforilcolina, mientras que en el caso de los glicoesfingolípidos es un azúcar.

Los esfingolípidos, se consideraron hasta hace aproximadamente dos décadas, como meros integrantes estructurales y estáticos de las membranas biológicas. Actualmente, se han caracterizado como componentes funcionales y dinámicos que además de sus importantes funciones estructurales en las células eucariotas, intervienen en las cascadas de transducción de señales que regulan procesos como el crecimiento, la diferenciación celular, el transporte intracelular de membranas y la muerte celular, entre otros. Además, son capaces de regular la dinámica de las membranas biológicas formando parte de las bolsas lipídicas (del inglés "*lipid rafts*") juntamente con el colesterol y los glicolípidos (Carter *et al.*, 1947; Futerman & Hannun, 2004; Dickson, 2008; Pruett *et al.*, 2008).

3.1. Metabolismo de los esfingolípidos y su papel fisiológico

Entre los principales esfingolípidos de la membrana plasmática se incluyen la ceramida, la esfingosina, la ceramida-1-fosfato y la esfingosina-1-fosfato. Entre ellos destaca la ceramida, una molécula hidrofóbica cuya producción se incrementa ante estímulos de estrés y que es considerada como el centro de la ruta de síntesis y degradación de los esfingolípidos.

El catabolismo de los esfingolípidos tiene lugar principalmente en los lisosomas y en menor extensión, en la membrana plasmática. Los diferentes esfingolípidos llegan a los lisosomas vía caveolas y/o mediante endocitosis dependiente de clatrina. Los productos derivados del catabolismo, como la esfingosina, acceden al citosol y pueden ser reutilizados en la vía de recuperación de la ceramida o actuar en sus efectores (Marks & Pagano, 2002).

El metabolismo de los esfingolípidos consiste básicamente en tres pasos. El primero de ellos es la **síntesis de ceramida**, que puede producirse mediante varios mecanismos: (1) un mecanismo de síntesis *de novo*, que se lleva a cabo en el retículo endoplasmático y el aparato de Golgi, a partir de precursores sencillos, empezando por la condensación de la serina y palmitoil CoA dando lugar a cetoesfinganina.; (2) mediante la degradación de la esfingomielina de la membrana mediante la intervención de las enzimas esfingomielinasas, dando lugar a ceramida y fosforilcolina. Esta segunda vía es considerada la responsable de la ceramida como transductor de señales de muerte celular (Andrieu-Abadie & Levade, 2002); o (3) mediante la vía de reciclaje o de

"salvamento", que ocurre mediante la acilación de la esfingosina y otras bases esfingoides procedentes de la degradación de esfingolípidos complejos.

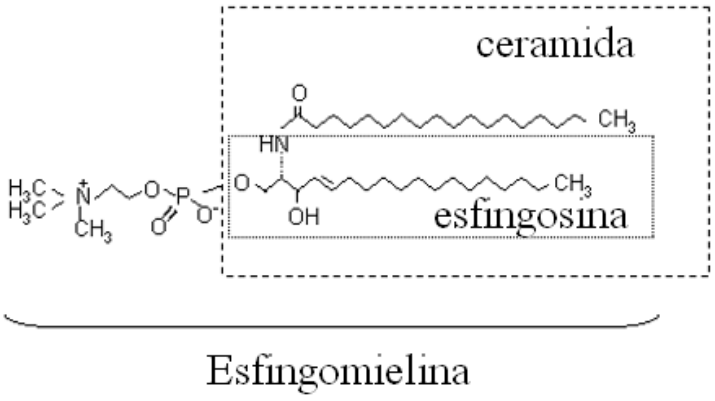

Figura 10: Estructura de la esfingosina, ceramida y esfingomielina.

El segundo paso del metabolismo ocurre mediante la **degradación de las ceramidas** formando ceramida-1-fosfato, esfingosina y esfingosina-1-fosfato. Las ceramidas son sustrato de las enzimas ceramidasas originando esfingosina y el ácido graso correspondiente.

En el tercer paso, la esfingosina liberada bajo la acción de las ceramidasas puede ser reutilizada para originar de nuevo ceramida (vía de reciclaje o salvamiento) mediante la reacción catalizada por la ceramida sintasa, o transformarse en esfingosina-1-fosfato en la reacción catalizada por esfingosina cinasa. Por otro lado, la conversión de ceramida a ceramida-1-fosfato está catalizada por la ceramida cinasa **(Figura 11).**

Uno de los aspectos más interesantes de la función biológica de los esfingolípidos es su papel en la decisión del destino celular. Mientras que la ceramida activa señales de muerte, la ceramida-1-fosfato y la esfingosina-1-fosfato activan señales de supervivencia celular. Por lo tanto, los niveles relativos de estos metabolitos son fundamentales para determinar funciones vitales de la célula. También se ha descrito una implicación en la vía de muerte y supervivencia celular para las enzimas que catalizan la síntesis de estos metabolitos. Por otro lado, al controlar los niveles de esfingomielina y ceramida, se ha descrito que las esfingomielinasas de membrana pueden estar implicadas en la modulación funcional de la formación de las denominadas bolsas lipídicas. También se ha demostrado que la ceramida controla los niveles de

receptores para acetilcolina en la membrana plasmática, pudiendo tener implicaciones importantes en el desarrollo de diversas enfermedades (Gallegos *et al.*, 2008).

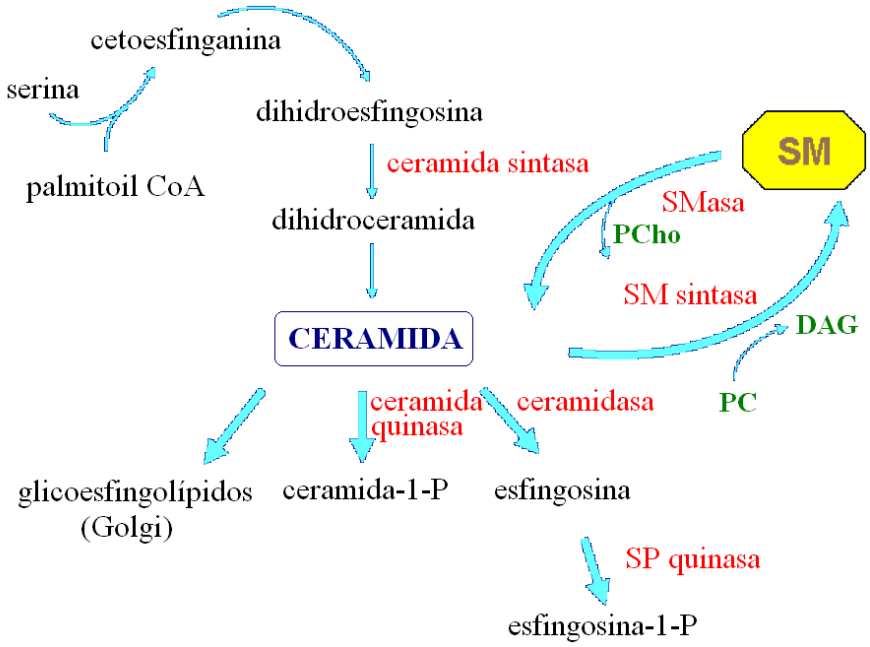

Figura 11: Síntesis y degradación de los esfingolípidos

3.2. Papel de los esfingolípidos en el proceso exo-endocitótico

Siendo la exocitosis y endocitosis procesos que involucran las membranas enriquecidas en lípidos, algunos estudios han abordado el papel del metabolismo de los lípidos en la liberación de neurotransmisores.

En lo que respecta al posible efecto de los esfingolípidos de membranas sobre los procesos de exocitosis, se ha descrito que a actividad de la esfingomielinasa se asocia a una regulación de la liberación de neurotransmisores de las neuronas del cerebelo y mesencéfalo, así como de las células PC12 (Blochl & Sirrenberg, 1996; Numakawa *et al.*, 2003; Jeon *et al.*, 2005). De forma similar, la esfingosina-1-fosfato regula al alza la secreción de glutamato en las neuronas del hipocampo (Kajimoto *et al.*, 2007), así como la liberación de acetilcolina en la unión neuromuscular de rana (Brailoiu *et al.*, 2002). Por último, un reciente estudio muestra que la liberación de

neurotransmisor está aumentada en presencia de esfingosina en las células cromafines, en la unión neuromuscular de rana, en sinaptosomas y en melanotrofos (Darios *et al.*, 2009). Este papel regulador parece deberse a la acción de las esfingosinas sobre las sinaptobrevinas que forman el complejo SNARE. Por otro lado, la esfingosina-1-fosfato se ha relacionado con la salida de Ca^{2+} del retículo endoplasmático de las células cromafines bovinas desencadenando una respuesta secretora en ausencia de despolarización (Pan *et al.*, 2006), así como una disminución de la corriente de calcio y de los procesos exocitóticos y endocitóticos (Pan *et al.*, 2007).

Por el contrario, el posible papel de los esfingolípidos en el mecanismo endocitótico ha sido hasta ahora poco estudiado. La primera observación de la acción de las esfingomielinasas en la formación vesicular se llevó a cabo en eritrocitos humanos en 1988 por Allan y Walklin (Allan & Walklin, 1988). Una década más tarde, Zha y colaboradores (1998) describieron que este proceso ocurría en zonas lejanas a la membrana plasmática, y que era independiente de ATP (Zha *et al.*, 1998). El mecanismo por lo cual se activa la endocitosis es incierto, pero se supone que las esfingomielinasas provocan una deformación hacia el interior de la bicapa lipídica generando una curvatura inversa más bien por acción mecánica que por activación de proteínas o enzimas.

4. LA CÉLULA CROMAFÍN COMO MODELO NEUROSECRETOR

Como hemos mencionado anteriormente, uno de los modelos experimentales que hemos utilizado para el desarrollo de la presente Tesis es la célula cromafín de la médula de la glándula suprarrenal. Este tipo celular constituye un excelente modelo para el estudio de la síntesis, el almacenamiento, la liberación por exocitosis de neurotransmisores y la endocitosis, de la modulación de canales de Ca^{2+} dependientes de voltaje (CCDV) y de los movimientos intracelulares de Ca^{2+}, entre otros.

4.1. La glándula suprarrenal

La glándula suprarrenal, también conocida como glándula adrenal, está encerrada en una cápsula de tejido conjuntivo vascularizado. Posee una corteza y una médula, que a pesar de tener un origen filogenético diferente y funciones diversas, forman un órgano

homogéneo. La rica irrigación vascular de la glándula es conducida hacia el interior a través de los elementos de tejido conectivo derivados de la cápsula (**Figura 11**).

La **corteza**, derivada del epitelio mesodérmico, está subdividida en tres regiones o zonas concéntricas; la zona glomerular, la más externa y angosta ubicada justo por debajo de la cápsula; la zona fasciculata, la más extensa, cuyas células se organizan en cordones o columnas y la zona reticular, la más interna, se dispone en cordones anastomosados de células formando un tejido laxo en forma de malla que limita con la médula. La corteza suprarrenal produce tres tipos de hormonas: mineralcorticoides (zona glomerular), glucocorticoides (zona fasciculata y parte de la zona reticular) y andrógenos (zona fasciculata y zona reticular).

La **médula** de la glándula suprarrenal deriva embriológicamente de la cresta neural, teniendo por tanto un origen común con las neuronas simpáticas (Euler, 1972). Las células de la médula suprarrenal son poliédricas, exhiben una granulación muy fina y están distribuidas en cordones rodeados por redes capilares que las nutren y, a la vez, recogen sus productos de secreción **(Figura 12B).** A causa de su afinidad por las sales de cromo, las células de la médula suprarrenal se bautizaron con el nombre de células cromafines (Coupland, 1965). Las células cromafines son responsables de la síntesis, almacenamiento y secreción de las catecolaminas (dopamina, adrenalina y noradrenalina), además de actuar sobre el metabolismo de los glúcidos y lípidos; en la redistribución del volumen sanguíneo circulante; en el aumento de la presión arterial, la frecuencia cardíaca y en el SNC incrementan la atención y la vigilia.

5.2. La célula cromafín como modelo de neurona secretora: el término *paraneurona*

A mediados de los años 70, Tsuneo Fujita (Fujita, 1977) y Shigeru Kobayashi (Kobayashi, 1977) introdujeron el término ***paraneurona*** para describir a las células neuroendocrinas con propiedades similares a las neuronas en cuanto a su origen, estructura, función y metabolismo. En base a estos criterios, las células cromafines de los mamíferos podrían considerarse paraneuronas, ya que presentan un gran parentesco con las neuronas simpáticas postganglionares: ambos tipos de células derivan de la cresta neural; poseen vesículas sinápticas y/o de secreción; tienen función neurosecretora (las células cromafines liberan catecolaminas en respuesta a la

estimulación por acetilcolina (ACh) liberada por nervios originados en la médula espinal).

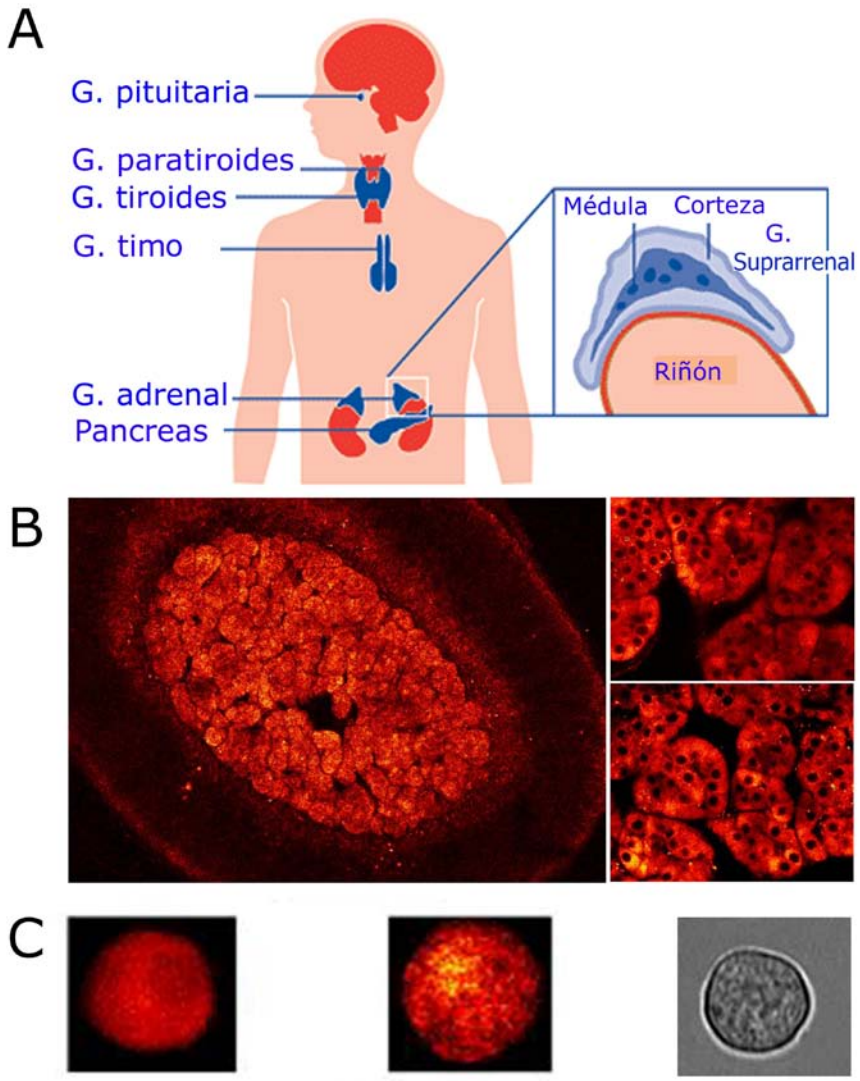

Figura 12: Panel A: Ubicación de la glándula suprarrenal en el organismo humano. **Panel B**: Imagen confocal de una rodaja de glándula adrenal de ratón de 150 µm de grosor, marcada con la sonda fluorescente Lysotracker Red que permite visualizar las vesículas de secreción. A la derecha, detalles de la organización en "acinos" o racimos de las células cromafines. Nótese su forma poliédrica. **Panel C**: células cromafines de ratón en cultivos primarios marcadas con la sonda fluorescente Lysotracker Red. A la derecha, imagen de transmisión de las células. Nótese aquí la diferencia con las células en el tejido intacto (Panel B) y su forma esférica, con un diámetro aproximado de 15 µm. Adaptada de (Fuentealba, 2004)

Ambos tipos de células comparten además otras características funcionales: así, las células cromafines poseen receptores nicotínicos (Douglas & Rubin, 1961; Wilson & Kirshner, 1977) y muscarínicos (Douglas & Poisner, 1965) sobre los que actúa la ACh; disparan potenciales de acción (Biales *et al.*, 1976; Brandt *et al.*, 1976; Kidokoro & Ritchie, 1980); poseen canales sensibles a voltaje de Na^+, Ca^{2+} y K^+ (Fenwick *et al.*, 1982b; Artalejo *et al.*, 1993; Garcia *et al.*, 2006) o exhiben facilitación de corrientes de calcio por prepulsos despolarizantes repetidos (Ikeda, 1991; Gandia *et al.*, 1993b; Albillos *et al.*, 1996a). Las células cromafines también presentan similitudes morfológicas con las neuronas postganglionares simpáticas, ya que emiten prolongaciones al co-cultivarlas con astroglia o al exponerlas al factor de crecimiento nervioso (Unsicker *et al.*, 1980).

Por todo lo expuesto anteriormente y porque se pueden aislar y mantener en cultivo primario con facilidad (Livett, 1984; Moro *et al.*, 1990), las células cromafines se han empleado ampliamente como modelo neurosecretor y mucho de lo que se conoce sobre la síntesis y liberación exocitótica de neurotransmisores se lo debemos a ellas. Por otra parte, el hecho de presentar la maquinaria para el mecanismo endocitótico las convierten en un valioso modelo para estudiar los eventos y función de la retirada de membrana tras el proceso exocitótico

5. ENFERMEDAD DE ALZHEIMER

La Enfermedad de Alzheimer (EA) es una enfermedad neurodegenerativa que se caracteriza por afectar a los sistemas colinérgicos, glutamatérgicos y serotonérgicos, produciéndose una pérdida progresiva de la memoria y de otras capacidades mentales. La EA fue identificada a principios del siglo por el psiquiatra y neurólogo alemán **Aloysius "Alois" Alzheimer** al encontrarse con una paciente (*Auguste Deter*) que presentaba un llamativo cuadro clínico de trastorno mental.

Las principales características de esta enfermedad son la disminución de la neurotransmisión colinérgica y la muerte neuronal, sobre todo a nivel del Núcleo basal de Meynert, resultando en una gran pérdida cognitiva (Whitehouse *et al.*, 1982a; Whitehouse *et al.*, 1982b). Este núcleo que se encuentra próximamente al hipocampo, contiene principalmente neuronas colinérgicas y emite sus prolongaciones nerviosas hasta regiones importantes como córtex prefrontal, occiptal e hipocampo. Estudios en

cerebros posmortem de pacientes demostraron una pérdida masiva del tamaño del cerebro sobretodo en la región de Meynert, así como una disminución de la colina acetil transferasa (CAT), acetilcolina esterasa (AChE) y del número de receptores para acetilcolina. Todos estos hechos han llevado a la formación de la *Hipótesis Colinérgica* postulada por Bartus y colaboradores en 1982 (Bartus *et al.*, 1982) y que ha llevado a que, actualmente, la terapia para el tratamiento de los pacientes con EAen sus estadios iniciales se base principalmente en aumentar la transmisión colinérgica con el uso de inhibidores de la acetilcolinesterasa como la galantamina, la rivastigmina y el donepezilo. La excitotoxicidad por glutamato, el estrés oxidativo, los procesos inflamatorios y el gen de la apoproteína-4 (ApoE-4), también han sido relacionados con la muerte neuronal en la EA.

La enfermedad de Alzheimer también pose características histológicas bien definidas como la acumulación de ovillos neurofibrilares y placas seniles. Los ovillos neurofibrilares están formados por un acumulo de proteína Tau hiperfosforilada. La fosforilación de tau es mediada por una serie de proteínas quinasas y fosfatasas (Ekinci *et al.*, 2003). Las placas seniles están compuestas por el péptido β-amiloide (Aβ), producto de la degradación de la proteína precursora de amiloide (APP) presente en la membrana de las células (Santos *et al.*, 2009). La APP es cortada fisiológicamente por enzimas secretasas dando lugar a dos fragmentos proteicos. Uno de ellos es el fragmento soluble de la proteína precursora de amiloide (APPs) que tiene propiedades promotoras del crecimiento y que puede jugar un papel en la formación de las neuronas, tanto antes como después del nacimiento. En este proceso fisiológico están relacionadas las enzimas α-secretasa y γ-secretasa. El otro fragmento es el péptido β-amiloide procedente de la acción consecutiva de la β-secretasa y γ-secretasa (Wu & Yao, 2009). En situaciones normales, existe un equilibrio entre la producción y la degradación. Sin embargo, una alteración en la expresión o en la actividad de APP puede llevar a cambios en la estabilidad y/o agregación del péptido, pudiendo dar inicio a una cascada de eventos intra y extracelulares, con alteraciones en la homeostasia del Ca^{2+} y un daño oxidativo por la formación de radicales libres, llevando progresivamente a la muerte neuronal.

5.1. Canales de Ca^{2+} y Enfermedad de Alzheimer

Diferentes estudios *in vitro* e *in vivo* han demostrado que la forma insoluble y agregada del fragmento del péptido β -amiloide posee propiedades neurotóxicas en diferentes modelos experimentales (Weiss *et al.*, 1994; Ueda *et al.*, 1997; Ekinci *et al.*, 1999; Ekinci *et al.*, 2003; Clementi *et al.*, 2005; Santos *et al.*, 2009; Yu *et al.*, 2009). Estos efectos tóxicos han sido descritos para los diferentes fragmentos del péptido conocidos: $A\beta_{1-42}$, $A\beta_{1-40}$, $A\beta_{25-35}$ y $A\beta_{31-35}$ (Clementi *et al.*, 2005).

Aún no se sabe el mecanismo exacto por el cual el péptido Aβ produce la muerte celular, pero se piensa que la alteración en la homeostasia del Ca^{2+} podría estar relacionada, ya que *per se* el Aβ es capaz de elevar la $[Ca^{2+}]_c$ (Mattson *et al.*, 1992; Ueda *et al.*, 1997). Puesto que, como he comentado anteriormente, los CCDV constituyen la principal vía de entrada de Ca^{2+} a la célula y por esta razón, se han desarrollado diversos estudios con el fin de investigar la posible implicación de los CCDV en el aumento de Ca^{2+} intracelular provocado por el péptido Aβ.

Actualmente existen en la literatura grandes controversias en relación al papel de los difeferentes CCDV en el efecto neurotóxico del péptido Aβ. Sin embargo, muchos hallazgos llevan a pensar en una participación del canal del subtipo L en la neurotoxicidad del péptido Aβ. Así, se ha descrito que la inhibición de los canales L, pero no de los canales N y PQ, es capaz de disminuir la muerte celular. Igualmente, mediante técnicas electrofisiológicas se ha demostrado un aumento de las corrientes L en preparaciones expuestas al péptido Aβ (Weiss *et al.*, 1994; Ueda *et al.*, 1997; Santos *et al.*, 2009).

Por otro lado, se ha descrito que el ácido okadaico (AO), un inhibidor de las proteínas fosfatasas 1 y 2A (PP1 y PP2A) que es utilizado como modelo experimental para la hiperfosforilación de la proteína tau (otra característica histopatológica encontrada en los cerebros de pacientes con Alzheimer) ejerce su acción sobre la fosforilación de tau principalmente mediante la fosforilación por MAP-kinasas de los canales de Ca^{2+} del subtipo L (Ekinci *et al.*, 2003).

5.2. Esfingolípidos y Enfermedad de Alzheimer

Entre los diversos lípidos presentes en la membrana plasmática, en los últimos años ha crecido el interés en los estudios relacionados con el metabolismo de los

esfingolípidos y su posible implicación en el desarrollo de la Enfermedad de Alzheimer, animados por el hallazgo de la localización de las secretasas que cortan la APP en un dominio transmembrana, hipotetizándose que una alteración en el grosor de la membrana plasmática podría cambiar la zona de corte de la APP favoreciendo así el inicio de la ruta amiloidogénica (Grziwa *et al.*, 2003).

A este respecto, se ha descrito que las esfingomielinas pueden disminuir la producción de péptido Aβ al inhibir la actividad de las γ-secretasas. Igualmente, la inhibición de la actividad de las esfingomielinasas, responsables de la degradación de las esfingomielinas de membrana, también han sido relacionadas con una menor producción de Aβ, al aumentar la cantidad de esfingomielinas con esta inhibición (Grimm *et al.*, 2005). Las esfingosinas también pueden alterar el metabolismo de la APP por actuar sobre la proteína cinasa C (PKC), que a su vez activa las α-secretasas (Smith *et al.*, 2000).

Por otro lado, la ceramida, el producto de la degradación de las esfingomielinas por las esfingomielinasas, se ha relacionado con la activación de proteínas próapoptóticas, lo que podría ser relevante en la EA por la muerte neuronal (Jana *et al.*, 2009; Qin *et al.*, 2010).

Adicionalmente, en cerebros de pacientes postmorten se ha observado un aumento de la actividad de las esfingomielinasas y ceramidasas, lo que llevaría a un incremento de los niveles de ceramida y esfingosina y a una disminución de las esfingomielinas y esfingomielina1 fosfato (S1P) (He *et al.*, 2008). En los últimos años, se ha descrito que los efectos neuroprotectores presentados por S1P se deben principalmente por su actuar en la PKCε y por disminuir el potencial de membrana mitocondrial, con consiguiente disminución del Ca^{2+} en la mitocondria (Agudo-Lopez *et al.*, 2010). Así, se postula que la disminución de los niveles de S1P y el aumento de las ceramidas, podrían estar contribuyendo en el desarrollo de la enfermedad provocando una deposición del péptido β-amiloide (He *et al.*, 2008).

Por último, el aumento de ceramida, sea por forma directa o por su síntesis endógena mediante esfingomielinasas disminuyen el número de receptores para acetilcolina en la membrana. Este hecho es altamente relevante, desde que la transmisión nicotínica se encuentra disminuida en la EA (Gallegos *et al.*, 2008).

5.3. Alteraciones en el mecanismo endocitótico en la Enfermedad de Alzheimer y su relación con los esfingolípidos de membrana

Diversas alteraciones en la endocitosis han sido relacionadas con diversas patologías, entre ellas la Enfermedad de Alzheimer. Poco se conoce de la posible relación entre los procesos endocitóticos de membrana y la EA. Sin embargo, los resultados obtenidos a partir de estudios con tejido neuronal de pacientes postmorten con EA, sugieren que la endocitosis se encuentra aumentada en las fases iniciales de la enfermedad. El aumento de la formación de los endosomas podría llevar a una mayor producción de Aβ.

Tanto en cerebros de pacientes con EA como en cultivos celulares, se ha observado un aumento del número y del tamaño de las vesículas endocitóticas y endosomas. Estas alteraciones se han identificado incluso antes de que se produzca la deposición de Aβ y en fases iniciales de la enfermedad (Cataldo *et al.*, 2000), sugiriendo que la EA podría ser el resultado de unsecuestro y/o una inapropiada degradación de proteínas de la membrana plasmática con vital importancia para el buen funcionamiento de la célula, como los factores tróficos y los receptores. Por otro lado, en fases tardías de la enfermedad, se ha observado una reducción de las proteínas reguladoras de la endocitosis por clatrina: dinamina y AP180 (Yao & Coleman, 1998; Yao *et al.*, 2003).

Dentro de los endosomas ocurre el procesamiento amiloidogénico de la APP, lo que indica que el proceso endocitótico va a determinar como será procesada la APP (Nordstedt *et al.*, 1993). Holtzman y colaboradores fueron los pioneros en sugerir que la endocitosis regulada (la iniciada tras un estímulo exocitótico) aumenta la internalización de la APP, resultando en un aumento de la producción y liberación de péptido Aβ (Cirrito *et al.*, 2005; Cirrito *et al.*, 2008). Por el contrario, la inhibición de la endocitosis vía caveolas disminuye la muerte de neuronas en cultivo por el tratamiento con Aβ (Yu *et al.*, 2009). Al inhibirse una de las vías que median la endocitosis lenta, el péptido Aβ no se translocaría al citosol de la célula inhibiéndose así la activación de las rutas de muerte.

Por otro lado, como se ha descrito anteriormente, los procesos endocitóticos son dependientes de proteínas que se localizan en la membrana plasmática. En este sentido,

se ha descrito que las esfingomielinasas presentes en la membrana plasmática pueden ser activadas por el péptido Aβ, llevando a una degradación de las esfingomielinas y un aumento de ceramida y esfingosina favorecería la formación de vesículas endocitóticas, por lo que se ha postulado una posible relación entre EA y alteraciones en los procesos endocitóticos controlados por los esfingolípidos.

III. HIPÓTESIS Y OBJETIVOS

El proceso de neurosecreción y neurotransmisión es dependiente de dos mecanismos básicos: exocitosis, con consiguiente liberación del contenido vesicular, y endocitosis, que controla el tamaño celular y la cantidad de vesículas disponibles para liberación. Ambos procesos son regulados mediante la entrada de Ca^{2+} por los distintos CCDV. Dependiendo del estímulo secretor y protocolo utilizado para el estudio de los canales de calcio en la exocitosis, diferentes especializaciones de los CCDV han sido encontradas. Sin embargo, el papel del calcio en la endocitosis es controverso. Además, poco se sabe en relación al papel de los distintos canales de calcio en la endocitosis.

Se ha descrito que en las células cromafines bovinas, los canales de Ca^{2+} del tipo L son menos sensibles a los cambios de voltaje (Villarroya *et al.*, 1999) y a la inactivación dependiente de Ca^{2+} que los tipos N y PQ (Hernandez-Guijo *et al.*, 2001). Obviamente, este diferente patrón de inactivación de las señales de Ca^{2+} podrían dar lugar no sólo a diferentes señales de Ca^{2+} citosólico y exocitosis (Garcia *et al.*, 2006), sino también a un modelo diferente de control de la endocitosis. Por lo tanto, en esta Tesis Doctoral, estudiaremos como los canales de calcio modulan entre si su actividad, además de combinar técnicas electrofisiológicas de registros de corrientes de entrada de Ca^{2+} (I_{Ca} y Q_{Ca}) con medidas de capacidad de la membrana (C_m; exo-endocitosis) y técnicas fotométricas con la sonda FM1-43, para estudiar el papel de la entrada de Ca^{2+} a través de los diferentes subtipos de CCDV y verificar si el Ca^{2+} que entra en la célula a través de los canales L, N o PQ tras un estímulo despolarizante, modifica de igual forma las respuestas exo-endocitóticas. Por otro lado, estudiaremos como el Ca^{2+} intracelular puede afectar la endocitosis mediante la utilización de la técnica de fotoliberación de Ca^{2+} enjaulado. Con la ayuda del marcaje con anticuerpos específicos frente a los diferentes subtipos de CCDV y proteínas endocitóticas estudiaremos una posible co-localización en la maquinaria endocitótica.

Otro aspecto importante en la neurotransmisión es el acoplamiento de los procesos exo-endocitóticos. La endocitosis en células neuroendocrinas presenta una correlación positiva con la cantidad de cationes Ca^{2+} y la exocitosis. Se ha demostrado que los esfingolípidos de membrana, principalmente esfingosina, aumenta la liberación vesicular activando proteínas responsables por la fusión de las vesiculas. Ya que la endocitosis es directamente proporcional a la previa exocitosis, nos preguntamos que

papel podrían tener los esfingolípidos en la retirada de membrana y su relación con el Ca^{2+}.

Basándonos en estos antecedentes, en este estudio pretendemos caracterizar el papel de los canales de calcio en los procesos endocitóticos. Para ello nos hemos propuesto los siguientes objetivos concretos:

1. Estudiar los efectos de los bloqueantes de canales L (nifedipino), N (ω-conotoxina GVIA), PQ (ω-agatoxina IVA) y N-PQ (ω-conotoxina MVIIC) en la entrada de Ca^{2+} así como en los cambios en la capacidad de la membrana utilizando la técnica de patch clamp en la configuración de parche perforado y en fijación de voltaje (-80 mV);
2. Estudiar los efectos de los bloqueantes de canales L (nifedipino) y N (omega-conotoxina GVIA) y del activador de canales L (FPL64176) en las respuestas exocitóticas y endocitóticas utilizando la sonda FM1-43 y estímulos de alto potasio (59 mM);
3. Estudiar cómo el aumento del gradiente extracelular de Ca^{2+} afecta la respuesta endocitótica;
4. Estudiar cómo la respuesta endocitótica se afecta por la mayor entrada de Ca^{2+} por los canales L utilizando el activador FPL64176;
5. Estudiar cómo el aumento de la entrada de Ca^{2+} por la corriente de cola de los canales PQ por el activador roscovitina afecta la corriente de calcio, exocitosis y endocitosis en la célula cromafin;
6. Investigar como el aumento de la corriente L por el activador FPL64176 puede afectar la propiedad de inactivación dependiente de calcio) de los canales N y PQ;
7. Estudiar como la esfingomielinasa, la esfingosina y la esfingosina-1-fosfato afectan las respuestas exo-endocitóticas.

IV. MATERIALES Y MÉTODOS

1. Aislamiento y cultivo de células cromafines bovinas

Las células cromafines de la médula adrenal se aislaron a partir de glándulas de vacas, extraídas de animales en un matadero local y transportadas hasta el laboratorio en una solución de Locke sin Ca^{2+} ni Mg^{2+} compuesta por (en mM): 154 NaCl, 5.6 KCl, 3.6 $NaHCO_3$, 5.6 glucosa, 5 HEPES, pH 7.2; además de antibióticos (50 UI/ml de penicilina y 50 μg/ml de estreptomicina).

El protocolo utilizado para aislar las células cromafines de la médula adrenal ha sido el de digestión de la médula con colagenasa descrito por Livett en 1984 (Livett, 1984) con modificaciones introducidas por nuestro laboratorio (Moro *et al.*, 1990). Todos los procesos se realizan en condiciones de esterilidad en campana de flujo laminar.

Los cultivos de las células cromafines bovinas se realizaron a partir de 3-4 glándulas para la obtención de aproximadamente 80-100 millones de células/glándula. Una vez en la unidad de cultivos, se procede la limpieza de la glándula retirando el tejido graso periadrenal e inyectándole retrógradamente a través de la vena adrenolumbar (o medular central) solución Locke. Este lavado se repite varias veces y sirve para eliminar los eritrocitos del sistema vascular de la glándula y adecuar el tejido a nuestro líquido nutricio. A continuación se inyecta a través de la vena adrenolumbar una solución enzimática mixta (colagenasa al 0.25% + albúmina de suero bovina (BSA) al 0.5%) y se incuba la glándula a 37ºC para que la colagenasa actúe en condiciones óptimas. El tratamiento con colagenasa sirve para digerir el colágeno que está presente en la medula adrenal dejando libres las células cromafines. La albúmina protege las células de la acción excesiva de la colagenasa. Una vez inyectada la colagenasa, las glándulas permanecerán en Locke durante 15 minutos a 37ºC. Este proceso se repite hasta un total de 3 veces.

Finalizada la digestión enzimática, se secciona la glándula longitudinalmente y con la ayuda de una hoja de bisturí se extrae la médula digerida que se lava de colagenasa mediante la adicción de grandes volúmenes de Locke y filtración de la suspensión obtenida a través de una malla de nylon con un tamaño de poro de 217 μm, que permite eliminar fragmentos de médula no digeridos. La suspensión filtrada se centrifuga (120xg, 10 min, temperatura ambiente) para sedimentar las células. Se elimina el sobrenadante y el precipitado se resuspende en Locke, tras lo cual se obtiene

una nueva suspensión celular que se filtra a través de una malla de nylon con un tamaño de poro menor, de 82 μm, que permite la eliminación de grasa y fibras.

A continuación se separan y purifican las células mediante un gradiente de Percoll, para lo cual se añade una mezcla estéril de Percoll y Locke concentrado (10x) (pH=5) a la suspensión celular y se centrifuga (20.000xg, 20 min, 15^{o}C). Tras esta centrifugación se observan varias bandas en el gradiente, entre las que destacan una superior con una mezcla de células cromafínes adrenérgicas y noradrenérgicas y una inferior de cromafínes principalmente adrenérgicas. Se recogen las células comprendidas entre estas dos capas y se realiza un primer lavado del Percoll añadiendo grandes cantidades de Locke y centrifugando (120xg, 10 min, temperatura ambiente). Se elimina el sobrenadante y se resuspende el precipitado en medio DMEM (se realiza así un segundo lavado del Percoll) al que se le han añadido: 5% de suero bovino fetal, inhibidores de fibroblastos (10 μM de ácido cítidin de citosina y 10 μM de fluorodeoxiuridina) y antibióticos (50 UI/ml de penicilina y 50 μg/ml de estreptomicina).

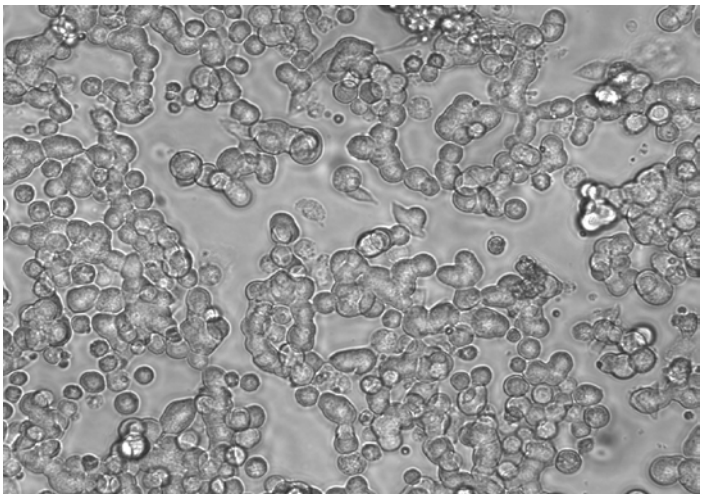

Figura 13: Microfotografía de células cromafínes en cultivo. Obsérvese la apariencia redondeada y la tendencia a agruparse en forma de pequeños racimos, imitando la situación que ocurre fisiológicamente en la médula suprarrenal.

Las células **(Figura 13)** se sembraron en cubreobjetos de vidrio de 1 cm de diámetro (previamente tratados con polilisina para facilitar la adhesión de las mismas) a una densidad de $5x10^4$ células/ml para los experimentos de *patch-clamp* o a una densidad de $1x10^5$células/ml para los experimentos de fluorescencia y co-localización.

Las células se mantuvieron a 37°C en un incubador con atmósfera saturada de agua y 5% de CO_2. El medio de cultivo se reemplazó por un DMEM libre de suero 24 h tras la siembra. Las células se emplearon 24-48 h tras la siembra.

2. Registro de corrientes iónicas mediante la técnica de *patch-clamp*

2.1. La técnica de *patch-clamp*

Las corrientes de calcio (I_{Ca}) generadas por la estimulación de una célula mediante la aplicación de estímulos despolarizantes se registraron mediante la técnica de *patch clamp* (Hamill *et al.*, 1981) en su modalidad de fijación de voltaje y configuración de célula entera o parche perforado (Korn & Horn, 1989; Gillis *et al.*, 1991).

La técnica de *patch-clamp* en su modalidad de fijación de voltaje consiste en mantener fija la diferencia de potencial de un parche de membrana de la célula con ayuda de un amplificador **(Figura 14)**. De este modo, si en respuesta a un determinado estímulo se produce alguna corriente de entrada o de salida de iones a través de los canales y/o receptores presentes en dicho parche, la medición de la corriente que es necesario inyectar para mantener fijo el Vm será equivalente al flujo de iones que se ha producido a través del parche de membrana de la célula.

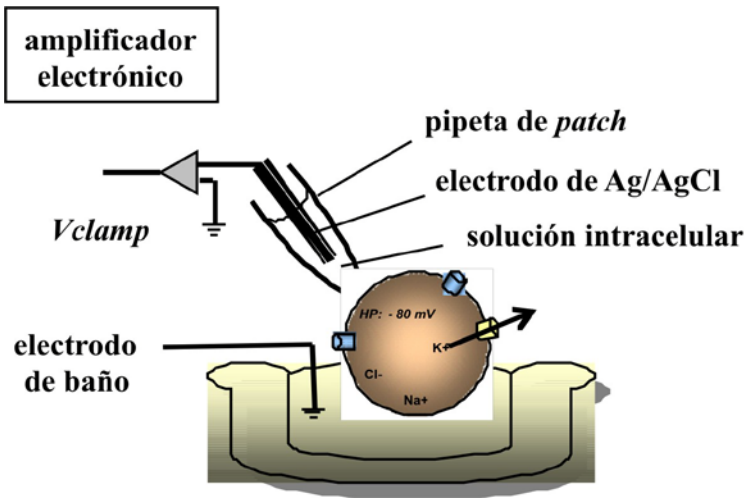

Figura 14: Patch-clamp. Representación esquemática de la técnica de *patch-clamp* en su modalidad de fijación de voltaje (*voltage clamp*).

Esta técnica emplea un único electrodo que simultanea a elevada frecuencia el registro de voltaje (para mantenerlo fijo en el parche de membrana) y el registro de corriente (la inyectada para mantener fijo el Vm). Sus ventajas con respecto a la clásica de fijación de voltaje de doble electrodo (Cole, 1949; Marmont, 1949; Hodgkin *et al.*, 1952) son que se puede aplicar a células pequeñas, en las que sería imposible introducir dos electrodos, y que presenta una buena relación señal-ruido, por lo que permite el registro de corrientes del orden de hasta pA.

El primer paso para ejecutar esta técnica es formar un sello de alta resistencia eléctrica entre la membrana celular y el electrodo de registro, para lo cual éste se introduce en el interior de una pipeta de vidrio cuya punta se pule al fuego hasta poseer un diámetro de aproximadamente 1µm. La pipeta se aproxima a la membrana de la célula y se presiona contra ella, con lo que se forma un sello eléctrico de alta resistencia (de unos 50 MΩ) que asegura que la mayor parte de corrientes originadas en el parche de membrana fluyan hacia el interior de la pipeta y de allí al circuito de medida de corriente.

Si la punta de la pipeta mantiene limpia su superficie, la aplicación de una ligera succión o presión negativa en su interior permite conseguir sellos de resistencia aún mayor, del orden de 10-100 GΩ, conocidos como *giga-sellos*, que reducen el ruido del registro y evitan el flujo de corriente entre la pipeta y el baño, lo que permite fijar el potencial de membrana. Se adquiere así la configuración de célula adherida o parche *in situ* (*cell attached*). Estos sellos son además mecánicamente muy estables, por lo que permiten diversas manipulaciones mecánicas que originarán las distintas configuraciones de la técnica (célula adherida, célula entera, parche perforado, parche escindido dentro-fuera y parche escindido fuera-fuera) **(Figura 15).**

Una variación de la configuración de célula entera es el llamado "parche-perforado". Esta configuración (Korn & Horn, 1989; Gillis *et al.*, 1991) es una variación de la configuración de célula entera que se obtiene por la inclusión de un antifúngico (en nuestro caso, amfotericina B) en la solución del interior de la pipeta de *patch*; los antifúngicos formarán poros en el parche de membrana que queda atrapado bajo la punta de la pipeta y permitirán así el acceso eléctrico al interior celular.

Para conseguir la configuración de parche perforado se parte de una célula adherida y se espera a que el antifúngico forme los poros en la membrana sin aplicar

succión alguna. Los antifúngicos forman canales en las membranas celulares que contienen colesterol o ergosterol que van a ser permeables a cationes monovalentes y a Cl^- (hasta nueve veces más permeables a cationes monovalentes que a Cl^-) e impermeables a iones multivalentes como el Ca^{2+} o el Mg^{2+} y a moléculas no electrolíticas de tamaño igual o superior al de la glucosa.

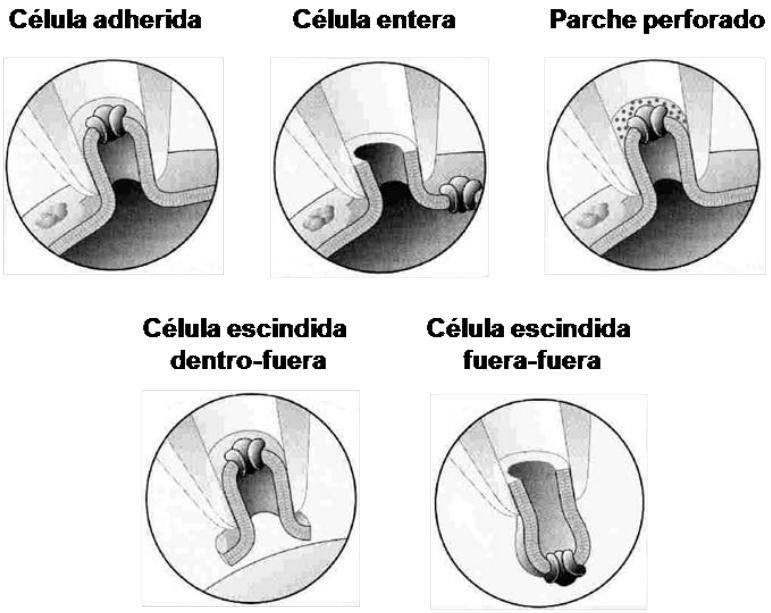

Figura 15: Configuraciones de la técnica de *patch-clamp*

Los experimentos presentados en esta Tesis se realizaron principalmente mediante la configuración de parche perforado, ya que es menos invasiva (se evita la succión para romper el parche de membrana) y, presenta un sello y resistencia de acceso al interior celular mucho más estables. Además, el parche perforado permite obtener registros de hasta 1 h de duración en una misma célula, resultando de especial utilidad para estudiar procesos celulares que sean dependientes de componentes intracelulares pues éstos no sufren un proceso de "lavado" o diálisis.

Sin embargo, la configuración de parche perforado presenta la desventaja de no permitir el control de la composición intracelular por parte del investigador. Por este motivo, en ocasiones se utilizó la configuración de célula entera, permitiendo la diálisis celular de herramientas farmacológicas.

Las pipetas de registro empleadas se fabricaron a partir de capilares de vidrio de borosilicato con ayuda de un estirador vertical de vidrio (PP-830, Narishige, Tokio, Japón) en dos pasos, puliéndose posteriormente la punta con ayuda de una microforja (MF-830, Narishige) hasta alcanzar un diámetro de aproximadamente 1 µm y una resistencia de 2-5 MΩ una vez rellenas con la correspondiente solución intracelular.

En todos los experimentos, las células se colocaron en una pequeña cámara de metacrilato situada en la plataforma de un microscopio invertido Nikon Diaphot. Una vez en la placa, las células se prefundieron con una solución de Krebs-Hepes control compuesta por (mM): 137 NaCl, 1 $MgCl_2$, 2 $CaCl_2$, 10 glucose, 10 HEPES, pH 7.4 ajustado con NaOH, con un flujo basal de 1-2 ml/min. En los experimentos para estudiar la dependencia al Ca^{2+}, han sido utilizadas diferentes concentraciones de calcio para la solución extracelular. En la configuración de célula entera, las células fueron dializadas con una solución intracelular presente en la pipeta compuesta de (mM) 10 NaCl, 100 CsCl, 20 TEA, 14 EGTA, 20 HEPES, 5 Mg.ATP, 03 Na.GTP, pH 7.2 ajustado con CsOH. En algunos experimentos, para medir capacidad de la membrana utilizando la configuración de célula entera, el EGTA ha sido omitido de la solución intracelular. Para los experimentos en configuración de parche perforado, las pipetas de registros se rellenaron con una solución interna compuesta de (mM) 135 CsGlutamato, 10 HEPES, 9 NaCl, pH 7.2 ajustado con CsOH; a la que se le añadió, con el fin de obtener la configuración de parche perforado, amfotericina B (0.5 mg/ml en DMSO). La anfotericina se añadía a partir de una solución madre de amfotericina B que se preparaba nueva en el día en dimetilsulfóxido (DMSO), a la concentración de 50 mg/ml, sonicándola hasta su completa solubilización protegida de la luz. La concentración final de amfotericina se obtenía añadiendo 10µl de esta solución madre a 1 ml de solución intracelular y sonicándola también protegida de la luz y del calentamiento hasta su completa homogenización; esta solución se mantenía en frío, se agitaba con frecuencia con vortex para evitar la adhesión del antifúngico a las paredes del recipiente contenedor (una jeringa) y se empleaba en el plazo de unas 3 h para asegurar que no se hubiese perdido la actividad del antifúngico.

Las pipetas de registro se sumergían brevemente (unos segundos) por la punta en solución intracelular sin amfotericina y a continuación se rellenaban por detrás con solución intracelular con amfotericina. De este modo se podía conseguir la configuración de célula adherida antes de que el antifúngico hubiese difundido hacia la

punta de la pipeta para empezar a formar los poros en la membrana (esto dificultaría la obtención del sello). El proceso de perforación (hasta alcanzar una resistencia en serie <20 MΩ) tardaba unos 5-15 min. Las células fueron perforadas hasta alcanzar una resistencia en serie de no más que 30 MΩ.

Para la estimulación celular y la adquisición de datos se empleó el programa PULSE (HEKA Elektronic) y un ordenador PC. Los registros se adquirieron con una frecuencia de muestreo de 5-10 kHz y se filtraron a 1-2 kHz. Los registros con una corriente de fuga superior a 30 pA se descartaron. También se descartaron aquellas células en las que la resistencia de acceso del transitorio capacitativo alcanzaba valores > 20 MΩ.

Las soluciones extracelulares que superfunden a las células se intercambiaron mediante un sistema de válvulas excluyentes controladas electrónicamente, acopladas a una pipeta de perfusión cuya punta se posicionaba a menos de 100 µm de la célula en experimentación. La velocidad de este sistema de perfusión es consecuencia de la presión por gravedad ejercida sobre el líquido, siendo de aproximadamente 1 ml/min, permitiendo el completo recambio de las soluciones experimentales en unos 50 ms.

El análisis de las corrientes se llevó a cabo mediante los programas IgorPro (Wavemetrics Inc., Oregon, USA) y PULSE.

2.2. Medida de la exocitosis y endocitosis mediante el estudio de la variación de la capacidad eléctrica de la membrana celular (ΔCm)

La medida de la capacidad eléctrica de la membrana celular nos proporciona de forma indirecta la medida de la secreción (exocitosis) y retirada de membrana (endocitosis) debido a la propiedad de la membrana de actuar como un condensador. De esta forma podemos registrar cambios en el tamaño de la superficie celular al producirse la exocitosis, ya que la membrana de las vesículas pasa a formar parte de la membrana plasmática, lo que conlleva un incremento en la superficie de la misma. Tras el proceso exocitótico, se puede observar una caída del registro de la capacidad de la membrana, indicándonos la existencia de un proceso endocitótico.

Para estimar estos cambios, utilizamos la técnica desarrollada por Lindau y Neher (Lindau & Neher, 1988), basada en la aplicación de una onda sinusoidal de voltaje a la membrana celular (1 kHz, 60 mV de amplitud), para lo que utilizamos

también el amplificador de *patch-clamp*, lo que además nos va a permitir simultanear el registro de los cambios de capacidad con los registros de corrientes iónicas **(Figura 16)**.

En los experimentos para estudiar los procesos exo/endocitóticos presentados en esta Tesis hemos utilizado protocolos experimentales en el que se registraba la capacidad de la membrana antes y después de la aplicación del pulso despolarizante. La exocitosis ha sido medida como la diferencia entre la capacidad de la membrana tras el estímulo despolarizante y la media basal. La endocitosis ha sido calculada como la diferencia entre el valor de la capacidad de la membrana tras estímulo y el valor al final del registro.

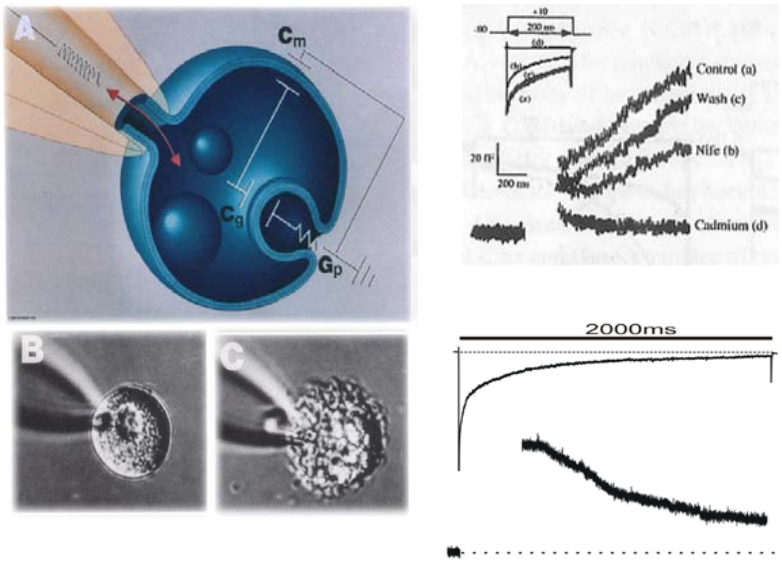

Figura 16: Técnica de registro de la capacidad de la membrana celular como una medida de la exocitosis. El panel A muestra la representación esquemática del comportamiento de la membrana celular como un condensador eléctrico. Los paneles B y C muestran el aspecto de un mastocito de rata antes (B) y después (C) de producirse la exocitosis masiva de histamina. Los paneles de la derecha muestran registros originales del incremento de la capacidad de la membrana en respuestas. Adaptado de Monck y Fernández (1992).

3. Estudio de las respuestas exocitóticas y endocitóticas mediante técnicas de fluorescencia con la sonda FM1-43

El uso de sondas fluorimétricas como marcadores exo-endocitóticos permite estudiar el reciclaje de vesículas sinápticas, corroborando los resultados obtenidos con las técnicas electrofisiológicas utilizadas en esta Tesis.

Las sondas de la familia FM presentan una serie de ventajas: (1) presentan en su estructura una extensión lipofílica que le confiere una alta afinidad por las membranas plasmáticas, marcando así éstas dede forma reversible; (2) poseen un grupo positivo que impide que sean eliminados de las vesículas endocitadas, siendo por el contrario rápidamente lavadas de la membrana plasmática; y (3) son 350 veces más fluorescentes en medio hidrofóbico (membrana celular) que en medio acuoso (Betz *et al.*, 1996; Henkel *et al.*, 1996; Smith & Betz, 1996; Cousin & Robinson, 1999). La aplicación de estas sondas en combinación con protocolos de estimulación nos permite estudiar el proceso endocitótico por marcaje de las vesículas tras estímulos despolarizantes. Entre estas sondas destaca particularmente el FM1-43 como una de las más empleadas para el estudio del reciclado vesicular.

Para llevar a cabo estos experimentos, se sigue el protocolo mostrado en la **Figura 17**. Se lavan las células 2 veces durante 5 minutos con solución extracelular Krebs-Hepes conteniendo 2 mM Ca^{2+}. Tras el proceso de lavado, se trasladan los cubres que contienen las células a un microscopio invertido Zeiss Axiovert, modelo 100S o Nikon Diaphot. En el microscopio, se realiza la medida basal de la fluorescencia celular que debe ser "zero" (**Figura 17I, basal**). Se incuban las células con FM1-43 (3 μM) durante 10 minutos. Las longitudes de onda utilizadas para la emisión/excitación de la sonda FM1-43 ha sido de 480/535 nM y las imágenes se capturaron a cada segundo. Tras los 10 minutos de incubación, la célula alcanza una fluorescencia máxima al cual normalizamos al 100% (**Figura 17II, FM1-43**). Se estimulan las células durante 3 min con una solución de alto potasio (59 mM K^+) en presencia de FM1-43. La despolarización producida por el potasio, fusiona las vesículas secretoras a la membrana plasmática, haciendo con que más sonda se una a la célula aumentado la intensidad de fluorescencia (**Figura 17III, K^+**). La diferencia entre el valor máximo de fluorescencia alcanzado tras la estimulación y el 100% se considerará el valor de la exocitosis. Al

finalizar la estimulación se procede el lavado de la sonda FM1-43 con solución control durante 20 min (**Figura 17IV, lavado**) que nos dará el valor de la endocitosis. Separadamente, en una región sin células se mide la fluorescencia de fondo, a la cual se resta al final del experimento de la fluorescencia total durante la totalidad del protocolo.

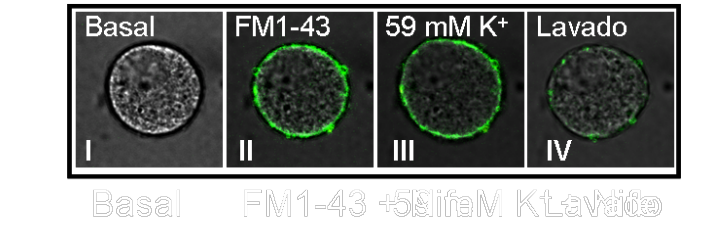

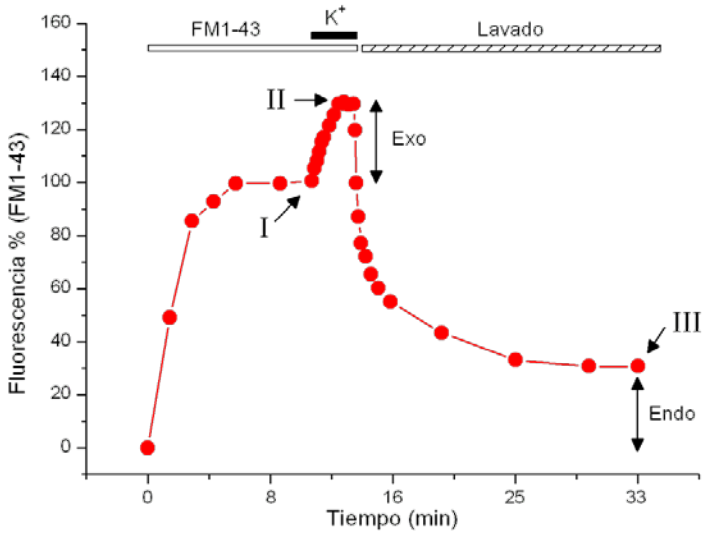

Figura 17: Imágenes secuenciales en una misma células del marcaje de membrana con la sonda FM1-43. (I) imagen de una célula cromafín en presencia de 4 μM de FM1-43. (II) después de 10 minutos de incubación con la sonda. (III) tras la aplicación de un estímulo de 59 mM K^+ durante 3-min. (IV) tras 10 minutos de lavado.

4. Medidas de las respuestas exo-endocitóticas con FM1-43 tras la fotoliberación de calcio "enjaulado"

La técnica de fotoliberación de Ca^{2+} enjaulado consiste en provocar una liberación masiva y homogénea de Ca^{2+} en el interior de la célula mediante la aplicación de un destello de luz rompiendo compuestos específicos. Los compuestos empleados en

esta técnica son moléculas muy similares a compuestos que tamponan Ca^{2+}, como el EGTA, pero que ante un estímulo de luz se rompen y pierden su afinidad por los iones de Ca^{2+}, dejándolos libres. Esta técnica permite controlar la cantidad de Ca^{2+} liberable en función de la intensidad y duración del destello de luz. Así pues, en una misma célula se puede incrementar la concentración de Ca^{2+} a niveles conocidos y así poder estudiar el fenómeno secretor con la combinación con otras técnicas, como por ejemplo, marcaje de la membrana con la sonda FM1-43 o medidas de la capacidad de la membrana.

El NP-EGTA.AM es uno de los compuestos utilizados para esta técnica. Esta molécula tiene la ventaja de ser permeable, sin necesidad de dializar la célula debido a su grupo acetoximetil (AM). Una vez en el interior de la célula, NP-EGTA.AM es convertido en NP-EGTA por acción de esterasas intracelulares, obteniendo una alta sensibilidad al Ca^{2+}.

Para la realización de los experimentos de fotoliberación de Ca^{2+} enjaulado, se incuban las células durante 45 min a temperatura ambiente, con 25 μM de NP-EGTA.AM disuelto en DMSO con ayuda del detergente aniónico ácido plurónico para facilitar la captación del compuesto fotoliberable. Finalizada la carga, se realizan tres lavados con KH para eliminar los restos del compuesto no captado por las células. El cubre es trasladado al microscopio y con la ayuda de un monocromador y una lámpara de xenón, se estimulan las células con un destello de luz UV de 5 ms, lo que provoca la ruptura de la molécula de NP-EGTA y la liberación del Ca^{2+} (Giner *et al.*, 2007). La liberación del Ca^{2+} enjaulado activará proteínas responsables de la respuesta secretora (exocitosis), con consiguiente retirada de membrana (endocitosis). Para la medida de las respuestas exo-endocitóticas producidas por la fotoliberación, se añade la sonda FM1-43 en la solución del baño. El protocolo que se sigue es similar al comentado en el apartado anterior, sin embargo, en vez de una estimulación despolarizante con alto potasio, se activa la fotoliberación de Ca^{2+} intracelular como estímulo secretagogo (Smith & Betz, 1996).

5. Medida de la concentración de Ca^{2+} citosólico en célula única

Las variaciones en la concentración de Ca^{2+} intracelular los experimentos de fotoliberación y FM1-43 se determinaron mediante el uso de sondas fluorescentes

sensibles al Ca^{2+}. Las sondas fluorescentes sensibles al Ca^{2+} son fluoróforos que pueden unirse de forma selectiva y reversible al Ca^{2+}, como resultado de lo cual varían sus propiedades ópticas: cambia su espectro de excitación o de emisión o bien la intensidad de la fluorescencia que emiten. El fluoróforo utilizado en los experimentos de calcio citosólico ha sido la sonda ratiométrica Fura-2 que posee los espectros de excitación a 340/380 nm.

Para la realización de los experimentos, se incubaron las células con 4 μM Fura-2 juntamente con NP-EGTA.AM o previamente a la incubación con la sonda FM1-43. La sonda se disuelve en DMSO a una concentración de 1 mM. Para la carga, se incubaron las células durante 45 min a 37ºC con Fura-2 y plurónico (para facilitar la carga) a la concentración final indicada en solución Krebs-Hepes control. Tras la incubación con la sonda, se lavaron las células durante 15 min con solución control a temperatura ambiente.

6. Soluciones experimentales empleadas

Para el desarrollo del presente trabajo de investigación se han utilizado los siguientes compuestos: colagenasa tipo I, nifedipino, Bay K8644, amfotericina B, D-esfingosina, *S. aureus* esfingomielinasa, N-oleoiletanolamina, dinasor, calmidazolium, esfingosina-1-fosfato, carbonilcianide-4-(trifluorometoxi)feenilhidrazona (FCCP), amitriptilina, genisteína, péptido $A\beta_{25-35}$ (Sigma, Madrid, España); FPL64176 (RBI, Natick, USA); roscovitina; olomoucine; medio de Eagle modificado por Dulbecco (DMEM), albumina bovina V, suero fetal bovino y antibióticos (Gibco, Madrid, España); agatoxina-IVA (Peptide Institute, Sandhausen, Alemania); ω-conotoxina GVIA y ω-conotoxina MVIIC (Bachem Feinchemikalien, Budendorf, Suiza); EGTA.AM (Calbiochem, Barcelona, España); FM1-43, o-nitrophenyl EGTA-AM (NP-EGTA.AM) y Fura2-AM (Molecular Probes Inc. Eugene, OR, USA).

En los experimentos orientados a caracterizar la participación de los diferentes subtipos de CCDV en la endocitosis, se añadió a la solución los bloqueantes específicos: nifedipino 3 μM para los canales del tipo L (nife); ω-conotoxina GVIA 1 μM para los canales del tipo N (GVIA); ω-agatoxina IVA 1 μM para los canales PQ (Aga); y ω-conotoxina MVIIC 2 μM para el bloqueo de los subtipos N y PQ (MVIIC). Para estudiar el efecto de la mayor entrada de calcio por los canales del tipo L, las

células fueron perfundidas con solución Krebs-Hepes control en presencia del agonista de canales L FPL64176 (1 μM; FPL). Nifedipino y FPL64176 fueron disueltos en DMSO. Las demás toxinas bloqueantes de canales N y/o PQ en agua destilada. Para el estudio de la participación del calcio extracelular en la maquinaria endocitótica, solución Krebs-Hepes en presencia de diferentes concentraciones de calcio extracelular fueron utilizadas. En los experimentos de fluorescencia, la solución madre (1 mM en agua) de la sonda FM1-43 fue diluida a una concentración de 3 μM en solución Krebs-Hepes control o en presencia de 59 mM K^+, protegida de la luz.

En los experimentos para estudiar la modulación de los canales N y PQ por la entrada de calcio por los canales del subtipo L, se perfundieron las células con solución Krebs-Hepes control en presencia de los agonistas de los canales L FPL (1 μM) o BayK (1 μM). Para eso, se preparó una solución madre de 1 mM en etanol (FPL) o en DMSO (BayK). En los experimentos para estudiar la participación del calcio por enlentecer la deactivación de los canales PQ, roscovitina y olomoucina se preparó en DMSO.

Para el estudio del efecto de los esfingolípidos de membrana en las respuestas exo-endocitóticas se prepararon las soluciones de esfingosina, esfingomielinasa, NOE, dinasor y calmidazolium en DMSO. La esfingosina-1-fosfato se disolvió en metanol.

Los experimentos orientados al estudio de los efectos del péptido Aβ en la endocitosis, se disolvió el péptido en DMSO a una concentración de 10^{-2} M y, luego en solución Krebs-Hepes control se agregó el péptido durante 2 horas en agitación a 37oC.

Todas las soluciones se conservaron a -20^{o}C.

7. Análisis estadístico

Para el análisis del pico de corriente (I_{Ca}) y la integral del área de la corriente (Q_{Ca}) producida por la entrada de Ca^{2+} en la célula durante el estímulo despolarizante, se excluyeron los 5-ms iniciales, con el fin de eliminar la corriente de Na^+ (debido al no uso de bloqueante de canales de sodio).

En este estudio, las respuestas exo- y endocitóticas fueron determinadas registrando los cambios en la capacidad de la membrana (Cm). La diferencia entre el valor de la capacidad basal de la célula en los 400-ms previos a la estimulación y aquellos obtenidos 50-ms después del término del estímulo fue considerada la medida

de la exocitosis. Tras el pico de exocitosis, se midieron los cambios en la Cm durante varios segundos. La endocitosis se calculó como la diferencia del valor de la Cm tras la aplicación del estímulo despolarizante y el valor de Cm al final del registro.

Para los estudios con la sonda FM1-43 La fluorescencia máxima alcanzada tras la perfusión de FM1-43 es considerada como 100% de la respuesta. La diferencia entre el valor de fluorescencia tras el estímulo y la fluorescencia 100% fue considerada la medida de la exocitosis. Tras el lavado, la fluorescencia remanente fue tomada como medida de la endocitosis (endocitosis = fluorescencia tras lavado – fluorescencia basal).

Los datos están expresados como la media ± e.e.m. del número de datos obtenidos, habiéndose utilizado siempre células de al menos 3 cultivos diferentes. Para la comparación de las medias de diferentes grupos de datos se realizó un análisis de la varianza (ANOVA) de una o dos vías, seguido de un test Newman-Keuls. Se consideró un valor de P menor de 0.05 como límite para considerar una diferencia significativa.

V. RESULTADOS

1- Participación de los canales de calcio en la endocitosis

Available online at www.sciencedirect.com
ScienceDirect
Biochemical and Biophysical Research Communications 357 (2007) 834–839
BBRC
www.elsevier.com/locate/ybbrc

L-type calcium channels are preferentially coupled to endocytosis in bovine chromaffin cells

Juliana Martins Rosa [a], Antonio M.G. de Diego [a], Luis Gandía [a], Antonio G. García [a,b,*]

[a] Instituto Teófilo Hernando, Departamento de Farmacología y Terapéutica, Facultad de Medicina, Universidad Autónoma de Madrid, C/ Arzobispo Morcillo 4, 28029 Madrid, Spain
[b] Servicio de Farmacología Clínica, Hospital de la Princesa, Universidad Autónoma de Madrid, c/ Diego de León 62, 28006 Madrid, Spain

Received 7 March 2007
Available online 16 April 2007

Abstract

Exocytosis and endocytosis are Ca^{2+}-dependent processes. The contribution of high-voltage activated Ca^{2+} channels subtypes to exocytosis has been thoroughly studied in chromaffin cells. However, similar reports concerning endocytosis are unavailable. Thus, we studied here the effects of blockers of L (nifedipine), N (x-conotoxin GVIA) and P/Q (x-agatoxin IVA) Ca^{2+} channel on Ca^{2+} currents (I_{Ca}), Ca^{2+} entry (Q_{Ca}), as well as on the changes in membrane capacitance (C_m) in perforated-patch voltage-clamped bovine adrenal chromaffin cells. Using 500-ms pulses to 0 or +10 mV, given from a holding potential of −80 mV and 2 mM Ca^{2+} we found that x-conotoxin GVIA affected little the exo-endocytotic responses while x-agatoxin IVA markedly blocked those responses. However, nifedipine blocked little exocytosis but almost completely inhibited endocytosis. We conclude that L-type Ca^{2+} channels seem to be selectively coupled to endocytosis.

Keywords: Calcium channels; L-type calcium channel; Exocytosis; Endocytosis; Chromaffin cell

The expression of multiple types of voltage-activated Ca^{2+} channels in neurones [1] and in adrenal medullary chromaffin cells [2] poses the interesting question of their specialization in controlling different functions. This seems clear in neurons where the geographical segregation of different Ca^{2+} channel subtypes to dendrites, axon terminals, or somata facilitates their specialization for specific functions. For instance N (Cav.2.2)- and P/Q (Cav2.1)-types of Ca^{2+} channels, which are predominantly found along the length of apical dendrites and in axon terminals that synapse on dendrites [3], control the release of various neurotransmitters [4]. On the other hand, L (Cav1.3)-type channels located on proximal dendrites and neuronal cell bodies [3,5,6] have been associated with the regulation of gene expression and enzyme activities in cortical and hippocampal neurons [7–9].

As neurons, adrenal medullary chromaffin cells express L-, N-, P/Q- and R (Cav2.3)-types of Ca^{2+} channels. But unlike neurons, these cells lack dendrites and axons. Thus, studies on the specialization of Ca^{2+} channel subtypes in cultured spherical chromaffin cells have provided unclear results [2]. Depending on the stimulus, stimulation pattern, animal specie, and the methods used to measure exocytosis or catecholamine release, certain specialization to modulate exocytosis has been suggested. For instance, L-type channels were preferentially associated to release responses in some studies [10,11]. Others attributed more protagonism to N channels [12] or to P/Q channels [13]. And some others concluded that exocytosis was proportional to Ca^{2+} entry and the density of Ca^{2+} current carried by each Ca^{2+} channel subtype, with no specialization at all [14].

As far as we know, studies aimed at defining whether a given Ca^{2+} channel subtype is preferentially coupled to endocytosis in chromaffin cells, are lacking. To maintain the size of nerve terminals and neurosecretory cells it is

* Corresponding author. Fax: +34 91 497 31 20.
E-mail address: agg@uam.es (A.G. García).

0006-291X/$ - see front matter
doi:10.1016/j.bbrc.2007.03.207

essential to keep equilibrium between the amount of vesicular membrane incorporated into the plasmalemma during exocytosis and the membrane retrieved during the subsequent endocytotic phase. This will also warrant that a given number of vesicles are available to participate in subsequent rounds of exocytosis during repetitive cell activation [15,16]. The cell retrieves membrane after exocytosis following at least two rate constants, rapid and slow [17–19]. On the other hand, Smith and Neher [15] and Engisch and Nowycky [20] also found two modes of endocytosis named compensatory (membrane retrieval equals the membrane added during a preceding exocytotic stimulus) and excess endocytosis (membrane retrieval was greater than that added during the preceding exocytosis). The transition between compensatory and excess endocytosis is commonly attributed to differences in Ca^{2+} affinity; thus, Chan and Smith [21], and Engisch and Nowycky [20] suggested that compensatory and excessive membrane retrieval after stimulation of bovine chromaffin cells represent two independent Ca^{2+}-regulated mechanisms of rapid internalization. The existence of these two different Ca^{2+} sensors is illustrated by data of Nucifora and Fox [22] in which Ca^{2+} and Ba^{2+} supported excessive membrane retrieval in bovine chromaffin cells; in contrast, in a previous study, rapid endocytosis was supported by Ca^{2+} but not by Sr^{2+} or Ba^{2+} ions, also in bovine chromaffin cells [19].

In bovine chromaffin cells, the L-type Ca^{2+} channels are more reluctant that N and P/Q channels to voltage- [23] and Ca^{2+}-dependent inactivation [24]. Obviously, this different inactivation pattern might give rise not only to different $[Ca^{2+}]_c$ signals and exocytotic responses [2], but also to a different pattern of endocytosis regulation. Therefore, in this study we explored whether the Ca^{2+} entering the cell through L-, N-, or P/Q-type of Ca^{2+} channels, following a depolarizing stimulus applied to voltage-clamped bovine chromaffin cells, equally modified the exocytotic and endocytotic responses. We discovered that Ca^{2+} entry through L-type Ca^{2+} channels was more efficacious to trigger endocytosis than exocytosis. To our knowledge, this is the first study that shows this kind of specialization of L-type channels in neuroendocrine cells.

Materials and methods

Isolation and culture of bovine chromaffin cells. Bovine adrenal glands were obtained from a local slaughterhouse. Chromaffin cells were isolated by digestion of the adrenal medulla with collagenase and maintained in culture for 2–5 days [25,26].

Recording of Ca^{2+} currents and membrane capacitance of chromaffin cells. All recordings in this study were obtained with the perforated-patch whole-cell configuration [27] of the patch-clamp technique [28]. During recording, cells were constantly perifused with a control Tyrode solution containing (mM): 137 NaCl, 1 $MgCl_2$, 2 $CaCl_2$, 10 glucose, 10 Hepes, pH 7.4 adjusted with NaOH. Perforated-patch (internal) solution had the following composition (mM): 135 CsGlutamate, 10 Hepes, 9 NaCl, pH 7.2 adjusted with CsOH. All experiments were performed at room temperature (25–28 C). Electrophysiological data were acquired with an EPC-9 amplifier under the control of Pulse software (HEKA Elektronik). Cell membrane capacitance (C_m) changes were estimated by the Lindau–Neher technique [29]. A 400-ms sinusoidal wave (1 KHz, 70 mV peak to peak amplitude) was then added before the depolarizing protocol and an 8 s sinusoidal wave of the same characteristics after it, to allow for the computation of membrane capacitance change. Membrane current was sampled at 20 KHz, and only cells with responses greater than 250 pA of peak I_{Ca} and 80 fF DC_m were selected. Cells were held at 80 mV, and single depolarizing pulses to voltages where I_{Ca} peak was reached (usually 0 or +10 mV) were applied at 5 min intervals. Cells were perforated to a series resistance of no more than 30 MX.

Data analysis. The whole-cell inward Ca^{2+} current peak (I_{Ca}), and the current area representing the total Ca^{2+} that entered the cell during a depolarizing stimulus (Q_{Ca}), were analyzed after the initial 20 ms of each depolarizing pulse, to get rid of the Na^+ current. In this study, exo- and endocytosis were measured by monitoring changes in cell capacitance (C_m). Exocytosis peak (DC_m) was measured by subtracting the basal mean C_m obtained 400 ms previous to depolarization, to that obtained 50 ms after the end of the depolarizing pulse, to avoid a possible Na^+ channel gating artefact [30]. After the exocytotic peak, C_m changes were measured during the ensuing 8-s period; endocytosis was calculated as the difference in C_m at the beginning and the end of such 8-s period. Comparisons between means of group data were performed by one-way analysis of variance (ANOVA) followed by Duncan post hoc test when appropriate. A p value equal or smaller than 0.05 was taken as the limit of significance.

Results and discussion

In preliminary experiments, voltage-clamped cells were challenged with square depolarizing pulses of different duration (20–2000 ms). The holding potential was held at 80 mV and the test potential was 0–10 mV (usually, the peak I_{Ca} was achieved at these voltages). Increased C_m jumps were obtained with pulses of 50 to 2000 ms; however, a clear endocytotic response was visible only with longer depolarizing pulses, from 200 ms onwards. Hence, we decided to use single 500 ms depolarizing pulses to study exo-endocytotic responses along this study.

When a voltage-clamped cell was challenged with a 500 ms depolarizing pulse an inward fast Na^+ current (I_{Na}) peaked in about a millisecond at near 1 nA (arrow at the bottom of the current trace in Fig. 1A). The peak I_{Na} relaxed to a slower inward Ca^{2+} current (I_{Ca}) (second arrow in Fig. 1A) that gradually inactivated to reach 50% of its initial value at the end of the 500ms test pulse (Fig. 1A). Cells kept this type of currents very reproducibly along a 30-min period, when challenged at 5-min intervals. Note for instance that the 5th pulse produced I_{Na} and I_{Ca} current traces that matched those currents elicited by the 1st pulse.

Fig. 1B shows the membrane capacitance changes elicited by the 500-ms pulse, and measured during a period beginning 10 ms after the pulse till the 8th second post-pulse. The initial sharp jump of 147.1 fF corresponds to the exocytotic response (DC_m). The peak DC_m (exocytosis; left double arrow in Fig. 1B) was immediately followed by a pronounced endocytotic response; the post-pulse 8-s recording period corresponds to membrane retrieval or the endocytotic response (arrow at the right of Fig. 1B).

In 52 cells I_{Ca} amounted to 442.7 ± 25 pA and Q_{Ca} was 106 ± 4.3 pC. DC_m was 147.1 ± 9.3 fF and the sum of

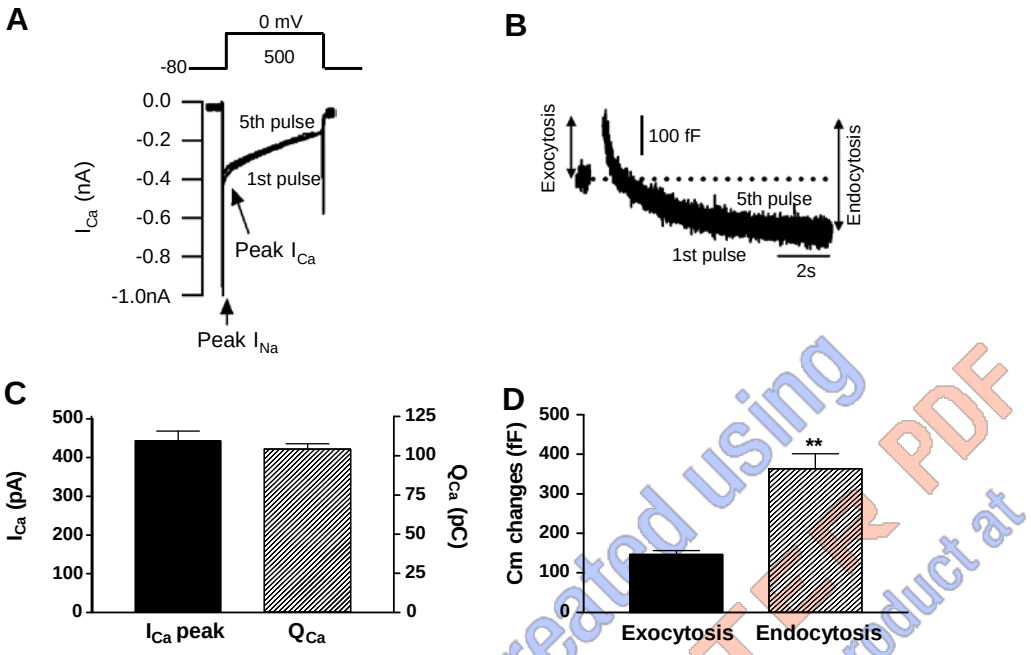

Fig. 1. Changes in membrane capacitance (C_m) elicited by inward whole-cell Ca^{2+} channel currents (I_{Ca}). The example I_{Ca} traces of (A) were obtained from a cell voltage-clamped at 80 mV, in 2 mM external Ca^{2+}. The cell was challenged with 500-ms depolarizing test pulses to 0 mV, given at 5-min intervals. (B) The C_m changes after the first and fifth depolarizing pulses, in the same cell. Exocytosis was measured as DC_m above basal C_m (left double-head arrow). Dotted line represents the basal C_m. (C) Averaged of I_{Ca} expressed in pA in the left ordinate. Total Ca^{2+} entry was determined by calculating the area under the I_{Ca} trace (pC, right ordinate). (D) C_m changes corresponding to those 52 cells. Data are means ± s.e.m. $^{**}p < 0.01$, compared to the exocytotic response.

compensatory plus excess endocytosis amounted to 368 ± 38 fF (Fig. 1D).

We next studied the current and exo-endocytotic responses in the presence of various selective Ca^{2+} channel blockers. Perifusion of voltage-clamped chromaffin cells with different blockers given for 30–120 s, dissect subcomponents of the whole-cell inward Ca^{2+} channel current, at the following maximal concentrations: 3 lM nifedipine for L-type channels, 1 lM x-conotoxin GVIA for N-type channels, and 1 lM x-agatoxin IVA for P/Q-type channels [2]. These were the blocker concentrations used throughout this study. As described above, the perforated-patch configuration allowed the recording of reproducible current and capacitance responses during five subsequent depolarizing pulses. Thus, we designed a sandwich-type experiment consisting in two initial control pulses, followed by two pulses in the presence of the blocker, which was perifused since 2 min before each stimulus; finally one or two more pulses were given after blocker washout.

In the original records of Fig. 2A, taken from a prototype cell, nifedipine reduced peak I_{Ca} by about 35%, without apparent change of inactivation. This is consistent with the well established observation that N and P/Q channels, that carry the current in the presence of nifedipine, suffer Ca^{2+}- [24] and voltage-dependent inactivation; inactivation is delayed in the case of L-type channels [23]. The C_m changes evoked by I_{Ca} in the cell of (A) are shown in (B). Note the drastic endocytotic response in control conditions and its complete inhibition in the presence of nifedipine. Quantitative data averaged from eight cells show that nifedipine significantly blocked I_{Ca} by 31% and Q_{Ca} by 53% (C); exocytosis was blocked by 27% ($p > 0.05$) while endocytosis (both compensatory and excessive) was practically abolished (D). These effects of nifedipine were completely reversed 2 min after its washout (data not shown).

We explored next how the suppression of the N-type component of I_{Ca} affected the C_m changes elicited by depolarizing pulses. Fig. 3A is a representative example of I_{Ca} traces obtained before (control) and 2 min after cell perifusion with x-conotoxin GVIA. Note that the toxin reduced peak I_{Ca} by about 35% and that inactivation was slowed down, in agreement with the observation previously commented that chromaffin cell L-type Ca^{2+} channels suffer little inactivation. In the C_m traces obtained from the same cell (B), endocytosis was reduced by about 20% during x-conotoxin GVIA treatment. Averaged pooled data from nine cells showed that x-conotoxin GVIA significantly reduced I_{Ca} by 30% and Q_{Ca} by 24% (C). It is interesting that in spite of the fact that peak I_{Ca} was reduced similarly by nifedipine and x-conotoxin GVIA, Q_{Ca} was inhibited much more by the former (53%) than the latter (24%). This is explained by the lesser inactivation of L-type channel current along the 500-ms depolarizing pulse (compare current traces of Fig. 2A and 3A).

We finally explored the effect of x-agatoxin IVA on I_{Ca}, Q_{Ca} and C_m changes (Fig. 4). (A) Shows I_{Ca} traces obtained from a representative cell. Note the drastic reduc-

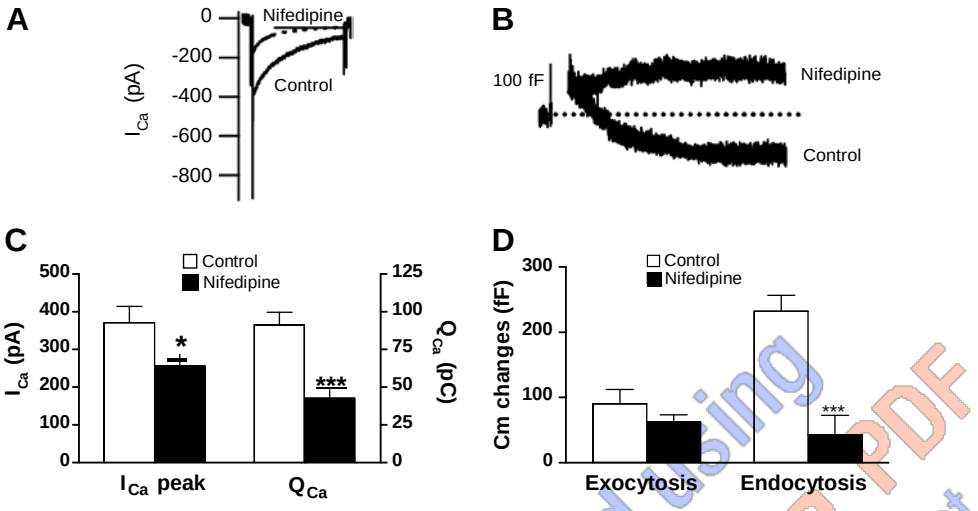

Fig. 2. Effects of nifedipine (3 **1**M) on I_{Ca} and C_m responses, following the protocol described in Fig. 1. (A) A control I_{Ca} trace, and a trace obtained after cell perifusion with nifedipine during 2-min before giving the pulse, and during the pulse. (B) The corresponding C_m traces obtained in the same cell. (C) Averaged pooled results of I_{Ca} (left ordinate in pA) and Q_{Ca} (right ordinate in pC), in the absence (white columns) and the presence of nifedipine (black columns); (D) The C_m changes (ordinate, in fF) corresponding to the same cells of (C). Data are means ± s.e.m. of eight cells from at least four different cultures. $^{*}p < 0.05$; $^{**}p < 0.001$ compared to control.

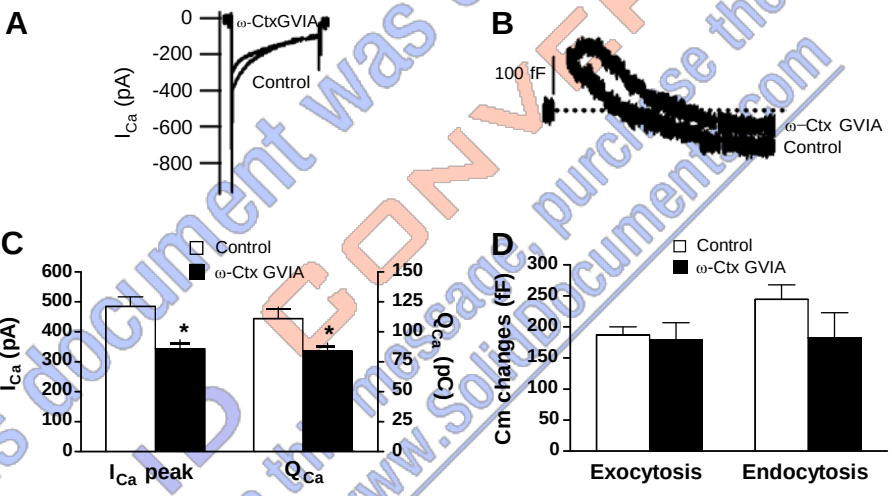

Fig. 3. Effects of x-conotoxin GVIA (x-Ctx GVIA, 1 **1**M) on I_{Ca} and the ensuing C_m changes. The protocol used here was as explained in Fig. 1. (A) Example I_{Ca} traces before (control) and after 2-min of cell perifusion with x-conotoxin GVIA (x-ctx GVIA). (B) The C_m traces elicited by depolarizing pulses that generated the corresponding I_{Ca} traces in the same cell of (A). (C) Pooled averaged results of peak I_{Ca} (left ordinate) and Q_{Ca} (right ordinate). (D) The exocytotic and endocytotic responses obtained in these cells. Data are means ± s.e.m. of nine cells from at least three different cultures. $^{*}p < 0.05$ compared to controls.

tion of peak I_{Ca} elicited by x-agatoxin IVA and the slow inactivation of the remaining current, likely due to the L-type component of such current. (B) Shows the exocytotic C_m jump and the ensuing pronounced endocytotic response, elicited by the control I_{Ca} of (A); x-agatoxin IVA drastically reduced the exocytotic as well as the endocytotic responses. This is better seen in the histogram of (C) and (D), showing that x-agatoxin reduced I_{Ca} by 68%, Q_{Ca} by 69%, exocytosis by 82%, and endocytosis by 68%.

Table 1 shows normalized data on the effects of the three Ca^{2+} channel blockers on Ca^{2+} entry, exocytosis and endocytosis. Thus, under the present experimental conditions (long 500-ms depolarizing pulses and 2 mM Ca^{2+}) N channel blockade affected little Q_{Ca} and the exo-endocytotic responses. In contrast, P/Q channel blockade markedly reduced, Q_{Ca} (69%), exocytosis (82%) and endocytosis (68%). This was not the case for nifedipine, that reduced by half Q_{Ca}, affected little exocytosis (27% blockade) but practically abolished endocytosis (92% blockade).

As referenced in the Introduction, the contribution of each channel type to Ca^{2+} entry and exocytosis greatly varies with the concentration (5–60 mM) and type of divalent cation used (Ca^{2+} or Ba^{2+}) and the stimulation pattern of chromaffin cells (K^{+} depolarization, short or longer depolarizing single pulses, trains of depolarizing pulses, trains of action potentials) (see [2] for a review). We selected here the

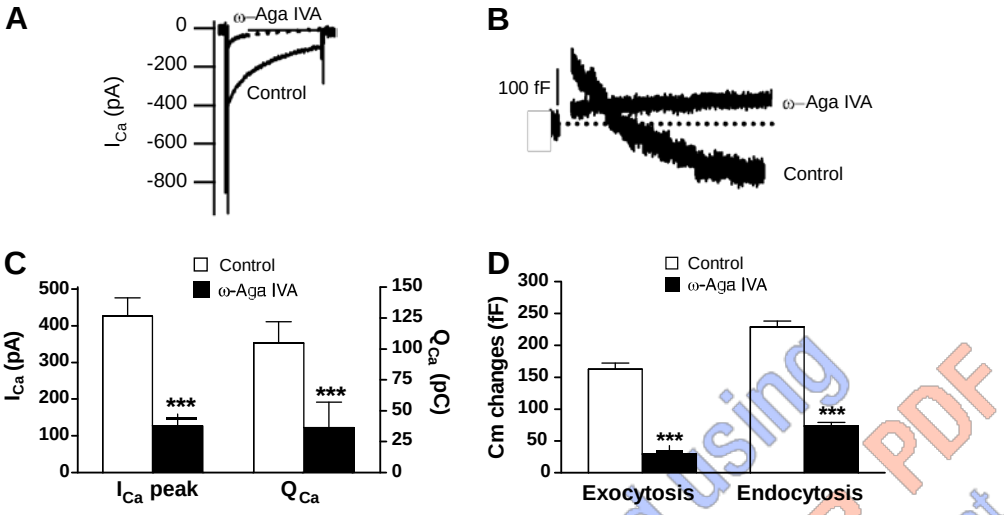

Fig. 4. Effects of x-agatoxin IVA (x-Aga, 1 **1**M) on I_{Ca} and the ensuing C_m changes evoked depolarizing pulses, as in Fig. 1. (A) The control I_{Ca} trace and that obtained after 2-min perifusion with x-agatoxin IVA. (B) The C_m traces from the same example cell of (A). (C) Averaged pooled results of I_{Ca} (left ordinate) and Q_{Ca} (right ordinate). (D) The averaged exocytotic and endocytotic responses of the same cells of (C). Data are means ± s.e.m. of four cells from three different cultures. ***$p < 0.001$ compared to controls.

Table 1
Normalized averaged data on the blockade of I_{Ca}, Q_{Ca}, exocytosis and endocytosis elicited by blockers of the three main high-voltage activated Ca^{2+} channels expressed by bovine chromaffin cells

Blockers	n	I_{Ca}	Q_{Ca}	Exocytosis	Endocytosis
Nifedipine (L-type Ca^{2+} channel blocker)	8	31.2 ± 2.9	53.2 ± 5	26.6 ± 2.2	92.1 ± 0.8
x-Conotoxin GVIA (N-type Ca^{2+} channel blocker)	9	29.7 ± 4.8	23.7 ± 2.9**	4.3 ± 0.5	33.2 ±
x-Agatoxin IVA (P/Q-type Ca^{2+} channel blocker)	4	68.3 ± 9.1***	69.4 ± 11.9*	81.6 ± 9.1**	67.8 ± 1.8

Data are expressed as % blockade with respect to control, and they are means ± s.e.m. of the number of cells shown in n.
* $p < 0.05$.
** $p < 0.01$.
*** $p < 0.001$ with respect to nifedipine.

physiological 2 mM Ca^{2+} concentration and single depolarizing pulses; we have chosen a long pulse duration (500 ms) because a pronounced endocytotic response was not seen with pulses shorter than 200 ms. Under these conditions, the degree of inactivation of each Ca^{2+} channel subtype will strongly condition the kinetics and the amount of Ca^{2+} entry. Thus, a low-inactivating Ca^{2+} channel such as the L-type, that contributes 31% to the initial peak I_{Ca}, will carry more than half of the total Ca^{2+} entry along the 500-ms depolarizing pulse. Conversely, the fast-inactivating N-type channel, that also contributes 30% to the initial I_{Ca} peak, only contributed 24% to Q_{Ca}. These data suggest that a low-rate, non-inactivating Ca^{2+} entry might be more critical to trigger compensatory as well as excess endocytosis. They are also compatible with the possibility that L-type Ca^{2+} channels are coupled to the endocytotic machinery more tightly than N-type Ca^{2+} channels. More difficult seems the interpretation of data obtained with x-agatoxin IVA. This toxin markedly inhibited exocytosis and thus an endocytotic response was unexpected; thus, it seems that when Ca^{2+} enters the cell through P/Q channels, exocytosis and endocytosis run in parallel.

Our findings are consistent with the hypothesis that not all Ca^{2+} channel subtypes in bovine chromaffin cells equally contribute to various cell functions. The recruitment of a particular Ca^{2+} channel subtype depends on the stimulation pattern [31] and varies amongst species [2]. In general, available data suggest that Ca^{2+}-dependent cell functions in bovine chromaffin cells (i.e. Ca^{2+} entry and its redistribution into organelles, exocytosis, ERK phosphorylation) are linked to the amount of Ca^{2+} entering into the cell, independently of the Ca^{2+} channel subtype involved [14,32,33]. Our present data may be considered the first to find a quite selective action for L-type Ca^{2+} channels for the control of endocytosis in bovine chromaffin cells, a function that seems to depend on Ca^{2+} entry through N- or P/Q-types of Ca^{2+} channels to a much lesser extent.

Acknowledgments

This work was supported by a ''Ministerio de Educación y Ciencia'' Grant Nos. BFI2003-02722 and SAF2006-03589 to A.G.G., and SAF2004-07307 to L.G. We thank ''Fundación Teófilo Hernando'' for continued support, Mr. Ricardo de Pascual and Mrs. Inés Colmena for the preparation of cell cultures. JM is a fellow of Fundación

Teófilo Hernando, and AMGD is a fellow of FPI program, Ministry of Education and Science, Madrid, Spain.

References

[1] B.M. Olivera, G.P. Miljanich, J. Ramachandran, M.E. Adams, Calcium channel diversity and neurotransmitter release: the omega- conotoxins and omega-agatoxins, Annu. Rev. Biochem. 63 (1994) 823–867.
[2] A.G. García, A.M. García-De-Diego, L. Gandía, R. Borges, J. García-Sancho, Calcium signaling and exocytosis in adrenal chromaffin cells, Physiol. Rev. 86 (2006) 1093–1131.
[3] R.E. Westenbroek, L. Hoskins, W.A. Catterall, Localization of Ca^{2+} channel subtypes on rat spinal motor neurons, nterneurons, and nerve terminals, J. Neurosci. 18 (1998) 6319–6330.
[4] D.B. Wheeler, A. Randall, R.W. Tsien, Roles of N-type and Q-type Ca^{2+} channels in supporting hippocampal synaptic transmission, Science 264 (1994) 107–111.
[5] M.K. Ahlijanian, R.E. Westenbroek, W.A. Catterall, Subunit structure and localization of dihydropyridine-sensitive calcium channels in mammalian brain, spinal cord, and retina, Neuron 4 (1990) 819–832.
[6] R.E. Westenbroek, M.K. Ahlijanian, W.A. Catterall, Clustering of L- type Ca^{2+} channels at the base of major dendrites in hippocampal pyramidal neurons, Nature 347 (1990) 281–284.
[7] H. Bading, D.D. Ginty, M.E. Greenberg, Regulation of gene expression in hippocampal neurons by distinct calcium signaling pathways, Science 260 (1993) 181–186.
[8] K. Deisseroth, E.K. Heist, R.W. Tsien, Translocation of calmodulin to the nucleus supports CREB phosphorylation in hippocampal neurons, Nature 392 (1998) 198–202.
[9] T.H. Murphy, P.F. Worley, J.M. Baraban, L-type voltage-sensitive calcium channels mediate synaptic activation of immediate early genes, Neuron 7 (1991) 625–635.
[10] M.G. Lopez, A. Albillos, M.T. de la Fuente, R. Borges, L. Gandía, E. Carbone, A.G. García, A.R. Artalejo, Localized L-type calcium channels control exocytosis in cat chromaffin cells, Pflugers Arch. 427 (1994) 348–354.
[11] R.R. Jimenez, M.G. Lopez, C. Sancho, R. Maroto, A.G. García, A component of the catecholamine secretory response in the bovine adrenal gland is resistant to dihydropyridines and omega-conotoxin, Biochem. Biophys. Res. Commun. 191 (1993) 1278–1283.
[12] M. O'Farrell, J. Ziogas, P.D. Marley, Effects of N- and L-type calcium channel antagonists and (+/-)-Bay K8644 on nerve-induced catecholamine secretion from bovine perfused adrenal glands, Br. J. Pharmacol. 121 (1997) 381–388.
[13] B. Lara, L. Gandía, R. Martinez-Sierra, A. Torres, A.G. García, Q- type Ca^{2+} channels are located closer to secretory sites than L-type channels: functional evidence in chromaffin cells, Pflugers Arch. 435 (1998) 472–478.
[14] E.A. Lukyanetz, E. Neher, Different types of calcium channels and secretion from bovine chromaffin cells, Eur. J. Neurosci. 11 (1999) 2865–2873.
[15] C. Smith, E. Neher, Multiple forms of endocytosis in bovine adrenal chromaffin cells, J. Cell Biol. 139 (1997) 885–894.
[16] S.A. Chan, R. Chow, C. Smith, Calcium dependence of action potential-induced endocytosis in chromaffin cells, Pflugers Arch. 445 (2003) 540–546.
[17] E. Neher, R.S. Zucker, Multiple calcium-dependent processes related to secretion in bovine chromaffin cells, Neuron 10 (1993) 21–30.
[18] P. Thomas, A.K. Lee, J.G. Wong, W. Almers, A triggered mechanism retrieves membrane in seconds after Ca^{2+}-stimulated exocytosis in single pituitary cells, J. Cell Biol. 124 (1994) 667–675.
[19] C.R. Artalejo, J.R. Henley, M.A. McNiven, H.C. Palfrey, Rapid endocytosis coupled to exocytosis in adrenal chromaffin cells involves Ca^{2+}, GTP, and dynamin but not clathrin, Proc. Natl. Acad. Sci. USA 92 (1995) 8328–8332.
[20] K.L. Engisch, M.C. Nowycky, Compensatory and excess retrieval: two types of endocytosis following single step depolarizations in bovine adrenal chromaffin cells, J. Physiol. 506 (Pt 3) (1998) 591–608.
[21] S.A. Chan, C. Smith, Physiological stimuli evoke two forms of endocytosis in bovine chromaffin cells, J. Physiol. 537 (2001) 871–885.
[22] P.G. Nucifora, A.P. Fox, Barium triggers rapid endocytosis in calf adrenal chromaffin cells, J. Physiol. 508 (Pt 2) (1998) 483–494.
[23] M. Villarroya, R. Olivares, A. Ruiz, M.F. Cano-Abad, R. de Pascual, R.B. Lomax, M.G. López, I. Mayorgas, L. Gandía, A.G. García, Voltage inactivation of Ca^{2+} entry and secretion associated with N- and P/Q-type but not L-type Ca^{2+} channels of bovine chromaffin cells, J. Physiol. 516 (Pt 2) (1999) 421–432.
[24] J.M. Hernández-Guijo, V.E. Maneu-Flores, A. Ruiz-Nuño, M. Villarroya, A.G. García, L. Gandía, Calcium-dependent inhibition of L, N, and P/Q Ca^{2+} channels in chromaffin cells: role of mitochondria, J. Neurosci. 21 (2001) 2553–2560.
[25] B.G. Livett, Adrenal medullary chromaffin cells in vitro, Physiol. Rev. 64 (1984) 1103–1161.
[26] M.A. Moro, M.G. López, L. Gandía, P. Michelena, A.G. García, Separation and culture of living adrenaline- and noradrenaline- containing cells from bovine adrenal medullae, Anal. Biochem. 185 (1990) 243–248.
[27] S.J. Korn, R. Horn, Influence of sodium–calcium exchange on calcium current rundown and the duration of calcium-dependent chloride currents in pituitary cells, studied with whole cell and perforated patch recording, J. Gen. Physiol. 94 (1989) 789–812.
[28] O.P. Hamill, A. Marty, E. Neher, B. Sakmann, F.J. Sigworth, Improved patch-clamp techniques for high-resolution current recording from cells and cell-free membrane patches, Pflugers Arch. 391 (1981) 85–100.
[29] K.D. Gillis, Techniques for membrane capacitance measurements, in: B. Sakamann, E. Neher (Eds.), Single-Channel Recording, Plenum Press, New York, 1995, pp. 155–198.
[30] F.T. Horrigan, R.J. Bookman, Releasable pools and the kinetics of exocytosis in adrenal chromaffin cells, Neuron 13 (1994) 1119–1129.
[31] A.M. García-de-Diego, J.J. Arnáiz, L. Gandía, J.M. Hernández- Guijo, A.G. García, A comparison between acetylcholine-

like actionpotentials and square depolarizing pulses in triggering calcium entry and exocytosis in bovine chromaffin cells, J. Mol. Neurosci. 30 (2006) 57–58.

[32] I.E. Mendoza, O. Schmachtenbeg, E. Tonk, J. Fuentealba, P. Diaz-Raya, V.L. Lagos, A.G. García, A.M. Cá rdenas, Depolarization- induced ERK phosphorylation depends on the cytosolic Ca^{2+} level rather than on the Ca^{2+} channel subtype of chromaffin cells, J. Neurochem. 86 (2003) 1477–1486.

[33] M. Montero, M.T. Alonso, A. Albillos, I. Cuchillo-Ibáñez, R. Olivares, C. Villalobos, J. Alvarez, Effect of inositol 1,4,5-trisphosphate receptor stimulation on mitochondrial [Ca^{2+}] and secretion in chromaffin cells, Biochem. J. 365 (2002) 451–459.

American Journal of Physiology original article (under review)

Different modes of calcium entry through PQ and L channels into chromaffin cells serve to control respectively exocytosis and endocytosis

Juliana M. Rosa[1,2], Cristina J. Torregrosa-Hetland[4], Inés Colmena[1,2], Luis M. Gutiérrez[4], Antonio G. García[1,2,3] and Luis Gandía[1,2*]

[1]Instituto Teófilo Hernando, [2]Departamento de Farmacología y Terapéutica, [3]Servicio de Farmacología Clínica, IIS del Hospital Universitario de la Princesa; Facultad de Medicina, Universidad Autónoma de Madrid, Madrid, Spain. [4]Instituto de Neurociencias, Centro Mixto CSIC-Universidad Miguel Hernández, Campus de San Juan, Alicante, Spain.

Rosa JM, Torregrosa-Hetland CJ, Colmena I, Gutiérrez LM, García AG and Gandía L. Calcium (Ca^{2+})-dependent endocytosis has been linked to preferential Ca^{2+} entry through the L-subtype (α_{1D}, $Ca_V1.3$) of voltage-dependent Ca^{2+} channels (VDCCs). Considering that the Ca^{2+}-dependent exocytotic release of neurotransmitters is mostly triggered by Ca^{2+} entry through N-(α_{1B}, $Ca_V2.2$) or PQ VDCCs (α_{1A}, $Ca_V2.1$) and that exocytosis and endocytosis are coupled, the supposition that the different channel subtypes are specialised to control different steps of secretion is attractive. Here we have explored this hypothesis in primary cultures of bovine adrenal chromaffin cells, using patch-clamp and fluorescence techniques to measure the exo-endocytotic responses triggered by depolarising stimuli, in 2 or 10 mM concentrations of extracellular Ca^{2+} ($[Ca^{2+}]_e$). ω-conotoxin GVIA (N channel blocker) affected little the exo-endocytotic responses while ω-agatoxin IVA (PQ channel blocker) caused 80% blockade of exocytosis as well as endocytosis. In contrast, nifedipine (L channel blocker) only caused 20% inhibition of exocytosis but as much as 90% inhibition of endocytosis. FPL67146 (an activator of L VDCCs) augmented more the endocytotic, as compared with exocytotic responses. Photoreleased caged Ca^{2+} caused substantially smaller endocytotic responses, compared with those produced by K^+ depolarisation. Using fluorescence antibodies, no co-localisation between L, N, or PQ channels with clathrin, was found; a 20-30% co-localisation was found between dynamin and channel antibodies. Data supports the presence of a functional, but not a geographical co-localisation of L-subtype of VDCCs with the endocytotic machinery. It seems therefore then the mode of Ca^{2+} entry through inactivating PQ channels contributes preferentially to trigger rapid exocytosis, while the mode of Ca^{2+} entry through non-inactivating L-type channels is preferentially triggering endocytosis.

voltage-dependent calcium channels, endocytosis, L-type channel

Correspondence to: Luis Gandía; Instituto Teófilo Hernando, Facultad de Medicina, Universidad Autónoma de Madrid; Arzobispo Morcillo, 4 28029 Madrid, Spain. (luis.gandia@uam.es)

NEURONAL COMMUNICATION at synapses is exerted through a Ca^{2+}-dependent release mechanism (Katz & Miledi, 1969), an observation that is also true for neuroendocrine secretion (Douglas, 1968). Such process underlies fusion of storing vesicle membranes with the plasmalemma (exocytosis) and subsequent membrane retrieval (endocytosis). The coupling of these two processes is essential to keep equilibrium between the amount of vesicular membrane incorporated into the plasmalemma during exocytosis, and membrane retrieved during the subsequent endocytotic phase. This will preserve the size of nerve terminals and neurosecretory cells and will also warrant that a given number of secretory vesicles are available to participate in subsequent rounds of exocytosis during repetitive cell activation (Ceccarelli & Hurlbut, 1980; Smith & Betz, 1996; Smith & Neher, 1997; Chan & Smith, 2001; Royle & Lagnado, 2003).

Calcium has been suggested to affect endocytosis and vesicle recycling in synapses and neuroendocrine cells (Neher & Zucker, 1993; von Gersdorff & Matthews, 1994; Wang & Zucker, 1998). Much is known about Ca^{2+} dependence of exocytosis in these systems (Douglas & Rubin, 1964; Katz & Miledi, 1969; Neher, 1998; Garcia *et al.*, 2006); however, controversy exists over the manner in which membrane retrieval during endocytosis is affected by Ca^{2+}. For instance, compensatory and excess endocytosis represent two independent Ca^{2+}-regulated mechanisms of rapid internalisation in bovine chromaffin cells (Engisch & Nowycky, 1998; Chan & Smith, 2001). The existence of these two different Ca^{2+} sensors is supported by data of Nucifora et al. (1998) in which Ca^{2+} and Ba^{2+} support excessive membrane retrieval in bovine chromaffin cells (Nucifora & Fox, 1998). In contrast, a previous study in the same cells showed that rapid endocytosis was supported by Ca^{2+} but not by Sr^{2+} or Ba^{2+} (Artalejo *et al.*, 1995). There are additional studies in synapses concluding that Ca^{2+} was not required for endocytosis (Ryan *et al.*, 1996; Wu & Betz, 1996) or behaved even as inhibitory (Rouze & Schwartz, 1998).

An additional problem emerges when considering the Ca^{2+} pathway that controls exo-endocytotic processes. The expression in neurons of multiple types of voltage-dependent Ca^{2+} channels (VDCCs) (Olivera *et al.*, 1994; Ertel *et al.*, 2000; Gandía *et al.*, 2008) and in adrenal medullary chromaffin cells (Garcia *et al.*, 2006) poses the interesting question of their possible specialisation in controlling different functions. This seems clear in neurons, where the geographical segregation of different subtypes of VDCCs to dendrites, axon terminals, or somata facilitates their specialisation for specific functions. For instance N-(α_{1B}, $Ca_V2.2$) and PQ-types (α_{1A}, $Ca_V2.1$) VDCCs, which are preferentially found along the length of apical dendrites and in axon terminals that synapse with dendrites (Westenbroek *et al.*, 1998), control the release of various neurotransmitters (Wheeler *et al.*, 1994). On the other hand, L (α_{1D}, $Ca_V1.3$)-type channels located on proximal dendrites and neuronal cell bodies (Ahlijanian *et al.*, 1990; Westenbroek *et al.*, 1990; Westenbroek *et al.*, 1998) have been associated with the regulation of gene expression and enzyme activities in cortical and hippocampal neurons (Murphy *et al.*, 1991; Bading *et al.*, 1993; Deisseroth *et al.*, 1998).

As neurons, adrenal medullary chromaffin cells express L-, N-, PQ, and R (α_{1E}, $Ca_v2.3$)-type of VDCCs. But unlike neurons, these cells lack dendrites and axons. Thus, studies on the specialisation of VDCC subtypes in cultured spherical chromaffin cells have provided unclear results (Garcia *et al.*, 2006).

Depending on the stimulus, patterns of stimulation, animal specie, and the methods used to measure exocytosis or catecholamine release, certain specialisation to modulate exocytosis has been suggested. For instance, L-type channels have been preferentially associated to release responses in some studies (Jimenez *et al.*, 1993; Lopez *et al.*, 1994). Others attributed more protagonism to N channels (O'Farrell *et al.*, 1997) or to PQ channels (Lara *et al.*, 1998; Rosa *et al.*, 2007; Wykes *et al.*, 2007; Alvarez *et al.*, 2008). And some others concluded that exocytosis was proportional to Ca^{2+} entry and the density of Ca^{2+} current carried by each Ca^{2+} channel subtype, with no specialisation at all (Lukyanetz & Neher, 1999).

Concerning the possible specialisation of VDCC subtypes in controlling endocytosis, we provided evidence that L channels were much more relevant than N or PQ channels in controlling endocytosis in voltage-clamped bovine adrenal chromaffin cells after application of single depolarising pulses (DPs) of long duration (Rosa *et al.*, 2007). This functional coupling between L channels and endocytosis was also found at the mouse neuromuscular junction (Perissinotti *et al.*, 2008). The present study was planned to explore the hypothesis that the mode of Ca^{2+} entry through a given VDCC subtype, rather than the total amount of Ca^{2+} entry into the cell, is more relevant to trigger exocytosis and the subsequent endocytosis. In spite that the density of L channels of bovine chromaffin cells accounts for only 20% of total whole-cell current through VDCCs (Albillos *et al.*, 1993; Gandia *et al.*, 1993a), Ca^{2+} entering through inactivating PQ channels seems to contribute preferentially to trigger rapid exocytosis, while Ca^{2+} entering through non-inactivating L-type channels seems to be functionally coupled to endocytosis. This supposition arises from experiments here presented, combining patch-clamp techniques, fluorescence techniques with the probe FM1-43, photorelease of caged Ca^{2+}, and co-localisation techniques through the fluorescence labelling of VDCC subtypes and of the endocytosis proteins clathrin and dynamin, in bovine adrenal chromaffin cells.

METHODS

Cell Culture. Bovine adrenal glands were obtained from a local slaughterhouse. Chromaffin cells were isolated by digestion of the adrenal medulla with collagenase following standard methods (Livett, 1984) with some modifications (Moro *et al.*, 1990). Cells were suspended in Dulbecco`s modified Eagle`s medium (DMEM) supplemented with 5% fetal calf serum, 10 µM cytosine arabinoside, 10 µM fluorodeoxyrudine, 50 IU ml^{-1} penicillin and 50 µg ml^{-1} streptomycin. Cells were plated on 12 mm-diameter polylisine-coated glass coverslips at a density of $5x10^4$ cells/coverslip for patch-clamp experiments or $5x10^5$ cells/coverslip for FM1-43 and flash-photolysis experiments. Cells were kept in a water-saturated incubator at 37°C, in a 5% CO_2 – 95% air atmosphere, and used 2-5 days thereafter.

Recording of Ca^{2+} currents and membrane capacitance. Calcium currents and membrane capacitance were measured under the perforated patch configuration of the patch-clamp technique (Hamill *et al.*, 1981; Korn & Horn, 1989; Gillis *et al.*, 1991). During recording, cells were constantly perifused with a control Tyrode solution at pH 7.4 containing (mM): 137 NaCl, 1 $MgCl_2$, 1, 2 or 10 $CaCl_2$, 10 glucose and 10

HEPES. Internal perforated-patch solution had the following composition (mM): 135 CsGlutamate, 10 HEPES and 9 NaCl, and pH 7.2 adjusted with CsOH. An amphotericin B stock solution was prepared every week at 50 mg/ml in DMSO, stored at 4°C and protected from light. Fresh perforated patch pipette solution was prepared every day by addition of 10 µl stock amphotericin B to 0.5 ml CsGlutamate internal solution; this solution was sonicated thoroughly, protected from light and kept in ice. Patch pipettes had their tips dipped in amphotericin-free solution for 5-10 s and back-filled with freshly mixed amphotericin-containing solution. For patching the cells, pipettes of approximately 2-3 MΩ resistance were pulled from borosilicate glass, partially coated with molten dental wax, and lightly fire polished. Cells were continuously perifused with external solution at a rate of 1 ml min^{-1} and all experiments were performed at room temperature (25-28°C). Electrophysiological data were carried out using an EPC-9 amplifier under the control of Pulse software (HEKA Elektronik). Cell membrane capacitance (Cm) changes were estimated by the Lindau-Neher technique (Lindau & Neher, 1988). A 400-ms sinusoidal wave (1 kHz, 60 mV peak to peak amplitude) was then added before the protocol and a 50-s sinusoidal wave of the same characteristics after it, to allow for the computation of membrane capacitance change. Membrane current was sampled at 20 kHz. Calcium channel blockers were perifused as indicated. Cells were held at -80 mV, and single depolarising pulses to voltages where I_{Ca} peak was reached were applied at 5-min intervals. Cells were perforated to a series resistance of no more than 30 MΩ, which usually happened within 10-min after sealing. External solutions were exchanged by a fast perifusion device consisting of a modified multi-barrelled pipette, the common outlet of which was positioned 50-100 µm from the cell. Control and test solutions were changed using miniature solenoid valves operated manually (Gandia *et al.*, 1993b).

For experiments with FPL64176 in perforated-patch clamp configuration, cells were preincubated during 45 min with 100 µM of the cell permeable EGTA.AM at 37°C; cells were then washed during 15 min at room temperature with the extracellular solution. Cell loading with EGTA was performed to prevent Ca^{2+}-dependent inactivation of VDCCs by excessive intracellular $[Ca^{2+}]_c$ rise (Rosa *et al.*, 2009).

Fluorescence imaging of exocytosis and endocytosis. Exocytosis and endocytosis were monitored using the membrane fluorescence indicator FM1-43 (Smith & Betz, 1996). The optical measurement of FM1-43 was performed as described previously (Perez Bay *et al.*, 2007). Before experiments, cells attached to the coverslip were washed twice for 5 min with standard external solution. Thereafter, the coverslip was mounted in the stage of a Zeiss Axiovert 100 S inverted microscope using a 100x Plan-Neofluor objective, and incubated in the standard external solution that contained 3 µM FM1-43 during 10 min. Fluorescence of FM1-43 was excited with 480 nm light and then collected at 535 nm. Images were acquired every second. Total cellular FM1-43 fluorescence was measured from individual cells and exo-endocytosis was monitored using the protocol described in Fig. 7. Background fluorescence was measured in the same way from regions containing no cells and was subtracted from total cellular fluorescence. Total cellular FM1-43 fluorescence was normalized with respect the total basal cell fluorescence after 10 min of FM1-43 exposition.

Flash photolysis experiments. Flash photolysis experiments were performed as described (Giner *et al.*, 2007). Photorelease of cytosolic caged Ca^{2+} was achieved using a 25 μM concentration of o-nitrophenyl EGTA.AM in Krebs-HEPES buffer with the following composition (in mM): 145 NaCl; 5.6 KCl; 1.2 $MgCl_2$; 2 $CaCl_2$; 10 glucose; 15 Hepes, pH adjusted to 7.4 using NaOH solution (Chen *et al.*, 2008). To facilitate cell loading with the indicator, stock solutions of NP-EGTA.AM were dissolved in DMSO with 10% w/v Pluronic F-127. After 45-min incubation, three washes were performed and the glass coverslip containing the cells was mounted in the stage of a Zeiss Axiovert 100 S inverted microscope using a 100x Plan-Neofluor objective. In this system a dual-port condenser allowed excitation of the specimen with a monochromator Polychrome IV (8% incoming light, Till-Photonics, Munich, Germany) and simultaneous application of a 5-ms UV flash using a pulsed Xenon arc lamp system (92% incoming light, UV Flash II, Till-Photonics), therefore allowing measurement $[Ca^{2+}]_c$ changes using Fura2 excitation at 340/380 nm (for this purpose, 4 μM Fura 2-AM was incubated simultaneously with the NP-EGTA.AM) (Giner *et al.*, 2007). Fluorescence emission from a 20X20-μm restricted area (Viewfinder III, Till-Photonics) was detected in a photomultiplier tube (Hamamatsu Inc., Hamamatsu, Japan). Control of excitation light and acquisition were performed with PCLAMP 8.0 software (Axon Instruments, Foster City, CA, USA) on a PC. FM1-43 was present at a concentration of 3 μM in the Krebs/Hepes buffer bathing the cells; in this manner, the rapid release of vesicles caused by the fast Ca^{2+} elevation could be detected by the increase in FM1-43 fluorescence following vesicle membrane incorporation by exocytosis (Smith & Betz, 1996). FM1-43 fluorescence after excitation at 475 nm was determined and integrated at 50-ms intervals using a fluorescein emission filter set.

Co-localisation studies using fluorescence-coupled antibodies. For immunofluorescence and confocal microscopy, cells were fixed using a 2% paraformaldehyde (PFA) in phosphate buffered saline solution (PBS) for 15 min at room temperature. Then cells were permeabilized with 0.1% Triton X-100 during 1 min incubation and washed twice with PBS within 10 min. To detect clathrin, the cells were incubated for 45 min with a mouse monoclonal anti-clathrin (X22) antibody (Brodsky, 1985); (Abcam, Cambridge, United Kingdom) diluted 1:100 in PBS containing 1% goat serum. To detect dynamin, mouse anti-dynamin (clone 41; an antibody that detects all dynamin isoforms (Ferguson *et al.*, 2007)) at a 1:100 dilution in PBS (containing 1% goat serum) was used as the primary antibody. After extensive washes, secondary goat anti-mouse antibodies coupled to Alexa-488 (1:1000 dilution in PBS, Invitrogen) were added and after 45 min unbound material was washed away using PBS.

Calcium channel subtypes were labeled using rabbit polyclonal antibodies (Alomone Labs, Jerusalem, Israel). Anti-L-type (Ca_V 1.3) channels were raised against a highly purified peptide corresponding to the residues 859–875 of the α_{1D} subunit of rat brain voltage-dependent calcium channels (Hui *et al.*, 1991) and affinity purified using a column immobilizing the same peptide. Anti-PQ (Ca_V 2.1)

channels were produced against residues 865–881 of α_{1A} subunit (Starr *et al.*, 1991) of rat brain voltage-dependent calcium channels. Similarly, anti-N-type (Ca_V 2.2) channels were produce against residues 851–867 of α_{1B} subunit from the same biological source (Westenbroek *et al.*, 1992). Immunolabeling was performed as described above using a 1:100 dilution of the antibodies and the non-specific labeling investigated using antibody solutions pre-incubated with 3 αg/ml of the corresponding peptides during 1 h at room temperature. Anti-rabbit secondary antibodies coupled to Alexa-546 (1:1000 dilution in PBS) were used to visualize epitope distribution. The stained cells were observed on a Leica TCS SP2 confocal microscope with a x100 objective.

Fluorescence was investigated using a Leica TCS SP2 confocal microscope with a x100 objective (spatial resolution based in this objective and the scanner characteristics was estimated in 60–80 nm for 2–3 pixel separations). This system allows for *z*-axis reconstruction with theoretical *z* slice of about 0.5_m thick and sequential mode studies in double labeling experiments. Images were processed using the LAS-AF (Leica Application Suite Advance Fluorescence; Leica Microsystems) program, and co-localization analysis were done using images with the same magnification.

Materials and solutions.The following materials were used: collagenase type I, nifedipine, FPL64176 and amphotericin B were from Sigma (Madrid, Spain); Dulbecco's modified Eagle's medium (DMEM), bovine serum albumin fraction V, fetal calf serum and antibiotics were from Gibco (Madrid, Spain). Agatoxin-IVA was from Peptide Institute (Sandhausen, Germany). ω-conotoxin GVIA and ω-conotoxin MVIIC were from Bachem Feinchemikalien (Budendorf, Switzerland). EGTA.AM was from Calbiochem (Barcelona, Spain). FM1-43, o-nitrophenyl EGTA-AM (NP-EGTA.AM) and Alexa-labelled secondary antibodies were from Invitrogen. (Eugene, OR, USA). ω-conotoxin GVIA and ω-conotoxin MVIIC were dissolved in distilled water and stored frozen in aliquots at 0.1 mM. Nifedipine 10 mM, NP-EGTA.AM 2.5 mM and Fura2-AM 2 mM were prepared in dimethylsulphoxide (DMSO); care was taken to protect solutions from light. FPL64176 at 1 mM was prepared in ethanol and was kept at -20 ºC in aliquots, and was protected from light. Final concentrations of drugs were obtained by diluting the stock solution directly into the extracellular solution. At these dilutions, solvents had no effect on the parameters studied. FM1-43 was dissolved in distilled water at a concentration of 1 mM.

Data analysis. The whole-cell inward Ca^{2+} current peak (I_{Ca}) were analysed after the initial 10-ms of each depolarising pulse to get rid of the Na^+ current (I_{Na}). In electrophysiology experiments, exo- and endocytosis were measured by monitoring changes in cell capacitance. Exocytosis peak was measured by subtracting the basal mean Cm obtained 400-ms previous to depolarisation to 50-ms after the end of the depolarising pulse to avoid a possible Na^+ channel gating artefact (Horrigan & Bookman, 1994). After the exocytotic peak, Cm changes were measured during the ensuing 50-s period; endocytosis was calculated as the difference in Cm at the beginning and the end of such 50-s period. For imaging experiments with FM1-

43 and flash photolysis, the initial size of the fluorescence signal after 10-min of FM1-43 perifusion was used to normalise subsequent fluorescence changes triggered by exocytosis. Endocytosis was calculated as the difference between fluorescence after wash and fluorescence before beginning the experiment (Perez Bay *et al.,* 2007). Comparisons between means of group data were performed by one-way analysis of variance (ANOVA) followed by Duncan post hoc test when appropriate. A p value equal or smaller than 0.05 was taken as the limit of significance.

RESULTS

Calcium gradients and the relationship between Ca^{2+} entry, exocytosis and endocytosis. All subtypes of VDCCs undergo a pronounced Ca^{2+}-dependent inactivation in voltage-clamped bovine chromaffin cells. However, such inactivation is substantially smaller for L, compared with N or PQ channels (Hernandez-Guijo *et al.,* 2001). It was therefore expected that the rate and amount of Ca^{2+} entry through each channel type could undergo visible changes in I_{Ca}, Q_{Ca}, ΔCm (exocytosis), and Cm decay (endocytosis), upon application of depolarising pulses (DPs) at different extracellular Ca^{2+} concentrations ($[Ca^{2+}]_e$). We therefore performed experiments to explore the variations of those four parameters under conditions of cell perifusion with external solutions containing 1 mM Ca^{2+} ($1Ca^{2+}$), 2 mM Ca^{2+} ($2Ca^{2+}$), or 10 mM Ca^{2+} ($10Ca^{2+}$). Cells were voltage-clamped at -80 mV and DPs were applied to generate I_{Ca} and the corresponding C_m changes. I-V curves revealed that maximum peak I_{Ca} was achieved upon application of test pulses to 0 mV at 1 and 2 mM $[Ca^{2+}]_e$, and to +10 mV at 10 mM $[Ca^{2+}]_e$. Thus, at the beginning of each experiment the test pulse giving maximum I_{Ca} was determined and used throughout the experiment. Concerning the length of the test pulse used here, we studied I_{Ca} and Cm changes generated by pulses of 50 to 2000 ms duration; however, a clear endocytotic response was visible from 200 ms onwards. Hence, we decided to use single DPs of 500 ms duration. With the perforated-patch configuration we learned in a previous report that the sequential application of 500 ms DPs to a cell at 5 min intervals, generated reproducible I_{Ca} and Cm changes (Rosa *et al.,* 2007). Thus, we applied this protocol here.

The supposition that variations of extracellular/intracellular Ca^{2+} gradients could distinctly affect ΔCm and Cm decay was tested in cells being perifused with extracellular solutions containing $1Ca^{2+}$, $2Ca^{2+}$ or $10Ca^{2+}$. The example I_{Ca} and Cm traces shown in Fig. 1A were obtained with different perifused extracellular solutions containing $1Ca^{2+}$, $2Ca^{2+}$ and $10Ca^{2+}$. Current traces show an initial current peak generated by Na^+ entry (I_{Na}) that inactivated quickly, giving rise to a slow inactivating I_{Ca}. Both I_{Ca} and ΔCm were substantially higher in $10Ca^{2+}$ as compared with $1Ca^{2+}$ and/or $2Ca^{2+}$. This is better seen in Fig. 1B,C,D where quantitative averaged results from 15 cells were plotted. I_{Ca} peak rose almost 3-fold when $1Ca^{2+}$ was switched to $10Ca^{2+}$ solution. This increase was even higher for Q_{Ca} that rose near 5-fold on switching the extracellular solution from $1Ca^{2+}$ to $10Ca^{2+}$. Cm changes paralleled the Ca^{2+} gradients. Both,

exocytotic and endocytotic responses rose as the Ca^{2+} gradient increased. For instance, exocytosis augmented 2.2-fold in $2Ca^{2+}$ and 6-fold in $10Ca^{2+}$, with respect to $1Ca^{2+}$. This increase was even more drastic for endocytosis that rose 4-fold in $2Ca^{2+}$ and near 10-fold in $10Ca^{2+}$, with respect to $1Ca^{2+}$. However, ratios between endocytosis and exocytosis were similar at the three $[Ca^{2+}]_e$ studied (Fig. 1D).

A quite close correlation between Ca^{2+} entry (Q_{Ca}) and Cm changes was found. This is better seen in Fig. 2 where regression plots on exocytosis/Q_{Ca} (A), endocytosis/Q_{Ca} (B), and endocytosis/exocytosis (C) are shown. There is a reasonable correlation between Ca^{2+} entry, exocytosis, and endocytosis, indicating that the three events are acting in a coordinated manner.

Blockade of VDCC subtypes does not always lead to parallel blockade of exocytosis and endocytosis. As described above, a positive correlation between an increased Ca^{2+} entry gradient, exocytosis and endocytosis was apparent. Because in bovine chromaffin cells the VDCC of the L-, N-, and PQ-subtypes contribute differently to exocytosis during stimulation (Garcia *et al.*, 2006), the question arose as to whether the Ca^{2+} entering through each channel type contributes similarly or differently to the control of exocytotic and endocytotic responses. To explore this question, selective blockers of those channels were used. We and many others have widely used these blockers in bovine chromaffin cells and found that 3 μM nifedipine, 1 μM ω-conotoxin GVIA (GVIA), or 1 μM ω-agatoxin IVA (Aga-IVA) fully block L, N, or PQ channels, respectively (reviewed by (Garcia *et al.*, 2006). These were the concentrations used in this study. The experiments were performed using 2 and 10 mM external Ca^{2+} as charge carrier. Sandwich-type experiments were performed: two initial control depolarising pulses were applied, followed by another two pulses given in the presence of the blocker that was perifused since 2 min before and during the two pulses. Figures 3-4 and table 1 display the results obtained with the three blockers.

In 10 mM Ca^{2+}, nifedipine caused 31% and 55% reduction of I_{Ca} and Q_{Ca}. Greater reduction of Q_{Ca} was likely due to higher Ca^{2+}-dependent inactivation of N and PQ channels (Hernandez-Guijo *et al.*, 2001; Rosa *et al.*, 2009). This led to a 22% reduction of ΔCm and to as much as 93% reduction of Cm decay (Fig. 3; table 1). In 2 mM Ca^{2+} nifedipine caused similar effects on the four parameters, namely 31%, 53%, 26%, and 92% reduction for respectively I_{Ca}, Q_{Ca}, ΔCm, and Cm decay (table 1).

GVIA blocked I_{Ca} to an extent similar to nifedipine i.e. 29% in $2Ca^{2+}$ and 37% in $10Ca^{2+}$. However, Q_{Ca} blockade was significantly lower that of nifedipine, namely 23% in $2Ca^{2+}$ and 35% in $10Ca^{2+}$. This could be explained by greater Ca^{2+} entry along the 500-ms pulse, via non-inactivating L channels. Exocytosis was unaffected and endocytosis was reduced 33% in $2Ca^{2+}$ and 40% in $10Ca^{2+}$ (Fig. 3, table 1).

At 1 μM, Aga-IVA reduced I_{Ca} by as much as 68% in $2Ca^{2+}$ and 51% in $10Ca^{2+}$. Q_{Ca} was reduced to a similar extent, 69% in $2Ca^{2+}$ and 64% in $10Ca^{2+}$. Exocytosis was markedly reduced, i.e. 82% in $2Ca^{2+}$ and 66% in $10Ca^{2+}$, and endocytosis was also largely reduced, i.e. 68% in $2Ca^{2+}$ and 90% in $10Ca^{2+}$ (Fig. 3, table 1).

Thus, it seemed that a defined blockade of a subcomponent of I_{Ca} and Q_{Ca} did not always lead to parallel inhibitions of ΔCm and Cm decay. This is clearer when looking at the ratios between endocytotic and exocytotic responses (Fig. 3; Endo/Exo). At 10 mM Ca^{2+}, the ratio Endo/Exo in nifedipine treated cells was 0.19, meaning that the exocytotic response was much more pronounced than the endocytotic response and that nifedipine was markedly blocking endocytosis with scarce exocytosis blockade. In the case of GVIA-treated cells, such ratio was 0.77, indicating the presence of a good endocytotic response. Aga-IVA treated cells showed an intermediate behaviour: both exo and endocytotic responses were markedly blocked and thus the Endo/Exo ratio was 0.54.

It seemed interesting to compare the behaviour of cells treated with nifedipine with others treated with Aga-IVA, but at a concentration that blocked I_{Ca} and Q_{Ca} to an extent similar that produced by nifedipine. In doing so, it was plausible that cell exocytotic and endocytotic responses differed provided the supposition was true that Ca^{2+} entry through L channels was more prone to trigger endocytosis, compared with Ca^{2+} entering through PQ channels. At 10 mM Ca^{2+} (Fig. 4 and table 1), 200 nM Aga-IVA caused 45% reduction of I_{Ca} and 59% reduction of Q_{Ca}; these values were comparable with those of nifedipine. In spite of this, 200 nM Aga-IVA reduced endocytosis only by 37% while nifedipine caused 84% inhibition. Conversely nifedipine caused 33% inhibition of exocytosis while 200 nM AgaIVA caused 41% blockade (**$p < 0.01$). Thus, it seems that more relevant than the total Ca^{2+} entry into the cell during the 500-ms depolarising pulse is the pathway used by Ca^{2+} to trigger endocytosis, i.e. the non-inactivating L subtype of VDCCs.

Enhanced Ca^{2+} entry through L-type VDCCs selectively augments endocytosis. If restriction of Ca^{2+} entry via L channels aborts endocytosis, then augmentation of Ca^{2+} entry through this pathway should enhance this response. This supposition was tested using the L-type Ca^{2+} channel activator FPL64176 (FPL). To unmask FPL-elicited augmentation of I_{Ca} under the perforated patch-configuration of the patch-clamp technique, we recoursed to cell loading with EGTA.AM before doing the experiments. In this manner, we could prevent Ca^{2+}-dependent inactivation of VDCCs and see augmentation of I_{Ca} (Rosa *et al.*, 2009).

Fig. 5A shows two pairs of I_{Ca} traces generated by 500-ms DPs to -10 mV (left) and 0 mV (right). In the presence of 1 μM FPL, I_{Ca} inactivated more slowly and deactivated also at a slower rate. Cm traces shown in Fig. 5B had a similar ΔCm; however, the trace obtained in the presence of FPL showed a drastic increment of endocytosis, compared with the trace obtained before the compound. Fig. 4C,D are averaged results showing that FPL caused around 11% and 18% increase of I_{Ca} and Q_{Ca}, respectively. Augmentation of Ca^{2+} entry gave rise to an almost 3-fold increase of the Endo/Exo ratio.

Although this experiment supported the supposition of enhanced endocytosis by augmented Ca^{2+} entry via L channels, an additional experiment with isolation of L from N/PQ channels was performed. To block N/PQ channels, 2 μM ω-conotoxin MVIIC (MVIIC) was used (Garcia *et al.*, 2006). Fig. 6A shows three Cm recordings obtained upon challenging a cell with three 500-ms DPs given before (control), during

MVIIC treatment, and after combined MVIIC plus FPL treatment. MVIIC reduced the endocytotic response; when given on top of MVIIC, FPL augmented endocytosis well above the control level. Averaged data are plotted in Fig. 6B-F. MVIIC reduced I_{Ca} by 51% and Q_{Ca} by 59%. Added on top of MVIIC, FPL restored I_{Ca} to 80% of the initial control and Q_{Ca} to 75% of the initial control. This enhanced Ca^{2+} entry exclusively through the L channel doubled the ratio Endo/Exo, indicating a selective augmentation of endocytosis.

Monitoring exo-endocytosis responses with FM1-43 dye: effects of VDCC blockers. To get further insight into the supposition that the various VDCC pathways contribute differently to exocytotic and endocytotic responses, chromaffin cells were challenged with a high-K^+ solution in the presence of FM1-43, a styryl hydrophilic dye widely used to study vesicle recycling. In response to long-lasting depolarisation; the dye inserts into the outer leaflet on the plasma membrane and is internalised during vesicle retrieval (Smith & Betz, 1996). Since the remaining extracellular dye is quickly washed away, the internalised fluorescence persisting within the cell is considered a good marker of endocytosis.

Upon addition of FM1-43, the dye stained the cell plasmalemma; fluorescence increased during the initial 10-min equilibration period, to reach a steady-state plateau (Fig. 7Aa, Ba). Upon challenging the cell with a solution containing 59 mM K^+ and 2 mM Ca^{2+}, fluorescence rapidly rose to reach a plateau in about a minute of K^+ exposure, an indication that vesicles were undergoing exocytosis and more membrane that was being incorporated into the plasmalemma, entered in contact with FM1-43; such increment was around 30% of fluorescence after 10-min loading. After the depolarising K^+ pulse, cells were washed; fluorescence due to extracellular dye fades off to a new plateau above basal. The height of such plateau was due to FM1-43 trapped within the membrane vesicle retrieved, an indication of endocytosis (Fig. 7Ac, Bc). Fluorescence tended to accumulate nearby the plasmalemma, a behaviour indicating Ca^{2+}-dependent vesicle cycling (Lagnado *et al.*, 1996). In this example cell, endocytosis was 30% of total fluorescence. Non-specific cell loading with FM1-43 was tested in non-stimulated cells; under these conditions, dye fluorescence indicating endocytosis did not occur (Fig. 7C, open circles).

Variations in the $[Ca^{2+}]_c$ were tested in cells loaded with Fura-2, subjected to a protocol similar that used for the FM1-43 experiment described above. The ratio 340/380 augmented 1.6-fold (Fig. 7D). This K^+-evoked $[Ca^{2+}]_c$ transient was evidently sufficient to trigger the exo-endocytotic responses measured with FM1-43.

The effect of VDCC blockers on the FM1-43 exo-endocytotic responses after 3-min K^+ challenging, were tested in another series of experiments. The Endo/Exo relationship was not affected by GVIA, a result similar that obtained with Cm change monitoring. However, MVIIC reduced by 40% the Endo/Exo ratio. In the case of nifedipine, a 53% reduction of Endo/Exo ratio was observed; this effect was lower, compared with the nifedipine action on endocytosis measured with Cm change monitoring, that practically abolished the endocytotic response (Fig. 3E). This difference could be explained on the basis of the two different types of stimuli used, i.e. 500 ms DPs under voltage clamp in Fig. 3 and 3-min K^+

stimulation here. FPL did not change the Endo/Exo ratio when given alone; however reverted the decrease of the Endo/Exo when applied on top of MVIIC (Fig. 7D). Although less clearly than data derived from patch-clamp experiments, the FM1-43 data however support the view that Ca^{2+} entering through L-type VDCCs seemed to be preferentially coupled to endocytosis.

Exo-endocytotic responses triggered by photoreleased Ca^{2+}, monitored with FM1-43 fluorescence. Experiments so far described explored the exo-endocytotic responses triggered by Ca^{2+} entry through VDCCs. Under this frame, the question arose on whether Ca^{2+} directly released into the cytosol without the intervention of those channels, could trigger responses similar to those activated by DPs. To this purpose, cells were loaded with NP.EGTA and fura-2. A 5-ms UV flash caused the rapid Ca^{2+} transient shown in the inset to Fig. 8A. This transient caused the exo- and endocytotic responses defined by the double-head arrows of Fig. 8A. Differences between variations in the $[Ca^{2+}]_c$ are shown in Fig. 8B. In Fig. 8C, the time courses of FM1-43 fluorescence changes evoked by photoreleased Ca^{2+} and K^+, were superimposed; this clearly shows that while the exocytotic responses had similar time courses, endocytosis was smaller in the case of cell stimulation with photoreleased Ca^{2+} compared with K^+ (double-head arrows to the right of panel B). This is quantitatively shown in Fig. 8D where the Endo/Exo ratios are plotted; this ratio was 2.5-fold higher for K^+, as compared with photoreleased Ca^{2+}.

Co-localisation of calcium channels with dynamin or clathrin. Confocal microscopy was used to identify the possible co-localisation of the different calcium channel subtypes with the endocytosis-related proteins dynamin and/or clathrin. Figure 9 shows a representative experiment in which a chromaffin cell was simultaneously labeled with an anti-L-type (Ca_V 1.3) channel antibody (panel A) and anti-dynamin antibody (panel B). Panel C shows merge image that correspond to co-localisation of both pixels labeled with both antibodies in the same cell. Fig. 9E shows averaged data on co-localisation rate for the different combinations of dynamin and clathrin with the three calcium channels subtypes studies. As shown, the co-localisation of clathrin was practically negligible with the three calcium channel subtypes (Ca_V 1.3, Ca_V2.1 and Ca_V2.2). A mild (about 20-30%) co-localisation rate was observed for dynamin with calcium channels, without significant differences between the different calcium channel subtypes (Fig. 9E).

DISCUSSION

Upon stimulation with DPs, chromaffin cells respond with an exocytotic response that is followed by an endocytotic response. Both processes are activated by a $[Ca^{2+}]_c$ elevation and are terminated when the cytosolic Ca^{2+} transient is cleared by the mitochondrion, the endoplasmic reticulum, and the plasmalemmal Ca^{2+} transporters (Garcia *et al.*, 2006). This exo-endocytotic coupling by Ca^{2+} is clearly shown in the experiments of Figs. 1 and 2 where both processes increase in parallel with augmentation of the Ca^{2+} gradient between the extracellular and intracellular compartments. A priori, these experiments support the

view that exo-endocytosis is a simple function of the amount of Ca^{2+} (Q_{Ca}) entering the cell, whatever the pathways used by the cation, i.e. L, N, or PQ VDCCs. However, these channel subtypes are expressed with different densities, and inactivate at different rates when they are recruited by long DPs as those used here, namely 200 ms in the perforated-patch recording (Figs. 1-5) and 3 min in the fluorescence studies using FM1.43 to monitor the exo-endocytotis responses triggered by K^+ (Figs. 7-8). L channels are resistant to $[Ca^{2+}]_c$-dependent and voltage-dependent inactivation, while N and PQ channels are more prone to inactivation (Villarroya *et al.*, 1999; Hernandez-Guijo *et al.*, 2001).

Such differences in inactivation rates may explain that blockade by nifedipine of L channels caused 31% blockade of peak I_{Ca} and 53% blockade of Q_{Ca}, while Aga-IVA caused similar blockade of peak I_{Ca} and Q_{Ca}, near 70% in 2 mM $[Ca^{2+}]_e$ (table 1). Considering that channel densities are 20% for L channels and 50% for PQ channels in bovine chromaffin cells (Albillos *et al.*, 1993; Gandia *et al.*, 1993a), it seems that over 50% blockade of Q_{Ca} by nifedipine is explained by a slower but sustained Ca^{2+} entry through L channels along a DP, as compared with a faster and greater initial Ca^{2+} entry followed by rapid decay when Ca^{2+} enters through PQ channels. These two modes of $[Ca^{2+}]_c$ increases is compatible with the idea that fast exocytosis requires a subplasmalemmal rapid increment of Ca^{2+} in the ten of even more micromolar levels (Neher, 1998; Garcia *et al.*, 2006), that may be better achieved when Ca^{2+} enters the cell through PQ channels; endocytosis, however, is a slower process that could require lower but more sustained elevations of $[Ca^{2+}]_c$, a signal that is better provided when Ca^{2+} enters the cell through L channels.

Our results are compatible with the above supposition, since L channel blockade (that cause little inhibition of exocytosis) suppressed the endocytotic response when triggered by electrical DPs (Fig. 3D), and caused a drastic inhibition of endocytosis when FM1.43 and K^+ pulses were used (Fig. 9E). Conversely, enhanced activation of L channels by FPL (that caused a mild enhancement of exocytosis), elicited a drastic augmentation of endocytosis, either under the perforated-patch technique (Figs. 5 and 6), or when using the FM1.43 dye (Fig. 7D). This considerably differed from the changes afforded by Aga-IVA; suppression of Ca^{2+} entry through PQ channels led to a parallel drastic inhibitions of exocytotic and endocytotic responses (Fig. 3); this was also true for MVIIC, a blocker of N and PQ channels (Fig. 6). However, partial blockade of PQ channels by a low Aga-IVA concentration (to an extent similar that produced by 3 μM nifedipine to cause a full L channel blockade) caused 40% and 20% inhibition of exocytosis, respectively for the former and the latter. The opposite was found with endocytosis that was inhibited by 37% by Aga-IVA and by as much as 84% by nifedipine (Fig. 4, table 1).

Being a spherical cell when maintained in a primary culture, and expressing at least the three subtypes of VDCCs having a rich pharmacology to manipulate them, the bovine chromaffin cell has become a model amply used to discern the relationship between the regulation of Ca^{2+} entry and exo-endocytotic responses, as well as the specialisation of L, N, and PQ channels to control different Ca^{2+}-dependent phenomena. From a physiological point of view, this question has a high relevance because it may throw light on two important questions: (1) is the expression of different VDCC subtypes a mere redundant mechanisms?; and (2) could every VDCC subtype serve different Ca^{2+}-dependent functions,

through the facilitation of different modes of Ca^{2+} entry, rather than the absolute quantity of Ca^{2+} entering the cell during a given stimulus? The contribution of each channel type to exocytosis has been widely studied in chromaffin cells. Depending on the stimulus and $[Ca^{2+}]_e$, PQ channels (Lara *et al.*, 1998; Chan *et al.*, 2005) have been suggested to be preferentially coupled to exocytosis; other authors have shown that the contribution of each channel type to exocytosis is only a function of both channel density and the Ca^{2+} entering the cell (measured as I_{Ca} peak) (Lukyanetz & Neher, 1999). Until recently, similar studies focusing on endocytosis were not available (Rosa *et al.*, 2007).

The present study reports a quite ample set of different experiments consistent with the supposition that L VDCCs are coupled more tightly to the endocytotic machinery while N or PQ channels exhibit a lesser degree of coupling. However, the immunofluorescence experiments showed no coupling of VDCC subtypes with clathrin and only about 20-30% coupling with dynamin, two proteins of the endocytotic machinery (Fig. 9). This is not against the concept that a functional coupling may exist between L channels and endocytosis, that we will try to explain in the context of the functional triad, a hypothesis arising from experiments performed in bovine chromaffin cells (Montero *et al.*, 2000; Alonso *et al.*, 2006; Garcia *et al.*, 2006).

Using mitochondria-targeted aequorins with different Ca^{2+} affinities, we found that about 50% of mitochondria located nearby VDCCs at subplasmalemmal sites, were taken up vast amounts of the Ca^{2+} entering through VDCCs. Considering that the mitochondrial Ca^{2+} uniporter has low affinity for Ca^{2+}, this rapid Ca^{2+} uptake that allowed to reach near millimolar $[Ca^{2+}]$ in the mitochondrial matrix, could be possible only near the VDCCs where large Ca^{2+} changes in the tens of micromolar concentrations are reached during cell activation (Neher, 1998). The functional consequences of such mitochondrial Ca2+ sink were unmasked by interrupting the mitochondrial Ca^{2+} uptake by protonophores, that obviously elicited a large potentiation of exocytosis (Giovannucci *et al.*, 1999; Montero *et al.*, 2000; Cuchillo-Ibanez *et al.*, 2004). Having a K_D for Ca^{2+} of 6 μM (Uceda *et al.*, 1995) the uniporter will see the large local Ca^{2+} transients generated by PQ channels, that account for about 50% of the whole population of VDCCs expressed by bovine chromaffin cells (Albillos *et al.*, 1993; Gandia *et al.*, 1993a); this will help to dissipate the Ca^{2+} transient and to quickly terminate the exocytotic response. In contrast, Ca^{2+} entering via L channels that account for only 15-20%, will generate lower but more sustained $[Ca^{2+}]_c$ elevations that will be affected little by subplasmalemmal mitochondria; this may serve to modulate the slower endocytotic process, as discussed above.

In conclusion, data reported here are compatible with the supposition that the different modes of Ca^{2+} entry through inactivating PQ-type of VDCCs and non-inactivating L-type of VDCCs may preferentially control respectively exocytosis and endocytosis in bovine chromaffin cells. This is consistent with the idea of the specialisation of VDCCs subtypes even when expressed within the same cell.

ACKNOWLEDGENTS

We thank *Fundación Teófilo Hernando* for continued support.

GRANTS

This work was partially supported from the following grants from Spanish institutions to AGG: (1) SAF2006-03589, *Ministerio de Ciencia e Innovación*, Spain; (2) NDE 07/09, *Agencia Laín Entralgo, Comunidad de Madrid*; (3) PI016/09, *Fundación C.I.E.N., Instituto de Salud Carlos III*; (4) RD 06/0026 RETICS, *Instituto de Salud Carlos III*; (5) S-SAL-0275-2006, *Comunidad de Madrid*. Also by grant SAF2007-65181, *Ministerio de Ciencia e Innovación*, Spain, to LG.

DISCLOSURES

We are not aware of financial conflict(s) with the subject matter or materials discussed in this manuscript with any of the authors, or any of the author's academic institutions or employers.

REFERENCES

1. **Ahlijanian MK, Westenbroek RE, and Catterall WA.** Subunit structure and localization of dihydropyridine-sensitive calcium channels in mammalian brain, spinal cord, and retina. *Neuron* 4: 819-832, 1990.
2. **Albillos A, Garcia AG, and Gandia L.** omega-Agatoxin-IVA-sensitive calcium channels in bovine chromaffin cells. *FEBS Lett* 336: 259-262, 1993.
3. **Alonso MT, Villalobos C, Chamero P, Alvarez J, and Garcia-Sancho J.** Calcium microdomains in mitochondria and nucleus. *Cell Calcium* 40: 513-525, 2006.
4. **Alvarez YD, Ibanez LI, Uchitel OD, and Marengo FD.** PQ Ca^{2+} channels are functionally coupled to exocytosis of the immediately releasable pool in mouse chromaffin cells. *Cell Calcium* 43: 155-164, 2008.
5. **Artalejo CR, Henley JR, McNiven MA, and Palfrey HC.** Rapid endocytosis coupled to exocytosis in adrenal chromaffin cells involves Ca^{2+}, GTP, and dynamin but not clathrin. *Proc Natl Acad Sci U S A* 92: 8328-8332, 1995.
6. **Bading H, Ginty DD, and Greenberg ME.** Regulation of gene expression in hippocampal neurons by distinct calcium signaling pathways. *Science* 260: 181-186, 1993.
7. **Brodsky FM.** Clathrin structure characterized with monoclonal antibodies. I. Analysis of multiple antigenic sites. *J Cell Biol* 101: 2047-2054, 1985.
8. **Ceccarelli B and Hurlbut WP.** Ca^{2+}-dependent recycling of synaptic vesicles at the frog neuromuscular junction. *J Cell Biol* 87: 297-303, 1980.
9. **Cuchillo-Ibanez I, Lejen T, Albillos A, Rose SD, Olivares R, Villarroya M, Garcia AG, and Trifaro JM.** Mitochondrial calcium sequestration and protein kinase C cooperate in the regulation of cortical F-actin disassembly and secretion in bovine chromaffin cells. *J Physiol* 560: 63-76, 2004.
10. **Chan SA, Polo-Parada L, and Smith C.** Action potential stimulation reveals an increased role for PQ-calcium channel-dependent exocytosis in mouse adrenal tissue slices. *Arch Biochem Biophys* 435: 65-73, 2005.
11. **Chan SA and Smith C.** Physiological stimuli evoke two forms of endocytosis in bovine chromaffin cells. *J Physiol* 537: 871-885, 2001.
12. **Chen X, Gao Y, Hossain M, Gangopadhyay S, and Gillis KD.** Controlled on-chip stimulation of quantal catecholamine release from chromaffin cells using photolysis of caged Ca^{2+} on transparent indium-tin-oxide microchip electrodes. *Lab Chip* 8: 161-169, 2008.
13. **Deisseroth K, Heist EK, and Tsien RW.** Translocation of calmodulin to the nucleus supports CREB phosphorylation in hippocampal neurons. *Nature* 392: 198-202, 1998.

14. **Douglas WW.** Stimulus-secretion coupling: the concept and clues from chromaffin and other cells. *Br J Pharmacol* 34: 451-474, 1968.
15. **Douglas WW and Rubin RP.** The Effects of Alkaline Earths and Other Divalent Cations on Adrenal Medullary Secretion. *J Physiol* 175: 231-241, 1964.
16. **Engisch KL and Nowycky MC.** Compensatory and excess retrieval: two types of endocytosis following single step depolarizations in bovine adrenal chromaffin cells. *J Physiol* 506 (Pt 3): 591-608, 1998.
17. **Ertel EA, Campbell KP, Harpold MM, Hofmann F, Mori Y, Perez-Reyes E, Schwartz A, Snutch TP, Tanabe T, Birnbaumer L, Tsien RW, and Catterall WA.** Nomenclature of voltage-gated calcium channels. *Neuron* 25: 533-535, 2000.
18. **Ferguson SM, Brasnjo G, Hayashi M, Wolfel M, Collesi C, Giovedi S, Raimondi A, Gong LW, Ariel P, Paradise S, O'Toole E, Flavell R, Cremona O, Miesenbock G, Ryan TA, and De Camilli P.** A selective activity-dependent requirement for dynamin 1 in synaptic vesicle endocytosis. *Science* 316: 570-574, 2007.
19. **Gandia L, Albillos A, and Garcia AG.** Bovine chromaffin cells possess FTX-sensitive calcium channels. *Biochem Biophys Res Commun* 194: 671-676, 1993.
20. **Gandia L, Garcia AG, and Morad M.** ATP modulation of calcium channels in chromaffin cells. *J Physiol* 470: 55-72, 1993.
21. **Gandía L, Montiel C, García A, and López M.** *Seafood and Freshwater Toxins: Pharmacology, physiology and detection*. Boca Raton, 2008.
22. **Garcia AG, Garcia-De-Diego AM, Gandia L, Borges R, and Garcia-Sancho J.** Calcium signaling and exocytosis in adrenal chromaffin cells. *Physiol Rev* 86: 1093-1131, 2006.
23. **Gillis KD, Pun RY, and Misler S.** Single cell assay of exocytosis from adrenal chromaffin cells using "perforated patch recording". *Pflugers Arch* 418: 611-613, 1991.
24. **Giner D, Lopez I, Neco P, Rossetto O, Montecucco C, and Gutierrez LM.** Glycogen synthase kinase 3 activation is essential for the snake phospholipase A2 neurotoxin-induced secretion in chromaffin cells. *Eur J Neurosci* 25: 2341-2348, 2007.
25. **Giovannucci DR, Hlubek MD, and Stuenkel EL.** Mitochondria regulate the Ca^{2+}-exocytosis relationship of bovine adrenal chromaffin cells. *J Neurosci* 19: 9261-9270, 1999.
26. **Hamill OP, Marty A, Neher E, Sakmann B, and Sigworth FJ.** Improved patch-clamp techniques for high-resolution current recording from cells and cell-free membrane patches. *Pflugers Arch* 391: 85-100, 1981.
27. **Hernandez-Guijo JM, Maneu-Flores VE, Ruiz-Nuno A, Villarroya M, Garcia AG, and Gandia L.** Calcium-dependent inhibition of L, N, and PQ Ca^{2+} channels in chromaffin cells: role of mitochondria. *J Neurosci* 21: 2553-2560, 2001.
28. **Horrigan FT and Bookman RJ.** Releasable pools and the kinetics of exocytosis in adrenal chromaffin cells. *Neuron* 13: 1119-1129, 1994.
29. **Hui A, Ellinor PT, Krizanova O, Wang JJ, Diebold RJ, and Schwartz A.** Molecular cloning of multiple subtypes of a novel rat brain isoform of the alpha 1 subunit of the voltage-dependent calcium channel. *Neuron* 7: 35-44, 1991.
30. **Jimenez RR, Lopez MG, Sancho C, Maroto R, and Garcia AG.** A component of the catecholamine secretory response in the bovine adrenal gland is resistant to dihydropyridines and omega-conotoxin. *Biochem Biophys Res Commun* 191: 1278-1283, 1993.
31. **Katz B and Miledi R.** Spontaneous and evoked activity of motor nerve endings in calcium Ringer. *J Physiol* 203: 689-706, 1969.
32. **Korn SJ and Horn R.** Influence of sodium-calcium exchange on calcium current rundown and the duration of calcium-dependent chloride currents in pituitary cells, studied with whole cell and perforated patch recording. *J Gen Physiol* 94: 789-812, 1989.
33. **Lagnado L, Gomis A, and Job C.** Continuous vesicle cycling in the synaptic terminal of retinal bipolar cells. *Neuron* 17: 957-967, 1996.
34. **Lara B, Gandia L, Martinez-Sierra R, Torres A, and Garcia AG.** Q-type Ca^{2+} channels are located closer to secretory sites than L-type channels: functional evidence in chromaffin cells. *Pflugers Arch* 435: 472-478, 1998.
35. **Lindau M and Neher E.** Patch-clamp techniques for time-resolved capacitance measurements in single cells. *Pflugers Arch* 411: 137-146, 1988.

36. **Livett BG.** Adrenal medullary chromaffin cells in vitro. *Physiol Rev* 64: 1103-1161, 1984.
37. **Lopez MG, Villarroya M, Lara B, Martinez Sierra R, Albillos A, Garcia AG, and Gandia L.** Q- and L-type Ca^{2+} channels dominate the control of secretion in bovine chromaffin cells. *FEBS Lett* 349: 331-337, 1994.
38. **Lukyanetz EA and Neher E.** Different types of calcium channels and secretion from bovine chromaffin cells. *Eur J Neurosci* 11: 2865-2873, 1999.
39. **Montero M, Alonso MT, Carnicero E, Cuchillo-Ibanez I, Albillos A, Garcia AG, Garcia-Sancho J, and Alvarez J.** Chromaffin-cell stimulation triggers fast millimolar mitochondrial Ca^{2+} transients that modulate secretion. *Nat Cell Biol* 2: 57-61, 2000.
40. **Moro MA, Lopez MG, Gandia L, Michelena P, and Garcia AG.** Separation and culture of living adrenaline- and noradrenaline-containing cells from bovine adrenal medullae. *Anal Biochem* 185: 243-248, 1990.
41. **Murphy TH, Worley PF, and Baraban JM.** L-type voltage-sensitive calcium channels mediate synaptic activation of immediate early genes. *Neuron* 7: 625-635, 1991.
42. **Neher E.** Vesicle pools and Ca^{2+} microdomains: new tools for understanding their roles in neurotransmitter release. *Neuron* 20: 389-399, 1998.
43. **Neher E and Zucker RS.** Multiple calcium-dependent processes related to secretion in bovine chromaffin cells. *Neuron* 10: 21-30, 1993.
44. **Nucifora PG and Fox AP.** Barium triggers rapid endocytosis in calf adrenal chromaffin cells. *J Physiol* 508 (Pt 2): 483-494, 1998.
45. **O'Farrell M, Ziogas J, and Marley PD.** Effects of N- and L-type calcium channel antagonists and (+/-)-Bay K8644 on nerve-induced catecholamine secretion from bovine perfused adrenal glands. *Br J Pharmacol* 121: 381-388, 1997.
46. **Olivera BM, Miljanich GP, Ramachandran J, and Adams ME.** Calcium channel diversity and neurotransmitter release: the omega-conotoxins and omega-agatoxins. *Annu Rev Biochem* 63: 823-867, 1994.
47. **Perez Bay AE, Ibanez LI, and Marengo FD.** Rapid recovery of releasable vesicles and formation of nonreleasable endosomes follow intense exocytosis in chromaffin cells. *Am J Physiol Cell Physiol* 293: C1509-1522, 2007.
48. **Perissinotti PP, Giugovaz Tropper B, and Uchitel OD.** L-type calcium channels are involved in fast endocytosis at the mouse neuromuscular junction. *Eur J Neurosci* 27: 1333-1344, 2008.
49. **Rosa JM, de Diego AM, Gandia L, and Garcia AG.** L-type calcium channels are preferentially coupled to endocytosis in bovine chromaffin cells. *Biochem Biophys Res Commun* 357: 834-839, 2007.
50. **Rosa JM, Gandia L, and Garcia AG.** Inhibition of N and PQ calcium channels by calcium entry through L channels in chromaffin cells. *Pflugers Arch* 458: 795-807, 2009.
51. **Rouze NC and Schwartz EA.** Continuous and transient vesicle cycling at a ribbon synapse. *J Neurosci* 18: 8614-8624, 1998.
52. **Royle SJ and Lagnado L.** Endocytosis at the synaptic terminal. *J Physiol* 553: 345-355, 2003.
53. **Ryan TA, Smith SJ, and Reuter H.** The timing of synaptic vesicle endocytosis. *Proc Natl Acad Sci U S A* 93: 5567-5571, 1996.
54. **Smith C and Neher E.** Multiple forms of endocytosis in bovine adrenal chromaffin cells. *J Cell Biol* 139: 885-894, 1997.
55. **Smith CB and Betz WJ.** Simultaneous independent measurement of endocytosis and exocytosis. *Nature* 380: 531-534, 1996.
56. **Starr TV, Prystay W, and Snutch TP.** Primary structure of a calcium channel that is highly expressed in the rat cerebellum. *Proc Natl Acad Sci U S A* 88: 5621-5625, 1991.
57. **Uceda G, Garcia AG, Guantes JM, Michelena P, and Montiel C.** Effects of Ca^{2+} channel antagonist subtypes on mitochondrial Ca^{2+} transport. *Eur J Pharmacol* 289: 73-80, 1995.
58. **Villarroya M, Olivares R, Ruiz A, Cano-Abad MF, de Pascual R, Lomax RB, Lopez MG, Mayorgas I, Gandia L, and Garcia AG.** Voltage inactivation of Ca^{2+} entry and secretion associated with N- and PQ-type but not L-type Ca^{2+} channels of bovine chromaffin cells. *J Physiol* 516 (Pt 2): 421-432, 1999.
59. **von Gersdorff H and Matthews G.** Inhibition of endocytosis by elevated internal calcium in a synaptic terminal. *Nature* 370: 652-655, 1994.

60. **Wang C and Zucker RS.** Regulation of synaptic vesicle recycling by calcium and serotonin. *Neuron* 21: 155-167, 1998.
61. **Westenbroek RE, Ahlijanian MK, and Catterall WA.** Clustering of L-type Ca^{2+} channels at the base of major dendrites in hippocampal pyramidal neurons. *Nature* 347: 281-284, 1990.
62. **Westenbroek RE, Hell JW, Warner C, Dubel SJ, Snutch TP, and Catterall WA.** Biochemical properties and subcellular distribution of an N-type calcium channel alpha 1 subunit. *Neuron* 9: 1099-1115, 1992.
63. **Westenbroek RE, Hoskins L, and Catterall WA.** Localization of Ca2+ channel subtypes on rat spinal motor neurons, interneurons, and nerve terminals. *J Neurosci* 18: 6319-6330, 1998.
64. **Wheeler DB, Randall A, and Tsien RW.** Roles of N-type and Q-type Ca2+ channels in supporting hippocampal synaptic transmission. *Science* 264: 107-111, 1994.
65. **Wu LG and Betz WJ.** Nerve activity but not intracellular calcium determines the time course of endocytosis at the frog neuromuscular junction. *Neuron* 17: 769-779, 1996.
66. **Wykes RC, Bauer CS, Khan SU, Weiss JL, and Seward EP.** Differential regulation of endogenous N- and PQ-type Ca^{2+} channel inactivation by Ca^{2+}/calmodulin impacts on their ability to support exocytosis in chromaffin cells. *J Neurosci* 27: 5236-5248, 2007.

Received September 1, 2010; currently under review

Table 1. Normalised quantitative pooled data on the blockade of I_{Ca}, Q_{Ca}, exocytosis, endocytosis and ratios between endocytosis and exocytosis (Endo/Exo), elicited by nifedipine (blocker of L channels), ω-conotoxin GVIA (blocker of N channels), and ω-agatoxin IVA (blocker of PQ channels). Data are expressed as % blockade with respect to the control initial response of each individual cell; they are means ± s.e.m. of the number of cells shown in n. *p<0.05; ** p<0.01; ***p<0.001 with respect to nifedipine.

Blockers	**[Ca^{2+}] (mM)**	**n**	**I_{Ca}**	**Q_{Ca}**	**Exocytosis**	**Endocytosis**	**Endo/Exo**
Nifedipine (3 μM) *(L-type Ca^{2+} channel blocker)*	2	8	31 ± 2.9	53 ± 5	26 ± 2.2	92 ± 0.8	97 ± 1.1
	10	6	43 ± 5.2	50 ± 3.4	20 ± 3.5	84 ± 9.6	82 ± 6.2
ω-Conotoxin GVIA (1 μM) *(N-type Ca^{2+} channel blocker)*	2	9	29 ± 4.8	23 ± 2.9**	4.3 ±0.5	33 ± 19**	18 ± 8***
	10	5	33 ± 4.6	34 ± 7.6	8.0 ±2.1	48 ± 21*	27 ± 11**
ω-Agatoxin IVA (1 μM) *(PQ-type Ca^{2+} channel blocker)*	2	4	68 ± 9.1***	69 ± 11.9*	81 ± 9.1**	67 ± 1.8	10 ± 5.3***
	10	3	90 ± 0.5***	85 ± 0.6***	85 ± 9*	91 ± 1.2	50 ± 7*
ω-Agatoxin IVA (200 nM) *(PQ-type Ca^{2+} channel blocker)*	10	9	45 ± 9	59 ± 13	40 ± 12	37 ± 9**	30 ± 9**

Figure 1

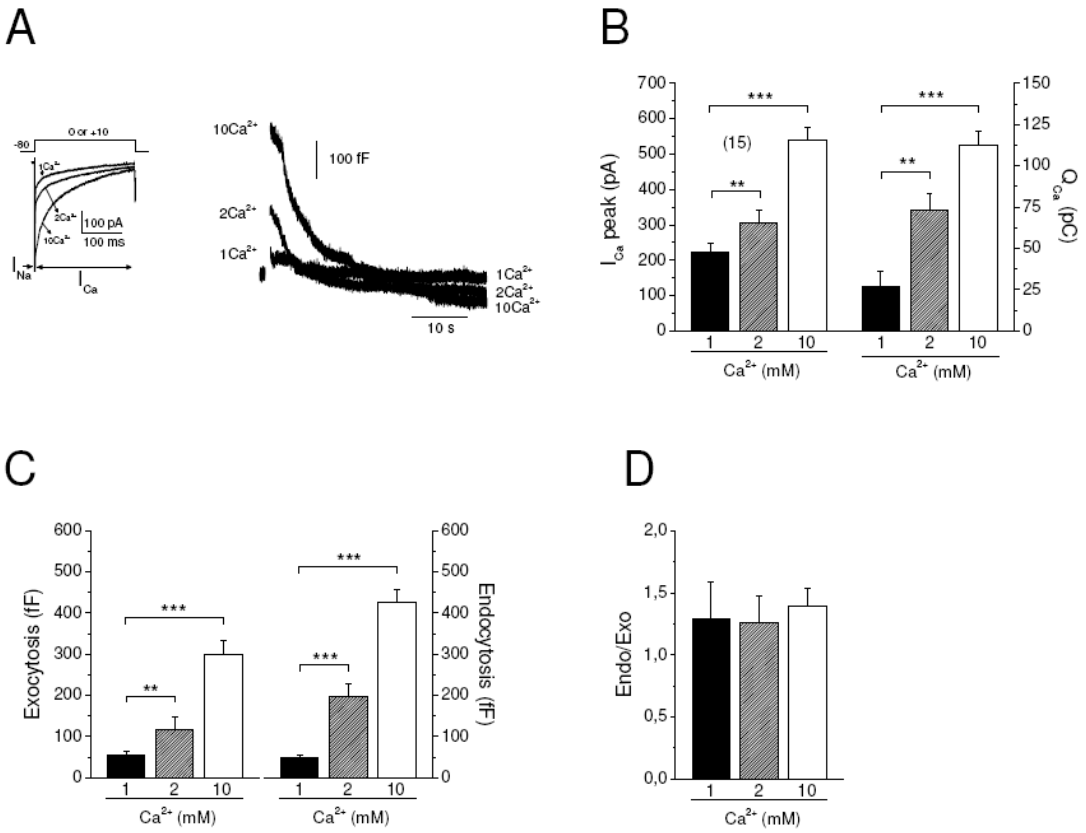

Fig. 1. Ca^{2+} currents (I_{Ca}) and membrane capacitance (Cm) changes induced by depolarising pulses applied to voltage-clamped chromaffin cells perifused with extracellular solutions containing 1 mM Ca^{2+} ($1Ca^{2+}$), 2 mM Ca^{2+} ($2Ca^{2+}$) or 10 mM Ca^{2+} ($10Ca^{2+}$). Cells were voltage-clamped at -80 mV, under the perforated-patch configuration of the patch-clamp technique and were stimulated at 5-min intervals with 500-ms pulses to 0 mV (when in 1 or 2 mM external Ca^{2+}) or to +10 mV (when in 10 mM Ca^{2+}) . **A**, inward Na^{+} currents (I_{Na}, arrow) and Ca^{2+} currents (I_{Ca}, horizontal double arrow) obtained using the top protocol, in a cell perifused first with $1Ca^{2+}$, and then with $2Ca^{2+}$ and $10Ca^{2+}$ solutions. **B**, Cm changes (fF, ordinate) elicited by the I_{Ca} shown in **A**; exocytosis (ΔCm) in $1Ca^{2+}$, $2Ca^{2+}$ and 10 Ca^{2+} is indicated by left vertical double-head arrows and endocytosis (Cm decay) by right vertical double-head arrows. Dotted line represents basal Cm. **C**, I_{Ca} peak (pA, left ordinate) and Q_{Ca} (Ca^{2+} entry as determined by I_{Ca} area, Q_{Ca} in pC, right ordinate). **D**, exocytosis measured as initial Cm jump (ΔCm in fF, ordinate). **E**, ratios between endocytosis and exocytosis (Endo/Exo). Data in bar graphs **B** to **E** are means ± s.e. of 15 cells from at least 3 different cultures. ** $p< 0.01$, compared with $1Ca^{2+}$.

Figure 2

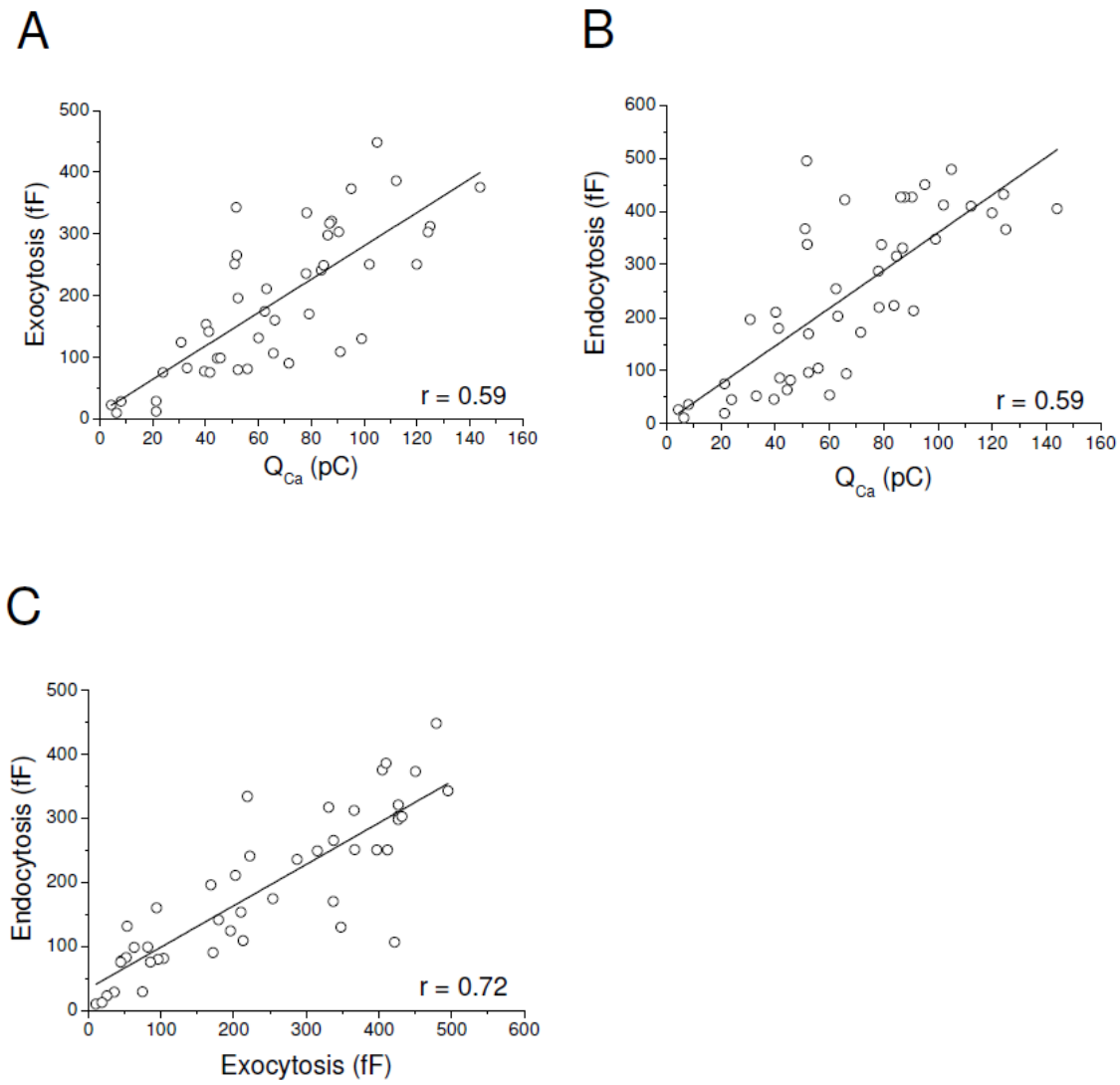

Fig. 2: Regression plot of the relationship between total Ca^{2+} entry (Q_{Ca}) evoked by 500-ms pulses, exocytosis, and endocytosis. Data from all cells of Fig. 1 in 1, 2, or 10 mM Ca^{2+}, were plotted together to find out the correlation coefficients (r) of exocytosis versus Q_{Ca} (**A**), endocytosis versus Q_{Ca} and endocytosis versus exocytosis (**C**).

Figure 3

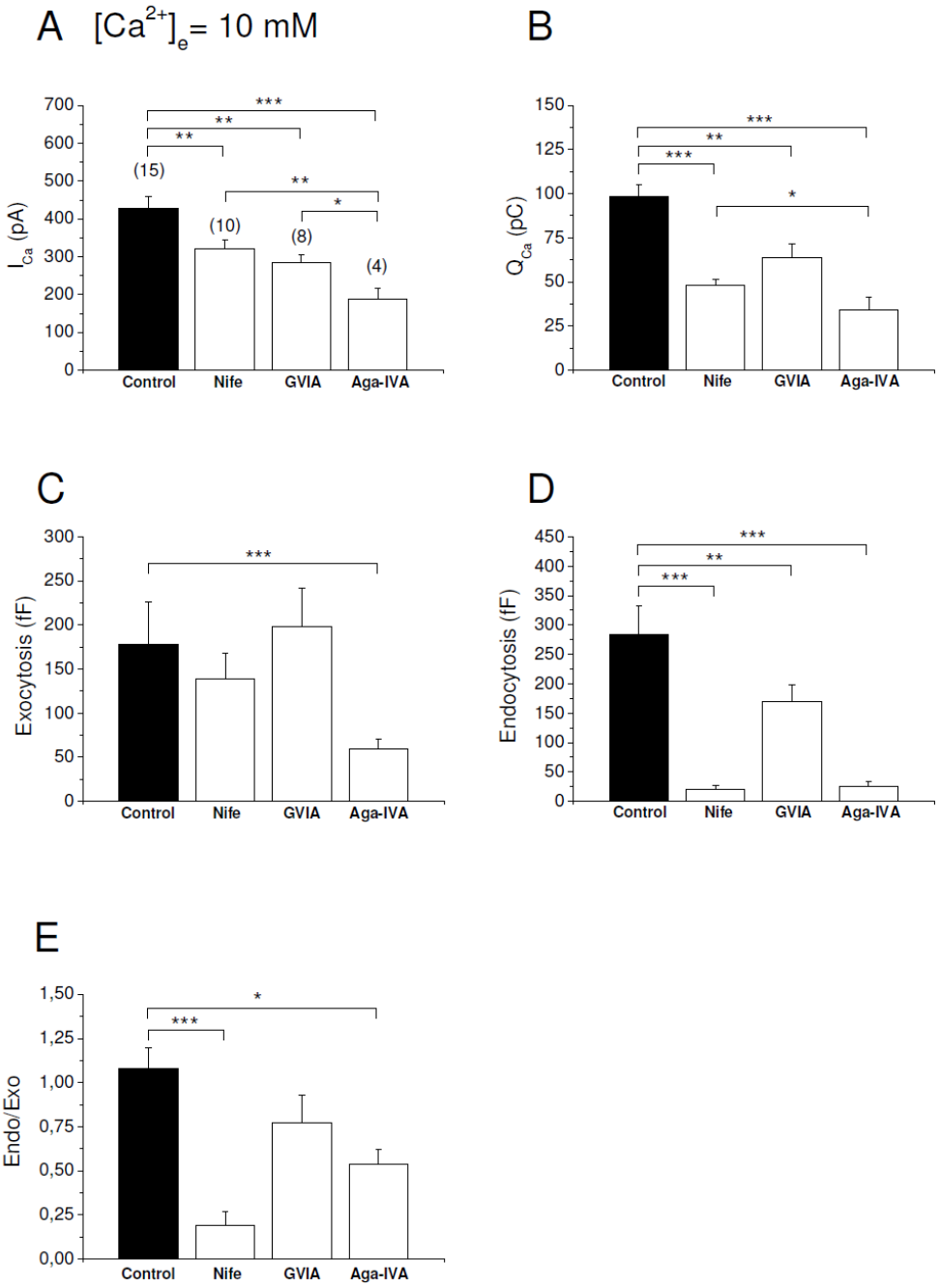

Fig. 3: Effects VDCC blockers on I_{Ca}, Q_{Ca}, exocytosis and endocytosis. Cells voltage-clamped at -80 mV were challenged with 500-ms depolarising test pulses to +10 mV, in 10 mM external Ca^{2+}. Blockers were added separately with external solutions and cells were perifused with them for 2 min prior to stimulation. Averaged pooled results of I_{Ca} **(A)** and Q_{Ca} **(B)** in the absence (black columns) and the presence of blockers (white columns). **C,** exocytotic responses. **D,** endocytotic responses. **E,** Endo/Exo relationship corresponding to the same cells of **C** and **D**. Data are means ± s.e.m. of cell number shown in parentheses from at least three different cultures. *p<0.05; **p<0.01; ***p<0.001 compared to control.

Figure 4

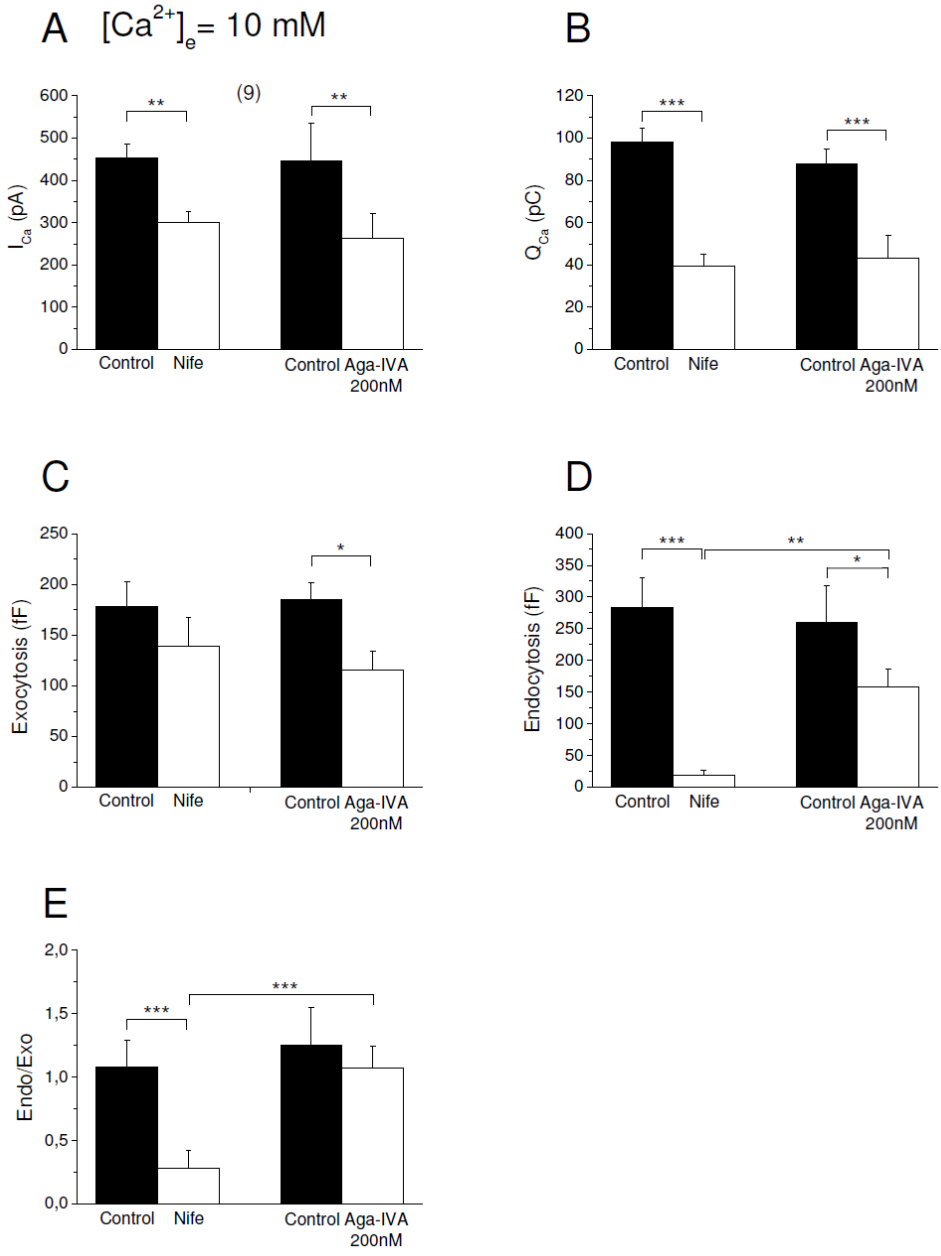

Fig. 4: Comparison of the effects of a low concentration of Aga-IVA (200 nM) and nifedipine on I_{Ca}, Q_{Ca}, exocytosis and endocytosis. Cells were voltage-clamped at -80 mV and stimulated with 500-ms depolarising pulses in the absence (black columns) or presence of L-type VDCC blocker (nifedipine, 3 μM) or PQ-type calcium channel blocker (AgaIVA; 0.2 μM) (white columns). Averaged data of I_{Ca} and Q_{Ca} were represented in **A** and **B**. **C** and **D** represents the capacitance changes from the same cells of A and B. Endo/Exo relationships are shown in **E**. Data are means ± s.e.m. from 9 cells belonging to three different cultures. *p<0.05; **p<0.01; ***p<0.001.

Figure 5

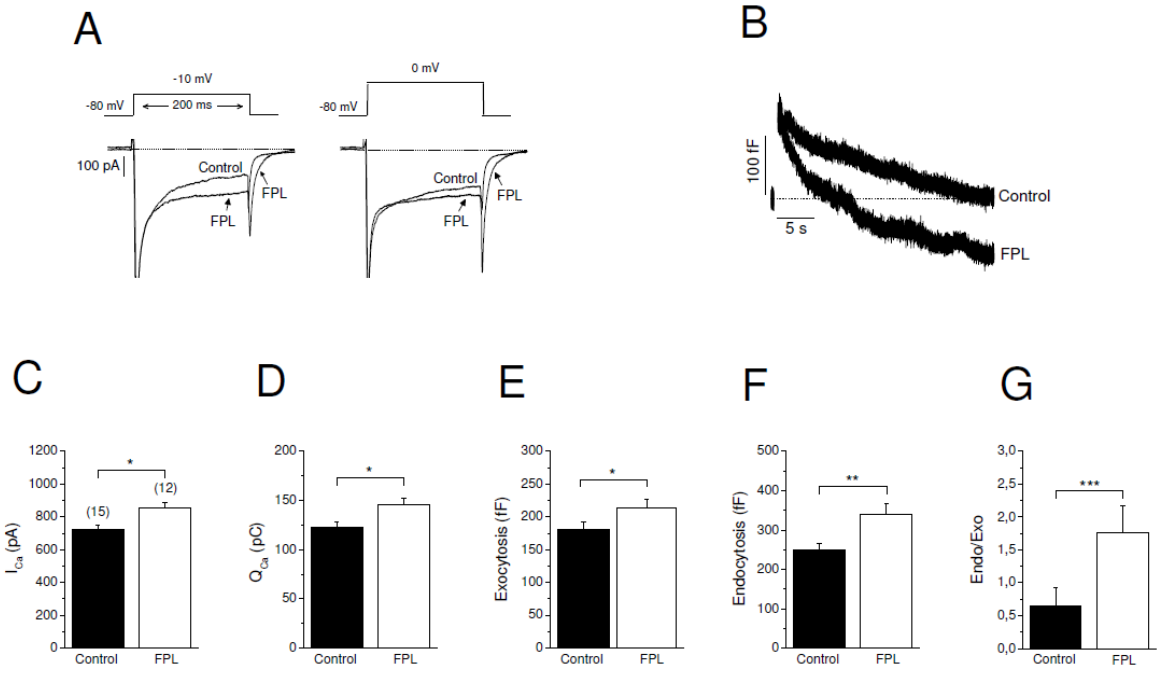

Fig. 5: Increase of L calcium current elicited by FPL64176 (FPL, 1 μM) augments endocytotic responses. Cells were incubated during 45 min with cell permeable EGTA.AM at 37ºC and subsequently washed during 15 min at room temperature. Then, cells were patched, voltage-clamped at -80 mV, and stimulated with 500-ms depolarising pulses using the usual protocols. **A** Example trace currents generated by test pulses to the voltages indicated at the protocol on top, before (control) and at 2 min of FPL treatment. (B) Cm traces originated by depolarising pulses in the absence (control) or presence of FPL. **C** and **D**, pooled results on the effects of FPL on I_{Ca} and Q_{Ca}. **E,** Endo/Exo relationship. Data are means ± s.e.m. of cell number shown in parentheses from at least three different cultures. *p<0.05; **p<0.01; ***p<0.001 compared to control.

Figure 6

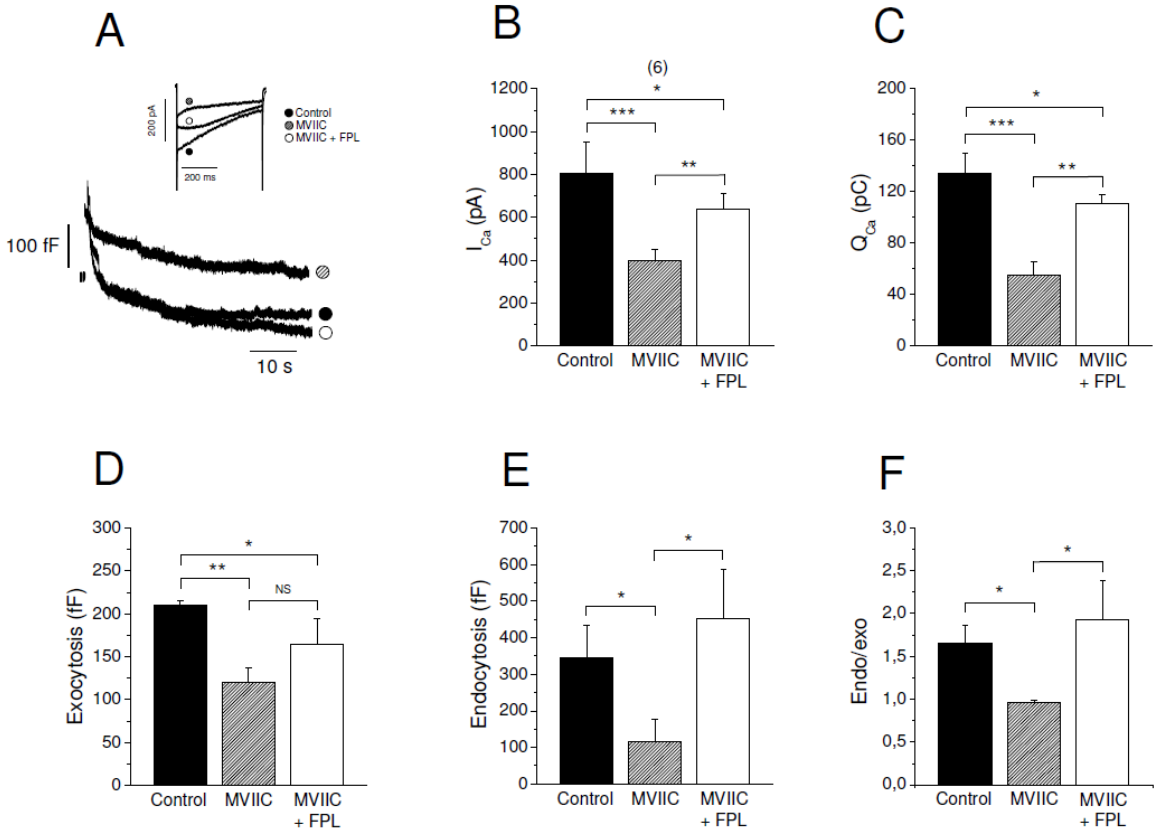

Fig. 6: Augmentation of Ca^{2+} entry through L-type VDCCs by FPL64176 (FPL; 1 μM) increased the endocytotic responses in cells treated with ω-conotoxin MVIIC (MVII, 2 μM). Cells were voltage-clamped at -80 mV and stimulated with 500-ms depolarising pulses. **A,** example traces of I_{Ca} (top) and capacitance changes (bottom) generated by depolarising pulses given before (control), at 2 min of MVIIC treatment, and at 2 min of combined MVIIC+FPL treatment. **B** and **C,** Pooled averaged results of peak I_{Ca} and Q_{Ca}, respectively. **D** and **E,** the endocytosis and exocytosis responses produced by I_{Ca} in the same cells. **F,** ratios between endocytotic and exocytotic responses (Endo/Exo, ordinate). Data are means ± s.e.m. of 6 cells from 3 different cultures. *p<0.05; **p<0.01; ***p<0.001.

Figure 7

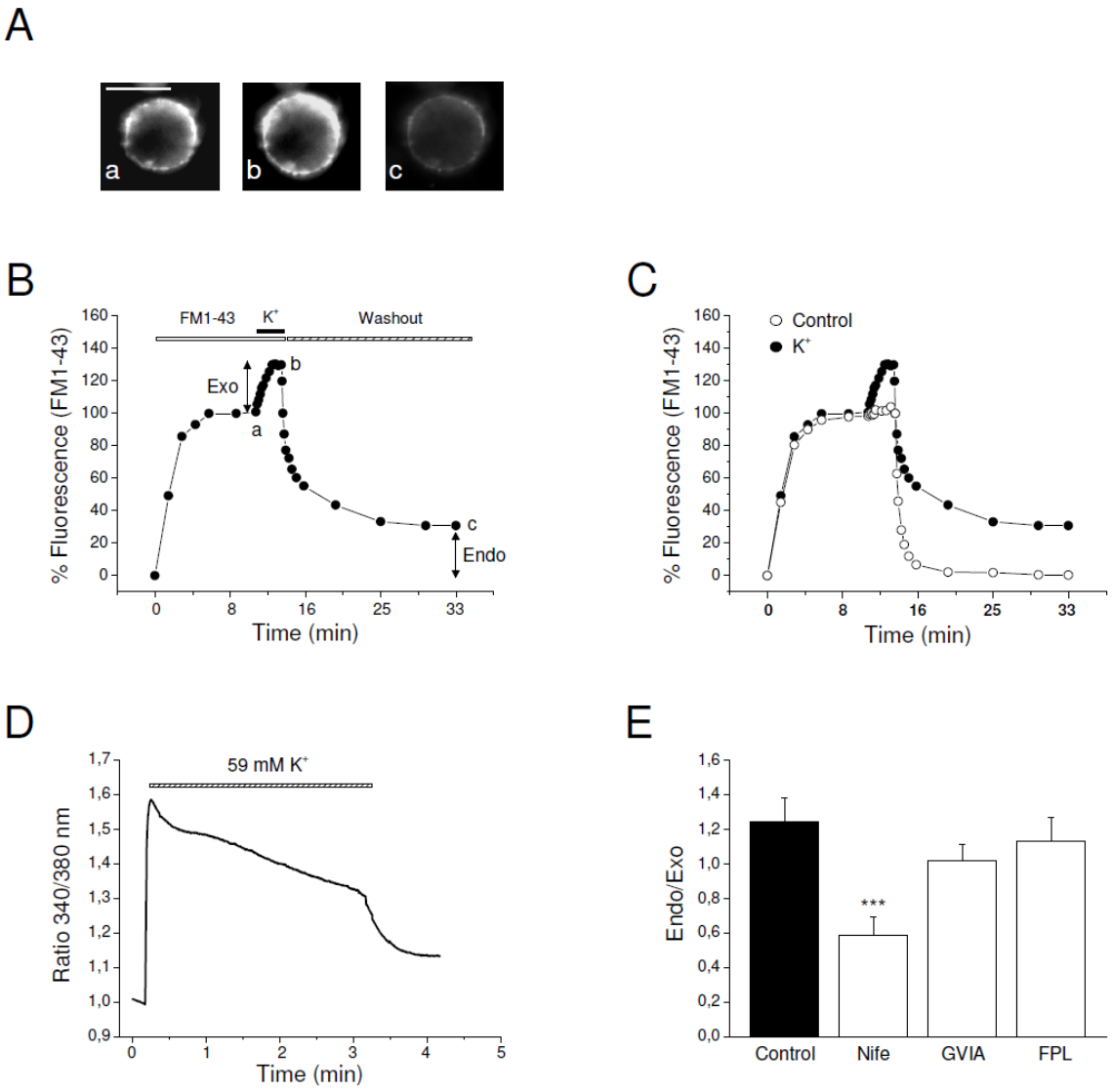

Fig. 7: Exocytotic and endocytotic responses monitored with FM1-43 dye, in cells stimulated with a high-K^+ solution: effects of VDCC modulators. Cells were incubated with FM1-43 and stimulated with a 3-min pulse of a 59 mM K^+ solution (K^+). **A,** FM1-43 fluorescence distribution in a cell under resting conditions (a), at the end of the K^+ pulse (b), and at the end of the washout period. **B,** time course of the fluorescence variations in the cell of panel A, in the presence of FM1-43 before (100% fluorescence) and during the 3-min period of K^+ stimulation. The increase of fluorescence above the resting plateau indicates exocytosis triggered by K^+ (double-head arrow). Upon washout of FM1-43 and K^+, fluorescence decayed to a plateau that indicates the FM1-43 taken up by the cell due to membrane retrieval (endocytosis) (double-head arrow to the right); letter a, b, and c correspond to the microphotographs shown in A. Time course of FM1-43

fluorescence variations in a resting cell (control), superimpose to the curve shown in B, where the cell was stimulated with K^+. **D**, variations of the cytosolic $[Ca^{2+}]_c$ concentrations elicited by K^+ in the same cell, loaded with fura-2. **E,** effects of 3 μM nifedipine (Nife), 1 μM ω-conotoxin GVIA (GVIA), 1 μM ω-conotoxin MVIIC (MVIIC) and 1 μM FPL64176 (FPL) on the ratios between the endocytotic and exocytotic responses (Endo/Exo, ordinate) measured with the protocol shown in B; data are means ± s.e.m. of 15 cells from 4 different cultures. ***$p<0.001$.

Figure 8

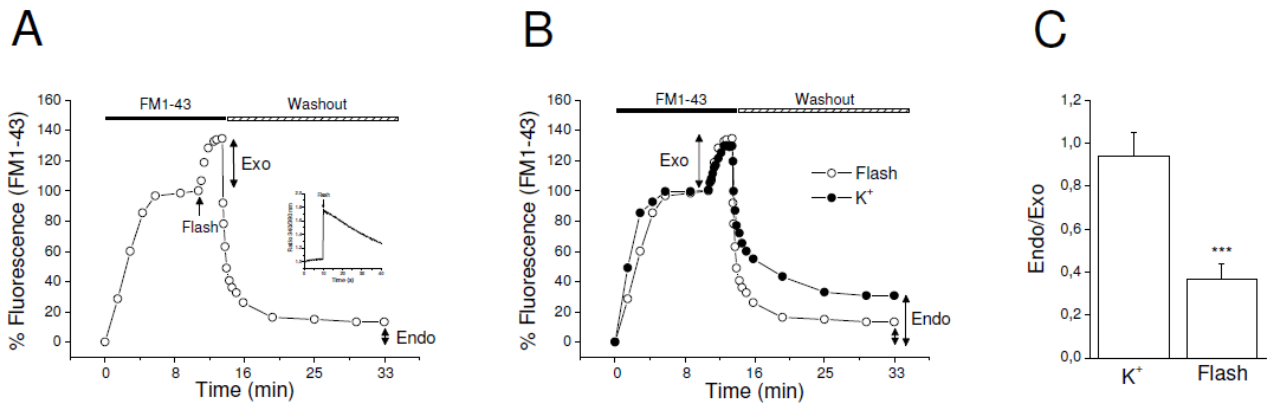

Fig. 8: Exocytotic and endocytotic responses triggered by photoreleased caged Ca^{2+}, monitored with FM1-43. **A,** example cell loaded with o-nitrophenyl EGTA.AM, with FM1-43; fluorescence reached an equilibrium plateau after 10 min (100 % fluorescence); then, the cell was stimulated with the light flash, followed by FM1-43 washout. The exocytotic and endocytotic responses are shown by double-head arrows. Inset, time course of $[Ca^{2+}]_c$ variations evoked by the light flash. **B,** comparative exo- and endocytotic responses triggered by the light flash and by K^+ in a control cell. **C,** ratios between endocytotic and exocytotic responses (Endo/Exo, ordinate) triggered by K^+ or light flash pulses; data are means ± s.e.m. of 12 cells from 4 different cultures. ***p<0.001.

Figure 9

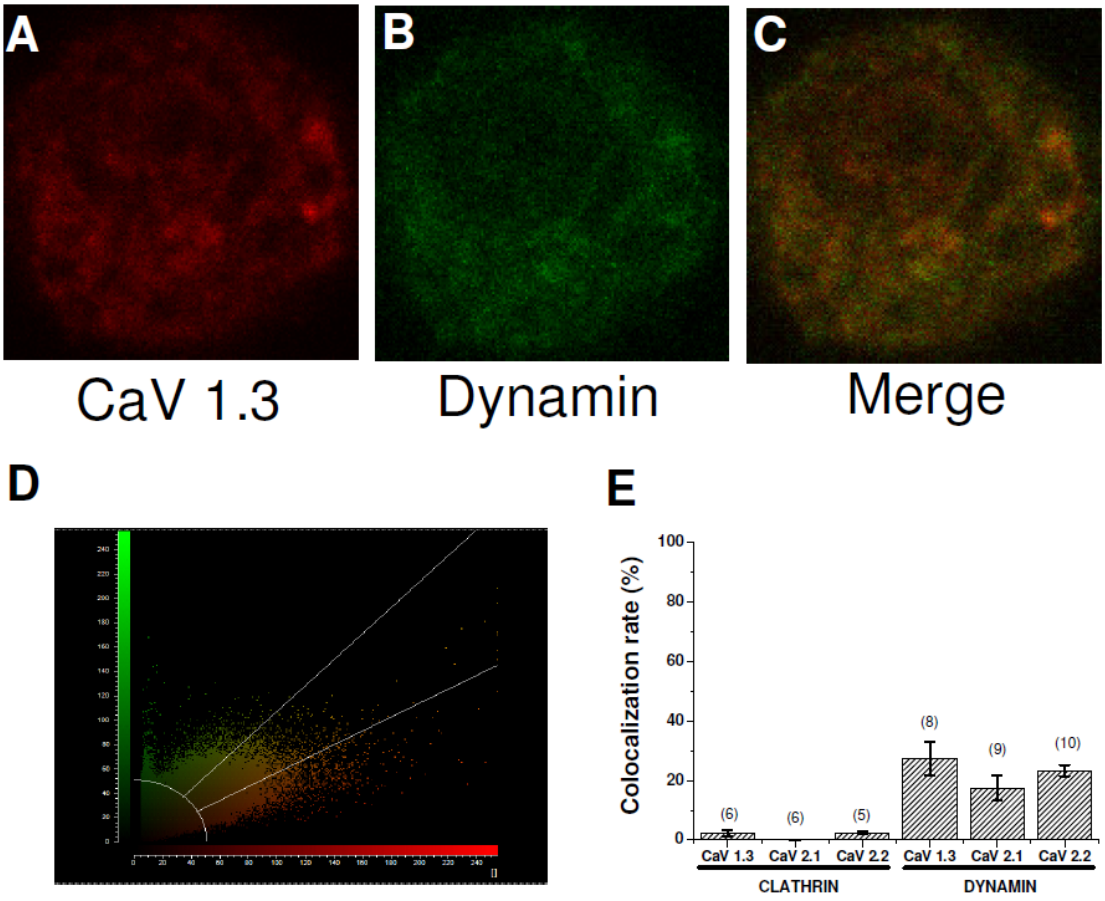

Fig. 9: Coupling of dynamin or clathrin with the different calcium channel subtypes present in bovine chromaffin cells. Figure shows representative examples of high magnification confocal images of cultured bovine chromaffin cells presenting anti-CaV 1.3 (**A**) or anti-dynamin (**B**) labeling. Co-localization was observed as spatially matched pixels in both channels (**C**). Panel **D** shows a representative scattergram to indicate the limits used to analyse the co-localisation of dynamin or clathrin with the three calcium channel subtypes studied. Panel **E** shows average data obtained on the co-localisation rate (%) of anti-clathrin or anti-dynamin labeling with anti-CaV1.3, anti-CaV2.1 or anti-CaV2.2 labelling. Data are means $\pm$ s.e.m. of 5-9 cells from at least 3 different cultures.

Journal of Neurochemistry original article (under review)

Ca^{2+} entry during PQ calcium channel deactivation matters for the control of exocytosis and endocytosis

Juliana M. Rosa[1,2], Angela Orozco[1,2], Inés Colmena[1,2], Ricardo de Pascual[1,2], Antonio G. García[1,2,3] and Luis Gandía[1,2*]

[1]Instituto Teófilo Hernando, [2]Departamento de Farmacología y Terapéutica, [3]Servicio de Farmacología Clínica del Hospital Universitario de la Princesa; Facultad de Medicina, Universidad Autónoma de Madrid, Madrid, Spain.

Abstract: Neuroendocrine cells and neurons express different types of voltage-dependent calcium channels (VDCCs). Why cells express then and whether a given channel is specialized to perform a specific function are puzzling and unanswered questions. Many pharmacological tools have been used to study biophysical and pharmacological properties of VDCCs, some of them as antagonistic. L-type calcium channel is the only subtype of VDCC to possess activators (e.g. FPL64176 and Bay K8466) that augment the calcium entry at hyperpolarised potentials and slow the current deactivation. Depending on the stimulus, stimulation pattern, animal specie, and the methods used to measure exocytosis or catecholamine release, certain specialization to modulate exocytosis has been suggested. Identifying novel pharmacological activators will provide new answers for understanding the role of these channels in the secretory mechanisms. Roscovitine has been reported to slow the deactivation of Cav2, although many controversies have been found as far as calcium channel subtypes are concerned. Here, we studied the effects of roscovitine on calcium entry and exocytosis on chromaffin cells that express L-, N- and PQ-type VDCCs. Roscovitine augments the tail current in a concentration-dependent manner without affecting the calcium current peak. ω-conotoxin MVIIC (N- and PQ-blocker) and ω-agatoxin AgaIVA (PQ-blocker), but not nifedipine (L-blocker) or ω-conotoxin GVIA (N-bloker) eliminated the roscovitine-elicited activator effect, suggesting an action on PQ-channels. On the other hand, using a train of depolarising pulses roscovitine was able to increase the exocytotic response. This effect was seen in a better way when N- and L-channels were blocked. In addition, augmenting the calcium entry by L-tail current using the activator FPL64176 (1 μM) did not modify the exocytotic response. Our data demonstrate that the augment of calcium entry by slowing deactivation of PQ-type calcium channel, but not by L-channels, increase the exocytotic response using a train of depolarising pulses, suggesting a specific role of calcium entry by PQ-channels on secretory mechanisms. **Key Words:** roscovitine, PQ-calcium channels, exocytosis, endocytosis, tail current.

Correspondence to: Luis Gandía; Instituto Teófilo Hernando, Facultad de Medicina, Universidad Autónoma de Madrid; Arzobispo Morcillo, 4 28029 Madrid, Spain. (luis.gandia@uam.es)

Tail currents (I_{tail}) are generated during the closing of a voltage-dependent pulse (DP) used to elicit its opening finalises (Hille et al., 2000). In the case of high-voltage activated (HVA) calcium channels the amount of Ca^{2+} entering the cell during the duration of I_{tail}, accounts for only a small fraction of the whole-cell current elicited by a DP. For instance, in a bovine adrenal chromaffin cell voltage-clamped at -80 mV, a 100-ms DP produces 100 pC of total Ca^{2+} entry using 2 mM external Ca^{2+} as charge carrier. In contrast, Ca^{2+} entering the cell during I_{tail}, accounts for only 10 pC (de Diego et al., 2008). The question therefore arises to whether the minute amount of Ca^{2+} entering the cell during I_{tail} has any physiological role in many Ca^{2+}-dependent processes of excitable cells among others, exocytosis and endocytosis (Neher, 1998; Garcia *et al.*, 2006; Neher, 2006).

In trying to provide some clues to answer this question we recoursed to the bovine adrenal chromaffin cells for various reasons (Garcia et al., 2006): (i) various of the HVA calcium channels are expressed in these cells, namely L-type (α_{1D}, $Ca_v1.3$), N-type (α_{1B}, $Ca_v2.2$), and PQ-type (α_{1A}, $Ca_v2.1$); (ii) the role of such channels in controlling exocytosis and endocytosis has been widely studied; (iii) selective blockers for such channels are available, namely nifedipine for L channels, ω-conotoxin GVIA (GVIA) for N channels, ω-agatoxin IVA (AgaIVA) for PQ channels, and ω-conotoxin MVIIC (MVVIC) for N and PQ channels; (iv) this spherical, readily available cell became an excellent model soon after the patch-clamp techniques appeared (Hamill et al., 1981), for studies of ion currents, Ca^{2+} signalling, exocytosis, and endocytosis (Neher, 1998).

The discovery of 1,4-dihydropiridine (DHP) derivatives as blockers of cardiac and smooth muscle L-type HVA calcium channels constituted a therapeutic hallmark for the treatment of various cardiovascular diseases (Fleckenstein, 1977). But in addition to this clinically relevant facet, nifedipine and other numerous DHPs have extensively been used as pharmacological tools to explore the many cell functions regulated by L-type channels. This field underwent a breakthrough with the discovery of BayK8644 (BayK), a DHP derivative with a molecular structure similar to nifedipine but having just the opposite effects, i.e. vasoconstriction, tachycardia and augmentation of the strength of heart contraction (Schramm et al., 1983). This was the beginning of a pleyade of studies that used BayK as a pharmacological tool to explore several Ca^{2+}-dependent functions linked to Ca^{2+} entry through L VDCCs. Because of the therapeutic potential of BayK, several pharmaceutical companies soon synthesised new DHP derivatives to activate L channels, namely Sandoz 200-791 (Kongsamut et al., 1985) or compounds having non-DHP moieties but acting as potent L channel agonists, for instance FPL64176 (FPL) (Zheng et al., 1991).

The study of L calcium channel gating and permeation has been greatly facilitated by BayK, +202-791, and FPL that increase channel open time over a wide range of voltages, slows their deactivation kinetics and prolong the tail current (I_{tail}) (Hess *et al.*, 1984; Kokubun & Reuter, 1984; Nowycky *et al.*, 1985; Zheng *et al.*, 1991; Kunze & Rampe, 1992; Tavalin *et al.*, 2004). This is not the case for N or PQ channels that until recently, only toxin blockers of such channels were

available, for instance ω-conotoxin GVIA (GVIA) for N channels, ω-agatoxin IVA (AgaIVA) for PQ channels, and ω-conotoxin MVIIC (MVIIC) for N and PQ channels (Olivera *et al.*, 1994; Garcia *et al.*, 2006; Gandía *et al.*, 2008). However, Yan et al reported in 2007 that the cyclin-dependent

kinase (cdk) inhibitor roscovitine (Hellmich et al., 1994; Tsai et al., 1994) slowed the deactivation of HVA calcium channels that were insensitive to DHPs; this effect was erased by MVIIC, a finding that led the authors to conclude that roscovitine targets PQ channels. However, the micromolar concentrations of MVIIC used by Yan et al (2002) also block N channels (Grantham *et al.*, 1994; Gandia *et al.*, 1997), leaving open the question of whether the compound also targeted N channels. In fact, roscovitine was later on found to also slow N channel deactivation in bullfrog sympathetic neurons (Buraei et al., 2005) as well as in the tsA201 cell line expressing the N channel (DeStefino et al., 2010). Furthermore, roscovitine was later on found to behave as a kind of promiscuous compound since it slows the deactivation of all calcium channels belonging to the Ca_v2 family (N, PQ, R) and blocked several potassium channels, i.e. $K_v1.3$, $K_v2.1$ and $K_v4.2$ (Buraei et al., 2007).

If roscovitine slows calcium channel deactivation of N and PQ channels, it was expected that this could lead to enhanced Ca^{2+} entry and neurotransmitter release, as the case is for BayK acting on L channels, that drastically augments K^+-evoked catecholamine release from chromaffin cells (Garcia et al., 1984). In fact, roscovitine enhances glutamate release at presynaptic terminals of hippocampal neurons, as monitored with the vesicle dye FM1-43 (Yan et al., 2002) and also augments neurotransmitter release at the neuromuscular junction (Cho & Meriney, 2006).

In this report, we present a study aimed at characterising the effects of roscovitine on whole-cell I_{Ca} as well as on exocytotic and endocytotic responses triggered by depolarising pulses (DPs) applied to voltage-clamped bovine adrenal chromaffin cells. We found that roscovitine only targeted the PQ-type of calcium channels, leaving untouched the L or N channels. Furthermore, we found that roscovitine did not affect the amplitude or kinetics of I_{Ca} through PQ channels, but caused a pronounced slowing of current deactivation. This led to enhanced exocytosis and to the reversal of nifedipine-inhibited endocytotic responses (Rosa et al., 2007).

Methods

Isolation and culture of bovine chromaffin cells. Bovine adrenal glands were obtained from a local slaughterhouse. Chromaffin cells were isolated by digestion of the adrenal medulla with collagenase following standard methods (Livett, 1984) with some modifications (Moro *et al.*, 1990). Cells were suspended in Dulbecco`s modified Eagle`s medium (DMEM) supplemented with 5% fetal calf serum, 10 µM cytosine arabinoside, 10 µM fluorodeoxyrudine, 50 IU ml^{-1} penicillin and 50 µg ml^{-1} streptomycin. Cells were plated on 12 mm-diameter polylisine-coated

glass coverslips at a density o f $5x10^4$ cells/coverslip for patch-clamp experiments or $5x10^5$ cells/coverslip for FM1-43 and flash-photolysis experiments. Cells were kept in a water-saturated incubator at 37°C, in a 5% CO_2 – 95% air atmosphere, and used 2-5 days thereafter.

Recording of Ca^{2+} currents and membrane capacitance. Calcium currents (I_{Ca}) and membrane capacitance (Cm) were measured under the perforated patch configuration of the patch-clamp technique (Hamill *et al.*, 1981; Korn & Horn, 1989; Gillis *et al.*, 1991). During recording, cells were constantly perifused with a control Tyrode
solution at pH 7.4 containing (mM): 137 NaCl, 1 $MgCl_2$, 10 glucose and 10 HEPES. To perform the experiments to study the effects of roscovitine on currents, 10 mM Ba^{2+} was added to the extracellular solution. In experiments to study the secretory response, 10 mM Ca^{2+} was used as charge carrier instead of Ba^{2+}. Internal perforated-patch solution had the following composition (mM): 135 CsGlutamate, 10 HEPES, and 9 NaCl, and the pH was adjusted to 7.2 with CsOH. An amphotericin B stock solution was prepared every week at 50 mg ml^{-1} in DMSO, stored at 4°C and, protected from light. Fresh perforated patch pipette solution was prepared every day by the addition of 10 µl of the amphotericin B stock solution to 1 ml CsGlutamate internal solution. This solution was sonicated thoroughly, protected from light and kept on ice. Patch pipettes had their tips dipped in amphotericin-free solution for 5-10 s and then were back-filled with freshly mixed amphotericin-containing solution. Cells were perforated to a series resistance of no more than 30 MΩ, which usually happened within 10-min after sealing. For patching the cells, pipettes of approximately 2-3 MΩ resistance were pulled from borosilicate glass, partially coated with molten dental wax, and lightly fire polished. Cells were continuously perifused with external solution at a rate of 1 ml min^{-1} and all experiments were performed at room temperature (25-28°C). Electrophysiological data was carried out using an EPC-9 amplifier under the control of Pulse software (HEKA Elektronik). Cell membrane capacitance (Cm) changes were estimated by the Lindau-Neher technique (Lindau & Neher, 1988). A 400-ms sinusoidal wave (1 kHz, 60 mV peak to peak amplitude) was then added before the protocol and a 50-s sinusoidal wave of the same characteristics after it, to allow for the computation of membrane capacitance change. Membrane current was sampled at 20 kHz. VDCC blockers were perifused as indicated.

Cells were held at -80 mV and I_{Ba} were generated by depolarising voltage steps of 50-ms duration to sequentially increasing test potentials by 10 mV-step increments from -50 to +50 mV. Test pulses were delivered at 10-s intervals to minimise the rundown of Ca^{2+} currents (Fenwick *et al.*, 1982a). To generate an exocytotic response, a train of 10x20 ms step depolarisations from -80 to +10 mV at 80 ms intervals was applied. Between each pulse, a 40-ms sinusoidal wave (1 kHz, 60 mV peak to peak amplitude) was added.

Materials and solutions. Collagenase type I, nifedipine, roscovitine and amphotericin B were purchased from Sigma (Madrid, Spain). Dulbecco's modified Eagle's medium (DMEM), bovine serum albumin fraction V, foetal calf serum and antibiotics were purchased from Gibco (Madrid, Spain). Agatoxin-IVA was from Peptide Institute (Sandhausen, Germany). ω-conotoxin GVIA and ω-conotoxin MVIIC were came from Bachem Feinchemikalien (Budendorf, Switzerland). ω-conotoxin GVIA and ω-conotoxin MVIIC were dissolved in distilled water and stored frozen in aliquots at 0.1 mM. Nifedipine and roscovitine (10^{-2} M) was prepared in dimethylsulphoxide (DMSO) and protected from light. Final concentrations of drugs were obtained by diluting the stock solution directly into the extracellular solution. At these dilutions, solvents had no effect on the parameters studied.

Data analysis. The whole-cell inward Ca^{2+} or Ba^{2+} current peak (I_{Ca} and I_{Ba}), and the current area representing the total Ca^{2+} that entered the cell during a depolarising stimulus (Q_{Ca}), were analyzed after the initial 10-ms of each depolarising pulse, to get rid of the Na^+ current. In order to measure the component of the tail current, a second
cursor was approximately placed 3-ms after the end of the test pulse. Q_{total} was analyzed as the whole I_{Ca} integral area to 3-ms after repolarisation and Q_{tail} as the area of the end of the test pulse to 3-ms. I_{Ca} was not leak subtracted, and only cells with a leak current <30 pA were included in the analysis. Exocytosis steps were measured by subtracting the basal mean Cm obtained 400-ms previous to depolarisation to 50-ms after the end of the depolarising pulse to avoid a possible Na^+ channel gating artefact (Horrigan & Bookman, 1994). After the exocytotic peak, Cm changes were measured during the ensuing 50-s period; endocytosis was calculated as the difference in Cm at the beginning and the end of such 50-s period. Comparisons between means of group data were performed by one-way analysis of variance (ANOVA) followed by the Duncan post-hoc test when appropriate. A $P \leq 0.05$ was taken as the limit of significance. Data are expressed as mean ± s.e.

Results

Roscovitine increases the amplitude of the tail current but doesn't affect the current peak.
Firstly, we designed experiments to test how roscovitine, a calcium-kinase dependent inhibitor, modified the amplitude and charge of peak and tail current generated by depolarising pulses. In the example records of Fig. 1A, a cell perifused with 10 mM Ba^{2+} in presence or absence of roscovitine was voltage-clamped at -80 mV and a 50-ms pulse to 10 mV was applied to generate an inward current (I_{Ba}). The current trace exhibited an initial fast-inactivating Na^+ current (I_{Na}), that was followed by the non-inactivating I_{Ba} and finally by a deactivating tail current (I_{tail}) generated by channel closing upon returning to -50 mV (see protocol on top of Fig. 1A). After 30 s of perifusion with 100 μM roscovitine, no modifications of the peak and current kinetics were

observed. However, a drastic difference was observed as far as I_{tail} was concerned (open circle in Fig. 1A). The tail current component (measured at 3 ms after the initiation of repolarisation) had greater amplitude and lasted longer in the presence of roscovitine than in control cells (Fig. 1B). So, we asked whether roscovitine could be shifting the I-V curve having its effects at more negative or positive voltages. For this, cells were stimulated with depolarising pulses of increasing strength (see indicated voltages in abscissa scale, Fig. 1C) given at 10-s intervals, before and after perifusion with roscovitine. In the presence of roscovitine no shifts of the I-V curve were observed on peak current (the currents generated are plotted on the ordinate scale). In addition, the enhancement of the long lasting component of the tail current measured at different voltages was greater and greater, suggesting that the actions of roscovitine on I_{tail} are voltage-dependent (Fig. 1D). Concentration-response curves showed that at 1-100 μM, roscovitine did not affect the amplitude of I_{Ba} peak (Fig. 1E); however, I_{tail} measured at +10 mV was enhanced by roscovitine in a concentration-dependent manner, exhibiting an EC50 of 20 uM.

Effects of roscovitine on the I_{Ba} remaining after treatment with nifedipine or ω-conotoxin GVIA. Bovine chromaffin cells express VDCCs at different densities, i.e. 20% L-type channel, 30% N-type channel and 50% PQ-type channel (Albillos *et al.*, 1993; Gandia *et al.*, 1993a). Perifusion of voltage-clamped chromaffin cells with different blockers given for 30-120 s, dissect subcomponents of the whole-cell inward Ca^{2+} channel current, at the
following maximal concentrations: 3 μM nifedipine for L-type channels, 1 μM ω-conotoxin GVIA for N-type channels, and 1 μM ω-agatoxin IVA for PQ-type channels (Garcia *et al.*, 2006). To study the effects of roscovitine on I_{tail} of the different VDCC subtypes, we designed an experiment consisting in an I-V control curve, followed by other I-V curve in the presence of the blocker which was perifused since 2 min before each I-V curve, and subsequently with the combination of roscovitine plus a given blocker during a 30-s period before the stimulus; finally one I-V curve was once more obtained after blocker plus roscovitine washout. To plot the normalised values, the original traces of I_{Ba} and I_{tail} were measured at a test potential of +10 mV.

Fig. 2 shows the effects of various blockers on I_{Ba} and I_{tail} in presence or absence of roscovitine (100 μM). Fig. 2Aa shows example traces from one cell stimulated with depolarising pulses and perifused with 10 mM Ba^{2+} in control conditions (tilled circle), in presence of N-type channel blocker GVIA plus roscovitine (open circle) and after washout (tilled triangle). The blockade of N-channels by GVIA has been described to be ~30% and does not recover upon washout (Gandia *et al.*, 1993a; Garcia *et al.*, 2006). When co-applied with GVIA, roscovitine did not change I_{Ba} peak (Fig. 2A), but increased the tail current by 5.3-fold that was fully recovered upon washout (Fig. 2A). Nifedipine (3 μM, nife) plus roscovitine quickly diminished I_{Ba} (about ~20%, Fig. 2B) that was proportional to the density of L-type VDCCs expressed by bovine

chromaffin cells (~20%) (Gandía et al., 2008). Again, roscovitine did not affect I_{Ba} peak (Fig. 2Bb). However, the compound augmented the I_{tail} by 7.7-fold (Fig. 2Bc); washout led to current recovery (Fig. 2Bc). MVIIC blocks N- and PQ-types of calcium channel; although its blocking actions are mitigated in 10 mM Ba^{2+} (Albillos *et al.*, 1996b). Co-application of MVIIC plus roscovitine decreased I_{Ba} by 40%, suggesting that roscovitine did not affect I_{Ba} peak (Fig. 2Ca,b). On the other hand, the blockade of N- and PQ-type channels inhibited the augmentation of I_{tail} elicited by roscovitine (Fig. 2C). These data suggest that the effect of roscovitine on augmentation of I_{tail} is exerted at PQ channels. To confirm this hypothesis, we used ω-agatoxin IVA (AgaIVA) to inhibit specifically PQ-type channels. Under these conditions, roscovitine did not augment the I_{tail}, reinforcing the view of a specific effect of roscovitine on PQ-type VDCCs (Fig. 2Da,b,c).

Roscovitine did not affect the exocytotic response triggered by a single depolarising pulse. In a recent study from our laboratory, we explored how the variations in Ca^{2+} entry with DPs of increasing length (50-2000 ms) changed the membrane capacitance on chromaffin cells. In this study we measured Cm changes during the 8-s period that followed the DP, and found that exocytotic responses (ΔCm) augmented as a function of DP duration; however, endocytotic responses (Cm decline after peak ΔCm) were absent with short DPs (50-200 ms) and were visible and pronounced with longer DPs (500-2000 ms) (de Diego *et al.*, 2008). Based on these data, we made tentative experiments with 200 ms-DPs (that caused an intermediate exocytotic response) to explore whether the size of the initial exocytotic Cm jump could be increased by augmenting Ca^{2+} entry secondary to I_{tail} slowing by the action of roscovitine on PQ channels. On the other hand, we used 500 ms-DPs to explore whether roscovitine could also change the endocytotic response. Cells were voltage-clamped at -80 mV and single depolarising pulses
at +10 mV (the voltage where maximum peak I_{Ca} was achieved) were applied in control conditions and after 30-s perifusion with 100 μM roscovitine. These experiments were performed in 10 mM external Ca^{2+}, using the perforated patch configuration of the patch clamp technique.

Fig. 3 shows example Cm traces from cells stimulated with 200 and 500-ms DPs in control conditions (control) and after roscovitine application (Ros). Although roscovitine augmented I_{tail} and hence Ca^{2+} entry this Ca^{2+} was not able to modify neither exocytotic (Fig. 3A) nor endocytotic responses (Fig. 3B).

Roscovitine augments exocytosis triggered by a train of depolarising pulses. Increasing Ca^{2+} entry by slowing deactivation of PQ-channels using the pharmacological tool rosocovitine did not modify the exocytosis evoked by single pulses. In trying to perform other experimental protocols to unmask a potential of roscovitine on exocytosis, we recoursed to the more physiological train of DPs. So, a train of 10 DPs of 20 ms duration delivered at 60 ms intervals was applied on cells from

-80 mV to +10 mV, before and after roscovitine application. $\sum Q_{total}$ was measured after the initial 10 ms at 3 ms at the end of each DP. $\sum Q_{tail}$ represents the area of the last 3 ms of I_{tail}. As shown in Fig. 4A, the application of DP train decreased I_{Ca} peak from 900 pA at the 1st DP to 400 pA at the last DP. This is in agreement with literature that demonstrates a Ca^{2+}-dependent component in the process of I_{Ca} inactivation in bovine chromaffin cells (Hernandez-Guijo et al., 2001). Roscovitine did not modify I_{Ca} peak nor I_{Ca} inactivation. Then, we analysed the averaged $\sum Q_{Ca}$ influx occurring during the 10 DPs. Under control conditions, $\sum Q_{Ca}$ rose to 85 ± 11 pC. Roscovitine did not modify the current peak, so $\sum Q_{Ca}$ influx was not significantly different when compared with control currents (96 ± 10 pC) (Fig. 4B). On the other hand, we analysed separately $\sum Q_{tail}$ before and after roscovitine perifusion. Roscovitine increased Q_{tail} from 1.2 ± 0.7 to 4.2 ± 0.7 pC at the 1st DP and from 8.5 ± 2.5 to 20 ± 1.3 pC at the 10th DP, as shown in Fig. 4C.

Fig. 4D represents an example of the exocytotic response in the same cell before (Control) and after roscovitine perifusion (Ros). Changes of membrane capacitance were measured ~30 ms after each step depolarisation, representing the exocytotic activity that occurs during the interpulse intervals and plotted with respect to the DP number. In control cells, the maximal exocytotic response (10th DP) reached 148 ± 4 fF. When roscovitine was present, this value increased to 212 ± 16 fF (Fig. 4E). These results suggest that even though roscovitine did not increase total $\sum Q_{Ca}$, the enhanced Ca^{2+} entering through PQ channels during their closure (I_{tail}) caused a 40% increase of exocytosis.

In bovine chromaffin cells, PQ channel currents accounts to approximately 50% of the whole-cell current; the rest is carried through N- and L- channels (Albillos *et al.*, 1993; Lopez *et al.*, 1994; Garcia *et al.*, 2006). In these cells, 3 μM nifedipine and 1 μM GVIA suppresses the L and N components of the whole cell inward current through Ca^{2+} channels. Therefore, in order to investigate the effect of PQ-tail current enhancement in conditions of isolation of PQ I_{Ca}, we recoursed to nifedipine and GVIA to block L and N currents, leaving the cell with its PQ current intact.

Under WCC recording, control cells exhibited I_{Ca} that were inhibited about 40% when an extracellular solution containing GVIA plus nifedipine was perifused, as shown in the original traces of Fig. 5A. Under these conditions where the remaining current was carried only through PQ channels, roscovitine did not affect I_{Ca} amplitudes (Fig. 5A). This is better seen when plotting cumulative Q_{Ca} (Fig. 5B). So, nifedipine and GVIA reduced Q_{Ca} by 43% in the 10th DP. When added on top of blockers, roscovitine did not modify Q_{Ca}. However, changes on tail charge were observed. $\sum Q_{tail}$ reached 4.3 ± 0.2 pC in control cells. This Q_{tail} value decreased to 3.6 ± 0.06 pC when blockers were perifused. However, roscovitine increased Q_{tail} to 5.08 ± 0.06 pC demonstrating its effect on PQ-I_{tail} (Fig. 5C). We therefore asked the question whether the enhancement of tail calcium entry by roscovitine through PQ channels could increase the

exocytotic response. In order to study the roscovitine effect on PQ-tail calcium induced exocytosis, membrane capacitance was measured before and after a depolarising train.

Fig. 5D and 5E show results obtained from experiments performed with the blockers in absence or presence of roscovitine. In control cells, the exocytosis amounted to 128 ± 19 fF. Data obtained in cells perifused with N and L channel blockers produced and exocytotic response of 51 ± 6.5 fF. However, in the presence of roscovitine such response underwent a pronounced activation of exocytosis that reached as much as 104 ± 14 fF. It seems therefore that roscovitine is acting on PQ channels slowing its closing and increasing the exocytotic response triggered by a train of DPs.

Enhanced Ca^{2+} entry through PQ-tail current selectively augments exocytosis. L-type calcium channel is the only subtype of VDCCs having specific activators (i.e. FPL64176 and Bay K8466) that augment Ca^{2+} entry and slow the I_{tail}. The effect on I_{Ca} peak is observed only at negative potentials; however, the effects on tail current is voltage-dependent (Liu et al., 2003; Rosa et al., 2009). FPL and BayK have been described to increase the exocytotic response at negative potentials where there is a maximum increase of Ca^{2+} entry through L-channels (XXXX). However, no studies about the role of Ca^{2+} entry through tail current on exocytosis were done in those studies. Therefore, here we designed an experiment to compare the effects on I_{tail} and exocytosis of roscovitine and FPL. To this purpose, cells were voltage-clamped at -80 mV and were stimulated with a DP train to +20 mV in the presence of FPL alone or given together with roscovitine. At +20 mV we did not observe an effect of FPL on I_{Ca} peak; however, an increase of I_{tail} was seen (Fig. 6A). Application of 1 μM FPL alone enhanced tail current to 5.2 ± 0.3 pC at 9.7 ± 0.8 pC (1.8-fold). Co-application of the two compounds induced an additive enhancement of tail currents of 2.3-fold (11.7 ± 1.1 pC). The clear additive effect of roscovitine and FPL-induced potentiation of tail currents suggests that these two drugs target different subtypes of calcium channels namely PQ and L, respectively.

We also made experiments to test the effects of FPL given alone or in the presence of roscovitine on exocytosis. Fig. 6B shows example traces from one cell stimulated with a DP train in control conditions, after 1-min perifusion with FPL and FPL plus roscovitine. The ΔCm reached 80 ± 16 fF in control cells and 85 ± 5.7 fF when FPL was applied. On the other hand, when roscovitine was co-applied with FPL, the additive effect on tail current induced a 1.6-fold augmentation of exocytosis (Fig. 6C). This result suggests that the increase of L-tail current by FPL does not modify the exocytotic response; however, enhancement of I_{tail} through PQ channels did give rise to enhanced exocytosis.

Roscovitine reverses the inhibitory effects of nifedipine on exocytosis and endocytosis. In a previous work, we demonstrated that the Ca^{2+} entering through L-type VDCCs is preferentially coupled to endocytosis in chromaffin cells (Rosa et al., 2007). This was corroborated in another study where endocytosis was partially inhibited by L channel blockers at the neuromuscular junction (Perissinotti et al., 2008). Here, we explored whether by enhancing Ca^{2+} entry via PQ channel I_{tail}, could reverse the inhibitory effects of nifedipine on exocytosis and endocytosis. Fig. 7A shows example traces from one cell stimulated with a DP train. In control conditions, the train induced an exocytotic response of 131 ± 15 fF and an endocytotic response of 95 ± 13 fF (Fig. 7B). Nifedipine decreased exocytosis to 98 ± 17 fF, indicating a 20% blockade of secretion. On the other hand, nifedipine reduced the endocytotic response to 31 ± 5 fF (Fig. 7C). In the presence of nifedipine, roscovitine augmented ΔCm to 149 ± 22 fF thereby promoting the full recovery of the endocytotic response (110 ± 20 fF). These data help to understand the endocytotic mechanisms in chromaffin cells and suggest a role of deactivation of PQ-channels on membrane retrieval and exocytosis.

Discussion

Roscovitine was firstly described as an activator of PQ-channels (Yan *et al.*, 2002). In this previous study, the increase of I_{tail} by roscovitine was inhibited when N and PQ channels were blocked with ω-conotoxin MVIIC, suggesting an action on PQ channels. However, there are many controversies about the calcium channel subtype that roscovitine acts. Some data have been demonstrated that roscovitine increases the I_{tail} to bind to N-type calcium channel (Buraei *et al.*, 2007; DeStefino *et al.*, 2010). These experiments were made in a cell preparation containing around 90% of N-type calcium channel or expressing heterologiouly different subtypes of VDCC. Our data corroborate that roscovitine binds to PQ channel increasing its time opening and the calcium entry by I_{tail}. Here, we used different blockers of VDCCs: nifedipine to L-channels, GVIA to N-channels, MVIIC to N- and PQ-channels and AgaIVA to PQ-channels (Garcia *et al.*, 2006; Gandía *et al.*, 2008). Nifedipine was not able to inhibit the slow deactivation presented by roscovitine as well as GVIA. When we used MVIIC to suppress N and PQ current we observed a total inhibition of I_{tail} augment. However, MVIIC has been known to inhibit inespecifically no-L calcium channel (Gandia *et al.*, 1997). For this reason we perifused the cells with AgaIVA to block only PQ channels observing a non-effect of roscovitine on I_{tail}. It is clear that roscovitine is delaying the PQ channel close and increasing the calcium entry into the cell.

In chromaffin cells and nerve terminals, PQ channels account almost 50% of the totality of VDCCs. These channels play an important role in stimulus-secretion coupling upon depolarisation stimuli. Until now, L-channel type was the only VDCCs subtype to have pharmacological tools to

increase the calcium entry. FPL64176 and BayK8644 augment the I_{Ca} peak at hyperpolarised potentials and slow the deactivation of L-channels allowing a calcium entrance during more time. Since the role of calcium augment by PQ-channels on exocytosis is poor owing to the fact of agonists of PQ-channels is lack, we considered that roscovitine could help to understand some aspects of neurotransmission by PQ-channels. On the other hand, knowledge about drugs, which interact with VDCC, especially new agonists, could prove information about structure and function of these ion channels.

The question is whether this calcium that entry into the cell by I_{tail} could induce an enhancement of exocytotic response or modify the endocytosis. Yan et al. (2002) observed a little enhancement of exocytosis on hippocampal synapses when stimulated with 1500 APs at 10 Hz and measuring the exocytotic response with FM1-43 dye. In addition, roscovitine increased the neurotransmitter release at the adult frog neuromuscular junction acting on presynaptic N-type Ca^{2+} channels (Cho & Meriney, 2006). In trying to elucidate the role of roscovitine on large-dense core vesicles release, we first stimulated chromaffin cells with a single DP, the little I_{tail} was not able to change exo-endocytotic responses. However, when a series of depolarisations pulses were applied, the cumulative calcium that entry into the cell increased the vesicle release. To confirm the specific effect of PQ tail current on exocytosis, we made experiments using the L-channels agonist FPL that at depolarised (positive) potentials does not change the I_{Ca} peak but increase the I_{tail}. Similar to FPL at positive potentials, roscovitine slows the deactivation of the calcium channel prolonging the mean open time of such channel without modify the I_{Ca} peak. Our data demonstrated that instead FPL augments in a similar manner the cumulative calcium entry, no changes on exocytosis were observed. These results suggest a specific role of PQ calcium in the activation of Ca^{2+}-dependent proteins preparing the machinery of exocytosis.

L-type calcium channels have been demonstrated to be tightly coupled to endocytosis while N/PQ channels are more weakly coupled to endocytosis (Rosa *et al.*, 2007; Perissinotti *et al.*, 2008; Kuromi *et al.*, 2010). However, a difficult question about the specialisation of L channels on endocytosis is unanswered. Is the control of endocytosis dependent of the calcium entry manner through L channels or its geographical coupling to endocytotic proteins? In our laboratory, we have evidences indicating a role of how calcium entry by L channels induces the endocytosis (unpublished data). L channels posses a different kinetics of calcium entry to N- and PQ-channels. These channels present a slow inactivation during the depolarisation. This characteristic induces a more prolonged entrance of calcium into the cell. We do think that the calcium that entry at the beginning of the stimulation is used to activate exocytotic proteins and at the end of the stimulation, the calcium is responsible to initiate the endocytotic process. Then, we though that inhibiting the endocytosis with L-channels blocker nifedipine and slow the deactivation of PQ-channels using roscovitine, we will allow a slow calcium entry into the cell at the end of the stimulation and the inhibited endocytotic response could be reversed. We found that roscovitine is

able to maintain an endocytotic response even though the calcium entry through L-channels, that is the responsible to initiate the membrane retrieval, is inhibited. This finding suggests that a prolonged calcium entry during stimulation has a clear role to promote the endocytosis on chromaffin cells.

In conclusion, the central finding of this study is that roscovitine, a cyclin-dependent kinase (cdk) inhibitor, slowed the PQ-channel deactivation increasing Ca^{2+} entry through I_{tail} of voltage-clamped bovine chromaffin cells enhancing the exocytotic response and maintaining the retrieval membrane. These findings corroborate with our hypothesis around the specialisation of VDCCs in controlling different cell functions on bovine chromaffin cells.

Acknowledgements

This work was partially supported from the following grants from Spanish institutions to AGG: (1) SAF2006-03589, *Ministerio de Ciencia e Innovación*, Spain; (2) NDE 07/09, *Agencia Laín Entralgo, Comunidad deMadrid*; (3) PI016/09, *Fundación C.I.E.N., Instituto de Salud Carlos III*; (4) RD 06/0026 RETICS, *Instituto deSalud Carlos III*; (5) S-SAL-0275-2006, *Comunidad de Madrid*, also by grant SAF2007-65181, *Ministerio de Ciencia e Innovación*, Spain, to LG. We thank *Fundación Teófilo Hernando* for continued support.

Albillos A, Garcia AG & Gandia L. (1993). omega-Agatoxin-IVA-sensitive calcium channels in bovine chromaffin cells. *FEBS Lett* **336,** 259-262.

Albillos A, Garcia AG, Olivera B & Gandia L. (1996). Re-evaluation of the PQ Ca^{2+} channel components of Ba^{2+} currents in bovine chromaffin cells superfused with solutions containing low and high Ba^{2+} concentrations. *Pflugers Arch* **432,** 1030-1038.

Buraei Z, Anghelescu M & Elmslie KS. (2005). Slowed N-type calcium channel ($Ca_V2.2$) deactivation by the cyclin-dependent kinase inhibitor roscovitine. *Biophys J* **89,** 1681-1691.

Buraei Z, Schofield G & Elmslie KS. (2007). Roscovitine differentially affects CaV2 and Kv channels by binding to the open state. *Neuropharmacology* **52,** 883-894.

Cho S & Meriney SD. (2006). The effects of presynaptic calcium channel modulation by roscovitine on transmitter release at the adult frog neuromuscular junction. *Eur J Neurosci* **23,** 3200-3208.

de Diego AM, Arnaiz-Cot JJ, Hernandez-Guijo JM, Gandia L & Garcia AG. (2008). Differential variations in Ca2+ entry, cytosolic Ca2+ and membrane capacitance upon steady or action potential depolarizing stimulation of bovine chromaffin cells. *Acta Physiol (Oxf)* **194,** 97-109.

DeStefino NR, Pilato AA, Dittrich M, Cherry SV, Cho S, Stiles JR & Meriney SD. (2010). (R)-roscovitine prolongs the mean open time of unitary N-type calcium channel currents. *Neuroscience* **167,** 838-849.

Fenwick EM, Marty A & Neher E. (1982). A patch-clamp study of bovine chromaffin cells and of their sensitivity to acetylcholine. *J Physiol* **331,** 577-597.

Fleckenstein A. (1977). Specific pharmacology of calcium in myocardium, cardiac pacemakers, and vascular smooth muscle. *Annu Rev Pharmacol Toxicol* **17,** 149-166.

Gandia L, Albillos A & Garcia AG. (1993). Bovine chromaffin cells possess FTX-sensitive calcium channels. *Biochem Biophys Res Commun* **194,** 671-676.

Gandia L, Lara B, Imperial JS, Villarroya M, Albillos A, Maroto R, Garcia AG & Olivera BM. (1997). Analogies and differences between omega-conotoxins MVIIC and MVIID: binding sites and functions in bovine chromaffin cells. *Pflugers Arch* **435,** 55-64.

Gandía L, Montiel C, García A & López M. (2008). *Seafood and Freshwater Toxins: Pharmacology, physiology and detection*. Boca Raton.

Garcia AG, Garcia-De-Diego AM, Gandia L, Borges R & Garcia-Sancho J. (2006). Calcium signaling and exocytosis in adrenal chromaffin cells. *Physiol Rev* **86,** 1093-1131.

Garcia AG, Sala F, Reig JA, Viniegra S, Frias J, Fonteriz R & Gandia L. (1984). Dihydropyridine BAY-K-8644 activates chromaffin cell calcium channels. *Nature* **309,** 69-71.

Gillis KD, Pun RY & Misler S. (1991). Single cell assay of exocytosis from adrenal chromaffin cells using "perforated patch recording". *Pflugers Arch* **418,** 611-613.

Grantham CJ, Bowman D, Bath CP, Bell DC & Bleakman D. (1994). Omega-conotoxin MVIIC reversibly inhibits a human N-type calcium channel and calcium influx into chick synaptosomes. *Neuropharmacology* **33,** 255-258.

Hamill OP, Marty A, Neher E, Sakmann B & Sigworth FJ. (1981). Improved patch-clamp techniques for high-resolution current recording from cells and cell-free membrane patches. *Pflugers Arch* **391,** 85-100.

Hellmich MR, Kennison JA, Hampton LL & Battey JF. (1994). Cloning and characterization of the Drosophila melanogaster CDK5 homolog. *FEBS Lett* **356,** 317-321.

Hernandez-Guijo JM, Maneu-Flores VE, Ruiz-Nuno A, Villarroya M, Garcia AG & Gandia L. (2001). Calcium-dependent inhibition of L, N, and PQ Ca2+ channels in chromaffin cells: role of mitochondria. *J Neurosci* **21,** 2553-2560.

Hess P, Lansman JB & Tsien RW. (1984). Different modes of Ca channel gating behaviour favoured by dihydropyridine Ca agonists and antagonists. *Nature* **311,** 538-544.

Horrigan FT & Bookman RJ. (1994). Releasable pools and the kinetics of exocytosis in adrenal chromaffin cells. *Neuron* **13,** 1119-1129.

Kokubun S & Reuter H. (1984). Dihydropyridine derivatives prolong the open state of Ca channels in cultured cardiac cells. *Proc Natl Acad Sci U S A* **81,** 4824-4827.

Kongsamut S, Kamp TJ, Miller RJ & Sanguinetti MC. (1985). Calcium channel agonist and antagonist effects of the stereoisomers of the dihydropyridine 202-791. *Biochem Biophys Res Commun* **130,** 141-148.

Korn SJ & Horn R. (1989). Influence of sodium-calcium exchange on calcium current rundown and the duration of calcium-dependent chloride currents in pituitary cells, studied with whole cell and perforated patch recording. *J Gen Physiol* **94,** 789-812.

Kunze DL & Rampe D. (1992). Characterization of the effects of a new Ca2+ channel activator, FPL 64176, in GH3 cells. *Mol Pharmacol* **42,** 666-670.

Kuromi H, Ueno K & Kidokoro Y. Two types of Ca2+ channel linked to two endocytic pathways coordinately maintain synaptic transmission at the Drosophila synapse. *Eur J Neurosci* **32,** 335-346.

Lindau M & Neher E. (1988). Patch-clamp techniques for time-resolved capacitance measurements in single cells. *Pflugers Arch* **411,** 137-146.

Liu L, Gonzalez PK, Barrett CF & Rittenhouse AR. (2003). The calcium channel ligand FPL 64176 enhances L-type but inhibits N-type neuronal calcium currents. *Neuropharmacology* **45,** 281-292.

Livett BG. (1984). Adrenal medullary chromaffin cells in vitro. *Physiol Rev* **64,** 1103-1161.

Lopez MG, Villarroya M, Lara B, Martinez Sierra R, Albillos A, Garcia AG & Gandia L. (1994). Q- and L-type Ca2+ channels dominate the control of secretion in bovine chromaffin cells. *FEBS Lett* **349,** 331-337.

Moro MA, Lopez MG, Gandia L, Michelena P & Garcia AG. (1990). Separation and culture of living adrenaline- and noradrenaline-containing cells from bovine adrenal medullae. *Anal Biochem* **185,** 243-248.

Neher E. (1998). Vesicle pools and Ca2+ microdomains: new tools for understanding their roles in neurotransmitter release. *Neuron* **20,** 389-399.

Neher E. (2006). A comparison between exocytic control mechanisms in adrenal chromaffin cells and a glutamatergic synapse. *Pflugers Arch* **453,** 261-268.

Nowycky MC, Fox AP & Tsien RW. (1985). Long-opening mode of gating of neuronal calcium channels and its promotion by the dihydropyridine calcium agonist Bay K 8644. *Proc Natl Acad Sci U S A* **82,** 2178-2182.

Olivera BM, Miljanich GP, Ramachandran J & Adams ME. (1994). Calcium channel diversity and neurotransmitter release: the omega-conotoxins and omega-agatoxins. *Annu Rev Biochem* **63,** 823-867.

Perissinotti PP, Giugovaz Tropper B & Uchitel OD. (2008). L-type calcium channels are involved in fast endocytosis at the mouse neuromuscular junction. *Eur J Neurosci* **27,** 1333-1344.

Rosa JM, de Diego AM, Gandia L & Garcia AG. (2007). L-type calcium channels are preferentially coupled to endocytosis in bovine chromaffin cells. *Biochem Biophys Res Commun* **357,** 834-839.

Rosa JM, Gandia L & Garcia AG. (2009). Inhibition of N and PQ calcium channels by calcium entry through L channels in chromaffin cells. *Pflugers Arch* **458,** 795-807.

Schramm M, Thomas G, Towart R & Franckowiak G. (1983). Novel dihydropyridines with positive inotropic action through activation of Ca2+ channels. *Nature* **303,** 535-537.

Tavalin SJ, Shepherd D, Cloues RK, Bowden SE & Marrion NV. (2004). Modulation of single channels underlying hippocampal L-type current enhancement by agonists depends on the permeant ion. *J Neurophysiol* **92,** 824-837.

Tsai LH, Delalle I, Caviness VS, Jr., Chae T & Harlow E. (1994). p35 is a neural-specific regulatory subunit of cyclin-dependent kinase 5. *Nature* **371,** 419-423.

Yan Z, Chi P, Bibb JA, Ryan TA & Greengard P. (2002). Roscovitine: a novel regulator of PQ-type calcium channels and transmitter release in central neurons. *J Physiol* **540,** 761-770.

Zheng W, Rampe D & Triggle DJ. (1991). Pharmacological, radioligand binding, and electrophysiological characteristics of FPL 64176, a novel nondihydropyridine Ca2+ channel activator, in cardiac and vascular preparations. *Mol Pharmacol* **40,** 734-741.

Figure 1

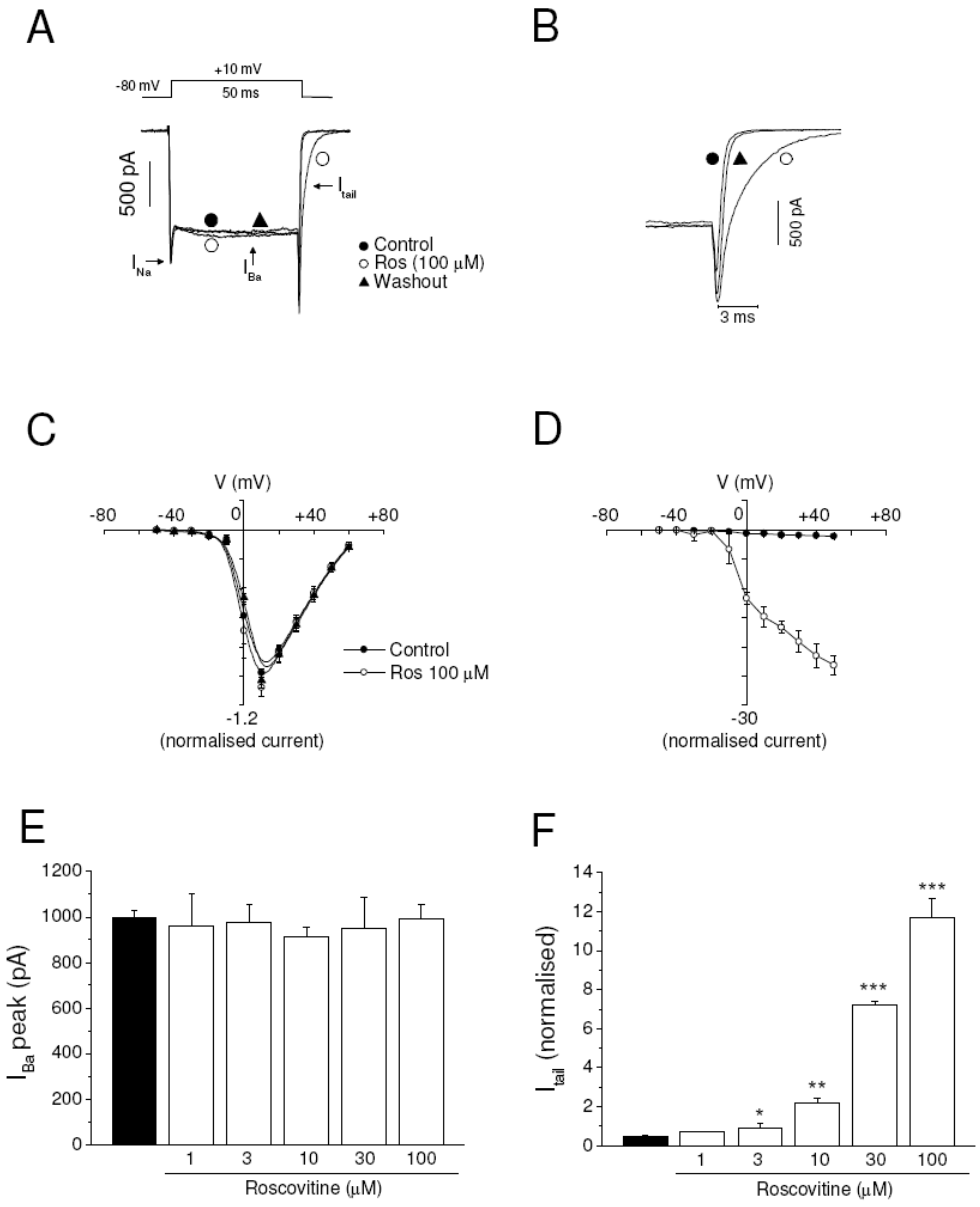

Fig. 1: Roscovitine (Ros) augmented I_{tail} in a concentration-dependent manner, but did not modify I_{Ba} peak. Bovine chromaffin cells perifused with an extracellular solution containing 10 mM Ba^{2+}, were voltage-clamped at -80 mV under the whole-cell configuration of the patch-clamp technique. Inward currents (I_{Ba}) were generated by 50-ms depolarising test pulses (DPs) to +10 mV. **A**, example trace currents generated by test pulse to the voltage indicated at the protocol on top, before (control; ●), at 1-min of roscovitine treatment (Ros; ○) and after washout (washout; ▲). **B,** I_{tail} trace from the same cell on A. **C,** current-voltage relationship (I-V) of I_{Ba}, before (control) and during roscovitine treatment. **D,** IV of I_{tail} before and during roscovitine treatment. These curves

were obtained by measuring I_{Ba} amplitude after the initial 10-ms of each depolarising pulse or I_{tail} amplitude 3-ms after the end of the test pulse; currents were generated by successive test potentials given at increasing 10-mV steps from -50 to +50 mV. **E, F,** pooled results of I_{Ba} amplitude and I_{tail} (measured at 3-ms after returning to HP -80 mV) at different concentration. Data are mean ± s.e. of the number of cells shown in parenthesis from four different cultures. ***$p<0.001$, **$p<0.01$, and *$p<0.05$.

Figure 2

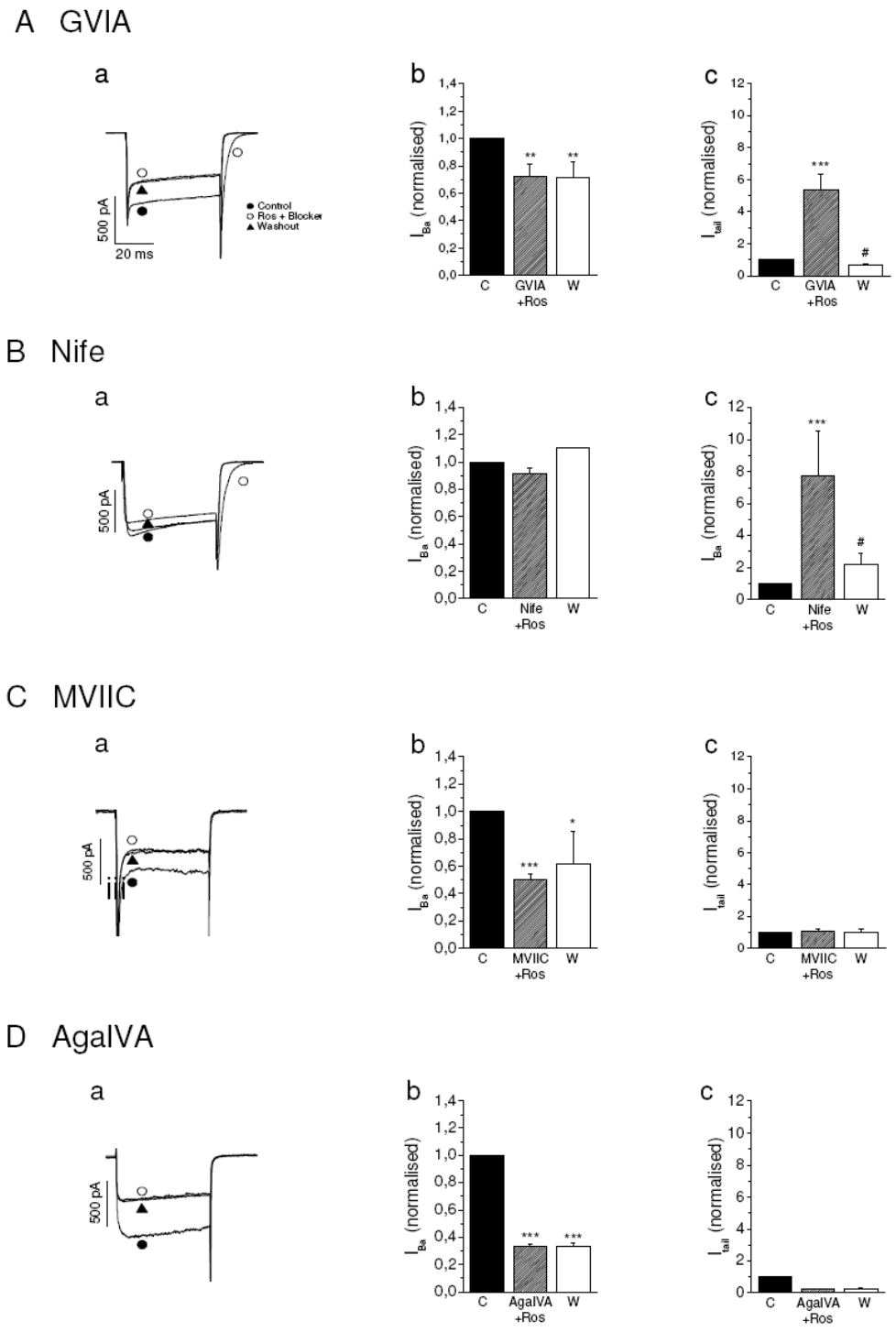

Fig. 2: Effects of calcium channels blockers on I_{tail}, following the protocol described in Fig. 1. **A,** control I_{Ba} trace, and a trace obtained after cell perifusion with GVIA plus roscovitine during 1-min before giving

the pulse and after washout (a). Averaged pooled results of I_{Ba} (b) and I_{tail} (c) in absence and the presence of GVIA plus roscovitine. **B,** example I_{Ba} traces before (control) and after 3-min of cell perifusion with nifedipine (a). Pooled averaged results of peak I_{Ba} (b) and I_{tail} (c). **C,** example I_{Ba} traces before (control) and after 1-min of cell perifusion with MVIIC (a). Pooled averaged results of peak I_{Ba} (b) and I_{tail} (c). **D,** example I_{Ba} traces before (control) and after 1-min of cell perifusion with AgaIVA (a). Pooled averaged results of peak I_{Ba} (b) and I_{tail} (c). Data are mean ± s.e. of the number of cells shown in parenthesis from four different cultures. ***$p<0.001$, **$p<0.01$, and *$p<0.05$.

Figure 3

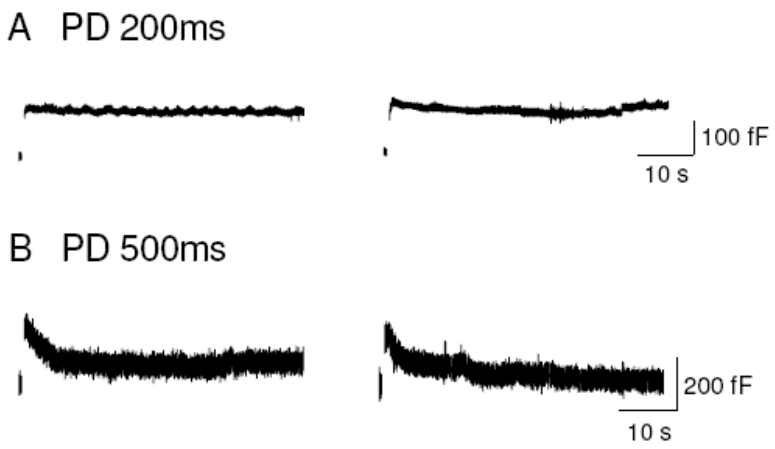

Fig. 3: Roscovitine does not facilitate the exocytosis or endocytosis upon single depolarising pulses. Cells voltage-clamped at -80 mV were perifused with an extracellular solution containing 10 mM Ca^{2+}. Changes of membrane capacitance (Cm) were generated by 200-ms or 500-ms depolarising test pulses (DPs) to +0 mV. **A,** example traces of Cm changes from a control cell (left) and a cell perifused with roscovitine 100 μM (right) upon 200-ms DP. **B,** example traces of Cm changes from a control cell (left) and a cell perifused with roscovitine 100 μM (right) upon 500-ms DP.

Figure 4

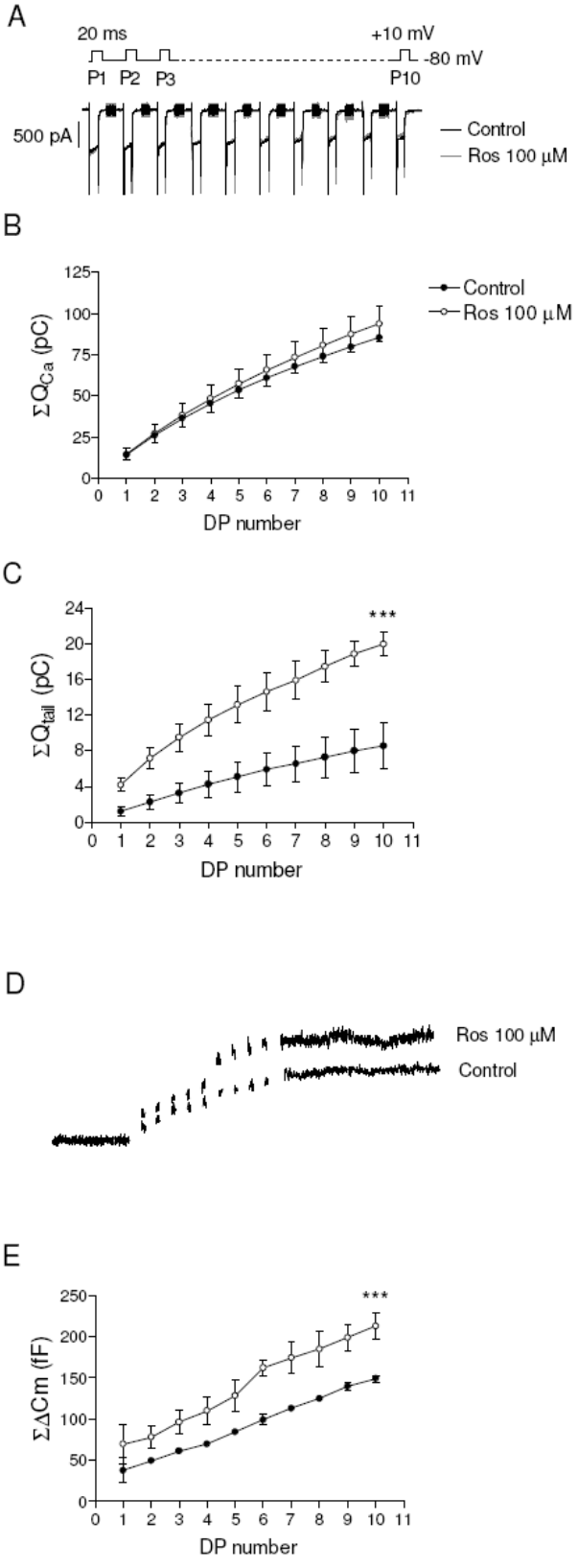
A
20 ms
+10 mV
-80 mV
P1 P2 P3
P10
500 pA
Control
Ros 100 µM
B
Control
Ros 100 µM
ΣQCa (pC)
DP number
C
***
ΣQtail (pC)
DP number
D
Ros 100 µM
Control
E
***
ΣΔCm (fF)
DP number

Fig. 4: Roscovitine favours the activation of an exocytotic response. Bovine chromaffin cells perifused with an extracellular solution containing 10 mM Ca^{2+}, were voltage-clamped at -80 mV under the perforated patch-clamp configuration of the patch-clamp technique. Inward calcium currents (I_{Ca}) and changes of membrane capacitance (Cm) were generated by a series of 10x20-ms depolarising test pulses (DPs) to +10 mV at 60-ms intervals. **A**, example of I_{Ca} trace in a control cell and after roscovitine (100 μM) perifusion, obtained using the top protocol. **B,** cumulative calcium charge ($\sum Q_{Ca}$) upon depolarising train in control conditions and after roscovitine application; this area, expressed in pC, indicates the total Ca^{2+} entering the cell during a train. **C,** cumulative tail charge ($\sum Q_{tail}$) in pC upon depolarising train in control conditions and after roscovitine application measured during the 3-ms period after repolarisation. **D,** example traces of Cm from a control cell and a cell perifused with 100 μM roscovitine. **E,** averaged cumulative exocytotic responses ($\sum$Cm) in control and roscovitine cells. Data are means ± s.e. of the number of cells shown in parenthesis from 4 different cultures. ***$p < 0.001$.

Figure 5

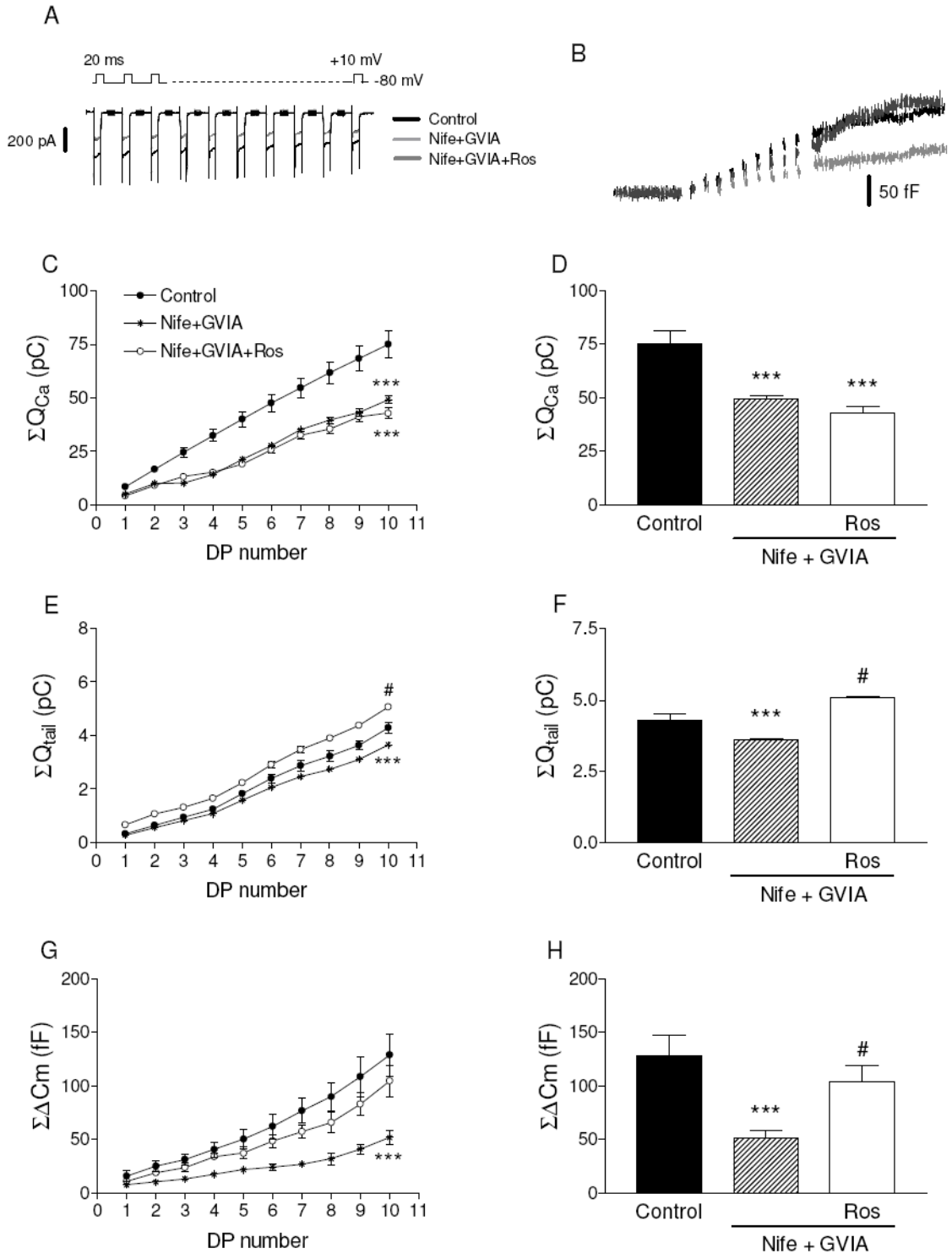

Fig. 5: Effect of PQ-tail current elicited by roscovitine (100 μM, Ros) augments exocytotic responses in presence of N and L-channel blockers. Nifedipine (3 μM, nife) and ω-conotoxin GVIA (1 μM, GVIA)

were used to inhibit L and N-calcium channels, respectively. The same protocol of Fig. 4 was used to stimulate the cells. Example traces of I_{Ca} (**A**) and capacitance changes (**B**) generated by a train of depolarising pulses given before (control), at 2-min of Nife+GVIA treatment, and at 1-min of combined Nife+GVIA+Ros treatment. **C** and **D**, pooled averaged results of Q_{Ca} after depolarising train at each depolarising pulse and at the 10^{th} PD, respectively. **E** and **F**, pooled averaged results of Q_{tail} under the different treatment conditions. **G** and **H**, pooled averaged of Cm changes under the different treatment conditions. Data are means ± s.e. of the number of cells shown in parenthesis from 4 different cultures. ***$p < 0.001$.

Figure 6

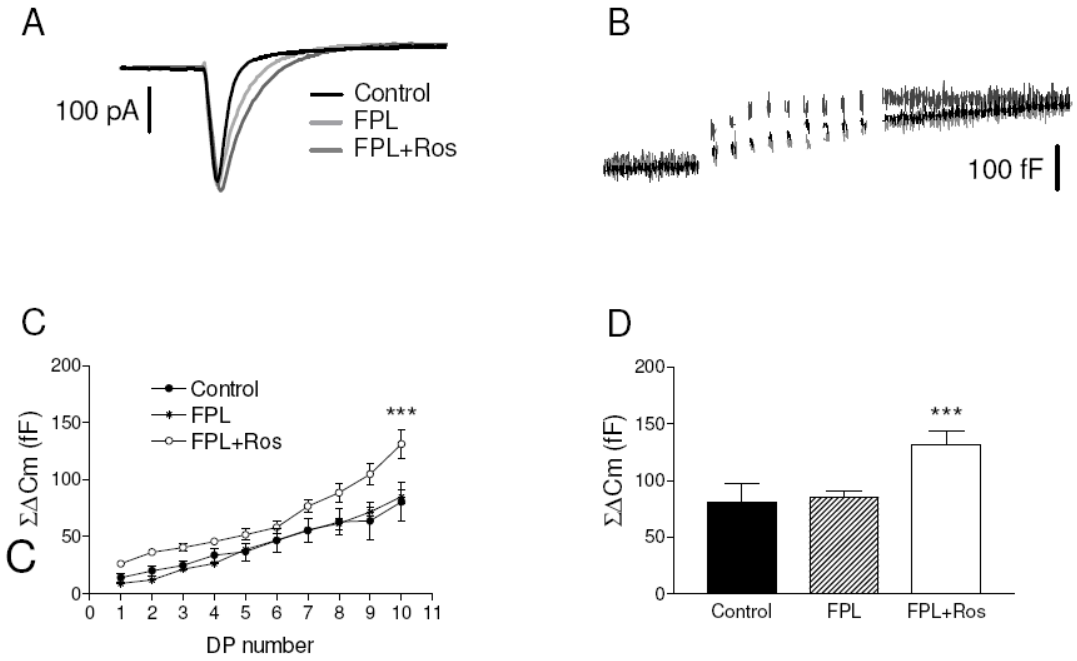

Fig. 6: The potentiation of I_{tail} caused by roscovitine and FPL64176 (FPL) was additive. Cells were voltage-clamped at -80 mV and a train of depolarising pulses were applied to +10 mV in presence of 10 mM Ca^{2+}. **A,** example traces of I_{tail} in control conditions, after FPL alone and co-application of FPL and roscovitine (FPL+Ros). **B,** Cm changes under the protocol used in A. **C,** averaged pooled results of Cm at each despolarisation. **D,** averaged pooled of exocytotic response at 10^{th} stimuli. Data are means ± s.e. of the number of cells shown in parenthesis from 4 different cultures. ***$p < 0.001$.

Figure 7

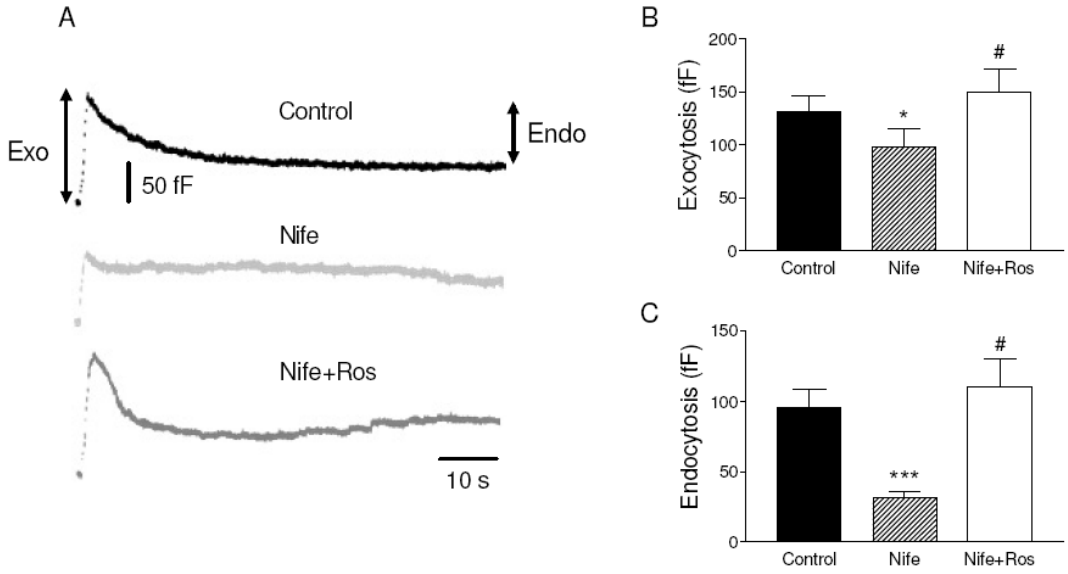

Fig. 7: Augmentation of Ca^{2+} entry through PQ-tail current by roscovitine (Ros; 1 μM) recovered the endocytotic responses in cells treated with nifedipine (nife, 3 μM). Cells were voltage-clamped at -80 mV and stimulated with 500-ms depolarising pulses at 5-min intervals. **A,** example of capacitance changes generated by depolarising pulses given before (control; bottom), at 3-min of nifedipine treatment (middle), and at 1-min of combined Nife+Ros treatment (under). **B** and **C,** pooled averaged results of exocytosis and endocytosis, in fF, respectively. Data are means ± s.e. of the number of cells shown in parenthesis from 4 different cultures. * < 0.05, ***p < 0.001.

2- Modulación de los canales de calcio

Pflugers Arch – Eur J Physiol
DOI 10.1007/s00424-009-0662-2

SIGNALING AND CELL PHYSIOLOGY

Inhibition of N and PQ calcium channels by calcium entry through L channels in chromaffin cells

Juliana M. Rosa & Luis Gandía & Antonio G. García

Received: 16 October 2008 / Revised: 9 February 2009 / Accepted: 1 March 2009

Abstract Why adrenal chromaffin cells express various subtypes of voltage-dependent Ca^{2+} channels and whether a given channel is specialized to perform a specific function are puzzling and unanswered questions. In this study, we have used the L Ca^{2+} channel activator FPL64176 (FPL) to test the hypothesis that enhanced Ca^{2+} entry through this channel favors the inhibition of N and PQ channels in voltage-clamped bovine adrenal chromaffin cells. Using 2 mM Ca^{2+} as charge carrier and under the perforated-patch configuration (PPC) of the patch-clamp technique, FPL caused a paradoxical inhibition of the whole-cell inward Ca^{2+} current (I_{Ca}). Such inhibition turned on into an augmentation upon cell loading with EGTA-AM. Also, under the whole-cell configuration (WCC) of the patch-clamp technique, FPL decreased I_{Ca} in the absence of EGTA from the pipette solution and increased the current in its presence. Using 2 mM Ba^{2+} as charge carrier, FPL augmented the Ba^{2+} current under both recording conditions, WCC and PPC. FPL augmented the residual current remaining after blockade of N and PQ channels with ω-conotoxin MVIIC or by holding the membrane potential at −50 mV. The data support the view that Ca^{2+} entering the cell through the lesser inactivating L channels serves to modulate the more inactivating N and PQ channels. They also suggest a close colocalization of L and N/PQ Ca^{2+} channels. This kind of L channel specialization may be relevant to cell excitability, exocytosis, and cell survival mechanisms.

Keywords L calcium channel · N calcium channel · PQ calcium channel · Chromaffin cells · Calcium current · FPL64176

J. M. Rosa : L. Gandía : A. G. García (*)
Instituto Teófilo Hernando, Facultad de Medicina,
Universidad Autónoma de Madrid,
Arzobispo Morcillo,
4. 28029 Madrid, Spain
e-mail: agg@uam.es

J. M. Rosa : L. Gandía : A. G. García
Departamento de Farmacología y Terapéutica,
Facultad de Medicina, Universidad Autónoma de Madrid,
Madrid, Spain

A. G. García
Servicio de Farmacología Clínica,
Hospital Universitario de la Princesa, Facultad de Medicina,
Universidad Autónoma de Madrid,
Madrid, Spain

Introduction

Bovine chromaffin cells express neuronal voltage-dependent Ca^{2+} channels of the subtypes L (α_{1D}, $Ca_v1.3$), N (α_{1B}, $Ca_v2.2$), and PQ (α_{1A}, $Ca_v2.1$) [22], having similar biophysical and pharmacological properties to those expressed by neurons [20, 23, 59]. Why these cells express L as well as non-L (N/PQ) Ca^{2+} channels is an intriguing question. There are reports suggesting different modulation of channel subtypes and different roles in controlling exocytosis, according to various experimental conditions and patterns of chromaffin cell stimulation. The following findings illustrate this point: (1) Ca^{2+} channel currents (I_{Ca}) are modulated by neurotransmitters in a voltage-dependent (N/PQ channels) or voltage-independent manner (L channels) [1, 18, 19, 30]; (2) depending on the experimental conditions, L channels may be preferentially coupled to exocytosis [40] or PQ channels may dominate the control of secretion [36]; (3) cell stimulation with action potentials (APs) produce a secretory response mostly controlled by PQ channels, while secretion stimulated with depolarizing pulses

Published online: 04 April 2009

is controlled by other channel subtypes [14]; (4) L channels are tightly coupled to endocytosis while N/PQ channels are more weakly coupled to endocytosis [60, 63]; (5) L channels are more resistant to voltage-dependent inactivation while N/PQ channels are more prone to such inactivation [31, 70]; and (6) L channels undergo Ca^{2+}-dependent inhibition at a rate slower than N/PQ channels [32].

The Ca^{2+}-dependent inactivation of Ca^{2+} channels was first suggested by Hagiwara and Nakajima [28], subsequently proven by Brehm and Eckert [9] and Tillotson [68] in mollusc neurons, and later on extended to various excitable cells [27]. It is interesting to note that not all Ca^{2+} channel subtypes are equally prone to Ca^{2+}-dependent inactivation. For instance, the cardiac and smooth muscle L channel is quickly inactivated upon depolarization [25, 37, 52] while the neuronal L channel inactivates more slowly [71]. Because the L channel inactivates more slowly in bovine chromaffin cells [32], it may be that Ca^{2+} entry through this channel could modulate N/PQ channels. In this study, we tested this hypothesis by measuring the whole-cell inward Ca^{2+} channels current (I_{Ca}) in voltage-clamped bovine adrenal chromaffin cells. We used the L channel activator FPL64176 (FPL) [44, 75] to enhance the I_{Ca} flowing through L channels to test its consequences on the inhibition of the I_{Ca} flowing through N and PQ channels. The results support the hypothesis implying the existence of a Ca^{2+}-mediated cross-talk between L and N/PQ Ca^{2+} channels.

Materials and methods

Isolation and culture of bovine chromaffin cells

Bovine adrenal glands were obtained from a local slaughterhouse. Chromaffin cells were isolated by digestion of the adrenal medulla with collagenase following standard methods [39] with some modifications [50]. Cells were suspended in Dulbecco's modified Eagle's medium (DMEM) supplemented with 5% fetal calf serum, 10 µM cytosine arabinoside, 10 µM fluorodeoxyrudine, 50 IU mL^{-1} penicillin, and 50 µg mL^{-1} streptomycin. Cells were plated on 13-mm diameter polylisine-coated glass coverslips at a density of 5×10^4 cells per coverslip. Cells were kept in a water-saturated incubator at 37°C in a 5% CO_2–95% air atmosphere and used 2–5 days thereafter.

Electrophysiological recordings

I_{Ca} were recorded in voltage-clamped cells under whole-cell configuration (WCC) or perforated-patch configuration (PPC) [26, 34] of the patch-clamp technique [29]. During recording, cells were continuously perfused (at a rate of 1 mL min^{-1}) with an external solution containing (in millimolar): 145 NaCl, 1.2 $MgCl_2$, 2 $CaCl_2$, 10 glucose, and 10 HEPES, pH adjusted to 7.4 with NaOH. In some experiments, equimolar Ba^{2+} was used instead of Ca^{2+} as charge carrier. For perforated-patch experiments, electrodes were filled with internal solution containing the following (in millimolar): 135 CsGlutamate, 10 HEPES, 1 $MgCl_2$, and 9 NaCl, pH 7.2 adjusted with CsOH. For this configuration, an amphotericin B stock solution was prepared every week at 50 mg mL^{-1} in dimethyl sulfoxide (DMSO), stored at −20°C, and protected from light. Fresh perforated-patch pipette solution was prepared every day by addition of 10 µL stock amphotericin B solution to 1 mL intracellular solution. This solution was sonicated thoroughly, protected from light, and kept in ice. Patch pipettes had their tips dipped in amphotericin-free solution for 2–10 s and backfilled with freshly mixed amphotericin-containing solution. For whole-cell experiments, cells were dialysed with an internal solution containing (in millimolar): 10 NaCl, 100 CsCl, 20 TEA-Cl, 14 EGTA, 20 HEPES, 5 MgATP, and 0.3 NaGTP, pH 7.2 adjusted with CsOH. When necessary, EGTA was omitted from the internal solution. For PPC, recordings started when the access resistance decreased below 25 MΩ, which usually happened within 10 min after sealing [61]. For WCC, the total pipette access resistance ranged from 2 to 3 MΩ.

Electrophysiological data were carried out using an EPC-9 amplifier under the control of Pulse software (HEKA Elektronik). Cells were held at −80 mV and I_{Ca} were generated by depolarizing voltage steps of 50-ms duration to sequentially increasing test potentials by 10-mV step increments from −50 to +50 mV. Test pulses were delivered at 10-s intervals to minimize the rundown of Ca^{2+} currents [16]. Cells with pronounced rundown were discarded. External solutions were exchanged by a fast superfusion device consisting of a modified multibarrelled pipette, the common outlet of which was positioned 50–100 µm from the cell. Control and test solutions were changed using miniature solenoid valves operated manually.

To determine the effects of L-type Ca^{2+} channel agonists under WCC or PPC, cells were perfused with external solutions containing either FPL (in most experiments) or BayK8644 (BayK; in a few experiments). All experiments were performed at room temperature (24±2°C).

Materials and solutions

The following materials were used: collagenase type I from Sigma (Madrid, Spain); DMEM, bovine serum albumin fraction V, fetal calf serum, and antibiotics were from Gibco (Madrid, Spain). Amphotericin B and BayK were from Sigma (Madrid, Spain) and FPL was from RBI (Natick, MA, USA); ω-conotoxin MVIIC (MVIIC) was from Bachem Feinchemikalien (Essex, UK).

FPL at 1 mM was prepared in ethanol and BayK at 1 mM in DMSO; both solutions were kept at −20°C in aliquots and were protected from light. MVIIC was dissolved in distilled water and stored frozen in aliquots at 0.1 mM. Final concentrations of drugs were obtained by diluting the stock solution directly into the external solution.

Data analysis

Under the appropriate conditions, FPL gradually augmented I_{Ca} along the 50-ms test depolarizing pulse (Fig. 1b). Therefore, the amplitude of I_{Ca} was always measured at the end of the test pulse (see double arrowheads in Fig. 1a). In order to measure the component of the tail current that occurred in the presence of L-type Ca^{2+} channel agonists, a second cursor was approximately placed 5 ms after the end of the test pulse. I_{Ca} was not leak subtracted, and only cells with a leak current <30 pA were included in the analysis. Comparisons between means of group data were performed by one-way analysis of variance followed by Duncan post hoc test when appropriate. A p value equal to or smaller than 0.05 was taken as the limit of significance. Data are expressed as means ± standard error (SE).

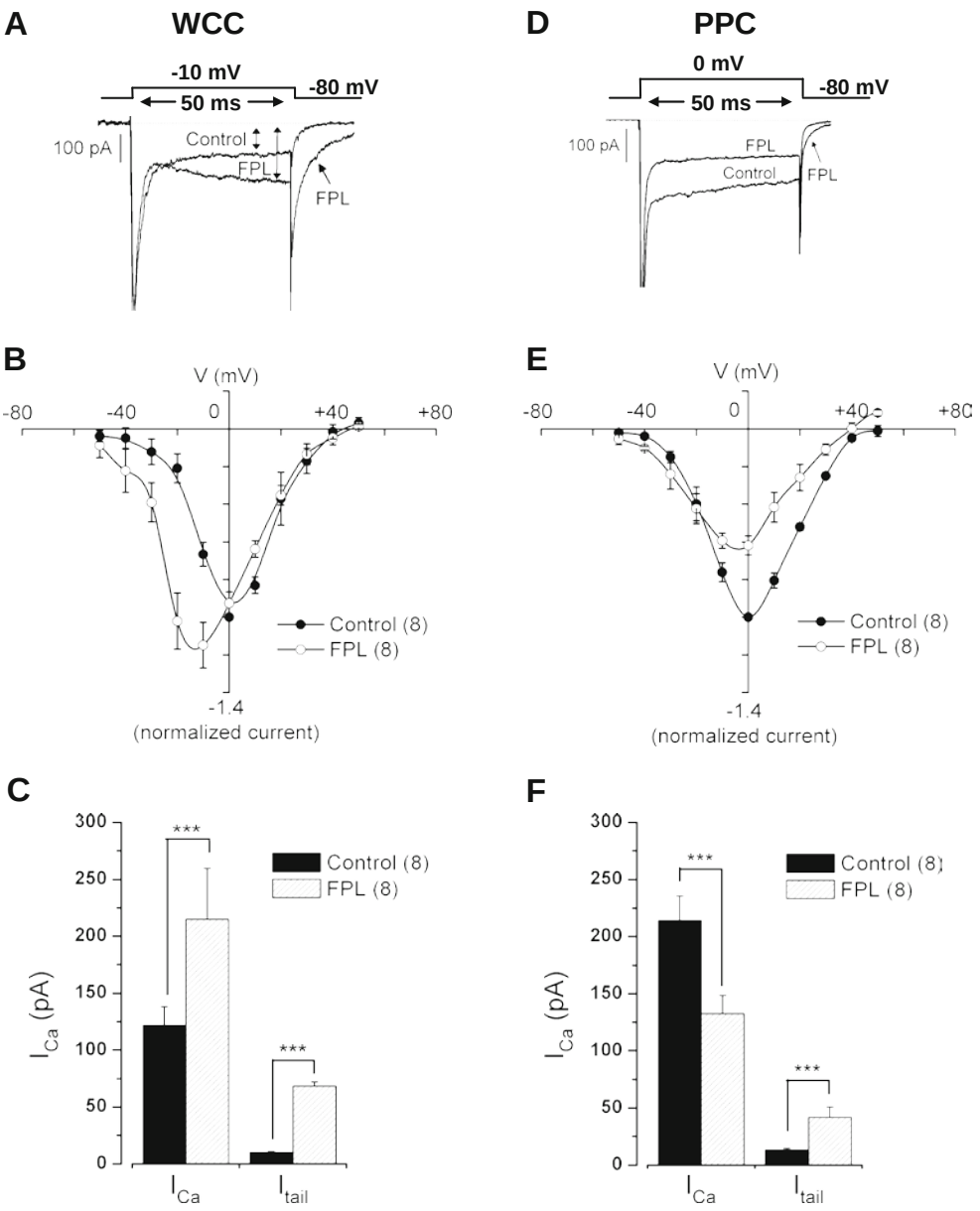

Fig. 1 FPL (1 μM) augmented I_{Ca} under WCC recording (a–c) and inhibited I_{Ca} under PPC recording (d–f). HP −80 mV; 2 mM external Ca^{2+}. a, d Example trace currents generated by test pulses to the voltages indicated at the protocol on top, before (control) and at 2 min of FPL treatment. b, e I–V relationship of I_{Ca}, before (control) and during FPL treatment. These curves were obtained by measuring I_{Ca} amplitude at the end of the test pulse (see double arrowhead in a); currents were generated by successive test potentials given at increasing 10-mV steps from −50 to +50 mV. c, f Pooled results of I_{Ca} amplitude (measured as indicated by the double arrowhead in a) and I_{tail} (measured at 5 ms after returning to HP −80 mV). Data are means ± SE of eight cells for each configuration, from at least four different cultures. ***p<0.001

Results

FPL augmented I_{Ca} under WCC but caused its inhibition under PPC

The fact that FPL increases $^{45}Ca^{2+}$ uptake into K^+ depolarized bovine chromaffin cells [70] suggested that the compound should also augment I_{Ca} in these cells. This $^{45}Ca^{2+}$ increase was maximal at 1 μM FPL; therefore, we used this concentration throughout this study. Generally, when a good seal was established in each experiment and access to the intracellular milieu was achieved, the targeted cell was voltage-clamped at −80 mV holding potential (HP). Then the cell was continuously perfused with an extracellular solution containing the physiological Ca^{2+} concentration of 2 mM. Unless otherwise indicated, under WCC recording, the pipette solution contained 14 mM EGTA; these are the conditions used in our and many other laboratories to prevent Ca^{2+} channel inactivation and optimize the recording of reproducible I_{Ca} current traces along the experiment. Under PPC recording, there was no point in adding EGTA to the pipette solution since this compound will not cross the perforated-patch pores; these are also the conditions thoroughly used to record I_{Ca} under PPC. In general, cells with leak currents greater than 30 pA were discarded (under WCC recording). Cells were usually challenged with test potentials given at different voltages at 10-s intervals.

In the example cell of Fig. 1a, a 50-ms pulse to −10 mV generated an inward current composed of (1) an initial fast-inactivating Na^+ current (we did not use tetrodotoxin in this study; however, the presence of 1 mM TTX fully suppressed the I_{Na} component of current traces); this current was large and, therefore, it appears truncated to facilitate the visualization of I_{Ca}; (2) a low-inactivating I_{Ca}; and (3) a deactivating tail current (I_{tail}) caused by Ca^{2+} channel closing upon returning to −80 mV (see protocol on top of Fig. 1a). After 1-min of perfusion with FPL, the current increased along the depolarizing pulse and was followed by an I_{tail} with a pronounced slowing down of current relaxation to zero baseline. These are typical effects of FPL on L channels [38, 42]. The characteristic effect of FPL on I_{Ca} suggested the convenience of expressing all quantitative data by measuring I_{Ca} at the end of the test pulse, as indicated by double arrowheads in the current traces of Fig. 1a. In this manner, when using the term I_{Ca} throughout this study, we mean the amplitude of I_{Ca} at the end of the test pulse. I_{tail} is the amplitude of the tail current measured 5 ms after the end of the test pulse in each cell. Figure 1b shows the typical shift to the left of the current–voltage (I–V) curve caused by activators of L channels [35, 75]. FPL augmented I_{Ca} only at steps in the negative range of the voltage scale. Figure 1c contains a summary of the averaged changes elicited by FPL: I_{Ca} augmented by 76% and I_{tail} by 5.8-fold.

A quite different picture emerged when I_{Ca} was recorded under PPC. I_{Ca} was halved when the example cell shown in Fig. 1d was treated with FPL; a tiny slowing down of I_{tail} was noted. FPL did not shift the I–V curve and caused its depression with respect to the control curve (Fig. 1e). The averaged data of Fig. 1f indicate that although FPL decreased I_{Ca} by 38%, I_{tail} was still augmenting 2.2-fold. This suggested that, in spite of I_{Ca} inhibition, FPL was still enhancing the open time of L channels.

In conclusion, under WCC recording, FPL augmented I_{Ca} and I_{tail} in the expected direction for an L Ca^{2+} channel activator. In contrast, under PPC recording, FPL blocked I_{Ca} and caused a lesser I_{tail} increase.

BayK mimicked the effects of FPL on I_{Ca}

BayK is the prototype L channel ligand that has been widely used since its discovery [65] as a tool to prolong the mean open time of such channel [57]. BayK drastically augments $^{45}Ca^{2+}$ uptake into K^+ depolarized bovine chromaffin cells [24]. Under these premises, we thought that BayK (a DHP derivative) should mimic the effects of FPL (a non-DHP derivative) on I_{Ca} and I_{tail}. We, therefore, performed experiments with designs similar to those used with FPL. As for FPL [70], we used 1 μM BayK, a concentration that maximally augments Ca^{2+} entry through Ca^{2+} channels in bovine chromaffin cells [24].

Under WCC, BayK augmented I_{Ca} and I_{tail} in the expected direction (Fig. 2a). The compound also shifted to the left the I–V curve by about 10 mV. Thus, BayK enhanced I_{Ca} at steps in the negative range of the voltage scale and depressed it in the positive range (Fig. 2b). This was similar to FPL that augmented I_{Ca} at negative voltage steps and mildly depressed it at positive steps (Fig. 1b). BayK augmented peak I_{Ca} by 61% and I_{tail} by 3.3-fold (Fig. 2c).

Under PPC recording, BayK had effects opposite to those found under WCC (Fig. 1). For instance, in the example trace of Fig. 2d, BayK caused a mild inhibition of I_{Ca}, and did not augment I_{tail}. The I–V curve underwent a meager depression with no shift (Fig. 2e). The averaged results indicate a 24% blockade of I_{Ca} and no effect on I_{tail} (Fig. 2f).

In conclusion, from a qualitative point of view, BayK affected I_{Ca} in a direction similar to FPL: augmentation under WCC recording and diminution under PPC. However, from a quantitative point of view, the effects of BayK were milder; therefore, we chose FPL to perform further experiments.

FPL enhanced I_{Ca} under both WCC and PPC recordings in conditions of L current isolation

As indicated in the Introduction section, we depart from the hypothesis that Ca^{2+} entry through L channels causes the

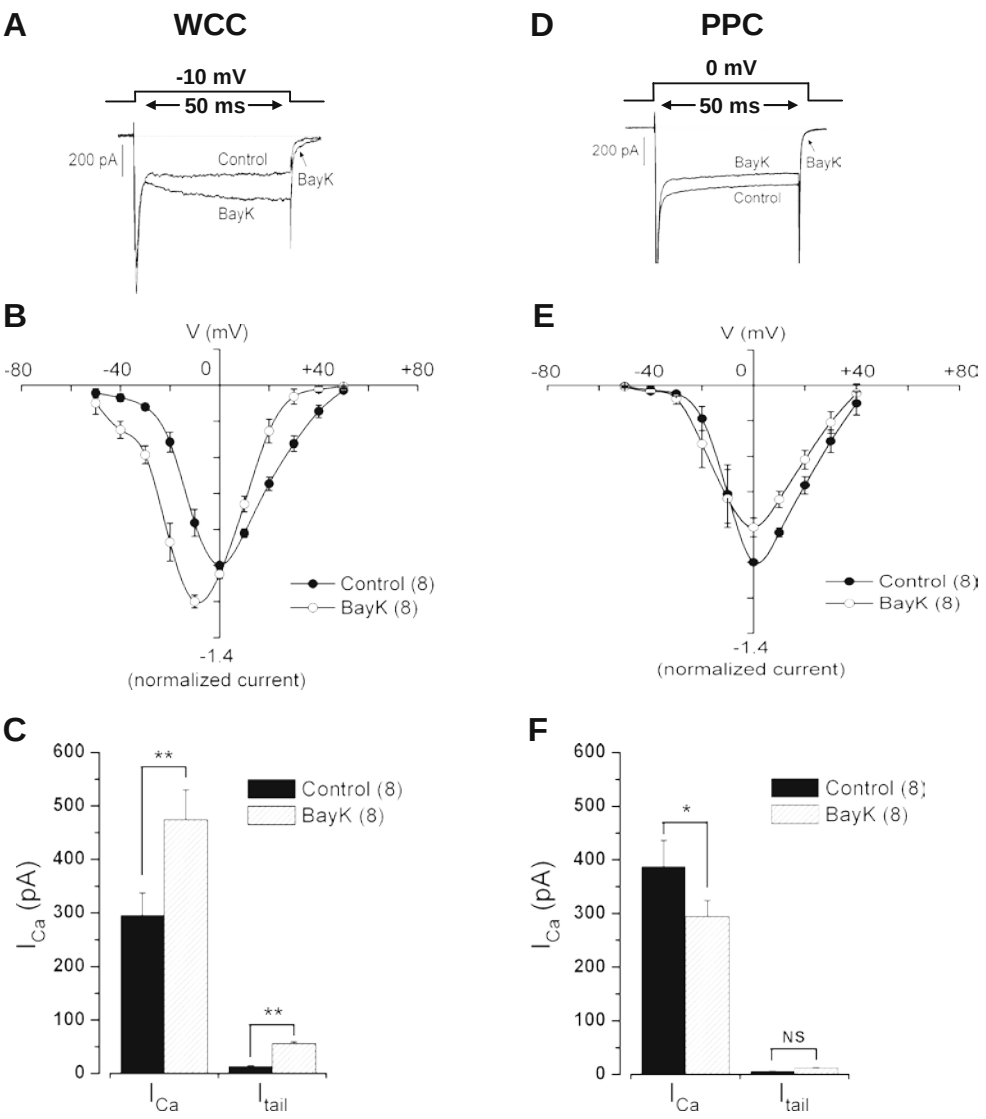

Fig. 2 BayK (1 μM) augmented I_{Ca} under WCC recording (a–c) and inhibited I_{Ca} under PPC recording (d–f). HP −80 mV; 2 mM external Ca^{2+}. a, d Example trace currents generated by test pulses to the voltages indicated at the protocol on top, before (control) and at 2 min of BayK treatment. b, e I–V relationship of I_{Ca}, before (control) and during BayK treatment. These curves were obtained by measuring I_{Ca} amplitude at the end of the test pulse; currents were generated by successive test potentials given at increasing 10-mV steps from −50 to +50 mV. c, f Pooled results of I_{Ca} and I_{tail} amplitudes. Data are means ± SE of eight cells for each configuration, from at least four different cultures. *p<0.05, ***p<0.001. NS nonsignificant

inhibition of N and PQ channels. In bovine chromaffin cells, L channel current accounts for only 20% of the whole-cell current; the rest is carried through N and PQ channels [2, 18, 40]. In these cells, 2 μM MVIIC suppresses the N and PQ components of the whole-cell inward current through Ca^{2+} channels [19]. Therefore, we recourse to 2 μM MVIIC to block N and PQ currents, leaving the cell with its L current intact.

Under WCC recording, MVIIC inhibited I_{Ca} by 43%, as exemplified in the original traces of Fig. 3a (inset i). When added on top of MVIIC, FPL augmented I_{Ca} and slowed down the relaxation of I_{tail} (inset ii) to near the control level. On the other hand, MVIIC depressed the I–V curve; when added with MVIIC, FPL shifted to the left the I–V curve and thus augmented I_{Ca} at step potentials in the negative voltage scale (Fig. 3b). The averaged I_{Ca} changes appear in Fig. 3c. MVIIC reduced I_{Ca} by 58% in the presence of the toxin, FPL augmented I_{Ca} to about 70% of the initial control current.

Under PPC recording, MVIIC reduced I_{Ca} by 67% in the example cell shown in Fig. 3d. When added on top of MVIIC, FPL augmented I_{Ca} and delayed I_{tail} relaxation (see inset ii in Fig. 3d). MVIIC depressed the I–V curve in a parallel manner. When added together with MVIIC, FPL augmented I_{Ca} to about 70% of the initial control I–V curve (Fig. 3e). Averaged results are summarized in Fig. 3f; I_{Ca} was inhibited 80% by MVIIC. Although this inhibited current was doubled by FPL, this increase was not significantly different.

Another way of isolating the L from N/PQ currents rests on the voltage-dependent inactivation of N/PQ channels. Shifting of the HP from −80 to −50 mV causes the gradual loss of 70–80% of current; the remaining current is blocked by nifedipine and is thus associated to noninactivating L channels [31, 70]. This was reproduced here under WCC

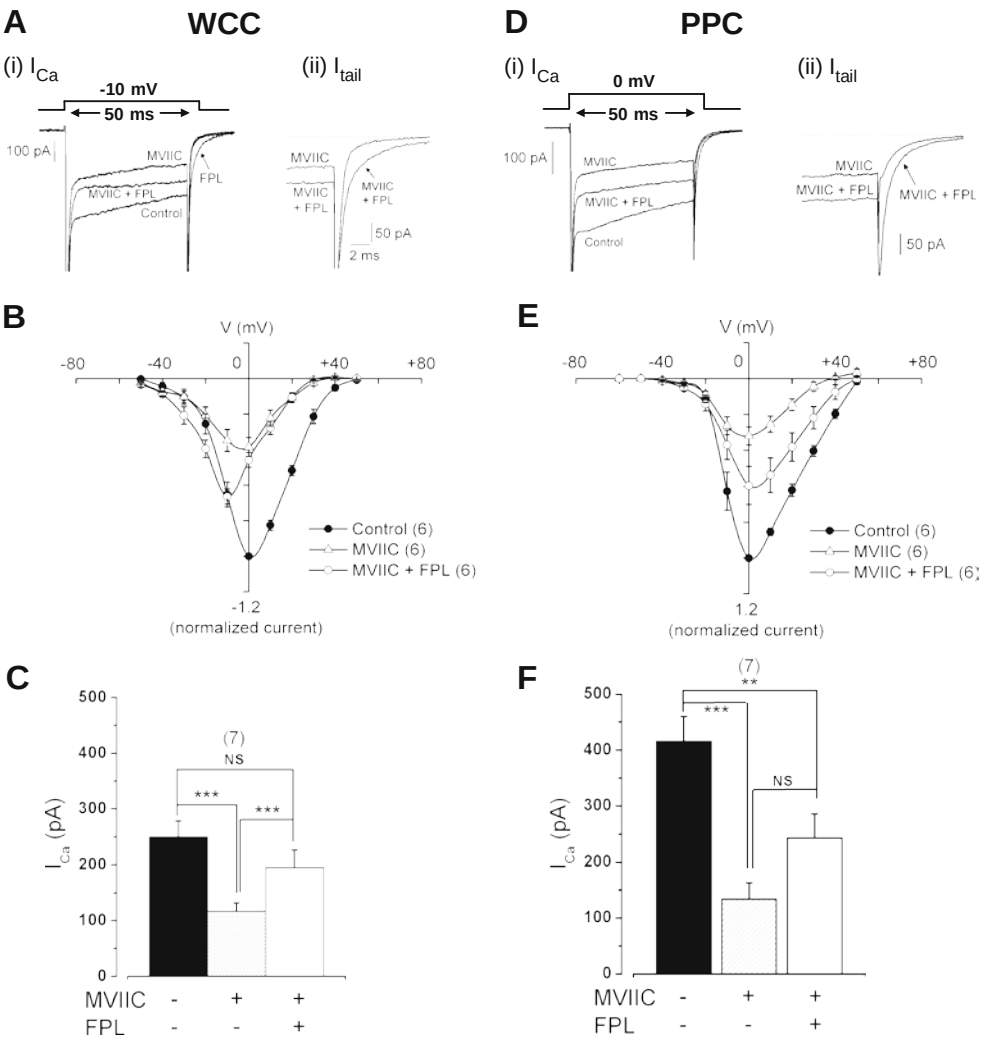

Fig. 3 FPL (1 μM) augmented I_{Ca} and I_{tail} under conditions of WCC recording (a–c) and PPC recording (d–f) in cells treated with ω-conotoxin MVIIC (MVIIC, 2 μM) to suppress N and PQ Ca^{2+} channel currents. HP −80 mV; 2 mM external Ca^{2+}. a, d Example trace currents generated by test pulses to the voltages indicated at the protocol on top, before (control), at 2 min of MVIIC treatment, and at 2 min of combined MVIIC + FPL treatment. b, e I–V relationship of I_{Ca}, during MVIIC treatment and during MVIIC + FPL treatment. These curves were obtained as described in Fig. 1. c, f Pooled results of I_{Ca} and I_{tail} amplitudes. Data are means ± SE of six cells for each configuration, from at least three different cultures. *p< 0.05, **p<0.01, ***p<0.001

recording. In the example cell shown in Fig. 4a, I_{Ca} declined to about 30% of initial current upon switching the HP from −80 to −50 mV. FPL gradually augmented I_{Ca} as well as I_{tail} to reach a plateau in about a minute. Current traces from this time course curves (a, b, c) are shown in Fig. 4b; note the progressive augmentation of I_{Ca} (i) and the drastic slowing down of I_{tail} relaxation (ii). Pooled data (Fig. 4c) indicate a voltage-dependent current loss of 54% and its augmentation to about 60% of the initial I_{Ca} upon FPL treatment. Particularly impressive was the eightfold increase of I_{tail}.

Under PPC recording, the reduction of I_{Ca} was also gradual and stabilized after a couple of minutes at −50 mV HP (Fig. 4d). FPL gradually augmented I_{Ca} and I_{tail} to reach a plateau after about 2 min. The example traces shown in Fig. 4e show the mild FPL-induced I_{Ca} increase (i) and the more pronounced slowing down of I_{tail} relaxation (ii). Pooled data (Fig. 4f) show a 60% decrease of I_{Ca} at −50 mV HP and 37% increase elicited by FPL with fivefold augmentation of I_{tail}.

In conclusion, under conditions of L current isolation, either with MVIIC or depolarized HP, FPL equally augmented I_{Ca} and I_{tail} under WCC and PPC recording conditions. This contrasts with the results obtained when I_{Ca} flows through all channel types where FPL augmented I_{Ca} under WCC recording but caused its inhibition under PPC. It seems, therefore, that this inhibition must be associated to N/PQ channels, rather than L channels.

The presence or absence of EGTA in the cytosol modifies the effects of FPL under WCC and PPC recordings

Under WCC recording, the intracellular solution contained 14 mM EGTA. Under these conditions, Ca^{2+} entering through Ca^{2+} channels will be chelated, the $[Ca^{2+}]_c$ will not increase, and the Ca^{2+}-dependent inhibition of Ca^{2+} channels will be prevented [32]. We, therefore, expected that an experiment performed in conditions similar to those of Fig. 1 under WCC recording, but using an intracellular

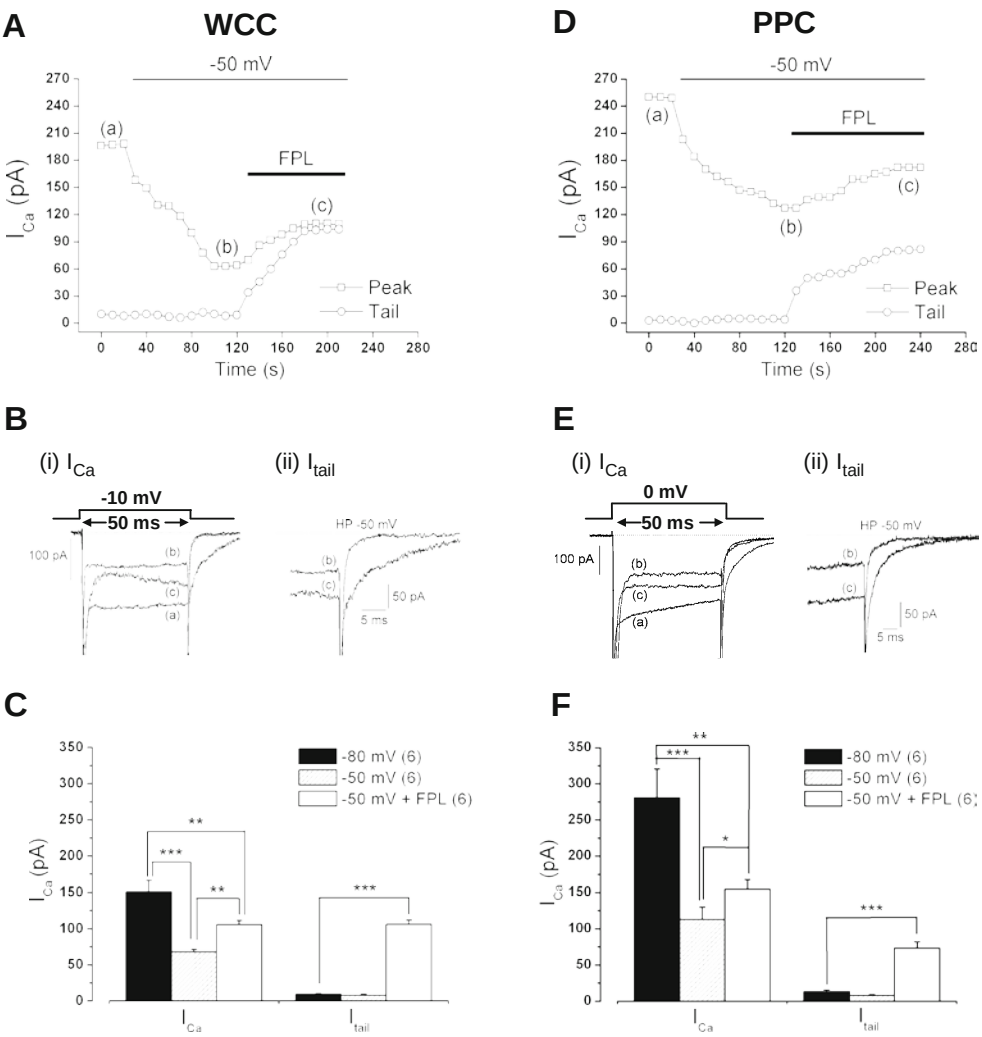

Fig. 4 FPL (1 μM) augmented I_{Ca} and I_{tail} under conditions of WCC recording (a–c) and PPC recording (d–f) in cells voltage-clamped at −50 mV in order to suppress N and PQ Ca^{2+} channel currents. HP was initially maintained at −80 mV; subsequently, HP was switched to −50 mV as indicated by the horizontal bars on top of a and d; 2 mM Ca^{2+} was present in the extracellular solution. a, d Time courses of I_{Ca} and I_{tail}. FPL was perfused during the time period indicated by the horizontal bars. Test pulses to −10 mV were applied at 10-s intervals. b, e Example I_{Ca} (i) and I_{tail} currents (ii) taken from experiments of a and d at the times indicated by a–c. c, f Pooled results on I_{Ca} and I_{tail} amplitudes calculated at the HP indicated and after 2 min perfusion with FPL. Data are means ± SE of six cells for each configuration, from at least three different cultures. *p<0.05, **p<0.01, ***p<0.001

solution deprived of EGTA, will favor the inhibition of N/PQ channel current.

The example I_{Ca} traces of Fig. 5a show that FPL inhibits I_{Ca} by 36% at a test potential of 0 mV and by 49% at +10 mV. There was a tiny slowing down of I_{tail}, particularly at +10 mV. This inhibition was seen only at depolarizing test potentials, as shown by the I–V curves of Fig. 5b. Pooled data indicate that the initial I_{Ca} of 350 pA was reduced 45% by FPL. This was a picture quite similar to that found under PPC recording with no EGTA in the cytosol (compare the I–V curves of Figs. 1e and 5b).

Under PPC recording, EGTA could not be given in the pipette solution because it will not cross the pores of the perforated membrane patch. Hence, we recourse to the cell-permeable EGTA-AM to load the cell cytosol with EGTA before doing the experiment. Figure 5d shows example I_{Ca} traces; a tiny augmentation of I_{Ca} and I_{tail} were seen upon FPL treatment both at −10 and 0 mV test potentials. FPL shifted the I–V curve to the left, indicating that FPL augmented I_{Ca} only at hyperpolarizing potentials (Fig. 5e). Pooled data show that FPL augmented I_{Ca} by 33% (Fig. 5f). These FPL effects were quite similar to those found under WCC recording with EGTA in the cytosol (compare the I–V curves of Figs. 1b and 5b).

In conclusion, under WCC, EGTA removal from the patch pipette turned FPL-induced I_{Ca} augmentation into inhibition; conversely, under PPC, the presence of EGTA in the cytosol converted FPL-induced I_{Ca} inhibition into potentiation. This supports the view that Ca^{2+}-dependent inactivation by Ca^{2+} entry through L channels is responsible for the inhibition of the fraction of the current carried through non-L channels.

Effects of FPL on Ca^{2+} channel currents using Ba^{2+} (instead of Ca^{2+}) as charge carrier, under WCC and PPC recordings

The Ca^{2+} inactivation of Ca^{2+} channels is prevented when using Ba^{2+} (instead of Ca^{2+}) as charge carrier. This is true for neurons [27] as well as bovine chromaffin cells [7, 72].

By using 2 mM Ba^{2+} (instead of 2 mM Ca^{2+}) as charge carrier, we expected to find similar effects of FPL on Ba^{2+} currents (I_{Ba}), under both WCC and PPC recordings.

Figure 6a shows example I_{Ba} traces obtained under WCC recording. FPL augmented I_{Ba} by 90% and caused a pronounced delay of I_{tail} relaxation. FPL shifted the entire I–V curve to the left, indicating I_{Ba} augmentation at steps in the negative range of the voltage scale and inhibition in the positive range (Fig. 6b). Pooled results show that FPL augmented I_{Ba} by 90% and I_{tail} by as much as sixfold (Fig. 6c).

Under PPC recording, the data came in a similar direction. For instance, the example traces of Fig. 6d show a progressive augmentation of I_{Ba} along the depolarizing pulse and a pronounced slowing down of the tail current. However, the I–V curve was shifted to the left only in the negative range of the voltage scale where I_{Ba} was augmented by FPL (Fig. 6e). Pooled results indicate that FPL enhanced I_{Ba} by 80% and I_{tail} by as much as sevenfold (Fig. 6f).

In conclusion, FPL modified I_{Ba} (peak and tail currents) in a similar way, irrespective of whether the recordings were made under WCC or PPC.

Discussion

The central finding of this study was that FPL, an enhancer of Ca^{2+} entry through L-type Ca^{2+} channels, caused a paradoxical inhibition of the whole-cell inward current flowing through Ca^{2+} channels during depolarization of voltage-clamped bovine chromaffin cells. Such inhibition was initially observed only under PPC recording since, under WCC recording, FPL augmented I_{Ca} and I_{tail} in the expected direction. We later on found that these opposing FPL actions could be explained by the absence or the presence of the mobile Ca^{2+} buffer EGTA in the intracellular solution used under PPC or WWC recordings, respectively.

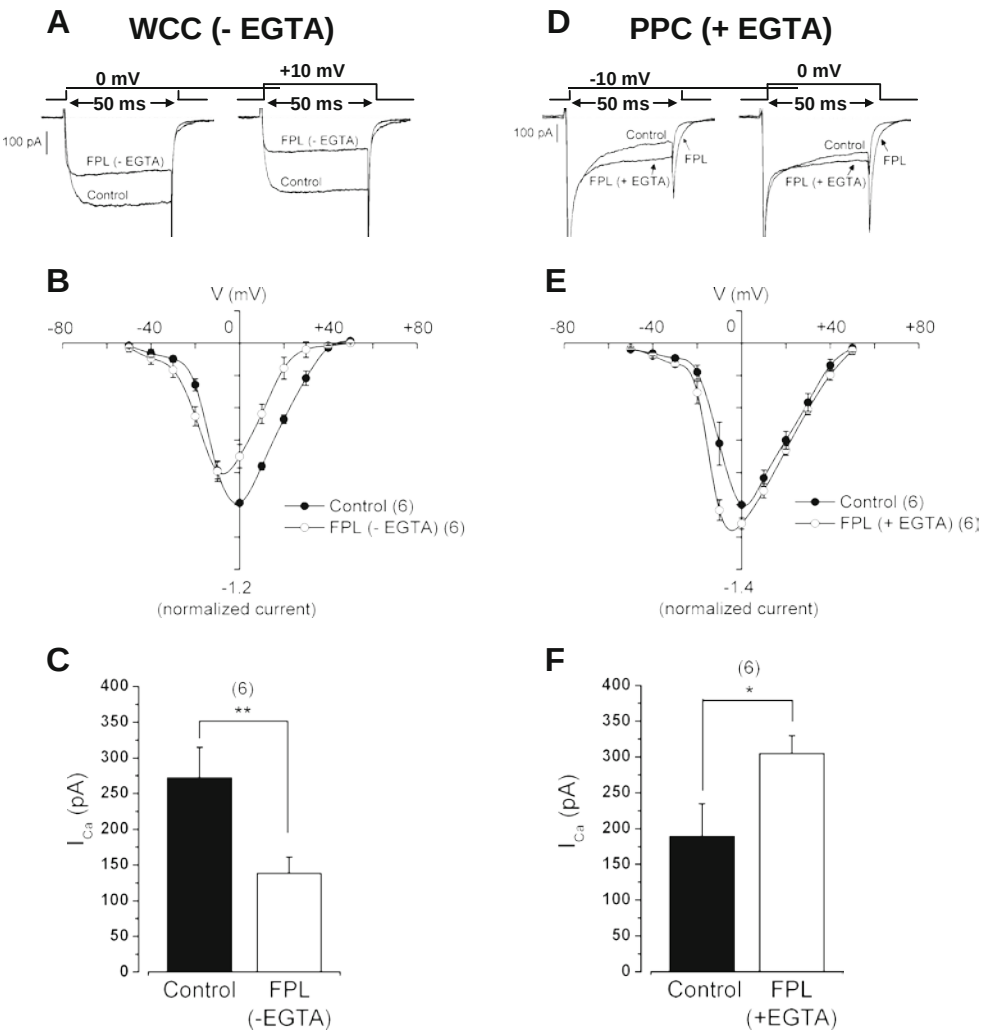

Fig. 5 Effects of EGTA on the changes of I_{Ca} elicited by FPL under WCC recording (a–c) and PPC recording (d–f) recording conditions. HP −80 mV; 2 mM external Ca^{2+}. Under WCC recording, the pipette solution contained no EGTA; under PPC recording, before the experiment, cells were incubated during 45 min with cell permeable EGTA-AM at 37°C. Cells were subsequently washed during 15 min at room temperature with the extracellular solution. Then, the cells were patched and the experiments were performed as usual under PPC recording. a, d Example trace currents generated by test pulses to the voltages indicated at the protocol on top, before (control) and at 2 min of FPL treatment. b, e I–V relationship of I_{Ca}, before (control) and during FPL treatment. c, f Pooled results on the effects of FPL on I_{Ca} (measured at 0 mV test potential). Data are means ± SE of six cells for each configuration, from at least three different cultures. *p<0.05, **p<0.01

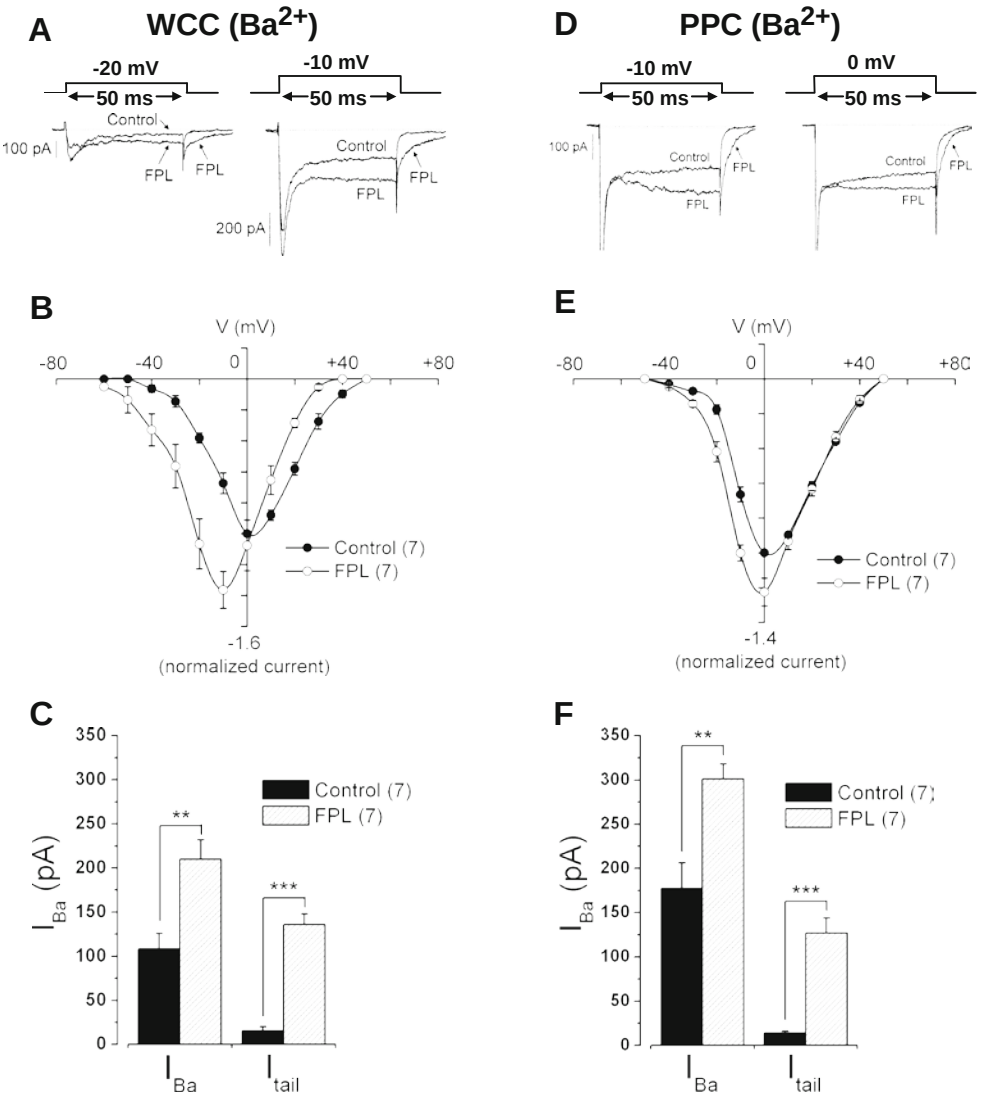

Fig. 6 FPL (1 μM) augmented I_{Ca} under both WCC (a–c) and PPC recording (d–f) if 2 mM Ba^{2+} (instead of 2 mM Ca^{2+}) was used as charge carrier. HP −80 mV; 2 mM external Ba^{2+}. a, d Example trace cur- rents generated by test pulses to the voltages indicated at the protocol on top, before (control) and at 2 min of FPL treatment. b, e I–V relationship of I_{Ba}, before (control) and during FPL treatment. These curves were made as indicated in Fig. 1. c, f Pooled results of I_{Ba} and I_{tail} amplitudes before and during FPL treatment. Data are means ± SE of seven cells for each con- figuration, from at least three different cultures. **p<0.01, *** p<0.001

The initial observation on FPL-induced I_{Ca} blockade was done under PPC recording (Fig. 1d). Thus, the possibility existed that, under this patch-clamp configuration, FPL caused a direct pharmacological inhibitory effect on some or all of the major Ca^{2+} channels expressed by bovine chromaffin cells, i.e., L, N, and PQ [23]. In fact, at 10 μM, FPL inhibited the majority of the whole-cell current in HEK cells expressing N channels; however, at 1 μM, the concentration used in this study, FPL did not block the N current [38].

I_{Ca} inhibition by FPL may rather be explained in a different context. For instance, under PPC, when FPL inhibited I_{Ca} amplitude, I_{tail} remained enhanced (Fig. 1d, f). This indicates that FPL was indeed augmenting I_{Ca} through L channels. However, these channels carry only about 15–20% of the whole-cell I_{Ca} in bovine chromaffin cells, the rest being carried by N and PQ channels [2, 3, 17, 40]. Therefore, the inhibition by FPL of N/PQ current compo- nents could mask its enhancing effects on the L current component. This was demonstrated to be the case in the experiment where N/PQ currents were blocked by MVIIC (Fig. 3) or by maintaining the HP at −50 mV (Fig. 4). Under these conditions of L current isolation, FPL always augmented I_{Ca} and I_{tail} regardless of the recording con- ditions, WCC or PPC (Figs. 3 and 4).

Various experimental data support the view that FPL was not directly inhibiting the N/PQ currents; rather, such inhibition was indirectly associated to enhanced Ca^{2+} entry through L channels that were kept open longer in the presence of FPL, as the following facts suggest: (1) under PPC recording, the presence of cytosolic EGTA turned the I_{Ca} inhibition into an I_{Ca} augmentation (Fig. 5); (2) conversely, under WCC recording, EGTA removal from the intracellular solution turned the augmented I_{Ca} into a depressed I_{Ca} (Fig. 5); (3) when using Ba^{2+} as charge carrier, which does not inactivate Ca^{2+} channels [7, 27],

FPL augmented I_{Ba} under both WCC and PPC recordings. Thus, FPL-induced I_{Ca} inhibition did not depend on the patch-clamp configuration used but on whether the experimental conditions allowed an elevation of $[Ca^{2+}]_c$ during the application of depolarizing pulses. The possibility existed that the effects of FPL were linked to the washout of a cytosolic factor that is the target of the Ca^{2+}; such factor could be removed under WCC recording. We did experiments in six cells, recording under WCC from the beginning of seal rupture. I_{Ca} amplitude was gradually augmented from about 40 pA at the moment of seal rupture to about 140 pA in 1 min thereafter. FPL caused a pronounced I_{Ca} augmentation from the beginning of seal rupture but only in the presence of EGTA. This indicates that the washout of a cytosolic factor is not involved in the FPL effects of I_{Ca}.

Now the question arises as to whether the amount of Ca^{2+} entering the cell during brief depolarizing pulses (50 ms in our present study) is sufficient to build up a local $[Ca^{2+}]_c$ transient to inactivate N/PQ Ca^{2+} channels. The averaged $[Ca^{2+}]_c$ peaks measured with Ca^{2+} probes do not detect the high $[Ca^{2+}]_c$ transients occurring at subplasmalemmal sites during cell depolarization [13, 54, 67]. Using pulsed laser imaging, Monck and workers [45] visualized hot spots of submembranous Ca^{2+} evoked by 50 ms depolarizing pulses, the same stimulation pattern used in the present study. These hot spots developed in 20–50 ms and extended laterally by several micrometers. Partial or complete submembranous rings of elevated $[Ca^{2+}]$ appeared at 50–100 ms after channel opening, and the Ca^{2+} gradient collapsed at 200–400 ms after the pulse began. This was interpreted as due to a limited Ca^{2+} diffusion because of rapid Ca^{2+} sequestration by immobile buffers [45, 76].

In bovine chromaffin cells, the cytosol has a Ca^{2+} binding capacity of 4 mmol/L cells. The endogenous Ca^{2+} buffer is scarcely mobile, has a low affinity for Ca^{2+} (k_d ~ 100 μM) and an activity coefficient of ~1/40 [74, 76]. The two-dimensional diffusion coefficient is ~40 $\mu m^2/s$ and shows inhomogeneities at the plasma membrane [51]. Brief openings of VDCCs generate $[Ca^{2+}]_c$ microdomains as high as 10 or even 100 μM [8, 55]. Using mitochondria as biosensors for $[Ca^{2+}]_c$ changes, we found that ACh or K^+ pulses caused $[Ca^{2+}]_c$ elevations of 20–40 μM at subplasmalemmal sites of bovine chromaffin cells [47]. Because of rapid diffusion of Ca^{2+} towards the surrounding cytosol, these Ca^{2+} microdomains are very much restricted in time and space [53, 54]. The presence of mobile Ca^{2+} buffers accelerates diffusion and oppose the development of high $[Ca^{2+}]_c$ microdomains during cell depolarization [4, 5, 56, 64]. For instance, at 50 μM, a high-affinity low-capacity Ca^{2+} buffer such as fura-2 increases the apparent rate of Ca^{2+} diffusion by as much as four times [76].

In our present experiments, we dialyzed the cytosol with 14 mM EGTA under WCC recording or we incubated the cells with EGTA-AM for PPC experiments. Being a strong buffer [43], EGTA will prevent the buildup of high Ca^{2+} microdomains at subplasmalemmal sites during cell stimulation with 50 ms depolarizing pulses, as happened to be the case with fura-2 [76]. Under these conditions, it is understandable that Ca^{2+} induced N/PQ channel inhibition was not taking place and that the dominant FPL effects were I_{Ca} and I_{tail} increase and slowing down of I_{tail} due to L channel activation.

As discussed above, the bovine chromaffin cell cytosol contains strong Ca^{2+} buffers that severely restrict the diffusion of the Ca^{2+} entering through Ca^{2+} channels. Therefore, we must admit that, to cause inactivation of N/PQ channels, the Ca^{2+} has to enter the cell through L channels located close by. This effect might occur under physiological stimulation of chromaffin cells. However, it could better be unmasked by FPL-induced enhanced Ca^{2+} entry through L channels. From a functional point of view, this possible colocalization of L and non-L channels can be further investigated using FPL as a pharmacological tool to selectively augment Ca^{2+} entry through L channels. A challenging question to explore is whether L, N, and PQ channels form functional clusters units to regulate diverse exocytotic responses tailored to specific needs. In this context, it is interesting to note that some authors have found hot spots of Ca^{2+} entry and release in bovine chromaffin cells [62]. Furthermore, active exocytotic zones have been found in bovine chromaffin cells [66, 73] and a functional polarization of secretory sites have been revealed using confocal fluorescence microscopy, also in bovine chromaffin cells [12]. However, this clustering of Ca^{2+} channel subtypes at specific plasmalemmal sites makes it difficult to understand how the Ca^{2+} entering through a given channel type may have a selective function distinct from the Ca^{2+} entering through other channel type. Also, the question emerges on why Ca^{2+} entering through N/PQ channels (about 80% of the I_{Ca}) is not eliciting the inactivation of such channels. Unfortunately, compounds that prevent the inactivation of N/PQ channels (as the case is for L channels with FPL and BayK) are not available to help answer these questions. Further insight into the possible colocalization of Ca^{2+} channel subtypes could be achieved through the judicious use of various concentrations of EGTA (slow Ca^{2+} chelator) and BAPTA (rapid Ca^{2+} chelator). This approach has been useful to study Ca^{2+} channel colocalization with the secretory machinery (reviewed in García et al. [23]). However, the extrapolation of this strategy to demonstrate colocalization of Ca^{2+} channel subtypes may be difficult in the context of the present experiments. Immunofluorescence experiments with specific antibodies for α1 subunits of L, N, and P/Q channels could also provide some information on the possible colocalization of these channels. An alternative

explanation may be linked to the different molecular mechanisms underlying the regulation of Ca^{2+} channel subtypes by the Ca^{2+}-binding protein calmodulin and/or intracellular messengers [11, 15, 37, 49]. It may be that the lower Ca^{2+} affinity of calmodulin lobe or another lower affinity Ca^{2+}-binding protein experiences activating concentrations in the microdomains around isolated L channels and then dissociates and travels to affect N/PQ channels.

Finally, the possible specialization of the various Ca^{2+} channel subtypes expressed within the same cell to perform specific functions deserves a comment. Since the discovery that bovine chromaffin cells expressed multiple Ca^{2+} channels, efforts have been made to find out a kind of specialization for each channel subtype to drive a specific cell function. For instance, concerning exocytosis, L channels [6, 33], PQ channels [36], or all channels [41, 69] drive the secretory process. This disparity may be due to different stimuli and experimental conditions used [23]. The possible specialization of Ca^{2+} channel subtypes in bovine chromaffin cells has been explored in functional aspects other than exocytosis. For instance, Ca^{2+} entry through L channels, but not through N and PQ channels, causes mitochondrial disruption and cell death by apoptosis [10]; also, Ca^{2+} entry through L channels are preferentially coupled to endocytosis [60, 63]. However, other studies do not attribute a special function to a given channel subtype. This is the case for tyrosine hydroxylase activation [58], SNAP-25 expression [21], ERK phosphorylation [48], or mitochondrial Ca^{2+} uptake [46]; these studies concluded that these cell functions depended more on critical $[Ca^{2+}]_c$ levels than on Ca^{2+} entry through a given Ca^{2+} channel subtype. The results of our present study, however, clearly indicate that the Ca^{2+} entering through L channels have a clear-cut function, the modulation of N and PQ channel activities during cell depolarization. To our knowledge, this is the first report suggesting this function for the L-type voltage-dependent Ca^{2+} channel.

To conclude, the L-type Ca^{2+} channel activator FPL caused opposing effects on I_{Ca}, i.e., augmentation under WCC recording and inhibition under PPC recording. The experiments done in this study to clarify these apparent paradoxical effects suggest that Ca^{2+} entry through L channels causes a Ca^{2+}-dependent inhibition of N and PQ channels. FPL seems to be a good tool to further explore functional aspects of this novel regulatory action of Ca^{2+} flux through L-type channels.

Acknowledgements This work was supported by grants from Ministerio de Ciencia e Innovación (SAF2006-03589 to AGG; SAF2007-65181 to LG); Instituto de Salud Carlos III (RETICS-RD06/0026); Comunidad Autónoma de Madrid (S-SAL-0275-2006); and Fundación Mutua Madrileña (to AGG and LG). JMR is a fellow of FPU program, Universidad Autónoma de Madrid, Spain. We thank Lorena Cortés and Inés Colmena for the preparation of excellent cell cultures and the "Fundación Teófilo Hernando" for the continued support.

References

1. Albillos A, Carbone E, Gandia L, Garcia AG, Pollo A (1996) Opioid inhibition of Ca^{2+} channel subtypes in bovine chromaffin cells: selectivity of action and voltage-dependence. Eur J Neurosci 8:1561–1570
2. Albillos A, Garcia AG, Gandia L (1993) omega-Agatoxin-IVA-sensitive calcium channels in bovine chromaffin cells. FEBS Lett 336:259–262
3. Albillos A, Garcia AG, Olivera B, Gandia L (1996) Re-evaluation of the P/Q Ca^{2+} channel components of Ba^{2+} currents in bovine chromaffin cells superfused with solutions containing low and high Ba^{2+} concentrations. Pflugers Arch 432:1030–1038
4. Alonso MT, Montero M, Carnicero E, Garcia-Sancho J, Alvarez J (2002) Subcellular Ca^{2+} dynamics measured with targeted aequorin in chromaffin cells. Ann N Y Acad Sci 971:634–640
5. Alonso MT, Villalobos C, Chamero P, Alvarez J, Garcia-Sancho J (2006) Calcium microdomains in mitochondria and nucleus. Cell Calcium 40:513–525
6. Artalejo CR, Adams ME, Fox AP (1994) Three types of Ca^{2+} channel trigger secretion with different efficacies in chromaffin cells. Nature 367:72–76
7. Artalejo CR, Garcia AG, Aunis D (1987) Chromaffin cell calcium channel kinetics measured isotopically through fast calcium, strontium, and barium fluxes. J Biol Chem 262:915–926
8. Augustine GJ, Neher E (1992) Calcium requirements for secretion in bovine chromaffin cells. J Physiol 450:247–271
9. Brehm P, Eckert R (1978) Calcium entry leads to inactivation of calcium channel in Paramecium. Science 202:1203–1206
10. Cano-Abad MF, Villarroya M, Garcia AG, Gabilan NH, Lopez MG (2001) Calcium entry through L-type calcium channels causes mitochondrial disruption and chromaffin cell death. J Biol Chem 276:39695–39704
11. Cens T, Rousset M, Leyris JP, Fesquet P, Charnet P (2006) Voltage- and calcium-dependent inactivation in high voltage-gated Ca^{2+} channels. Prog Biophys Mol Biol 90:104–117
12. Cuchillo-Ibáñez I, Michelena P, Albillos A, García AG (1999) A preferential pole for exocytosis in cultured chromaffin cells revealed by confocal microscopy. FEBS Lett 459:22–26
13. Chad JE, Eckert R (1984) Calcium domains associated with individual channels can account for anomalous voltage relations of CA-dependent responses. Biophys J 45:993–999
14. Chan SA, Polo-Parada L, Smith C (2005) Action potential stimulation reveals an increased role for P/Q-calcium channel-dependent exocytosis in mouse adrenal tissue slices. Arch Biochem Biophys 435:65–73
15. DeMaria CD, Soong TW, Alseikhan BA, Alvania RS, Yue DT (2001) Calmodulin bifurcates the local Ca^{2+} signal that modulates P/Q-type Ca^{2+} channels. Nature 411:484–489
16. Fenwick EM, Marty A, Neher E (1982) Sodium and calcium channels in bovine chromaffin cells. J Physiol 331:599–635
17. Gandía L, Albillos A, García AG (1993) Bovine chromaffin cells possess FTX-sensitive calcium channels. Biochem Biophys Res Commun 194:671–676
18. Gandía L, García AG, Morad M (1993) ATP modulation of calcium channels in chromaffin cells. J Physiol 470:55–72
19. Gandia L, Lara B, Imperial JS, Villarroya M, Albillos A, Maroto R, Garcia AG, Olivera BM (1997) Analogies and differences between omega-conotoxins MVIIC and MVIID: binding sites and functions in bovine chromaffin cells. Pflugers Arch 435:55–64
20. Gandía L, Montiel C, García AG, López MG (2008) Calcium channels for exocytosis: functional modulation with toxins. In: Botana L (ed) Seafood and freshwater toxins: pharmacology, physiology and detection. CRC Press, Boca Raton, FL, USA, pp 107–148

21. García-Palomero E, Montiel C, Herrero CJ, García AG, Alvarez RM, Arnalich FM, Renart J, Lara H, Cárdenas AM (2000) Multiple calcium pathways induce the expression of SNAP-25 protein in chromaffin cells. J Neurochem 74:1049–1058
22. García-Palomero E, Renart J, Andres-Mateos E, Solís-Garrido LM, Matute C, Herrero CJ, García AG, Montiel C (2001) Differential expression of calcium channel subtypes in the bovine adrenal medulla. Neuroendocrinology 74:251–261
23. García AG, García-De-Diego AM, Gandía L, Borges R, García-Sancho J (2006) Calcium signaling and exocytosis in adrenal chromaffin cells. Physiol Rev 86:1093–1131
24. García AG, Sala F, Reig JA, Viniegra S, Frias J, Fonteriz R, Gandía L (1984) Dihydropyridine BAY-K-8644 activates chromaffin cell calcium channels. Nature 309:69–71
25. Giannattasio B, Jones SW, Scarpa A (1991) Calcium currents in the A7r5 smooth muscle-derived cell line. Calcium-dependent and voltage-dependent inactivation. J Gen Physiol 98:987–1003
26. Gillis KD, Pun RY, Misler S (1991) Long-term monitoring of depolarization-induced exocytosis from adrenal medullary chromaffin cells and pancreatic islet B cells using "perforated patch recording". Ann N Y Acad Sci 635:464–467
27. Hagiwara S, Byerly L (1981) Calcium channel. Annu Rev Neurosci 4:69–125
28. Hagiwara S, Nakajima S (1966) Effects of the intracellular Ca ion concentration upon the excitability of the muscle fiber membrane of a barnacle. J Gen Physiol 49:807–818
29. Hamill OP, Marty A, Neher E, Sakmann B, Sigworth FJ (1981) Improved patch-clamp techniques for high-resolution current recording from cells and cell-free membrane patches. Pflugers Arch 391:85–100
30. Hernández-Guijo JM, Carabelli V, Gandía L, García AG, Carbone E (1999) Voltage-independent autocrine modulation of L-type channels mediated by ATP, opioids and catecholamines in rat chromaffin cells. Eur J Neurosci 11:3574–3584
31. Hernández-Guijo JM, Gandía L, de Pascual R, García AG (1997) Differential effects of the neuroprotectant lubeluzole on bovine and mouse chromaffin cell calcium channel subtypes. Br J Pharmacol 122:275–285
32. Hernández-Guijo JM, Maneu-Flores VE, Ruiz-Nuno A, Villarroya M, García AG, Gandía L (2001) Calcium-dependent inhibition of L, N, and P/Q Ca^{2+} channels in chromaffin cells: role of mitochondria. J Neurosci 21:2553–2560
33. Jiménez RR, López MG, Sancho C, Maroto R, García AG (1993) A component of the catecholamine secretory response in the bovine adrenal gland is resistant to dihydropyridines and omega-conotoxin. Biochem Biophys Res Commun 191:1278–1283
34. Korn SJ, Horn R (1989) Influence of sodium-calcium exchange on calcium current rundown and the duration of calcium-dependent chloride currents in pituitary cells, studied with whole cell and perforated patch recording. J Gen Physiol 94:789–812
35. Kunze DL, Rampe D (1992) Characterization of the effects of a new Ca^{2+} channel activator, FPL 64176, in GH3 cells. Mol Pharmacol 42:666–670
36. Lara B, Gandía L, Martinez-Sierra R, Torres A, García AG (1998) Q-type Ca^{2+} channels are located closer to secretory sites than L-type channels: functional evidence in chromaffin cells. Pflugers Arch 435:472–478
37. Liang H, DeMaria CD, Erickson MG, Mori MX, Alseikhan BA, Yue DT (2003) Unified mechanisms of Ca^{2+} regulation across the Ca^{2+} channel family. Neuron 39:951–960
38. Liu L, Rittenhouse AR (2003) Arachidonic acid mediates muscarinic inhibition and enhancement of N-type Ca^{2+} current in sympathetic neurons. Proc Natl Acad Sci U S A 100:295–300
39. Livett BG (1984) Adrenal medullary chromaffin cells in vitro. Physiol Rev 64:1103–1161
40. López MG, Villarroya M, Lara B, Martínez-Sierra R, Albillos A, García AG, Gandía L (1994) Q- and L-type Ca^{2+} channels dominate the control of secretion in bovine chromaffin cells. FEBS Lett 349:331–337
41. Lukyanetz EA, Neher E (1999) Different types of calcium channels and secretion from bovine chromaffin cells. Eur J Neurosci 11:2865–2873
42. McDonough SI, Mori Y, Bean BP (2005) FPL 64176 modification of Ca(V) 1.2 L-type calcium channels: dissociation of effects on ionic current and gating current. Biophys J 88:211–223
43. McGuigan JA, Luthi D, Buri A (1991) Calcium buffer solutions and how to make them: a do it yourself guide. Can J Physiol Pharmacol 69:1733–1749
44. McKechnie K, Killingback P, Naya I, O'Conner SE, Smith G, Warfam DG, Wells E, Whitehead YM, Williams G (1989) Calcium channel activator properties in a novel non-dihydropyridine-FPL64176. Br J Pharmacol 98:673–679
45. Monck JR, Robinson IM, Escobar AL, Vergara JL, Fernandez JM (1994) Pulsed laser imaging of rapid Ca^{2+} gradients in excitable cells. Biophys J 67:505–514
46. Montero M, Alonso MT, Albillos A, Cuchillo-Ibáñez I, Olivares R, García AG, García-Sancho J, Alvarez J (2001) Control of secretion by mitochondria depends on the size of the local $[Ca^{2+}]$ after chromaffin cell stimulation. Eur J Neurosci 13:2247–2254
47. Montero M, Alonso MT, Carnicero E, Cuchillo-Ibáñez I, Albillos A, García AG, García-Sancho J, Alvarez J (2000) Chromaffin-cell stimulation triggers fast millimolar mitochondrial Ca^{2+} transients that modulate secretion. Nat Cell Biol 2:57–61
48. Montiel C, Mendoza I, García CJ, Awad Y, García-Olivares J, Solís-Garrido LM, Lara H, García AG, Cárdenas AM (2003) Distinct protein kinases regulate SNAP-25 expression in chromaffin cells. J Neurosci Res 71:353–364
49. Morad M, Soldatov N (2005) Calcium channel inactivation: possible role in signal transduction and Ca^{2+} signaling. Cell Calcium 38:223–231
50. Moro MA, López MG, Gandía L, Michelena P, García AG (1990) Separation and culture of living adrenaline- and noradrenaline-containing cells from bovine adrenal medullae. Anal Biochem 185:243–248
51. Naraghi M, Muller TH, Neher E (1998) Two-dimensional determination of the cellular Ca^{2+} binding in bovine chromaffin cells. Biophys J 75:1635–1647
52. Neely A, Lingle CJ (1992) Two components of calcium-activated potassium current in rat adrenal chromaffin cells. J Physiol 453:97–131
53. Neher E (1998) Usefulness and limitations of linear approximations to the understanding of Ca^{++} signals. Cell Calcium 24:345–357
54. Neher E (1998) Vesicle pools and Ca^{2+} microdomains: new tools for understanding their roles in neurotransmitter release. Neuron 20:389–399
55. Neher E, Augustine GJ (1992) Calcium gradients and buffers in bovine chromaffin cells. J Physiol 450:273–301
56. Nowicky AV, Duchen MR (1998) Changes in $[Ca^{2+}]_i$ and membrane currents during impaired mitochondrial metabolism in dissociated rat hippocampal neurons. J Physiol 507:131–145
57. Nowycky MC, Fox AP, Tsien RW (1985) Three types of neuronal calcium channel with different calcium agonist sensitivity. Nature 316:440–443
58. O'Farrell M, Marley PD (2000) Differential control of tyrosine hydroxylase activation and catecholamine secretion by voltage-operated Ca^{2+} channels in bovine chromaffin cells. J Neurochem 74:1271–1278
59. Olivera BM, Miljanich GP, Ramachandran J, Adams ME (1994) Calcium channel diversity and neurotransmitter release: the omega-conotoxins and omega-agatoxins. Annu Rev Biochem 63:823–867

60. Perissinotti PP, Giugovaz Tropper B, Uchitel OD (2008) L-type calcium channels are involved in fast endocytosis at the mouse neuromuscular junction. Eur J Neurosci 27:1333–1344
61. Rae J, Cooper K, Gates P, Watsky M (1991) Low access resistance perforated patch recordings using amphotericin B. J Neurosci Methods 37:15–26
62. Robinson IM, Finnegan JM, Monck JR, Wightman RM, Fernan- dez JM (1995) Colocalization of calcium entry and exocytotic release sites in adrenal chromaffin cells. Proc Natl Acad Sci U S A 92:2474–2478
63. Rosa JM, de Diego AM, Gandía L, García AG (2007) L-type calcium channels are preferentially coupled to endocytosis in bovine chromaffin cells. Biochem Biophys Res Commun 357:834–839
64. Sala F, Hernández-Cruz A (1990) Calcium diffusion modeling in a spherical neuron. Relevance of buffering properties. Biophys J 57:313–324
65. Schramm M, Thomas G, Towart R, Franckowiak G (1983) Novel dihydropyridines with positive inotropic action through activation of $Ca2^{+}$ channels. Nature 303:535–537
66. Schroeder TJ, Jankowski JA, Senyshyn J, Holz RW, Wightman RM (1994) Zones of exocytotic release on bovine adrenal medullary cells in culture. J Biol Chem 269:17215–17220
67. Simon SM, Llinas RR (1985) Compartmentalization of the submembrane calcium activity during calcium influx and its significance in transmitter release. Biophys J 48:485–498
68. Tillotson D (1979) Inactivation of Ca conductance dependent on entry of Ca ions in molluscan neurons. Proc Natl Acad Sci U S A 76:1497–1500
69. Ulate G, Scott SR, Gonzalez J, Gilabert JA, Artalejo AR (2000) Extracellular ATP regulates exocytosis in inhibiting multiple Ca^{2+} channel types in bovine chromaffin cells. Pflugers Arch 439:304–314
70. Villarroya M, Olivares R, Ruiz A, Cano-Abad MF, de Pascual R, Lomax RB, Lopez MG, Mayorgas I, Gandia L, Garcia AG (1999) Voltage inactivation of Ca^{2+} entry and secretion associated with N- and P/Q-type but not L-type Ca^{2+} channels of bovine chromaffin cells. J Physiol 516:421–432
71. von Gersdorff H, Matthews G (1996) Calcium-dependent inacti- vation of calcium current in synaptic terminals of retinal bipolar neurons. J Neurosci 16:115–122
72. von Ruden L, Garcia AG, Lopez MG (1993) The mechanism of Ba^{2+}-induced exocytosis from single chromaffin cells. FEBS Lett 336:48–52
73. Wick PF, Trenkle JM, Holz RW (1997) Punctate appearance of dopamine-beta-hydroxylase on the chromaffin cell surface reflects the fusion of individual chromaffin granules upon exocytosis. Neuroscience 80:847–860
74. Xu T, Naraghi M, Kang H, Neher E (1997) Kinetic studies of Ca^{2+} binding and Ca^{2+} clearance in the cytosol of adrenal chromaffin cells. Biophys J 73:532–545
75. Zheng W, Rampe D, Triggle DJ (1991) Pharmacological, radio- ligand binding, and electrophysiological characteristics of FPL64176, a novel nondihydropyridine Ca^{2+} channel activator, in cardiac and vascular preparations. Mol Pharmacol 40:734–741
76. Zhou Z, Neher E (1993) Mobile and immobile calcium buffers in bovine adrenal chromaffin cells. J Physiol 469:245–273

3- Papel de los esfingolipidos en la endocitosis

Pflugers Arch – Eur J Physiol DOI 10.1007/s00424-010-0861-x

SIGNALING AND CELL PHYSIOLOGY

Permissive role of sphingosine on calcium-dependent endocytosis in chromaffin cells

Juliana M. Rosa & Luis Gandía & Antonio G. García

Received: 20 May 2010 / Accepted: 22 June 2010

Abstract Sphingosine has been shown to modulate neurotransmitter release. Because membrane fusion and fission involve lipid metabolism, we asked here whether sphingosine had a role in regulating endocytosis. To explore this hypothesis, we monitored changes of membrane capacitance (Cm) to study the effects of intracellular sphingosine on membrane retrieval after chromaffin cell stimulation with depolarising pulses (DPs). We found that: (1) sphingosine dialysis through the patch-clamp pipette (SpD) using the whole-cell configuration of the patch-clamp technique (WCC) favours the appearance of a pronounced endocytotic response; (2) SpD-elicited endocytosis was Ca^{2+}-dependent but Ba^{2+} did not substitute Ca^{2+}; (3) under WCC, such endocytotic response disappeared with repetitive DPs; (4) in cells preincubated with sphingomyelinase to augment endogenous sphingosine synthesis, and then voltage-clamped under the perforated-patch configuration of the patch-clamp technique (PPC), endocytosis decayed little with repeated stimulation; (5) sphingosine-1-phosphate (S1P), a metabolite of sphingosine, had a meagre effect on endocytosis; and (6) neither dynamin inhibitor dynasore nor calmodulin blocker calmidazolium affected the sphingosine elicited endocytosis. We believe this is the first report showing that sphingosine plays a permissive role in activating Ca^{2+}-dependent endocytosis during cell depolarisation. This effect requires high subplasmalemmal cytosolic Ca^{2+} concentrations and a cytosolic factor(s) that is dialysed with the pipette solution. Independence of dynamin and calmodulin suggests that sphingosine-dependent endocytosis could be a novel, more direct pathway for vesicle recycling under mild depolarisation stimuli.

Keywords Sphingosine · Endocytosis · Chromaffin cell · Sphingomyelinase · Sphingosine-1-phosphate

Introduction

The Ca^{2+}-dependent release of neurotransmitters [1] and hormones [2] tightly depends on the preservation of an equilibrium between the amount of vesicular membrane incorporated into the plasmalemma during exocytosis and membrane retrieval during endocytosis. This will ensure that the size of nerve terminals and endocrine cells is preserved during cell activity; it will also warrant that a given number of secretory vesicles are available to participate in subsequent rounds of exocytosis during repetitive cell activation [3–5].

Exocytosis (membrane fusion) and endocytosis (membrane fission) are processes that involve membranes enriched in lipids. Thus, some studies have addressed the role of lipid metabolism on neurotransmitter release. For instance, the activity of sphingomyelinase, an enzyme that synthesises sphingosine, has been associated to the regulation of neurotransmitter release from cerebellar and mesencephalic neurons, as well as from PC12 cells [6–8]. On the other hand, a genetic

J. M. Rosa : L. Gandía : A. G. García (*)
Instituto Teófilo Hernando Facultad de Medicina,
Universidad Autónoma de Madrid,
Arzobispo Morcillo, 4,
28029 Madrid, Spain
e-mail: agg@uam.es

J. M. Rosa : L. Gandía : A. G. García
Departamento de Farmacología y Terapéutica,
Facultad de Medicina, Universidad Autónoma de Madrid,
Madrid, Spain

A. G. García
Servicio de Farmacología Clínica, Hospital Universitario
de la Princesa, Universidad Autónoma de Madrid,
Madrid, Spain

Published online: 17 July 2010

study shows direct involvement of ceramidase in synaptic transmission [9]. Furthermore, a sphingosine metabolite upregulates glutamate secretion in hippocampal neurons [10], as well as acetylcholine release at the frog neuromuscular junction [11]. Finally, a recent study shows that sphingosine augments neurotransmitter release [12].

We planned the present study trying to answer the question of whether sphingomyelinase, sphingosine and its metabolite sphingosine-1-phosphate (S1P) are modulating the endocytotic response following cell depolarisation. We used chromaffin cells, a well established model to perform studies on the mechanisms involved in Ca^{2+}-dependent membrane fusion and membrane retrieval [13–15]. We investigated here the effects of sphingosine, sphingomyelinase and S1P on endocytosis in voltage-clamped bovine chromaffin cells stimulated with depolarising pulses. We found that sphingosine and sphingomyelinase promoted a large Ca^{2+}-dependent endocytosis upon mild stimulation of voltage-clamped cells. This effect was not inhibited by dynasore or calmidazolium, suggesting that sphingosine acts on an endocytotic pathway different from dynamin- and calmodulin-signalling pathways [5, 16–18].

Materials and methods

Isolation and culture of bovine chromaffin cells

Bovine adrenal glands were obtained from a local slaughterhouse. Chromaffin cells were isolated by digestion of the adrenal medulla with collagenase following standard methods [19] with some modifications [20]. Cells were suspended in Dulbecco's modified Eagle's medium (DMEM) supplemented with 5% foetal calf serum, 10 μM cytosine arabinoside, 10 μM fluorodeoxyrudine, 50 IU ml^{-1} penicillin and 50 μg ml^{-1} streptomycin. Cells were plated on 12-mm-diameter polylisine-coated glass coverslips at a density of 5×10^4 cells/coverslip. Cells were kept in a water-saturated incubator at 37°C, in a 5% CO_2–95% air atmosphere, and used 2−5 days thereafter.

Recording of Ca^{2+} currents and membrane capacitance of chromaffin cells

Ca^{2+} currents (I_{Ca}) were recorded in voltage-clamped cells under the whole cell configuration of the patch-clamp technique (WCC) [21] at 25°C. Cells were dialysed with a solution containing (mM): 10 NaCl, 100 CsCl, 20 TEA-Cl, 0.1 EGTA, 20 HEPES, 5 Mg.ATP, 0.3 Na.GTP, pH 7.2. During recordings, cells were continuously perifused with a Tyrode solution containing (mM): 137 NaCl, 1 $MgCl_2$, 10 $CaCl_2$, 10 glucose, 10 HEPES, pH 7.4. In the experiments to study the Ca^{2+}-dependent response, different external Ca^{2+} concentrations were used. In some experiments, equimolar Ba^{2+} was used instead of Ca^{2+} as charge carrier. For patching the cells, pipettes of 3−5 MΩ resistance were pulled from borosilicate glass, partially coated with molten dental wax, and lightly fire polished.

In some experiments, the perforated-patch configuration of the patch-clamp technique (PPC) was used; electrodes were filled with an intracellular solution containing (mM): 135 CsGlutamate, 10 HEPES, 9 NaCl, pH 7.2, adjusted with CsOH. For this configuration, an amphotericin B stock solution was prepared every week at 50 mg ml^{-1} in DMSO and stored at 4°C, and protected from light. Fresh perforated patch pipette solution was prepared every day by addition of 10 μl stock amphotericin B solution. This solution was sonicated thoroughly, protected from light and kept in ice. Patch pipettes (2−3 MΩ resistance) had their tips dipped in amphotericin-free solution for 2−10 s and back-filled with freshly mixed amphotericin-containing solution. Recordings started when the access resistance decreased below 25 MΩ, which usually happened within 10 min after sealing [22].

Electrophysiological data were acquired with an EPC-9 amplifier using the Pulse software (HEKA Elektronik). Cell membrane capacitance changes (Cm) were estimated by the Lindau-Neher technique [23]. A 400-ms sinusoidal wave (1 kHz, 60 mV peak-to-peak amplitude) was given before the depolarising protocol, followed by a 3-s sinusoidal wave of the same characteristics, allowing accurate calculations of membrane capacitance changes. Membrane current was sampled at 20 kHz. Cells were held at −80 mV, and single depolarising pulses to +10 mV were applied at 1-min intervals. Sphingosine (50 μM) or vehicle (1 μl/ml DMSO) was added in the pipette solution as indicated; this way of dialysing the cell cytosol with sphingosine under WCC was abbreviated as SpD throughout the manuscript.

Data analysis and statistics

The whole-cell inward Ca^{2+} current peak (I_{Ca}) and the current area representing the total Ca^{2+} that entered the cell during a depolarising stimulus (Q_{Ca}) were analysed after the initial 10 ms of each depolarising pulse to get rid of the Na^+ current. In this study, exo- and endocytosis were measured by monitoring changes in cell capacitance (Cm). After the exocytotic peak (capacitance was measured 40 ms after the end of the depolarising pulse), Cm changes were measured during the ensuing 3-s period; endocytosis was calculated as the difference in Cm at the beginning and the end of such 3-s period. Comparisons between means of group data were performed by one-way analysis of variance (ANOVA) followed by Newman-Keuls post hoc test when

appropriate. A p value equal to or smaller than 0.05 was taken as the limit of significance.

Materials and solutions

The following materials were used: DMEM, bovine serum albumin fraction V, foetal calf serum and antibiotics were from Gibco (Madrid, Spain). Collagenase type I, Amphotericin B, D-sphingosine, Staphylococcus aureus sphingomyelinase, N-oleoylethanolamine (NOE), dynasore monohydrate, calmidazolium, S1P and carbonylcyanide-4-(trifluoromethoxy) phenylhydrazone (FCCP) were from Sigma (Madrid, Spain). The solutions, except S1P, were prepared in dimethylsulphoxide (DMSO), kept at −20°C in aliquots and protected from light. S1P was dissolved in methanol. Final concentrations of drugs were obtained by diluting the stock solution directly into internal or external solution.

Results

Sphingosine favoured the activation of a pronounced endocytotic response

In preliminary experiments to explore the actions of sphingosine on endocytosis, we tested the various DP stimuli used in a recent study from our laboratory [24]. In this study, we analysed the differential variations in Ca^{2+} entry and membrane capacitance (Cm), under conditions of bovine chromaffin cell stimulation with DPs of increasing length. In this previous study, we measured Cm changes during the 8-s period that followed the DP and found that exocytotic responses (ΔCm) augmented as a function of DP duration; however, endocytotic responses (Cm decline after peak ΔCm) were absent with short DPs (50−200 ms) and were visible and pronounced with longer DPs (500−2,000 ms). In preliminary experiments, we found that cell dialysis with 50 μM sphingosine (SpD) augmented endocytosis, and this was better seen when using 10 mM Ca^{2+} in the extracellular solution and DPs shorter enough to prevent a pronounced endocytotic response that could mask the effect of sphingosine; therefore, we chose a 200-ms DP to perform all experiments reported here, and we measured Cm changes during the 3-s duration period that followed the DP.

Figure 1a shows example traces of the whole cell inward Ca^{2+} current (I_{Ca}, inset) and the Cm trace elicited by such current in a bovine chromaffin cell perifused with an extracellular solution containing 10 mM Ca^{2+} (to enhance ΔCm and thereby Cm decline), voltage-clamped at −80 mV under the whole-cell configuration of the patch-clamp technique (WCC) and stimulated with a 200-ms DP to +10 mV. I_{Ca} inactivated to about 20% of the initial peak current

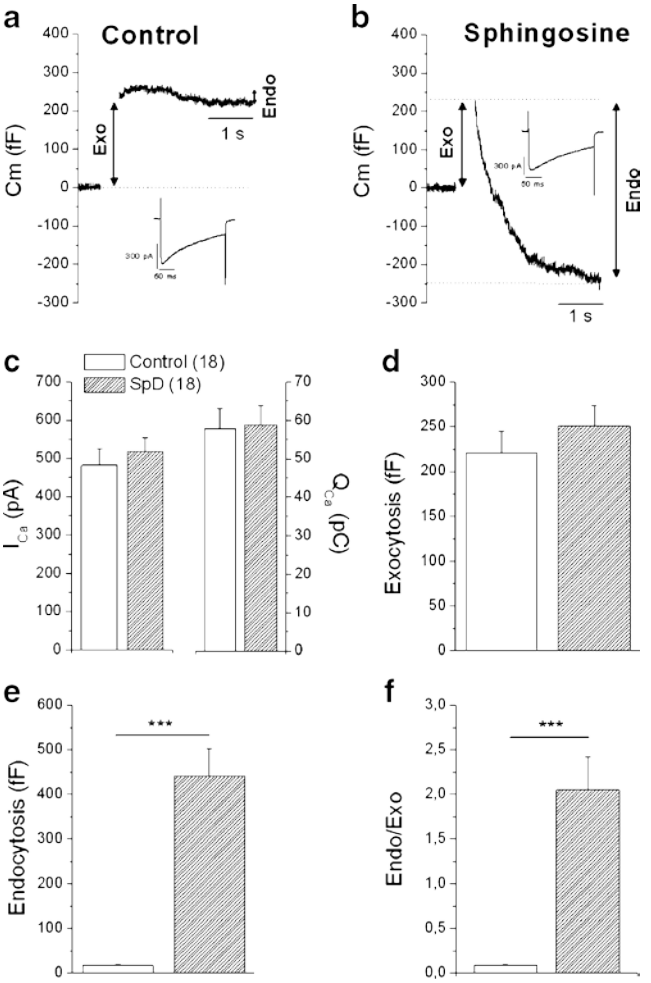

Fig. 1 Sphingosine favours the activation of a pronounced endocytotic response. Bovine chromaffin cells perifused with an extracellular solution containing 10 mM Ca^{2+} were voltage-clamped at −80 mV under the whole-cell configuration of the patch-clamp technique (WCC). Inward calcium currents (I_{Ca}) and changes of membrane capacitance (Cm) were generated by 200-ms depolarising test pulses (DPs) to +10 mV. a Example I_{Ca} trace (inset) and Cm changes in a control cell. b Example I_{Ca} trace (inset) and Cm changes in a cell dialysed with 50 μM sphingosine (SpD); the test pulse was applied after 2-min of breaking into the cell cytosol, to allow equilibrium between cytosol and pipette solution. Vertical arrows toward the right illustrate the definitions used in this study for the two components of Cm changes evoked by a DP, i.e. exocytotic response (Exo, left arrow) and endocytotic response (Endo, right arrow), measured durig the 3-s period that followed the DP. c Averaged I_{Ca} peak amplitude in pA, measured 10 ms after I_{Na} current inactivation in control and SpD cells (left ordinate) and I_{Ca} area in pC (right ordinate); the area was also measured from 10 ms after peak current to the end of trace; this area, expressed in pC, indicates the total Ca^{2+} entering the cell during a DP. d Averaged ΔCm increase (exocytosis), e Cm decrease (endocytosis), f ratios endocytosis/exocytosis (Endo/Exo). Data in panels c to f are means ± SE of the number of cells shown in parentheses in c, from four different cell cultures. ***p<0.001

amplitude, with a τ of 110 ms. Peak ΔCm was 250 fF, which was followed by a tiny Cm decay at the end of the 3-s recording period. Lack of endocytosis with 200-ms DP agrees with a previous study performed in voltage-clamped

bovine chromaffin cells where a 250-ms DP caused an exocytotic response that was not followed by endocytosis, using 3 mM Ca^{2+} in the external solutions (see Fig. 4 in [25]). In another study, 200-ms DP in 10 mM Ca^{2+} produced exocytosis, followed by endocytosis (see Fig. 1a in [26]). We have no explanation for these variable results in different laboratories. One possibility is that exocytosis and endocytosis are Ca^{2+}-dependent, but endocytosis has a higher threshold for activation by Ca^{2+}. The differences between stimulation and/or external solution Ca^{2+} concentrations could induce an endocytotic response. Figure 1b shows example traces of I_{Ca} (inset) and the Cm trace obtained in a cell dialysed through the patch pipette with an intracellular solution containing 50 μM sphingosine (SpD). I_{Ca} (inset) inactivated to about 20% of the initial peak current with a τ of 161 ms; so, it was similar to control current. In contrast, the Cm trace morphology sharply differed from control. The initial ΔCm of 210 fF was immediately followed by an abrupt decay that crossed baseline Cm and reached −245 fF. This pronounced endocytotic response (450 fF, double-head arrow to the right of Fig. 1b) was fitted to a single exponential with a τ of 411 ms.

Pooled data from 18 control and 18 SpD cells are also shown in Fig. 1. There were no differences in the peak I_{Ca} amplitudes neither in Q_{Ca} (panel c), indicating that differences in the endocytotic responses in control and SpD cells were not due to distinct rate and/or total Ca^{2+} entry through calcium channels. It seems, therefore, that sphingosine is not altering the kinetics of those channels, neither the lipid changed the mean ΔCm response (Fig. 1d). However, endocytosis that was barely expressed in control cells underwent a pronounced activation that reached as much as 441 fF in SpD cells (panel e). The mean ratios between endocytosis and exocytosis (Endo/Exo) are shown in Fig. 1f. Because ΔCm did not change, the Endo/Exo ratio augmented 22-fold in SpD cells, with respect to control cells.

Being a hydrophobic charged molecule, sphingosine had to be 'injected' and dialysed with the patch pipette; however, it was necessary to perform a control experiment to test whether the extracellular application of 50 μM sphingosine also augmented endocytosis in cells stimulated with 200-ms pulses to +10 mV. In seven control cells, we found that endocytosis amounted to 17.5±3 fF. Data obtained in another seven cells perifused with 50 μM sphingosine produced an endocytotic response of 15± 4.3 fF. It seems therefore that sphingosine is acting on an intracellular site to facilitate endocytosis; this site cannot be reached when the lipid was extracellularly applied.

Effect of Ca^{2+} ions on sphingosine-facilitated endocytosis

In spite of some controversy, there is agreement that endocytosis is a Ca^{2+}-dependent process (see 'Discussion' section). We therefore investigated if facilitation of endocytosis by sphingosine was Ca^{2+}-dependent. Figure 2 shows results obtained from experiments performed with the protocol of Fig. 1 under WCC, using 2, 5 or 10 mM Ca^{2+} as charge carrier. As in Fig. 1, we did not find differences of I_{Ca} in control compared with SpD cells at the three $[Ca^{2+}]_e$ tested, and so, we do not show them. Figure 2a displays example traces of Cm from cells perifused with different extracellular Ca^{2+} concentrations. In control cells perifused with 2 mM Ca^{2+}, the initial fast Cm jump was followed by a slow component of increasing exocytosis. In 5 and 10 mM $[Ca^{2+}]_e$, the initial Cm jump was followed by a plateau. Thus, using 200-ms duration DPs, no fast endocytosis occurred in the 3-s recording period; this was true irrespective of the $[Ca^{2+}]_e$ used. Figure 2b shows pooled results on ΔCm obtained in 2, 5 and 10 mM $[Ca^{2+}]_e$; a significant increase of ΔCm in SpD, in comparison with control cells, was seen, in agreement with the recent report of Darios et al. [12]. A pronounced augmentation of endocytosis was seen in 5 and 10 mM $[Ca^{2+}]_e$ in SpD cells. This increment was much higher than that seen in ΔCm that at 10 mM $[Ca^{2+}]_e$ was not statistically significant (Fig. 2b). The Endo/Exo ratio in 5 mM $[Ca^{2+}]_e$ was 13-fold and in 10 mM $[Ca^{2+}]_e$, 22-fold. A 500-ms DP given in 2 mM Ca^{2+} produced a sharp endocytotic response (see Fig. 1b in [14]). Up to a certain extent, Ca^{2+} entry into bovine chromaffin cells is a function of DP duration and the $[Ca^{2+}]_e$/$[Ca^{2+}]_i$ gradient [24]. It was therefore of interest to analyse whether a relationship existed between Ca^{2+} entry during the 200-ms DP and exo-endocytotic responses triggered by such pulse, at the three $[Ca^{2+}]_e$ used.

We plotted the amount of total Ca^{2+} entry (Q_{Ca}) during a 200-ms DP (calculated from the area of I_{Ca} in experiments of Fig. 2 made with 2, 5 and 10 mM Ca^{2+}) vs the changes of Cm obtained in each individual cell. A good correlation (r=0.91) was found between Q_{Ca}−ΔCm in control cells (Fig. 3a); however, such correlation was fully lost in SpD cells (Fig. 3b). A poor correlation between Q_{Ca} and endocytosis was found in control cells (r=0.75) that, as described above, exhibited a meagre endocytotic response when stimulated with 200-ms DPs (note the low Cm values for endocytosis in the ordinate of Fig. 3c). The correlation was somehow better in sphingosine-dialysed cells (r=0.82), as shown in Fig. 3d (note the large endocytotic values in the ordinate).

Effects of FCCP and SpD on exo-endocytotic responses when using 2 mM Ca^{2+} as charge carrier

SpD facilitated the triggering of endocytosis at 5 and 10 mM $[Ca^{2+}]_e$, but not at 2 mM, the physiological $[Ca^{2+}]_e$ (Fig. 2c). This indicated that the putative permissive role exerted by sphingosine on Ca^{2+}-dependent endocytosis required local high intracellular Ca^{2+} concentrations near exocytotic sites $[Ca^{2+}]_c$. A means of enhancing such local

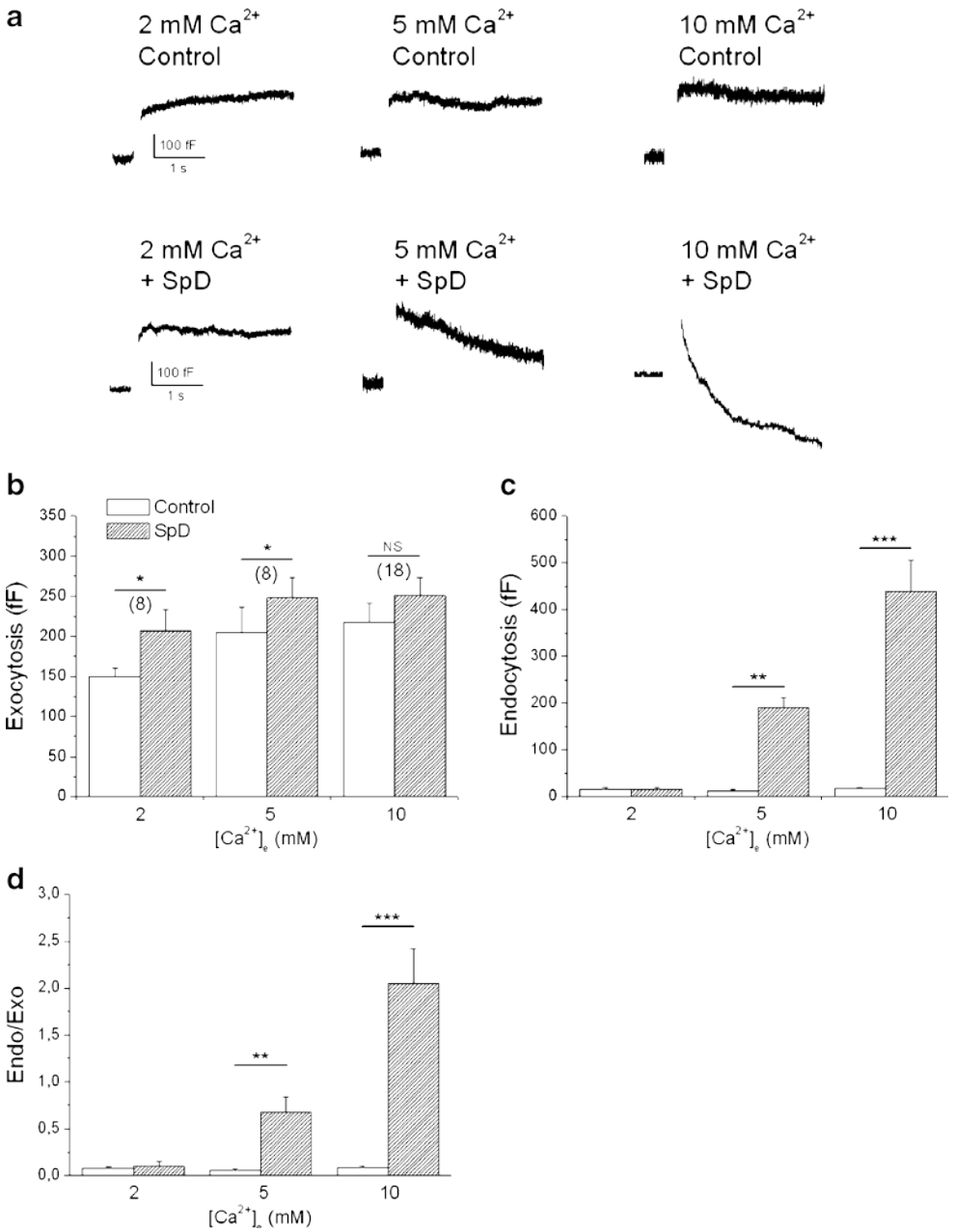

Fig. 2 Effects of the $[Ca^{2+}]_e$/$[Ca^{2+}]_i$ gradient on facilitation by sphingosine of exocytotic and endocytotic responses. Cells were voltage clamped at −80 mV under WCC and changes of membrane capacitance (Cm) were generated by 200-ms depolarising test pulses (DP) to 0 mV (when using 2 mM Ca^{2+}) or +10 mV (when using 5 and 10 mM Ca^{2+}) to get maximum peak I_{Ca}. Cells were perifused with external solutions containing the Ca^{2+} concentrations indicated in each panel. a Example traces of the Cm changes generated in six different cells perifused with 2 mM Ca^{2+} (left), 5 mM Ca^{2+} (middle) or 10 mM Ca^{2+} (right) in control conditions (top traces) or under sphingosine dialysis (SpD, 50 μM included in the pipette solution). b Averaged exocytotic responses in control and SpD cells, at the $[Ca^{2+}]_e$ shown in the abscissa; c averaged endocytotic responses in control and SpD cells, at the $[Ca^{2+}]_e$ shown in the abscissa. d Ratios between endocytotic and exocytotic responses (Endo/Exo, ordinate) in control and SpD cells, at the different $[Ca^{2+}]_e$ used. The averaged values in b, c, d represent the responses generated by the first 200-ms DP applied to each individual cell, at each $[Ca^{2+}]_e$. They are means ± SE of the number of cells shown in parentheses from at least three different cultures. *p<0.05, **p<0.01, ***p<0.001

$[Ca^{2+}]_c$ is the use of protonophores, which impair the Ca^{2+} sequestration by a subplasmalemmal subpopulation of mitochondria, discovered by using mitochondrially targeted aequorins with low affinity for Ca^{2+} in bovine chromaffin cells [27]. Protonophores that block mitochondrial Ca^{2+} uptake markedly potentiated exocytosis, measured with capacitance techniques in voltage-clamped bovine chromaffin cells [28]. We therefore decided to explore whether 1 μM of protonophore FCCP, given for a short time to prevent mitochondrial damage, could unmask the sphingosine-permissive effect on endocytosis in 2 mM Ca^{2+}.

Figure 4a shows I_{Ca} and Cm traces obtained from a control cell and from a cell perifused with FCCP that produced a similar peak I_{Ca}, although, in this cell, the current inactivated faster. FCCP enhanced ΔCm, but during the 3-s Cm recording period, endocytosis was not apparent. Figure 4a shows that SpD did not affect I_{Ca}; the Cm trace had no endocytosis. However, when treated with FCCP, the SpD cell exhibited a moderate endocytosis (Fig. 4a, right panel). Figure 4b, c show mean data on I_{Ca} and Q_{Ca} that were similar under all treatments. FCCP near doubled exocytosis in control cells, but this response was not increased further in SpD cells (Fig. 4d). FCCP caused

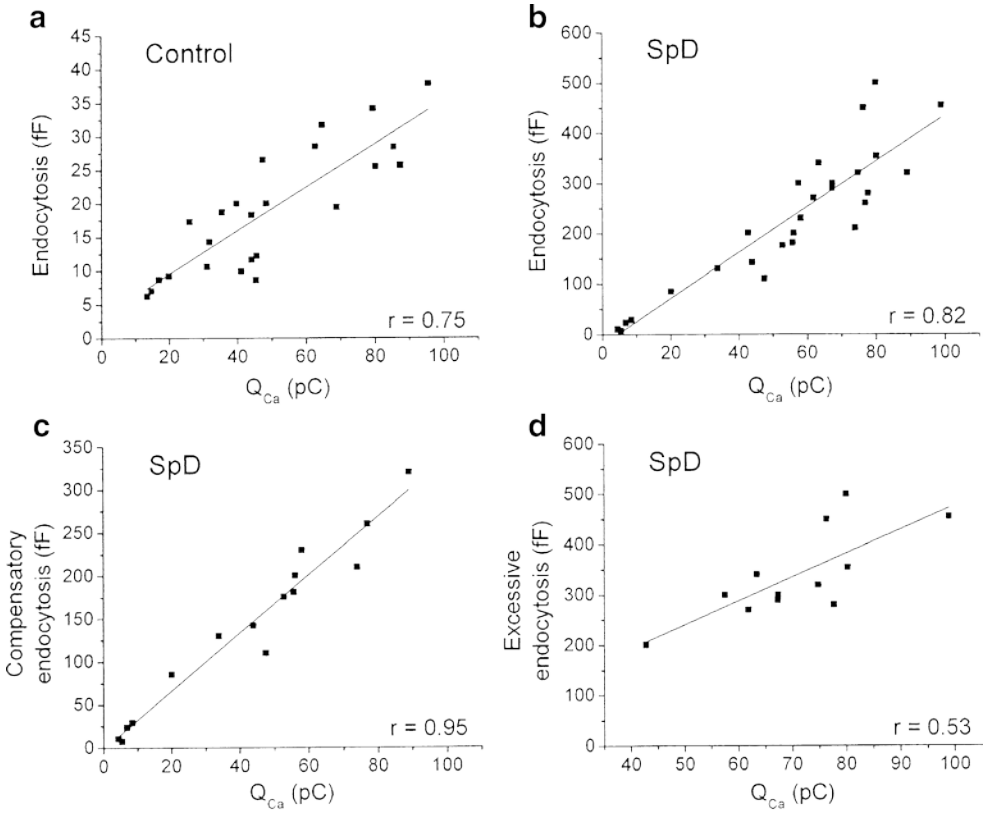

Fig. 3 Correlation between Ca^{2+} entry, exocytosis and endocytosis in control and sphingosine-dialysed cells (SpD), under WCC. Data on total Ca^{2+} entry (Q_{Ca}, in pC) represent I_{Ca} areas; endocytotic responses are given by the Cm changes generated by 200-ms DPs. All these data were calculated from the results shown in Fig. 2 obtained from cells perifused with 2, 5 or 10 mM Ca^{2+}, with or without sphingosine dialysis. Correlations between Q_{Ca} and exocytosis are shown in a (control) and b (SpD). Correlations between Q_{Ca} and endocytosis are shown in c (control) and d (SpD)

little augmentation of endocytosis in control cells (about 20 fF), but this increment was substantially larger in SpD cells (about 60 fF), suggesting that suppression of mitochondrial Ca^{2+} uptake unmasks at least partially the permissive role of sphingosine on Ca^{2+}-dependent endocytosis (Fig. 4e, f).

Exo-endocytosis responses in control and SpD cells using Ba^{2+} instead of Ca^{2+}, as charge carrier

Contradictory data were reported on whether Ba^{2+} ions supported endocytosis in bovine chromaffin cells. Thus, a study showed that rapid endocytosis is supported by Ca^{2+} but not Ba^{2+} [5]; in contrast, a latter study demonstrates that both Ca^{2+} and Ba^{2+} support excessive membrane retrieval [29]. Here, we also performed experiments using 10 mM Ba^{2+} instead of Ca^{2+}, as charge carrier.

Figure 5a shows example traces of I_{Ba} and ΔCm. In contrast to I_{Ca} (Fig. 1a, b) that underwent clear inactivation, I_{Ba} did not inactivate. The cell also responded with a Cm change that was slowly increasing along the 3-s recording period. In a SpD cell, I_{Ba} and Cm changes were similar to those recorded from a control cell (compare left and right traces of Fig. 5a). Figure 5b, c show averaged I_{Ba} and Q_{Ba} that were similar in control and SpD cells. Finally, Fig. 5d shows the peak exocytotic responses that were also similar in both cell types. In our experimental conditions, Ba^{2+} did not support endocytosis and the presence of intracellular sphingosine did not alter this pattern. These data suggest that the sphingosine elicited endocytosis is Ca^{2+}-dependent.

Effects of sphingosine and sphingomyelinase on endocytosis, upon repeated stimulation of voltage-clamped cells under WCC or PPC

Under WCC, cytosolic components are diluted by the intracellular pipette solution. This may lead to loss of particular cell functions that depend on threshold concentrations of those cytosolic factors. An illustrative example is the gradual loss of I_{Ca} upon repeated application of DPs to bovine chromaffin cells, coined with the term current washout in Neher's laboratory [30]. Also, when consecutive depolarisation pulses are applied to a bovine chromaffin cell voltage-clamped under the WCC, the endocytotic responses are washed out within 3 or 4 min, suggesting the need of cytosolic factors to maintain the secretion machine functional [25, 26]. We therefore asked the question whether the facilitation by sphingosine of endocytosis was also undergoing decay with repeated cell stimulation.

After seal formation, voltage-clamped cells under WCC were stimulated with three DPs to +10 mV, given at 1-min intervals (P1, P2 and P3). Figure 6a shows that I_{Ca} peaks

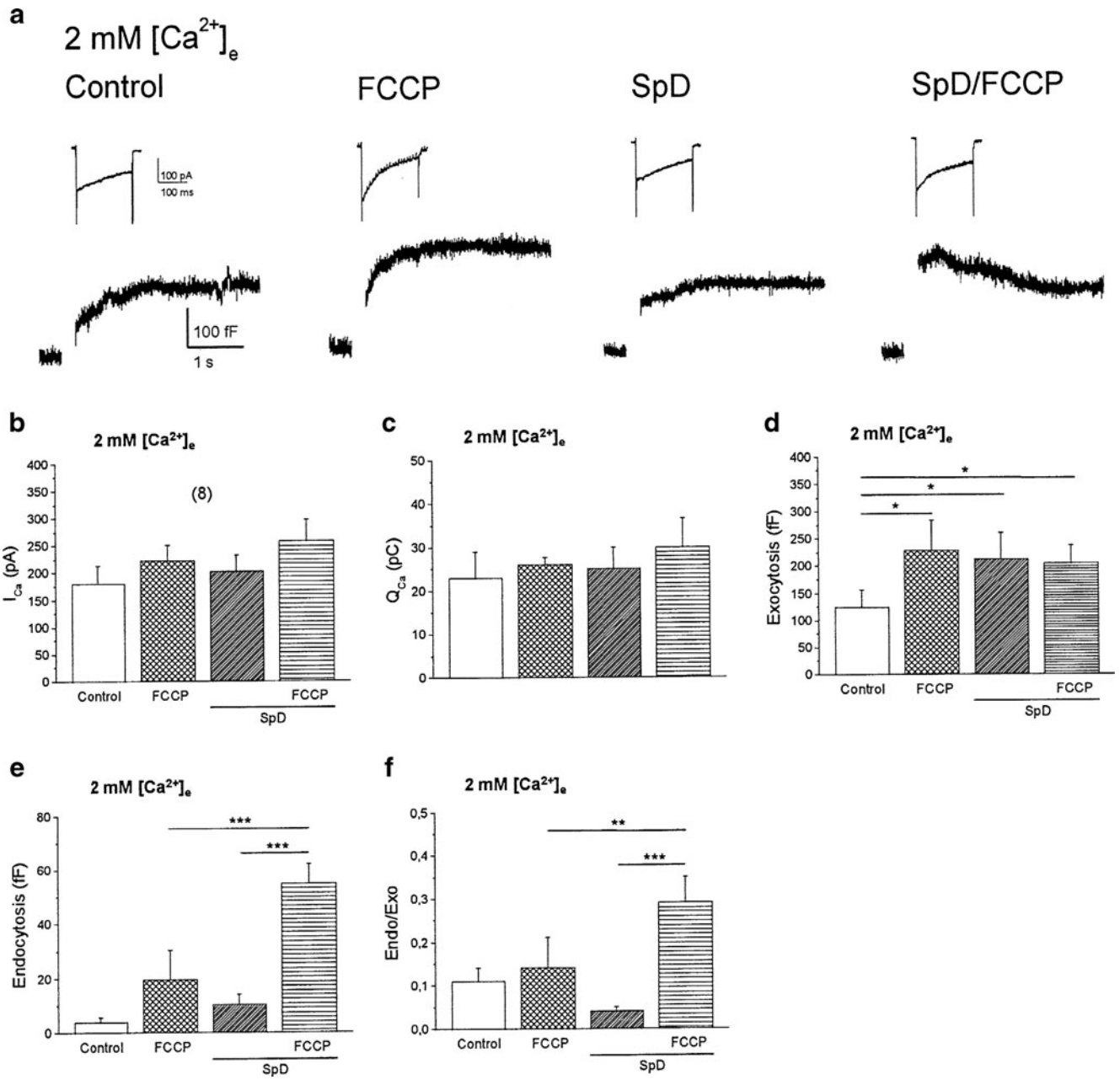

Fig. 4 Effect of FCCP on exo-endocytotic responses in control cells and cells dialysed with 50 μM sphingosine (SpD), using 2 mM Ca^{2+} as charge carrier. Cells were voltage-clamped at −80 mV under WCC. Inward whole-cell Ca^{2+} channel currents (I_{Ca}) and changes of membrane capacitance (Cm) were activated by 200-ms test depolarising pulses (DPs) to 0 mV. a I_{Ca} traces and Cm traces of an example control cell and an example cell perifused with 1 μM FCCP since 1 min before and during the application of the DP; example traces from SpD cell are shown in the middle part of a. b, c Averaged pooled results on I_{Ca} peak amplitude in pA and I_{Ca} area in pC, respectively, under the different treatment conditions. d Averaged exocytotic responses (ΔCm) measured as the initial Cm jump. e Averaged endocytotic responses measured at the end of the Cm trace (as indicated in Fig. 1b). e Ratios between endocytotic and exocytotic responses (Endo/Exo, ordinate). Data in b to f are means ± SE of the number of cells shown in parenthesis, from three different cultures. *p<0.05, **p<0.01, ***p<0.001

were similar in P1, P2 and P3 (around 500 pA) both in control and SpD cells. Q_{Ca} were also similar, around 60 pC (Fig. 6b). Figure 6c shows original Cm traces elicited by the three DPs. Again, ΔCm augmented by about 20−40% in SpD cells in P2 and P3 (Fig. 6d), in agreement with Darios et al. [12]. Figure 6e, f show that endocytosis was very poor in control cells (17.5 fF in P1 and 14.5 fF in P3). In contrast, in SpD cells endocytosis rose to as much as 440 fF during P1. During P2, however, the endocytotic response decayed to 82.3 fF and during P3 to 44 fF. In spite of such pronounced decay, it is worth noting that the endocytotic responses were always significantly higher in

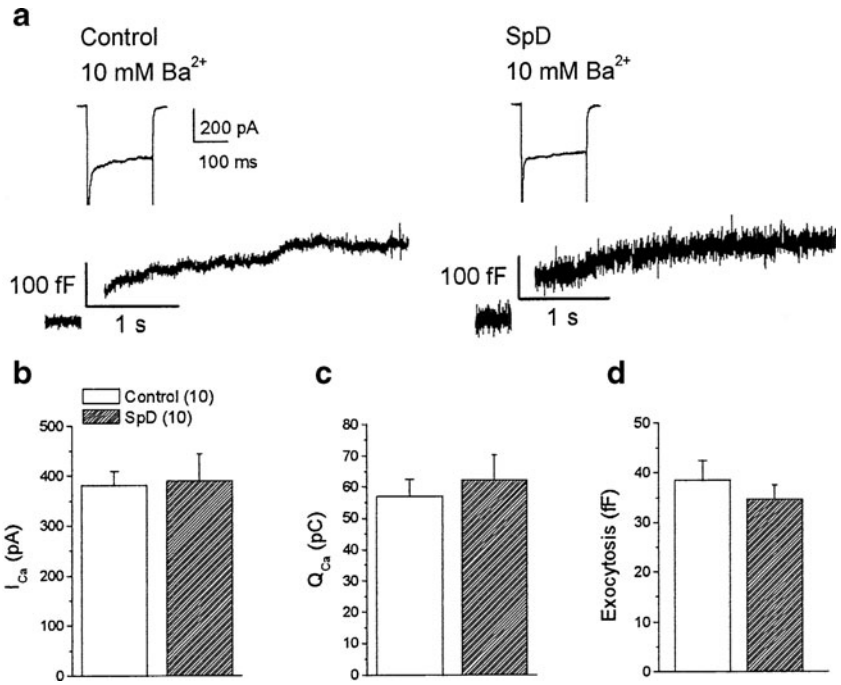

Fig. 5 Sphingosine does not facilitate the activation of endocytosis upon substitution of Ca^{2+} by Ba^{2+}. Cells voltage-clamped at −80 mV under WCC were perifused with an extracellular solution containing 10 mM Ba^{2+}, instead of Ca^{2+}. Whole-cell inward Ba^{2+} currents (I_{Ba}) and changes of membrane capacitance (Cm) were activated by 200-ms DPs to +10 mV. a Example traces of I_{Ba} and Cm from a control and a cell dialysed with 50 μM sphingosine (SpD). b, c Averaged I_{Ba} peak amplitude in pA and I_{Ba} area in pC. d Averaged ΔCm increase measured at the maximum Cm value. Data in b, c, d are means ± SE of the number of cells shown in parentheses

SpD cells, as compared with control cells both in P1, P2 and P3 (Fig. 6e).

The decay with time of endocytosis in SpD cells favours the view of the dilution with pipette dialysis of cytosolic factors required for endocytosis. Washout of these factors may not occur when using the perforated-patch configuration of the patch-clamp technique (PPC) [26]. However, these experiments could not be made with pipette dialysis of sphingosine because of its polar character that will not penetrate through the amphothericin B perforated patch. Therefore, we recoursed to cell pretreatment with sphingomyelinase (SMase, 1 unit ml^{-1}) to induce the endogenous synthesis of sphingosine via ceramide, leading to ATP-independent endocytosis [31]. Afterwards, cells were patch-clamped under PPC and subjected to an experimental protocol similar to that of Fig. 6, except for the fact that up to five DPs were applied instead of three.

Figure 7 shows the endocytotic responses of control cells and cells pretreated with SMase. Figure 7a represents original Cm traces showing the endocytotic responses. In sharp contrast with control cells that had very low endocytosis, SMase-treated cells showed a drastic augmentation of endocytosis (169 fF in P1 and 296 fF in P2) that was maintained reasonably well along the subsequent DPs (142 fF in P5) (Fig. 7a). Although some decay was visible, it was much less pronounced that seen under WCC (Fig. 6e). This difference was better seen when endocytotic responses induced by P3 were compared, i.e. 90% decay with respect to P1 under WCC (Fig. 6e) and only 10% decline under PPC (Fig. 7e). In contrast to endocytosis, neither I_{Ca}, Q_{Ca} nor exocytosis underwent decay upon repeated application of 200-ms DPs (Fig. 7b, c, d), exocytosis augmented by 10−25% in SMase-treated cells, with respect to control cells (Fig. 7d).

We also performed an additional experiment under PPC, trying to reverse the effects of SMase on Cm changes. To this aim, we preincubated cells with SMase (1 unit ml^{-1}) in presence of 150 μM of ceramidase inhibitor NOE (N-oleoylethanolamine), in order to prevent the formation of sphingosine [32]. After this pretreatment, cells were voltage-clamped under PPC and changes of Cm evoked by 200 DPs were recorded. I_{Ca} and Q_{Ca} were similar under pretreatment with SMase alone or with NOE plus SMase (not shown). Figure 7g shows the drastic augmentation of endocytosis in cells that had been preincubated with SMase, from around 20−25 fF in control or NOE treated cells, to as much as 200 fF, a tenfold increase. In cells coincubated with NOE and SMase, the endocytotic response was suppressed (Fig. 7g).

Effect of S1P on the endocytotic responses

It is believed that S1P is involved in Ca^{2+} homeostasis in various cell types and that it induces Ca^{2+} release from the

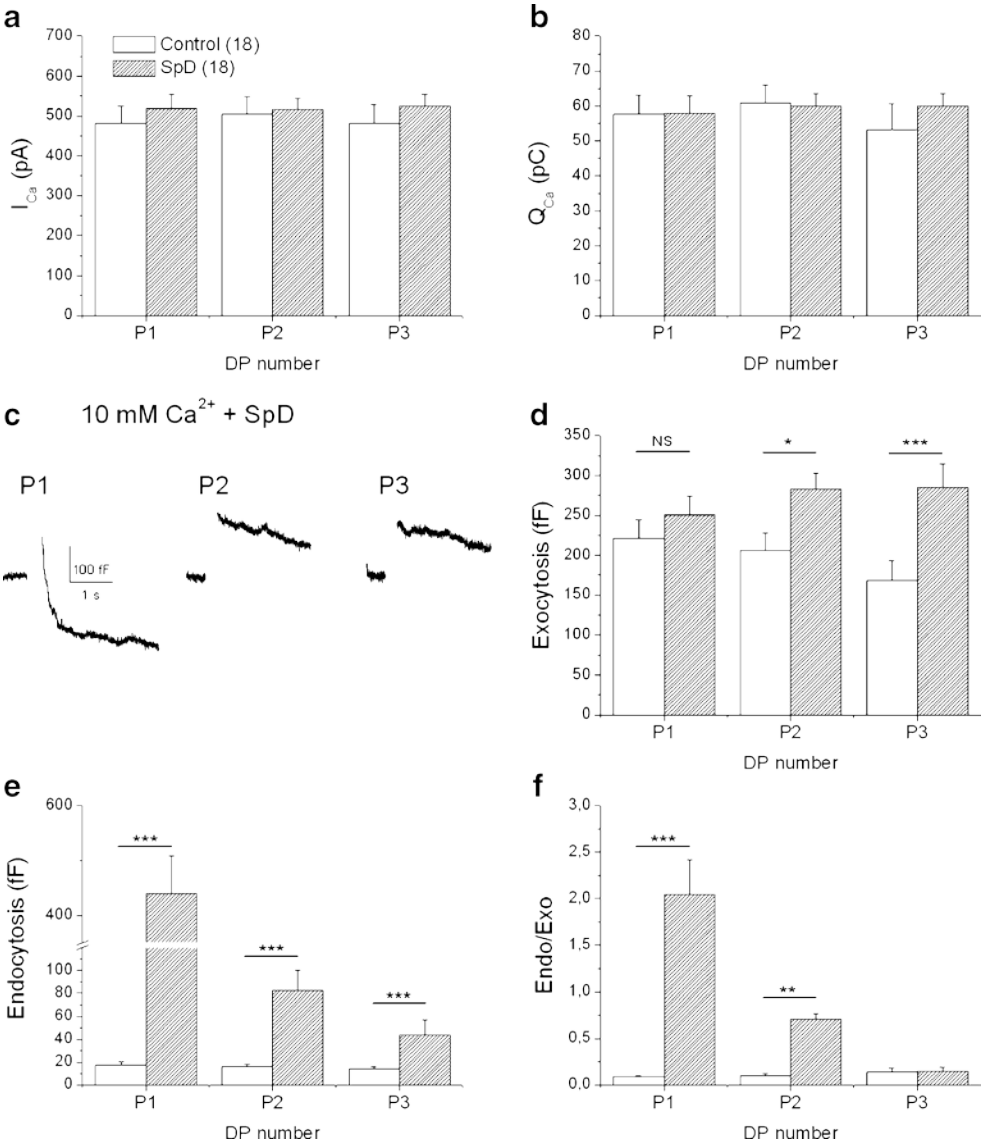

Fig. 6 Effects of repeated stimulation on I_{Ca} and Cm changes in control and sphingosine-dialysed cells (SpD). Cells were voltage-clamped at −80 mV under WCC and perifused with an extracellular solution containing 10 mM Ca^{2+}. They were sequentially stimulated with three DPs to +10 mV given at 1-min intervals. a I_{Ca} peak amplitude, b Q_{Ca} (an indication of total Ca^{2+} entry during a given DP), c Cm traces from each depolarising pulse, d averaged exocytotic responses, e endocytotic responses following the exocytotic jump, f ratio between endocytotic and exocytotic responses (Endo/Exo, ordinate). Data are means ± SE of the number of cells shown in parentheses (a) from at least four different cultures. *p<0.05, **p<0.01, ***p<0.001

endoplasmic reticulum [33, 34]. Since sphingosine can be metabolized by sphingosine-kinases into S1P, we addressed here the question of how S1P could affect the Cm changes under WCC. Cells were dialysed with an intracellular solution containing 50 μM S1P (S1PD), voltage-clamped to −80 mV under WCC and stimulated with a 200-ms DP to +10 mV. DPs were applied at 1-min intervals in presence of 10 mM extracellular Ca^{2+}.

Figure 8a shows example I_{Ca} and Cm traces obtained in control, S1PD and SpD cells; the three I_{Ca} traces were similar as far as peak and current inactivation were concerned. This is better seen in Fig. 8b, c, showing no differences between averaged I_{Ca} and Q_{Ca} of the three cell types. Concerning Cm changes, ΔCm peaks were similar, but the control cell exhibited no endocytosis, the S1PD cell showed moderate endocytosis and the SpD cell had a pronounced endocytotic response. These differences are better seen in panels d (mean exocytosis), e (mean endocytosis), and f (Endo/Exo ratios). It seems therefore clear that S1P was about fourfold less efficient than sphingosine in facilitating endocytosis.

Effects of dynasore and calmidazolium on the facilitation of endocytosis triggered by sphingosine

We attempted to clarify whether the pronounced endocytosis observed in SpD cells was linked to dynamin and/or calmodulin. We therefore recoursed to inhibitors of these two proteins to know their effects on endocytosis in control and SpD cells under WCC. At 50 μM, the dynamin inhibitor dynasore [18] decreased by 24% peak I_{Ca} and by 15.5% Q_{Ca} (Fig. 9a, b). In spite of this partial blockade of Ca^{2+} entry, the endocytotic responses were not affected by dynasore, neither in control nor in SpD cells (Fig. 9c, d).

A similar picture emerged with calmodulin inhibitor calmidazolium [16, 29] that at 20 μM did not significantly

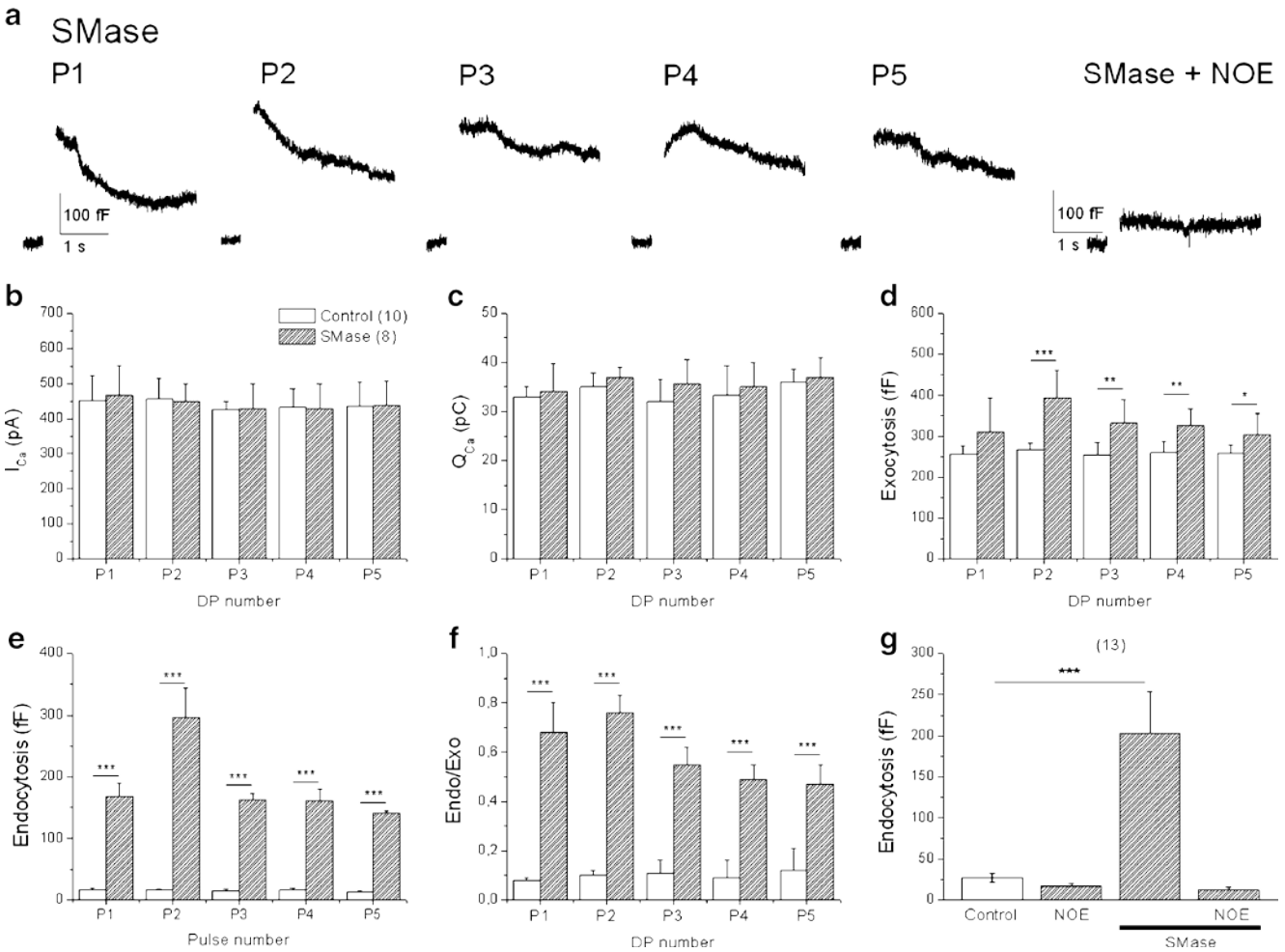

Fig. 7 Facilitation of endocytosis induced by sphingomyelinase (SMase) pretreatment was blocked by ceramidase inhibitor NOE (N-oleoylethanolamine). Before the experiment, cells were incubated during 30 min with sphingomyelinase (SMase; 1 unit ml^{-1}); control cells were incubated with vehicle (0.1% DMSO). In the experiments with NOE pretreatment, cells were preincubated with vehicle or NOE during 30 min before adding SMase. Cells were then voltage-clamped at −80 mV under PPC and perifused with an extracellular solution containing 10 mM Ca^{2+}. Five 200-ms DPs to +10 mV (P1 to P5) were sequentially applied at 1-min intervals to each cell. a Original Cm traces; b, c averaged pooled results on I_{Ca} peak amplitude (pA) and I_{Ca} area (pC), respectively, under the different experimental conditions, d averaged exocytotic responses; e endocytotic responses induced by SMase pretreatment; f ratio between endocytosis/exocytosis (Endo/Exo); g endocytotic responses after NOE and SMase pretreatment. Data are means ± SE of the number of cells shown in parentheses in B and C, from at least three different cultures. ***$p<0.001$

affect Ca^{2+} entry in control and SpD cells (Fig. 9a, b). Calmidazolium did not affect the endocytotic responses, neither in control nor in SpD cells (Fig. 9c, d).

Discussion

The central observation of this study is that sphingosine facilitated the generation of a fast endocytotic response under cell stimulation conditions that normally produced a sharp exocytotic response without endocytosis, i.e. 200-ms DP and Cm changes measured during the 3-s period that followed such pulse. Various experimental findings indicated that facilitation by sphingosine of endocytosis should be exerted at an intracellular site; this site is not accessible from the external plasmalemmal surface because (first) sphingosine application through pipette dialysis caused endocytosis (Fig. 1b); (second) extracellular sphingosine application was ineffective, surely because the lipid has a quaternary ammonium and so it can not cross the plasmalemma; (third) endogenously synthesised sphingosine mimicked the effect of SpD (Fig. 7) and (fourth) inhibition of endogenous sphingosine synthesis by ceramidase inhibitor NOE abolished the response (Fig. 7). The effect of sphingosine on endocytosis was only partially mimicked by its metabolite S1P (Fig. 8), indicating that sphingosine was quite selective in eliciting endocytosis under the experimental conditions studied here.

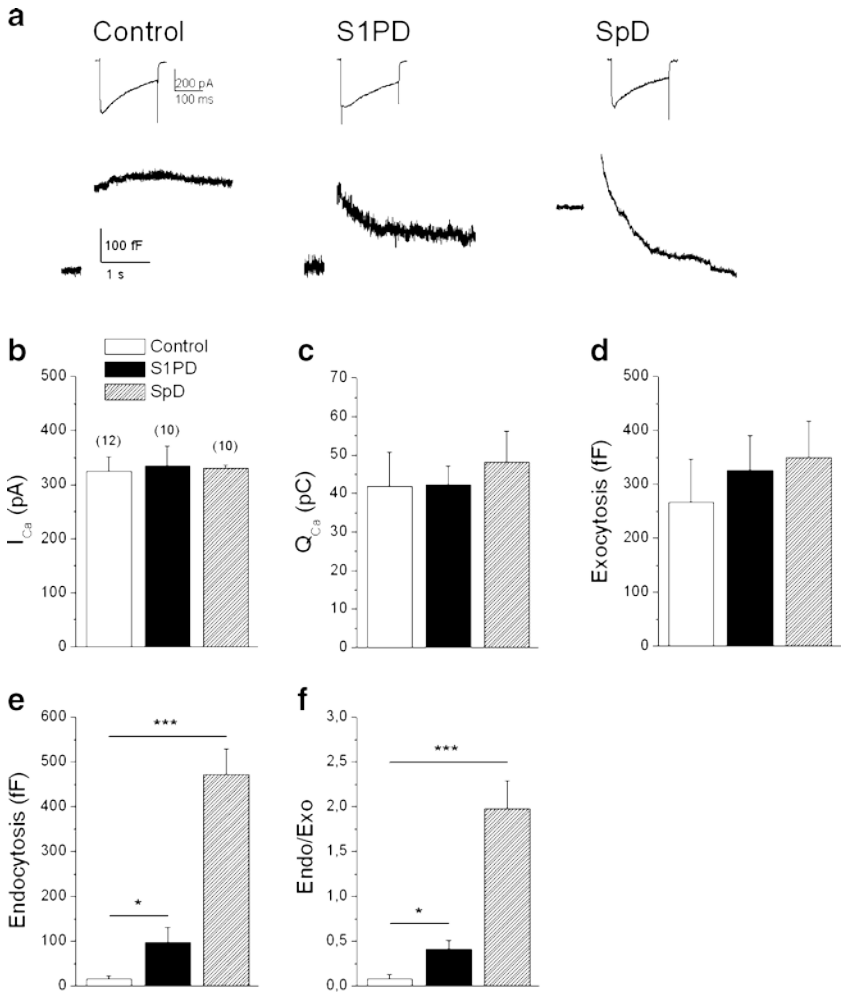

Fig. 8 Comparative effects of sphingosine and its metabolite S1P on endocytosis. Cells were voltage-clamped at −80 mV under WCC and perifused with an extracellular solution containing 10 mM Ca^{2+}. I_{Ca} and changes of membrane capacitance (Cm in fF) were elicited by 200-ms DPs to +10 mV. S1P (S1PD, 50 μM) and sphingosine (SpD, 50 μM) were dialysed with the pipette intracellular solution. a Example capacitance traces in a control cell (left), in a cell dialysed with S1P (middle) and in a cell dialysed with sphingosine (right). b, c I_{Ca} and Q_{Ca}; d averaged exocytotic response; e averaged data of endocytotic responses; f ratio endocytosis/exocytosis. Data are means ± SE of the number of cells shown in parentheses from three different cultures. *p<0.05, ***p<0.001

Another feature of interest was the Ca^{2+} dependence of endocytosis in SpD cells. A role for Ca^{2+} in endocytosis and vesicle recycling is extensively documented [35–37]. However, some studies in synapses concluded that Ca^{2+} was not required for endocytosis [38, 39] or behaved even as inhibitory [40, 41]. Another two studies reported contradictory data on the ability of Ba^{2+} to support Ca^{2+}-dependent endocytosis in bovine chromaffin cells. Thus, a study shows that rapid endocytosis is supported by Ca^{2+} but not Ba^{2+} [5]; in contrast, a latter study demonstrates that both Ca^{2+} and Ba^{2+} support excessive membrane retrieval [29]. Under our experimental conditions, Ba^{2+} could not substitute Ca^{2+}. It was intriguing that, in 2 mM Ca^{2+}, cell dialysis with sphingosine did not facilitate endocytosis. It could be that, with a single 200-ms pulse, the local $[Ca^{2+}]_c$ at subplasmalemmal sites did not reach a threshold to trigger sphingosine-dependent endocytosis; such $[Ca^{2+}]_c$ threshold was easily achieved with 5 mM Ca^{2+} and, particularly, with 10 mM Ca^{2+}. Mitochondria play an important role in removing Ca^{2+} from subplasmalemmal sites. Thus, when protonophore FCCP was used to block subplasmalemmal Ca^{2+} retrieval by mitochondria of bovine chromaffin cells, exocytosis was drastically potentiated [27, 28, 42]. We found here that FCCP also augmented sphingosine-triggered endocytosis in 2 mM Ca^{2+}, although this effect was mild. In any case, we interpret these data through the hypothesis that sphingosine could play a permissive role to favour endocytosis only under conditions of high $[Ca^{2+}]_c$ at subplasmalemmal sites [43], that can be reached only with high Ca^{2+} gradients (Fig. 2c) or with high-intensity stimulation patterns [24].

An interesting additional feature is that sphingosine could not maintain its effect on facilitation of endocytosis

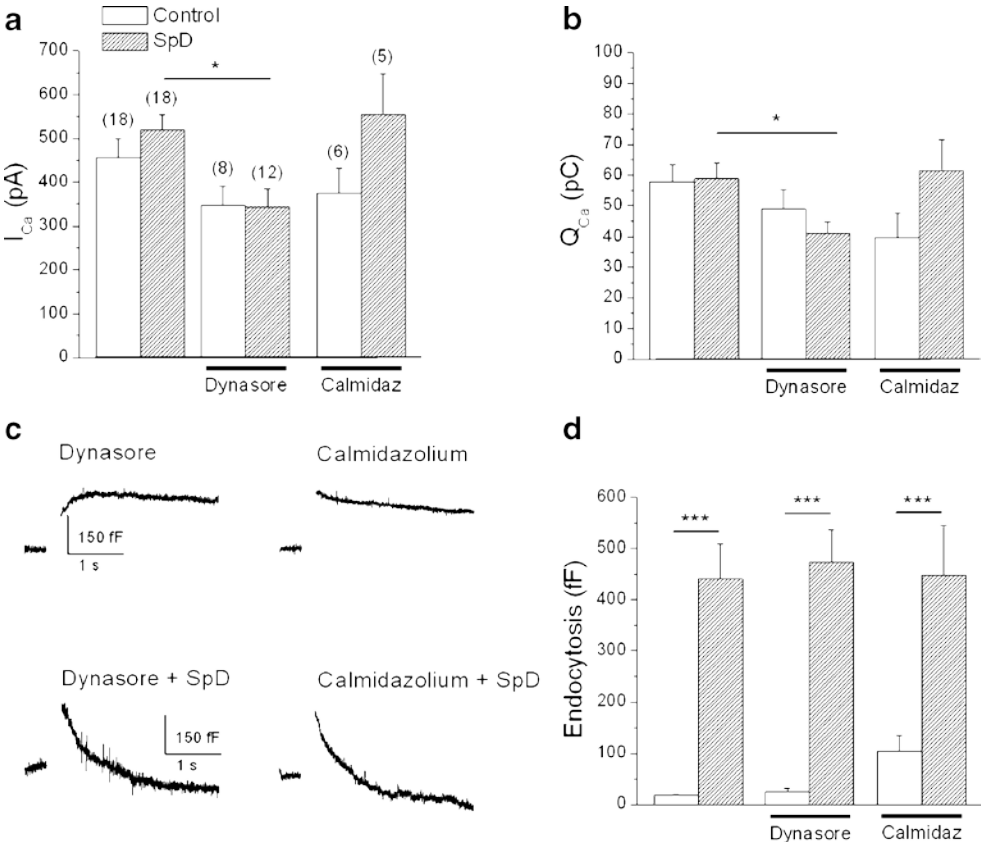

Fig. 9 Effects of dynamin blocker dynasore and calmodulin inhibitor calmidazolium (calmidaz) on sphingosine-elicited endocytotic responses generated by 200-ms DPs given to cells voltage-clamped at −80 mV, under WCC, and perifused with an extracellular solution containing 10 mM Ca^{2+}. a I_{Ca} amplitude; b I_{Ca} area (Q_{Ca}); c, d original traces and averaged data of endocytotic responses. These responses were measured after cell pretreatment with dynasore (50 μM) for 30 min at 37°C or 3 min after breaking into the cell cytosol with a pipette containing calmidazolium (20 μM). Data are means ± SE of the number of cells given in parentheses from three different cultures. *p<0.05, ***p<0.001

upon cell stimulation with repeated DPs under the WCC of the patch-clamp technique (Fig. 6c, e). This agrees with the previous observation of Burgoyne [25] that also showed the loss of endocytosis under repeated stimulation (cells were clamped at −60 mV and stimulated by depolarisation to +20 mV for 250 ms or 1 s) of bovine chromaffin cells, suggesting a differential loss of one or more endocytotic mechanisms during whole-cell recording. Our experiments using perforated patch agree with this concept (Fig. 7a, e). Furthermore, Smith and Neher [26] also showed the loss of endocytosis by the fourth minute of recording, while exocytosis persisted; we also found that exocytosis persisted (Fig. 6c, d).

On the other hand, Artalejo et al. [44] showed that Ca^{2+} currents and endocytosis remain intact even during long-term whole-cell recordings. We have no explanation for this discrepancy.

We attempted to determine whether the endocytotic-promoting effects of sphingosine were linked to calmodulin or dynamin. Ca^{2+} and calmodulin has just been shown to initiate all forms of endocytosis during cell depolarisation [16]. However, neither calmodulin inhibitor calmidazolium nor dynamin blocker dynasore affected the pronounced sphingosine elicited endocytotic response. In their recent study in the calyx synapse, Wu et al. [16] found that calmodulin and Ca^{2+} initiated all forms of endocytosis. On the other hand, under PPC, Tsai et al. [18] found that dynasore decreased the rapid exponential decay of Cm, after strong stimulation of bovine chromaffin cells with 10 DPs of 100-ms duration. Our stimulation pattern was milder (i.e. a single 200-ms DP) and did not evoke a substantial endocytosis in the 3-s recording time period following stimulation. Because sphingosine unmasked a pronounced endocytosis, under these mild stimulation conditions, it seems that the lipid might be acting either in a step previous to membrane pits formation and fission or may activate a different pathway.

It may well be that sphingosine is contributing to the initiation of membrane budded vesicles by changing the interaction lipid-proteins in a Ca^{2+}-dependent manner. This could explain why little endocytosis occurs with mild stimulation patterns based in action potentials that causes little Ca^{2+} entry, while it increases with stronger square depolarisations of bovine chromaffin cells that cause greater Ca^{2+} entry rates [24]. We hypothesise that sphingosine might play a Ca^{2+}-dependent permissive role in preparing specific areas of the plasmalemma to form endocytotic pits at early steps of the endocytotic process. However, this step does not seem to be necessary for dynamin- and calmodulin-dependent endocytosis [16, 18] because dynasore and calmidazolium did not inhibit sphingosine-triggered endocytosis.

In conclusion, to our knowledge, this is the first study showing that sphingosine has a Ca^{2+}-dependent permissive

role in the initiation of endocytosis; such action requires a soluble cytosolic factor that is washed out under the whole cell but not under the perforated patch configuration of the patch-clamp technique. The fact sphingosine-triggered endocytosis is independent of dynamin and calmodulin suggests the lipid may activate a different, more direct endocytotic pathway to recycle and reuse secretory vesicles.

Acknowledgements This work was partially supported from the following grants from Spanish institutions to AGG: (1) SAF2006-03589, Ministerio de Ciencia e Innovación, Spain; (2) NDE 07/09, Agencia Laín Entralgo, Comunidad de Madrid; (3) PI016/09, Fundación C.I.E.N., Instituto de Salud Carlos III; (4) RD 06/0026 RETICS, Instituto de Salud Carlos III; (5) S-SAL-0275-2006, Comunidad de Madrid, also by grant SAF2007-65181, Ministerio de Ciencia e Innovación, Spain, to LG. We thank Fundación Teófilo Hernando for continued support.

References

1. Katz B, Miledi R (1969) Spontaneous and evoked activity of motor nerve endings in calcium ringer. J Physiol 203:689–706
2. Douglas WW (1968) Stimulus-secretion coupling: the concept and clues from chromaffin and other cells. Br J Pharmacol 34:453–474
3. Ceccarelli B, Hurlbut WP (1980) Ca2+-dependent recycling of synaptic vesicles at the frog neuromuscular junction. J Cell Biol 87:297–303
4. Henkel AW, Almers W (1996) Fast steps in exocytosis and endocytosis studied by capacitance measurements in endocrine cells. Curr Opin Neurobiol 6:350–357
5. Artalejo CR, Henley JR, McNiven MA, Palfrey HC (1995) Rapid endocytosis coupled to exocytosis in adrenal chromaffin cells involves Ca2+, GTP, and dynamin but not clathrin. Proc Natl Acad Sci USA 92:8328–8332
6. Blochl A, Sirrenberg C (1996) Neurotrophins stimulate the release of dopamine from rat mesencephalic neurons via Trk and p75Lntr receptors. J Biol Chem 271:21100–21107
7. Numakawa T, Nakayama H, Suzuki S, Kubo T, Nara F, Numakawa Y, Yokomaku D, Araki T, Ishimoto T, Ogura A, Taguchi T (2003) Nerve growth factor-induced glutamate release is via p75 receptor, ceramide, and Ca(2+) from ryanodine receptor in developing cerebellar neurons. J Biol Chem 278:41259–41269
8. Jeon HJ, Lee DH, Kang MS, Lee MO, Jung KM, Jung SY, Kim DK (2005) Dopamine release in PC12 cells is mediated by Ca(2+)-dependent production of ceramide via sphingomyelin pathway. J Neurochem 95:811–820
9. Rohrbough J, Rushton E, Palanker L, Woodruff E, Matthies HJ, Acharya U, Acharya JK, Broadie K (2004) Ceramidase regulates synaptic vesicle exocytosis and trafficking. J Neurosci 24:7789–7803
10. Kajimoto T, Okada T, Yu H, Goparaju SK, Jahangeer S, Nakamura S (2007) Involvement of sphingosine-1-phosphate in glutamate secretion in hippocampal neurons. Mol Cell Biol 27:3429–3440
11. Brailoiu E, Cooper RL, Dun NJ (2002) Sphingosine 1-phosphate enhances spontaneous transmitter release at the frog neuromuscular junction. Br J Pharmacol 136:1093–1097
12. Darios F, Wasser C, Shakirzyanova A, Giniatullin A, Goodman K, Munoz-Bravo JL, Raingo J, Jorgacevski J, Kreft M, Zorec R, Rosa JM, Gandia L, Gutierrez LM, Binz T, Giniatullin R, Kavalali ET, Davletov B (2009) Sphingosine facilitates SNARE complex assembly and activates synaptic vesicle exocytosis. Neuron 62:683–694
13. Garcia AG, Garcia-De-Diego AM, Gandia L, Borges R, Garcia-Sancho J (2006) Calcium signaling and exocytosis in adrenal chromaffin cells. Physiol Rev 86:1093–1131
14. Rosa JM, de Diego AM, Gandia L, Garcia AG (2007) L-type calcium channels are preferentially coupled to endocytosis in bovine chromaffin cells. Biochem Biophys Res Commun 357:834–839
15. de Diego AM, Gandia L, Garcia AG (2008) A physiological view of the central and peripheral mechanisms that regulate the release of catecholamines at the adrenal medulla. Acta Physiol (Oxf) 192:287–301
16. Wu F, Yao PJ (2009) Clathrin-mediated endocytosis and alzheimer's disease: an update. Ageing Res Rev 8:147–149
17. Artalejo CR, Elhamdani A, Palfrey HC (1996) Calmodulin is the divalent cation receptor for rapid endocytosis, but not exocytosis, in adrenal chromaffin cells. Neuron 16:195–205
18. Tsai CC, Lin CL, Wang TL, Chou AC, Chou MY, Lee CH, Peng IW, Liao JH, Chen YT, Pan CY (2009) Dynasore inhibits rapid endocytosis in bovine chromaffin cells. Am J Physiol Cell Physiol 297:C397–C406
19. Livett BG (1984) Adrenal medullary chromaffin cells in vitro. Physiol Rev 64:1103–1161
20. Moro MA, López MG, Gandía L, Michelena P, García AG (1990) Separation and culture of living adrenaline- and noradrenaline-containing cells from bovine adrenal medullae. Anal Biochem 185:243–248
21. Hamill OP, Marty A, Neher E, Sakmann B, Sigworth FJ (1981) Improved patch-clamp techniques for high-resolution current recording from cells and cell-free membrane patches. Pflugers Arch 391:85–100
22. Rae J, Cooper K, Gates P, Watsky M (1991) Low access resistance perforated patch recordings using amphotericin B. J Neurosci Methods 37:15–26
23. Lindau M, Neher E (1988) Patch-clamp techniques for time-resolved capacitance measurements in single cells. Pflugers Arch 411:137–146
24. de Diego AM, Arnaiz-Cot JJ, Hernandez-Guijo JM, Gandia L, Garcia AG (2008) Differential variations in Ca2+ entry, cytosolic Ca2+ and membrane capacitance upon steady or action potential depolarizing stimulation of bovine chromaffin cells. Acta Physiol (Oxf) 194:97–109
25. Burgoyne RD (1995) Fast exocytosis and endocytosis triggered by depolarisation in single adrenal chromaffin cells before rapid Ca2+ current run-down. Pflugers Arch 430:213–219
26. Smith C, Neher E (1997) Multiple forms of endocytosis in bovine adrenal chromaffin cells. J Cell Biol 139:885–894
27. Montero M, Alonso MT, Carnicero E, Cuchillo-Ibanez I, Albillos A, Garcia AG, Garcia-Sancho J, Alvarez J (2000) Chromaffin-cell stimulation triggers fast millimolar mitochondrial Ca2+ transients that modulate secretion. Nat Cell Biol 2:57–61
28. Giovannucci DR, Hlubek MD, Stuenkel EL (1999) Mitochondria regulate the Ca(2+)-exocytosis relationship of bovine adrenal chromaffin cells. J Neurosci 19:9261–9270
29. Nucifora PG, Fox AP (1999) Tyrosine phosphorylation regulates rapid endocytosis in adrenal chromaffin cells. J Neurosci 19:9739–9746
30. Fenwick EM, Marty A, Neher E (1982) Sodium and calcium channels in bovine chromaffin cells. J Physiol 331:599–635
31. Zha X, Pierini LM, Leopold PL, Skiba PJ, Tabas I, Maxfield FR (1998) Sphingomyelinase treatment induces ATP-independent endocytosis. J Cell Biol 140:39–47
32. Strelow A, Bernardo K, Adam-Klages S, Linke T, Sandhoff K, Kronke M, Adam D (2000) Overexpression of acid ceramidase protects from tumor necrosis factor-induced cell death. J Exp Med 192:601–612
33. Ghosh TK, Bian J, Gill DL (1990) Intracellular calcium release mediated by sphingosine derivatives generated in cells. Science 248:1653–1656
34. Ghosh TK, Bian J, Gill DL (1994) Sphingosine 1-phosphate generated in the endoplasmic reticulum membrane activates release of stored calcium. J Biol Chem 269:22628–22635

35. Chan SA, Chow R, Smith C (2003) Calcium dependence of action potential-induced endocytosis in chromaffin cells. Pflugers Arch 445:540–546
36. Neher E, Zucker RS (1993) Multiple calcium-dependent processes related to secretion in bovine chromaffin cells. Neuron 10:21–30
37. Newcomb R, Szoke B, Palma A, Wang G, Chen X, Hopkins W, Cong R, Miller J, Urge L, Tarczy-Hornoch K, Loo JA, Dooley DJ, Nadasdi L, Tsien RW, Lemos J, Miljanich G (1998) Selective peptide antagonist of the class E calcium channel from the venom of the tarantula hysterocrates gigas. Biochemistry 37:15353–15362
38. Mattson MP, Cheng B, Davis D, Bryant K, Lieberburg I, Rydel RE (1992) beta-Amyloid peptides destabilize calcium homeostasis and render human cortical neurons vulnerable to excitotoxicity. J Neurosci 12:376–389
39. Wu LG, Betz WJ (1996) Nerve activity but not intracellular calcium determines the time course of endocytosis at the frog neuromuscular junction. Neuron 17:769–779
40. von Gersdorff H, Matthews G (1994) Inhibition of endocytosis by elevated internal calcium in a synaptic terminal. Nature 370:652–655
41. de Champlain J, Farley L, Cousineau D, van Ameringen MR (1976) Circulating catecholamine levels in human and experimental hypertension. Circ Res 38:109–114
42. Cuchillo-Ibáñez I, Lejen T, Albillos A, Rose SD, Olivares R, Villarroya M, García AG, Trifaró JM (2004) Mitochondrial calcium sequestration and protein kinase C cooperate in the regulation of cortical F-actin disassembly and secretion in bovine chromaffin cells. J Physiol 560:63–76
43. Neher E (1998) Vesicle pools and Ca2± microdomains: new tools for understanding their roles in neurotransmitter release. Neuron 20:389–399
44. Artalejo CR, Elhamdani A, Palfrey HC (2002) Sustained stimulation shifts the mechanism of endocytosis from dynamin-1-dependent rapid endocytosis to clathrin- and dynamin-2-mediated slow endocytosis in chromaffin cells. Proc Natl Acad Sci USA 99:6358–6363

VI. DISCUSION

Como mencionado en la Introducción, la contribución de cada subtipo de CCDV en la liberación de vesículas en las células cromafínes varia de acuerdo con la concentración de Ca^{2+}, catión divalente utilizado (Ba^{2+} o Ca^{2+}) y patrón de estimulación (despolarización por K^{+}, duración de pulsos despolarizantes, trenes de pulsos, potenciales de acción) (Garcia *et al.*, 2006). El bloqueo de cada subtipo de canal de Ca^{2+} condiciona la cantidad de iones Ca^{2+} que entran en las células tras un estímulo y con esto la activación de los procesos exocitóticos y/o endocitóticos. Desde un punto de vista fisiológico, la expresión de múltiples canales de Ca^{2+} con diferentes propiedades farmacológicas y biofísicas, nos presenta la interesante cuestión de la especialización de cada subtipo en desencadenar diferentes funciones intracelulares dependientes de Ca^{2+}.

En esta Tesis Doctoral hemos investigado el papel que desempeñan los diferentes subtipos de CCDV en el proceso endocitótico utilizando la célula cromafin de la médula adrenal bovina como modelo celular. Además, hemos estudiado el papel de calcio extra e intracelular en la endocitosis. Para ello, nos hemos servido de la técnica de patch-clamp y de la sonda FM1-43 para mediar las respuestas exo-endocitóticas. Por otro lado, hemos estudiado como los canales L modulan la entrada de Ca^{2+} por los canales N y PQ mediante el estudio de corrientes de calcio.

El proceso endocitótico está acoplado a la respuesta exocitótica (Engisch & Nowycky, 1996). Se ha demostrado que los esfingolípidos aumentan la liberación vesicular por activar proteínas del complejo SNARE (Darios *et al.*, 2009). En esta tesis, también hemos investigado el papel de los esfingolípidos en la retirada de membrana tras la aplicación de pulsos despolarizantes únicos.

A seguir, haremos una breve discusión de los temas abordados en este estudio.

1- Canales de calcio y endocitosis

En un primer abordaje experimental nos planteamos estudiar como el bloqueo de los diferentes CCDV afectaban el proceso endocitótico en la célula cromafin (artículo 1). En nuestro protocolo experimental inicial, hemos seleccionado la concentración de 2 mM Ca^{2+} extracelular y una estimulación mediante pulsos despolarizantes únicos de 500-ms de duración. La duración del PD fue seleccionada a partir de experimentos preliminares realizados por nuestro grupo en los cuales pulsos despolarizantes de diferentes duraciones (entre 50-ms y 2-s) se aplicaron desde -80 a 0 mV (de Diego *et al.*, 2008). En estos experimentos, los cambios en la capacidad de la membrana se

registraron mediante la técnica de patch-clamp en configuración de parche perforado. Las respuestas exocitóticas se obtuvieron con pulsos de duración mínima de 50-ms; sin embargo, una marcada respuesta endocitótica no fue apreciada con pulsos de duración inferior a 200-ms.

La aplicación de un pulso largo de 500-ms desencadenó una marcada respuesta endocitótica superior a la exocitótica que se reprodujo a lo largo del protocolo experimental. Tal reproducibilidad fue posible debido a la configuración de parche perforado utilizada en los experimentos. Esta configuración, permite que el contenido intracelular no sea dializado, manteniendo sus condiciones iniciales y perdurando las respuestas de entrada de Ca^{2+} y liberación de catecolaminas.

El bloqueo de los canales L, disminuyó la entrada de Ca^{2+} en un 30%. Este bloqueo abolió prácticamente toda la respuesta endocitótica, sin tocar significantemente la exocitosis. Curiosamente, el bloqueo de los canales N, que acarrea aproximadamente la misma cantidad de entrada de Ca^{2+} en la célula, no produjo cambios significativos en los procesos exo-endocitóticos. Estos datos demuestran que el bloqueo de la entrada de Ca^{2+} denota distintos efectos en la respuesta endocitótica según el subtipo de canal de Ca^{2+} afectado. Nuestras hipótesis en relación a estos datos se centran en dos posibles mecanismos intracelulares presentes en la célula cromafín: (1) la propiedad de lenta inactivación al Ca^{2+} y voltaje presentada por los canales tipo L en comparación con los canales N y PQ podría ser necesaria para activar la maquinaria endocitótica durante y después del estímulo; (2) una posible colocalización funcional de los canales L con proteínas de la endocitosis dependientes de Ca^{2+}.

Sin embargo, el bloqueo de los canales PQ produjo una marcada inhibición de ambas respuestas. En nuestro protocolo experimental, el bloqueo de los canales PQ disminuyó la respuesta exocitótica en un 81% y la endocitótica en un 64%. Estos datos nos indican que la endocitosis en nuestro modelo está relacionada con una previa exocitosis. Estos resultados están de acuerdo con Engisch y Nowycky (1998) que al aplicar pulsos despolarizantes de corta duración (40-ms) no apreciaron endocitosis (Engisch & Nowycky, 1998).

La sonda FM1-43 es ampliamente utilizada para medir los procesos exo-endocitóticos. Nosotros nos hemos servido de esta técnica fotométrica para corroborar los datos electrofisiológicos y estudiar el proceso endocitótico acoplado al canal L mediante la estimulación por alto potasio. Además, hemos investigando la modulación de la endocitosis en presencia de alta concentración de Ca^{2+} extracelular (artículo 2).

Con la sonda FM1-43 hemos obtenido resultados similares a los eletrofisiólogos donde el bloqueo de los canales L, inhibió en un 60% la respuesta endocitótica y en un 30% la respuesta exocitótica. Estos valores difieren de los encontrados en patch-clamp en el cual no se observaron cambios en la exocitosis y la endocitosis se bloqueó un 92%. Esta diferencia puede deberse por los distintos patrones de estimulación utilizados en las dos técnicas. En el protocolo anterior, las células fueron despolarizadas mediante PD de 500-ms de duración; sin embargo, para los experimentos de fluorescencia, un estímulo de 3-min de duración con 59 mM K^+ fue aplicado. La larga estimulación con K^+ podría estar activando algún otro mecanismo no dependiente de la entrada de Ca^{2+} por los canales L en la endocitosis, haciendo con que el uso de nifedipino disminuya apenas un pequeño porcentaje de la respuesta. Adicionalmente, el bloqueo de los canales tipo N no afectaron las respuestas exo-endocitóticas y la aplicación del agonista de canales L, FPL, aumentó considerablemente la endocitosis, pero apenas afectó la exocitosis. Por otro lado, hemos demonstrado que la participación del Ca^{2+} extracelular en iniciar la endocitosis tiene un papel importante, desde que la liberación de Ca^{2+} intracelular mediante fotoliberación activa en menor grado el proceso endocitótico.

La endocitosis es directamente proporcional a la entrada de Ca^{2+} y a la previa exocitosis (de Diego *et al.*, 2008). Variaciones en el gradiente de Ca^{2+} extra/intracelular podrían modificar la selectividad y la especialización del canal L en iniciar el proceso endocitótico. Para estudiar esta cuestión, hemos realizado experimentos de patch-clamp con medida de la capacidad de la membrana en configuración de parche perforado y aplicación de estímulos despolarizantes. Se perfundieron las células con soluciones extracelulares de diferentes concentraciones de Ca^{2+} (1, 2 y 10 mM). El aumento del gradiente extracelular de Ca^{2+}, con consiguiente aumento de la $[Ca^{2+}]_c$, aumenta la respuesta exocitótica en las células cromafines (de Diego *et al.*, 2008). Esta relación puede ser claramente observada en la figura 1 y 2 del artículo 2 de esta Tesis. El bloqueo de los canales N en presencia de 10 mM Ca^{2+}, disminuyó en un 35% la entrada de Ca^{2+}. Sin embargo, este bloqueo no fue capaz de inhibir la respuesta endocitótica. El bloqueo de los canales L, disminuyó en un 32% la entrada de Ca^{2+}; sin embargo, bloqueó casi por completo la respuesta endocitótica. Sin embargo, la siguiente pregunta se pone de manifiesto: ¿es la cantidad de calcio que entra en las células a través de los CCDV tras la despolarización que es responsable por la activación de la maquinaria endocitótica? o ¿es la entrada específica de calcio por los canales del tipo L?

La selectividad del calcio L en el proceso endocitótico ha sido estudiada utilizando un protocolo experimental bloqueando los canales PQ. Los canales PQ pueden ser bloqueados en su totalidad por la utilización de 1 µM de AgaIVA (Gandia *et al.*, 1993). El objetivo de este experimento, consistió en bloquear el canal PQ en presencia de 200 nM de AgaIVA (apenas una parte de los canales) y obtener una entrada de calcio (Q_{Ca}) similar a la adquirida en presencia del bloqueante de canales L nifedipino. Como resultado, obtuvimos un bloqueo de aproximadamente un 50% de la entrada de Ca^{2+} por ambos canales. Sin embargo, la respuesta endocitótica no ha sido bloqueada en presencia de AgaIVA. Estos resultados, nos demostran la selectiva participación de los canales L en el proceso endocitótico.

Otro dato que ponemos de manifiesto en nuestro trabajo, es el efecto de la exclusiva entrada de Ca^{2+} por los canales L en presencia del bloqueante de canales N y PQ MVIIC (Gandia *et al.*, 1997). El aumento de la entrada de Ca^{2+} por los canales L fue capaz de mantener las respuestas exocitóticas y endocitóticas en las células cromafines bovinas. Además, la aplicación del agonista de canales L FPL, produjo una mayor respuesta endocitótica.

Nuestros datos son consistentes con la hipótesis de que los distintos subtipos de canales de Ca^{2+} en la célula cromafín presentan papeles fisiológicos diferentes. El papel de cada CCDV depende del patrón de estimulación y de la especie animal estudiada. Nuestros datos pueden ser considerados los primeros a encontrar una acción selectiva de los canales de Ca^{2+} del tipo L en el control de la endocitosis en las células cromafines bovinas.

Los CCDV presentan la propiedad de inactivación por voltaje y por Ca^{2+} (Hernandez-Guijo *et al.*, 2001). Los canales L se inactivan más lentamente por ambos mecanismos que los canales N y PQ. De esta forma, la entrada de calcio por los canales L es más lenta y duradera. El papel que desempeñan los canales L en la endocitosis podría estar siendo mediado por dos procesos diferentes: (1) por una posible colocalización de las proteínas endocitóticas con los canales L; o (2) por la cinética lenta de entrada de Ca^{2+} por el canal L. En los estudios de marcaje con anticuerpos frente a clatrina y dinamina y CCDV, ninguna colocalización con la proteína clatrina ha sido observada. Sin embargo, todos los canales presentaron cierta colocalización con las dinaminas. Descartando la hipótesis de una exclusiva colocalización geográfica de los canales L con la maquinaria endocitótica. Para investigar si la endocitosis era debida a la forma de entrada del calcio por los canales L, nos hemos servido de una nueva

herramienta farmacológica que disminuye la deactivación de los canales PQ, la roscovitina (artículo 3). Este fármaco nos demostró ser un específico activador de los canales del subtipo PQ, que no afecta el pico de corriente (I_{Ca}) pero si la corriente de cola ($_{Itail}$). El resultado, es una mayor y más duradera entrada de Ca^{2+} por los canales PQ. Si la endocitosis se debe a la manera de entrada del calcio por los canales L (más lenta y duradera), la presencia de roscovitina mimetizaría esta lenta cinética en los canales PQ. En nuestros experimentos, el bloqueo de la endocitosis por nifedipino ha sido revertido por la presencia de roscovitina.

Como conclusión de esta parte experimental, podemos decir que los canales de calcio del tipo L son los responsables por la activación de la endocitosis en la célula cromafín. El mecanismo por lo cual los canales L participan de este proceso es mediante la cinética de entrada del Ca^{2+} y no por una colocalización con proteínas de la maquinaria endocitótica.

2- Modulación de los canales de calcio

La investigación realizada para describir el papel de los canales de calcio tipo L en la endocitosis, nos llevó a otro hallazgo experimental relacionado con la modulación que ejerce este subtipo de canal sobre los canales N y PQ. Como comentado en el apartado anterior, los canales de calcio se pueden modular por una acumulación de Ca^{2+} en la superficie interna de la membrana (Brehm & Eckert, 1978; Tillotson, 1979). La inactivación dependiente de calcio se debe a la unión del Ca^{2+} a la proteína calmodulina presente en las porciones N y C terminal de los canales N y PQ, las cuales cambian su configuración inactivando el canal. Los diferentes subtipos de canales de calcio presentan diferencias entre sí en cuanto a esta propiedad de inactivación por el propio Ca^{2+}. El hecho de que en la célula cromafín, el canal L se inactiva más lentamente que los canales N y PQ podría estar dando lugar a una modulación de los canales N y PQ, corroborando nuestra hipótesis de que no todo el Ca^{2+} que entra por los CCDV tiene la misma función.

El abordaje experimental utilizado en esta segunda etapa de esta Tesis Doctoral utilizó la técnica de patch-clamp para el estudio de las corrientes de calcio (artículo 4). Para ello, nos hemos servido de las configuraciones de parche perforado y célula entera utilizando el agonista FPL64176 como herramienta farmacológica para activar la entrada de calcio por los canales L. El principal hallazgo encontrado en este estudio, ha

sido que el FPL inhibió la corriente de calcio al utilizar la configuración de parche perforado, pero no en la configuración de célula entera. Estos resultados, también han sido obtenidos al utilizar el agonista dihidropiridínico de canales L BayK 8644. Ambos activadores, son conocidos por sus efectos en aumentar la I_{Ca} a potenciales negativos y disminuir la deactivación, aumentando así la I_{tail}. Por otro lado, el FPL ha sido capaz de aumentar la I_{Ca} cuando los canales N y PQ fueron bloqueados por MVIIC o por voltaje. Estos datos indican que la mayor entrada de calcio por los canales L, podría estar bloqueando los canales de calcio N y PQ en parche-perforado.

Ambas configuraciones de patch-clamp presentan diferencias entre sí. La paradójica inhibición de la corriente de calcio por FPL podría ser explicada por la ausencia del quelante de Ca^{2+} EGTA, en la configuración de parche perforado. En la configuración de célula entera la célula es dializada con una solución intracelular que contiene 14 mM EGTA. El Ca^{2+} tras entrar en la célula sería rápidamente quelado, impidiendo la inhibición dependiente de Ca^{2+}. Por otro lado, en parche perforado, el Ca^{2+} no es quelado e inactiva los canales de calcio. Para comprobar nuestra hipótesis, el EGTA presente en la solución intracelular de célula entera fue eliminado. En estas condiciones experimentales, la presencia de FPL inhibió las corrientes de calcio. Por el contrario, en parche-perforado, las células fueron pretratadas con EGTA.AM presentando una mayor entrada de calcio al utilizar FPL.

Desde que el calcio que entra por los canales L causa daño mitocondrial y muerte celular por apoptosis, así como es el responsable por la endocitosis en la célula cromafín, los resultados presentados en esta parte de esta Tesis Doctoral, ayudan a aclarar los mecanismos fisiológicos que pueden llevar a cabo los distintos CCDV.

3- Papel de los esfingolípidos en la endocitosis

Los procesos exocitóticos y endocitóticos requieren proteínas que se encuentran en la membrana plasmática. La esfingosina ha sido demostrada por actuar en la maquinaria exocitótica aumentando la liberación vesicular. Desde que la endocitosis está relacionada con la exocitosis, la esfingosina podría actuar en la maquinaria endocitótica. En este trabajo hemos estudiado el papel que desempeña los esfingolípidos (esfingosina, esfingosina-1-fosfato y esfingomielinasas) en la retirada de membrana tras la aplicación de un pulso despolarizante. Para ello, hemos utilizado la duración de 200-ms de estimulación que induce una considerable respuesta exocitótica, sin embargo, no

produce endocitosis. La diálisis intracelular de esfingosina indujo una respuesta endocitótica marcada. Los mismos resultados han sido obtenidos al pretratar las células con esfingomielinasas. Las esfingomielinasas a través de las esfingomielinas presentes en la membrana plasmática producen esfingosina endógena en el citosol. Este efecto fue revertido al bloquear una de las vías de síntesis de la esfingosina, la transformación de ceramida a esfingosina por ceramidasas. Por otro lado, el metabolito de la esfingosina, esfingosina-1-fosfato S1P, apenas indujo un proceso endoctitótico. La pequeña endocitosis tras la diálisis celular con S1P puede deberse al mecanismo retrógrado de síntesis de esfingosina.

El proceso endocitótico inducido por esfingosina ha sido dependiente de altas concentraciones de calcio (5 y 10 mM Ca^{2+}), desde que a concentraciones de 2 mM de Ca^{2+} extracelular, ninguna endocitosis fue observada. En condiciones fisiológicas, las esfingomielinasas son activadas tras estímulos estresantes como daño mitocondrial o reticular que aumentan la concentración de calcio citosólico. Estos datos corroboran con nuestros experimentos, ya que el tratamiento de las células con el protonóforo FCCP, que bloquea la captación de calcio por la mitocondria, y la presencia de 2 mM Ca^{2+} extracelular indujeron una marcada respuesta endocitótica.

La endocitosis, así como la exocitosis, es dependiente de factores citosólicos que son perdidos tras la diálisis celular. En nuestros experimentos, la esfingosina no pudo mantener la respuesta endocitótica en el tiempo al utilizar la configuración de célula entera, en la cual el interior celular es dializado con la solución presente en la pipeta. Sin embargo, la respuesta se mantiene al utilizar el parche perforado.

La dinamina es la proteína responsable por formar un anillo alrededor de la membrana de la vesícula fisionada, liberándola en el citoplasma. Por otro lado, la calmodulina ha sido relacionada por iniciar todos los procesos endocitóticos conocidos. Tanto la inhibición de las dinaminas o de la calmodulina, no abolió la endocitosis inducida por esfingosina. Estos datos nos revelan que el mecanismo endocitótico iniciado por la esfingosina no es dependiente ni de dinamina ni de calmodulina, sugiriendo un mecanismo totalmente diferente a los descritos hasta ahora. El mecanismo exacto por lo cual la esfingosina activa la endocitosis aún queda por aclarar.

II. Perspectivas Clínicas

Además de los resultados presentados en esta Tesis Doctoral, hemos obtenido datos que nos llevan a una perspectiva clínica en relación al papel que pueden tener los canales de calcio, la endocitosis y los esfingolípidos en la Enfermedad de Alzheimer.

Como mencionado en la Introducción, la muerte neuronal producida por el péptido Aβ podría estar relacionada con la alteración en la homeostasia del Ca^{2+}, ya que *per se* el Aβ es capaz de elevar la $[Ca^{2+}]_c$ y alterar la función de los canales de calcio voltaje-dependientes (Mattson *et al.*, 1992; Ueda *et al.*, 1997; Yu *et al.*, 2009). La elevación de los niveles de calcio citosólicos puede ser bloqueada mediante el uso de bloqueantes de canales de calcio del tipo L (Ueda *et al.*, 1997; Ho *et al.*, 2001). A modo de ejemplo, en el estudio de Ueda y colaboradores (1997) cuando se bloquearon los canales de calcio L con nimodipino se atenuó la toxicidad del péptido AB, no observándose este efecto protector cuando se utilizaron bloqueantes de los canales N y PQ. Los estudios electrofisiológicos mostraron un incremento de aproximadamente dos veces en la densidad de la corriente que fluye a través de los canales L (Ueda *et al.*, 1997).

Por otro lado, en los últimos años se ha postulado que alteraciones en los procesos de endocitosis preceden el depósito del péptido Aβ en el cerebro de pacientes con EA (Cataldo *et al.*, 2000; Keating *et al.*, 2006; Yuyama & Yanagisawa, 2009). Se ha sugerido que la endocitosis y el posterior procesamiento intracelular es lo que va a determianr la orma en que se procesa la proteína precursora de amiloid (APP) por las β- y γ-secretasas a nivel de los endosomas dando lugar al péptido toxico Aβ (Wu & Yao, 2009). En este sentido, se ha descrito que la endocitosis que se produce tras la actividad sináptica favorece la internalización de la APP, con lo que se va a favorecer la producción y liberación del Aβ (Cirrito *et al.*, 2008), así como el deposito de este (Yuyama & Yanagisawa, 2009).

En estrecha relación con estas alteraciones en los procesos de endocitosis, en la EA se ha descrito la existencia de alteraciones en el metabolismo de los fosfolípidos de membrana, principalmente en la vía ceramida/esfingomielina (tanto la ceramida como la esfingosina han sido descritas como pró-apoptóticas), habiéndose descrito una mayor activación de esta vía en presencia de Aβ, observándose que el contenido de esfingosina y ceramida se encontraban significantemente elevados en cerebros post-mortem de pacientes con EA, junto con un incremento de la actividad de la enzima esfingomielinasa, responsable por la producción de ceramida (He *et al.*, 2008).

A pesar de que los procesos que se producen durante el procesamiento por distintas secretasas de la proteína APP son bien conocidos, no lo son tanto los mecanismos que regulan la producción, liberación y depósito del péptido Aβ tóxico, lo cual puede ser la causa de que las distintas estrategias farmacológicas que se han venido ensayando con el objetivo de modificar el procesamiento de la proteína APP y, por ende, de la producción del Aβ como los bloqueantes β- y γ-secretasas, activadores de α-secretasas, estatinas, quelantes de Aβ, vacuna frente al Aβ, incremento de la eliminación de Aβ por proteasas (Wolfe, 2002) no hayan resultado satisfactorias y ninguna de ellas ha alcanzado la clínica todavía.

Por este motivo, consideramos que se hace altamente necesario profundizar en el estudio de los posibles mecanismos implicados en los efectos tóxicos del péptido Aβ que conducen al deterioro del paciente con EA. Puesto que, como hemos descrito en esta Introducción, existen evidencias recientes que sugieren que la toxicidad del Aβ se relaciona con una alteración de la actividad sináptica, así que el estudio de los posibles efectos de este péptido sobre distintos parámetros que controlan y/o regulan el proceso endocitótico y la actividad de los canales de calcio podría ser de gran interés para el desarrollo de nuevas dianas terapéuticas en la EA.

Resultados preliminares de este estudio, así como protocolos experimentales y una breve discusión pueden ser observados en el apartado “ANEXO 1”.

Estos resultados son datos preliminares de una investigación que continuará en el Instituto Teófilo Hernando. La hipótesis de un acoplamiento entre endocitosis – esfingolípidos – canales de calcio y EA (**Esquema 1**) ha surgido gracias a los resultados obtenidos mediante los estudios realizados en esta Tesis Doctoral y las colaboraciones realizadas entre los miembros de dentro y fuera del ITH. Sin duda, el porvenir de esta línea de investigación abrirá nuevos horizontes en el transcurso del entendimiento de patologías como la Enfermedad de Alzheimer.

VIII. Conclusiones

De los resultados de este trabajo y de su análisis y discusión, nos permitimos extraer las siguientes conclusiones:

1. Los diferentes modos de entrada de calcio a través de los canales de calcio PQ (más inactivantes) y L (menos inactivantes) controlan los procesos exocitotóticos y endocitóticos en la célula cromafin;
2. La endocitosis en la célula cromafin tras la aplicación de pulsos despolarizantes únicos, es dependiente del calcio que entra por los canales de calcio del tipo L;
3. La endocitosis es un proceso calcio dependiente y es directamente proporcional a la entrada de Ca^{2+};
4. La estimulación durante un largo período de tiempo (3-min) puede desencadenar otros mecanismos endocitóticos no dependientes exclusivamente del Ca^{2+} que entra por los canales L;
5. El calcio intracelular no presenta la misma eficacia de iniciar el proceso endocitótico;
6. Los diferentes subtipos de CCDV no están colocalizados con la proteínas endocitótica clatrina; sin embargo, presente una pequeña colocalización con las dinaminas;
7. El aumento de la entrada de calcio por los canales del tipo PQ, son capaces de controlar la endocitosis en la célula cromafin;
8. El aumento de la entrada de calcio por los canales L modula la entrada de calcio por los canales N y PQ;
9. Esfingosina y esfingomielinasas son capaces de activar la endocitosis, pero no la esfingosina-1-fosfato,
10. La respuesta endocitótica inducida por esfingosina es dependiente de altas concentraciones de calcio citosólico. Este puede darse a través del aumento del gradiente extracelular de Ca^{2+} o por la inhibición de la captación de Ca^{2+} por la mitocondria;
11. La endocitosis producida por esfingosina no es dependiente ni de calmodulina ni de dinaminas.

Agudo-Lopez A, Miguel BG, Fernandez I & Martinez AM. (2010). Involvement of mitochondria on neuroprotective effect of sphingosine-1-phosphate in cell death in an in vitro model of brain ischemia. *Neurosci Lett* **470,** 130-133.

Ahlijanian MK, Westenbroek RE & Catterall WA. (1990). Subunit structure and localization of dihydropyridine-sensitive calcium channels in mammalian brain, spinal cord, and retina. *Neuron* **4,** 819-832.

Albillos A, Artalejo AR, Lopez MG, Gandia L, Garcia AG & Carbone E. (1994). Calcium channel subtypes in cat chromaffin cells. *J Physiol* **477 (Pt 2),** 197-213.

Albillos A, Carbone E, Gandia L, Garcia AG & Pollo A. (1996a). Opioid inhibition of Ca2+ channel subtypes in bovine chromaffin cells: selectivity of action and voltage-dependence. *Eur J Neurosci* **8,** 1561-1570.

Albillos A, Garcia AG & Gandia L. (1993). omega-Agatoxin-IVA-sensitive calcium channels in bovine chromaffin cells. *FEBS Lett* **336,** 259-262.

Albillos A, Garcia AG, Olivera B & Gandia L. (1996b). Re-evaluation of the P/Q Ca2+ channel components of Ba2+ currents in bovine chromaffin cells superfused with solutions containing low and high Ba2+ concentrations. *Pflugers Arch* **432,** 1030-1038.

Ales E, Tabares L, Poyato JM, Valero V, Lindau M & Alvarez de Toledo G. (1999). High calcium concentrations shift the mode of exocytosis to the kiss-and-run mechanism. *Nat Cell Biol* **1,** 40-44.

Alonso MT, Villalobos C, Chamero P, Alvarez J & Garcia-Sancho J. (2006). Calcium microdomains in mitochondria and nucleus. *Cell Calcium* **40,** 513-525.

Alvarez YD, Ibanez LI, Uchitel OD & Marengo FD. (2008). P/Q Ca2+ channels are functionally coupled to exocytosis of the immediately releasable pool in mouse chromaffin cells. *Cell Calcium* **43,** 155-164.

Allan D & Walklin CM. (1988). Endovesiculation of human erythrocytes exposed to sphingomyelinase C: a possible explanation for the enzyme-resistant pool of sphingomyelin. *Biochim Biophys Acta* **938,** 403-410.

Andrieu-Abadie N & Levade T. (2002). Sphingomyelin hydrolysis during apoptosis. *Biochim Biophys Acta* **1585,** 126-134.

Ardiles AO, Gonzalez-Jamett AM, Maripillan J, Naranjo D, Caviedes P & Cardenas AM. (2007). Calcium channel subtypes differentially regulate fusion pore stability and expansion. *J Neurochem* **103,** 1574-1581.

Arroyo G, Aldea M, Fuentealba J, Albillos A & Garcia AG. (2003). SNX482 selectively blocks P/Q Ca2+ channels and delays the inactivation of Na+ channels of chromaffin cells. *Eur J Pharmacol* **475,** 11-18.

Artalejo AR, Garcia AG & Neher E. (1993). Small-conductance Ca^{2+}-activated K^{+} channels in bovine chromaffin cells. *Pflugers Arch* **423,** 97-103.

Artalejo CR, Adams ME & Fox AP. (1994). Three types of Ca^{2+} channel trigger secretion with different efficacies in chromaffin cells. *Nature* **367,** 72-76.

Artalejo CR, Elhamdani A & Palfrey HC. (1996). Calmodulin is the divalent cation receptor for rapid endocytosis, but not exocytosis, in adrenal chromaffin cells. *Neuron* **16,** 195-205.

Artalejo CR, Elhamdani A & Palfrey HC. (2002). Sustained stimulation shifts the mechanism of endocytosis from dynamin-1-dependent rapid endocytosis to clathrin- and dynamin-2-mediated slow endocytosis in chromaffin cells. *Proc Natl Acad Sci U S A* **99,** 6358-6363.

Artalejo CR, Henley JR, McNiven MA & Palfrey HC. (1995). Rapid endocytosis coupled to exocytosis in adrenal chromaffin cells involves Ca^{2+}, GTP, and dynamin but not clathrin. *Proc Natl Acad Sci U S A* **92,** 8328-8332.

Artalejo CR, Perlman RL & Fox AP. (1992). Omega-conotoxin GVIA blocks a Ca^{2+} current in bovine chromaffin cells that is not of the "classic" N type. *Neuron* **8,** 85-95.

Augustine GJ & Neher E. (1992). Neuronal Ca^{2+} signalling takes the local route. *Curr Opin Neurobiol* **2,** 302-307.

Bading H, Ginty DD & Greenberg ME. (1993). Regulation of gene expression in hippocampal neurons by distinct calcium signaling pathways. *Science* **260,** 181-186.

Barg S & Machado JD. (2008). Compensatory endocytosis in chromaffin cells. *Acta Physiol (Oxf)* **192,** 195-201.

Bartus RT, Dean RL, 3rd, Beer B & Lippa AS. (1982). The cholinergic hypothesis of geriatric memory dysfunction. *Science* **217,** 408-414.

Bean BP. (1989). Neurotransmitter inhibition of neuronal calcium currents by changes in channel voltage dependence. *Nature* **340,** 153-156.

Berrow NS, Brice NL, Tedder I, Page KM & Dolphin AC. (1997). Properties of cloned rat alpha1A calcium channels transiently expressed in the COS-7 cell line. *Eur J Neurosci* **9,** 739-748.

Bertolino M & Llinas RR. (1992). The central role of voltage-activated and receptor-operated calcium channels in neuronal cells. *Annu Rev Pharmacol Toxicol* **32,** 399-421.

Betz WJ, Mao F & Smith CB. (1996). Imaging exocytosis and endocytosis. *Curr Opin Neurobiol* **6,** 365-371.

Biales B, Dichter M & Tischler A. (1976). Electrical excitability of cultured adrenal chromaffin cells. *J Physiol* **262,** 743-753.

Blochl A & Sirrenberg C. (1996). Neurotrophins stimulate the release of dopamine from rat mesencephalic neurons via Trk and p75Lntr receptors. *J Biol Chem* **271,** 21100-21107.

Brailoiu E, Cooper RL & Dun NJ. (2002). Sphingosine 1-phosphate enhances spontaneous transmitter release at the frog neuromuscular junction. *Br J Pharmacol* **136,** 1093-1097.

Brandt BL, Hagiwara S, Kidokoro Y & Miyazaki S. (1976). Action potentials in the rat chromaffin cell and effects of acetylcholine. *J Physiol* **263,** 417-439.

Brehm P & Eckert R. (1978). Calcium entry leads to inactivation of calcium channel in Paramecium. *Science* **202,** 1203-1206.

Brodsky FM. (1985). Clathrin structure characterized with monoclonal antibodies. I. Analysis of multiple antigenic sites. *J Cell Biol* **101,** 2047-2054.

Buraei Z, Anghelescu M & Elmslie KS. (2005). Slowed N-type calcium channel ($Ca_V2.2$) deactivation by the cyclin-dependent kinase inhibitor roscovitine. *Biophys J* **89,** 1681-1691.

Buraei Z, Schofield G & Elmslie KS. (2007). Roscovitine differentially affects Ca_V2 and K_v channels by binding to the open state. *Neuropharmacology* **52,** 883-894.

Burgoyne RD. (1995). Fast exocytosis and endocytosis triggered by depolarisation in single adrenal chromaffin cells before rapid Ca^{2+} current run-down. *Pflugers Arch* **430,** 213-219.

Burley JR & Sihra TS. (2000). A modulatory role for protein phosphatase 2B (calcineurin) in the regulation of Ca^{2+} entry. *Eur J Neurosci* **12,** 2881-2891.

Cano-Abad MF, Garcia AG, Sanchez-Garcia P & Lopez MG. (2000). Ba^{2+}-induced chromaffin cell death: cytoprotection by Ca^{2+} channel antagonists. *Eur J Pharmacol* **402,** 19-29.

Cano-Abad MF, Villarroya M, Garcia AG, Gabilan N & Lopez MG. (2002). Contribution of calcium entry through L-type calcium channels to chromaffin cell death. *Ann N Y Acad Sci* **971,** 171-173.

Cano-Abad MF, Villarroya M, Garcia AG, Gabilan NH & Lopez MG. (2001). Calcium entry through L-type calcium channels causes mitochondrial disruption and chromaffin cell death. *J Biol Chem* **276,** 39695-39704.

Carabelli V, Carra I & Carbone E. (1998). Localized secretion of ATP and opioids revealed through single Ca^{2+} channel modulation in bovine chromaffin cells. *Neuron* **20,** 1255-1268.

Carabelli V, Giancippoli A, Baldelli P, Carbone E & Artalejo AR. (2003). Distinct potentiation of L-type currents and secretion by cAMP in rat chromaffin cells. *Biophys J* **85,** 1326-1337.

Carter HE, Haines WJ & et al. (1947). Biochemistry of the sphingolipides; preparation of sphingolipides from beef brain and spinal cord. *J Biol Chem* **169,** 77-82.

Cataldo AM, Peterhoff CM, Troncoso JC, Gomez-Isla T, Hyman BT & Nixon RA. (2000). Endocytic pathway abnormalities precede amyloid beta deposition in sporadic Alzheimer's disease and Down syndrome: differential effects of APOE genotype and presenilin mutations. *Am J Pathol* **157,** 277-286.

Catterall WA. (2000). Structure and regulation of voltage-gated Ca^{2+} channels. *Annu Rev Cell Dev Biol* **16,** 521-555.

Catterall WA, Perez-Reyes E, Snutch TP & Striessnig J. (2005). International Union of Pharmacology. XLVIII. Nomenclature and structure-function relationships of voltage-gated calcium channels. *Pharmacol Rev* **57,** 411-425.

Ceccarelli B & Hurlbut WP. (1980). Ca^{2+}-dependent recycling of synaptic vesicles at the frog neuromuscular junction. *J Cell Biol* **87,** 297-303.

Ceccarelli B, Hurlbut WP & Mauro A. (1973). Turnover of transmitter and synaptic vesicles at the frog neuromuscular junction. *J Cell Biol* **57,** 499-524.

Cena V, Nicolas GP, Sanchez-Garcia P, Kirpekar SM & Garcia AG. (1983). Pharmacological dissection of receptor-associated and voltage-sensitive ionic channels involved in catecholamine release. *Neuroscience* **10,** 1455-1462.

Cirrito JR, Kang JE, Lee J, Stewart FR, Verges DK, Silverio LM, Bu G, Mennerick S & Holtzman DM. (2008). Endocytosis is required for synaptic activity-dependent release of amyloid-beta in vivo. *Neuron* **58,** 42-51.

Cirrito JR, Yamada KA, Finn MB, Sloviter RS, Bales KR, May PC, Schoepp DD, Paul SM, Mennerick S & Holtzman DM. (2005). Synaptic activity regulates interstitial fluid amyloid-beta levels in vivo. *Neuron* **48,** 913-922.

Clementi ME, Marini S, Coletta M, Orsini F, Giardina B & Misiti F. (2005). Abeta 31-35 and Abeta 25-35 fragments of amyloid beta-protein induce cellular death through apoptotic signals: Role of the redox state of methionine-35. *FEBS Lett* **579,** 2913-2918.

Cole KS. (1949). Some physical aspects of bioelectric phenomena. *Proc Natl Acad Sci U S A* **35,** 558-566.

Coupland RE. (1965). (Electron Microscopic Observations on the Structure of the Rat Adrenal Medulla. I. the Ultrastructure and Organization of Chromaffin Cells in the Normal Adrenal Medulla.). *J Anat* **99,** 231-254.

Cousin MA & Robinson PJ. (1999). Mechanisms of synaptic vesicle recycling illuminated by fluorescent dyes. *J Neurochem* **73,** 2227-2239.

Cousin MA & Robinson PJ. (2001). The dephosphins: dephosphorylation by calcineurin triggers synaptic vesicle endocytosis. *Trends Neurosci* **24,** 659-665.

Cousin MA, Tan TC & Robinson PJ. (2001). Protein phosphorylation is required for endocytosis in nerve terminals: potential role for the dephosphins dynamin I and synaptojanin, but not AP180 or amphiphysin. *J Neurochem* **76,** 105-116.

Cox DH & Dunlap K. (1994). Inactivation of N-type calcium current in chick sensory neurons: calcium and voltage dependence. *J Gen Physiol* **104,** 311-336.

Cuchillo-Ibanez I, Lejen T, Albillos A, Rose SD, Olivares R, Villarroya M, Garcia AG & Trifaro JM. (2004). Mitochondrial calcium sequestration and protein kinase C cooperate in the regulation of cortical F-actin disassembly and secretion in bovine chromaffin cells. *J Physiol* **560,** 63-76.

Chan SA, Polo-Parada L & Smith C. (2005). Action potential stimulation reveals an increased role for P/Q-calcium channel-dependent exocytosis in mouse adrenal tissue slices. *Arch Biochem Biophys* **435,** 65-73.

Chan SA & Smith C. (2001). Physiological stimuli evoke two forms of endocytosis in bovine chromaffin cells. *J Physiol* **537,** 871-885.

Chan SA & Smith C. (2003). Low frequency stimulation of mouse adrenal slices reveals a clathrin-independent, protein kinase C-mediated endocytic mechanism. *J Physiol* **553,** 707-717.

Chen X, Gao Y, Hossain M, Gangopadhyay S & Gillis KD. (2008). Controlled on-chip stimulation of quantal catecholamine release from chromaffin cells using photolysis of caged Ca^{2+} on transparent indium-tin-oxide microchip electrodes. *Lab Chip* **8,** 161-169.

Cho S & Meriney SD. (2006). The effects of presynaptic calcium channel modulation by roscovitine on transmitter release at the adult frog neuromuscular junction. *Eur J Neurosci* **23,** 3200-3208.

Darios F, Wasser C, Shakirzyanova A, Giniatullin A, Goodman K, Munoz-Bravo JL, Raingo J, Jorgacevski J, Kreft M, Zorec R, Rosa JM, Gandia L, Gutierrez LM, Binz T, Giniatullin R, Kavalali ET & Davletov B. (2009). Sphingosine facilitates SNARE complex assembly and activates synaptic vesicle exocytosis. *Neuron* **62,** 683-694.

De Camilli P & Takei K. (1996). Molecular mechanisms in synaptic vesicle endocytosis and recycling. *Neuron* **16,** 481-486.

de Diego AM, Arnaiz-Cot JJ, Hernandez-Guijo JM, Gandia L & Garcia AG. (2008). Differential variations in Ca^{2+} entry, cytosolic Ca^{2+} and membrane capacitance

upon steady or action potential depolarizing stimulation of bovine chromaffin cells. *Acta Physiol (Oxf)* **194,** 97-109.

Deisseroth K, Heist EK & Tsien RW. (1998). Translocation of calmodulin to the nucleus supports CREB phosphorylation in hippocampal neurons. *Nature* **392,** 198-202.

DeStefino NR, Pilato AA, Dittrich M, Cherry SV, Cho S, Stiles JR & Meriney SD. (2010). (R)-roscovitine prolongs the mean open time of unitary N-type calcium channel currents. *Neuroscience* **167,** 838-849.

Dickson RC. (2008). Thematic review series: sphingolipids. New insights into sphingolipid metabolism and function in budding yeast. *J Lipid Res* **49,** 909-921.

Diverse-Pierluissi M, Dunlap K & Westhead EW. (1991). Multiple actions of extracellular ATP on calcium currents in cultured bovine chromaffin cells. *Proc Natl Acad Sci U S A* **88,** 1261-1265.

Doering CJ & Zamponi GW. (2003). Molecular pharmacology of high voltage-activated calcium channels. *J Bioenerg Biomembr* **35,** 491-505.

Douglas WW. (1968). Stimulus-secretion coupling: the concept and clues from chromaffin and other cells. *Br J Pharmacol* **34,** 451-474.

Douglas WW, Kanno T & Sampson SR. (1967). Effects of acetylcholine and other medullary secretagogues and antagonists on the membrane potential of adrenal chromaffin cells: an analysis employing techniques of tissue culture. *J Physiol* **188,** 107-120.

Douglas WW & Poisner AM. (1965). Preferential release of adrenaline from the adrenal medulla by muscarine and pilocarpine. *Nature* **208,** 1102-1103.

Douglas WW & Rubin RP. (1961). Mechanism of nicotinic action at the adrenal medulla: calcium as a link in stimulus-secretion coupling. *Nature* **192,** 1087-1089.

Douglas WW & Rubin RP. (1964). The Effects of Alkaline Earths and Other Divalent Cations on Adrenal Medullary Secretion. *J Physiol* **175,** 231-241.

Eckert R & Chad JE. (1984). Inactivation of Ca channels. *Prog Biophys Mol Biol* **44,** 215-267.

Egea J, Rosa AO, Sobrado M, Gandia L, Lopez MG & Garcia AG. (2007). Neuroprotection afforded by nicotine against oxygen and glucose deprivation in hippocampal slices is lost in alpha7 nicotinic receptor knockout mice. *Neuroscience* **145,** 866-872.

Ekinci FJ, Malik KU & Shea TB. (1999). Activation of the L voltage-sensitive calcium channel by mitogen-activated protein (MAP) kinase following exposure of

neuronal cells to beta-amyloid. MAP kinase mediates beta-amyloid-induced neurodegeneration. *J Biol Chem* **274,** 30322-30327.

Ekinci FJ, Ortiz D & Shea TB. (2003). Okadaic acid mediates tau phosphorylation via sustained activation of the L-voltage-sensitive calcium channel. *Brain Res Mol Brain Res* **117,** 145-151.

Engisch KL & Nowycky MC. (1996). Calcium dependence of large dense-cored vesicle exocytosis evoked by calcium influx in bovine adrenal chromaffin cells. *J Neurosci* **16,** 1359-1369.

Engisch KL & Nowycky MC. (1998). Compensatory and excess retrieval: two types of endocytosis following single step depolarizations in bovine adrenal chromaffin cells. *J Physiol* **506 (Pt 3),** 591-608.

Ertel EA, Campbell KP, Harpold MM, Hofmann F, Mori Y, Perez-Reyes E, Schwartz A, Snutch TP, Tanabe T, Birnbaumer L, Tsien RW & Catterall WA. (2000). Nomenclature of voltage-gated calcium channels. *Neuron* **25,** 533-535.

Euler USv. (1972). Synthesis, uptake and storage of catecholamines in adrenergic nerves. The effect of drugs. *Hand Exp Pharmacol* **33,** 186-230.

Feldberg W, Minz B & Tsudzimura H. (1934). The mechanism of the nervous discharge of adrenaline. *J Physiol* **81,** 286-304.

Fenwick EM, Marty A & Neher E. (1982a). A patch-clamp study of bovine chromaffin cells and of their sensitivity to acetylcholine. *J Physiol* **331,** 577-597.

Fenwick EM, Marty A & Neher E. (1982b). Sodium and calcium channels in bovine chromaffin cells. *J Physiol* **331,** 599-635.

Ferguson SM, Brasnjo G, Hayashi M, Wolfel M, Collesi C, Giovedi S, Raimondi A, Gong LW, Ariel P, Paradise S, O'Toole E, Flavell R, Cremona O, Miesenbock G, Ryan TA & De Camilli P. (2007). A selective activity-dependent requirement for dynamin 1 in synaptic vesicle endocytosis. *Science* **316,** 570-574.

Fesce R, Grohovaz F, Valtorta F & Meldolesi J. (1994). Neurotransmitter release: fusion or 'kiss-and-run'? *Trends Cell Biol* **4,** 1-4.

Fleckenstein A. (1977). Specific pharmacology of calcium in myocardium, cardiac pacemakers, and vascular smooth muscle. *Annu Rev Pharmacol Toxicol* **17,** 149-166.

Fox AP, Cahill AL, Currie KP, Grabner C, Harkins AB, Herring B, Hurley JH & Xie Z. (2008). N- and P/Q-type Ca2+ channels in adrenal chromaffin cells. *Acta Physiol (Oxf)* **192,** 247-261.

Fuentealba J. (2004). Señales de calcio y de exocitosis generadas por acetilcolina, colina y potasio, en la célula cromafín. *Tesis Doctoral Universidad Autónoma de Madrid*.

Fujita T. (1977). Concept of paraneurons. *Arch Histol Jpn* **40 Suppl,** 1-12.

Futerman AH & Hannun YA. (2004). The complex life of simple sphingolipids. *EMBO Rep* **5,** 777-782.

Gad H, Low P, Zotova E, Brodin L & Shupliakov O. (1998). Dissociation between Ca2+-triggered synaptic vesicle exocytosis and clathrin-mediated endocytosis at a central synapse. *Neuron* **21,** 607-616.

Gallegos CE, Pediconi MF & Barrantes FJ. (2008). Ceramides modulate cell-surface acetylcholine receptor levels. *Biochim Biophys Acta* **1778,** 917-930.

Gandia L, Albillos A & Garcia AG. (1993a). Bovine chromaffin cells possess FTX-sensitive calcium channels. *Biochem Biophys Res Commun* **194,** 671-676.

Gandia L, Borges R, Albillos A & Garcia AG. (1995). Multiple calcium channel subtypes in isolated rat chromaffin cells. *Pflugers Arch* **430,** 55-63.

Gandia L, Garcia AG & Morad M. (1993b). ATP modulation of calcium channels in chromaffin cells. *J Physiol* **470,** 55-72.

Gandia L, Lara B, Imperial JS, Villarroya M, Albillos A, Maroto R, Garcia AG & Olivera BM. (1997). Analogies and differences between omega-conotoxins MVIIC and MVIID: binding sites and functions in bovine chromaffin cells. *Pflugers Arch* **435,** 55-64.

Gandia L, Mayorgas I, Michelena P, Cuchillo I, de Pascual R, Abad F, Novalbos JM, Larranaga E & Garcia AG. (1998). Human adrenal chromaffin cell calcium channels: drastic current facilitation in cell clusters, but not in isolated cells. *Pflugers Arch* **436,** 696-704.

Gandía L, Montiel C, García A & López M. (2008). *Seafood and Freshwater Toxins: Pharmacology, physiology and detection*. Boca Raton.

Garcia-Palomero E, Cuchillo-Ibanez I, Garcia AG, Renart J, Albillos A & Montiel C. (2000). Greater diversity than previously thought of chromaffin cell Ca^{2+} channels, derived from mRNA identification studies. *FEBS Lett* **481,** 235-239.

Garcia AG, Garcia-De-Diego AM, Gandia L, Borges R & Garcia-Sancho J. (2006). Calcium signaling and exocytosis in adrenal chromaffin cells. *Physiol Rev* **86,** 1093-1131.

Garcia AG, Sala F, Reig JA, Viniegra S, Frias J, Fonteriz R & Gandia L. (1984). Dihydropyridine BAY-K-8644 activates chromaffin cell calcium channels. *Nature* **309,** 69-71.

Gillis KD, Pun RY & Misler S. (1991). Single cell assay of exocytosis from adrenal chromaffin cells using "perforated patch recording". *Pflugers Arch* **418,** 611-613.

Giner D, Lopez I, Neco P, Rossetto O, Montecucco C & Gutierrez LM. (2007). Glycogen synthase kinase 3 activation is essential for the snake phospholipase A2 neurotoxin-induced secretion in chromaffin cells. *Eur J Neurosci* **25,** 2341-2348.

Giovannucci DR, Hlubek MD & Stuenkel EL. (1999). Mitochondria regulate the Ca^{2+}-exocytosis relationship of bovine adrenal chromaffin cells. *J Neurosci* **19,** 9261-9270.

Graham ME, O'Callaghan DW, McMahon HT & Burgoyne RD. (2002). Dynamin-dependent and dynamin-independent processes contribute to the regulation of single vesicle release kinetics and quantal size. *Proc Natl Acad Sci U S A* **99,** 7124-7129.

Grantham CJ, Bowman D, Bath CP, Bell DC & Bleakman D. (1994). Omega-conotoxin MVIIC reversibly inhibits a human N-type calcium channel and calcium influx into chick synaptosomes. *Neuropharmacology* **33,** 255-258.

Grimm MO, Grimm HS, Patzold AJ, Zinser EG, Halonen R, Duering M, Tschape JA, De Strooper B, Muller U, Shen J & Hartmann T. (2005). Regulation of cholesterol and sphingomyelin metabolism by amyloid-beta and presenilin. *Nat Cell Biol* **7,** 1118-1123.

Grziwa B, Grimm MO, Masters CL, Beyreuther K, Hartmann T & Lichtenthaler SF. (2003). The transmembrane domain of the amyloid precursor protein in microsomal membranes is on both sides shorter than predicted. *J Biol Chem* **278,** 6803-6808.

Gutnick MJ, Lux HD, Swandulla D & Zucker H. (1989). Voltage-dependent and calcium-dependent inactivation of calcium channel current in identified snail neurones. *J Physiol* **412,** 197-220.

Hagiwara S & Byerly L. (1981). Calcium channel. *Annu Rev Neurosci* **4,** 69-125.

Hagiwara S & Nakajima S. (1966). Effects of the intracellular Ca ion concentration upon the excitability of the muscle fiber membrane of a barnacle. *J Gen Physiol* **49,** 807-818.

Hamill OP, Marty A, Neher E, Sakmann B & Sigworth FJ. (1981). Improved patch-clamp techniques for high-resolution current recording from cells and cell-free membrane patches. *Pflugers Arch* **391,** 85-100.

Harata NC, Aravanis AM & Tsien RW. (2006). Kiss-and-run and full-collapse fusion as modes of exo-endocytosis in neurosecretion. *J Neurochem* **97,** 1546-1570.

He X, Huang Y, Li B, Gong CX & Schuchman EH. (2008). Deregulation of sphingolipid metabolism in Alzheimer's disease. *Neurobiol Aging* **31,** 398-408.

Heidelberger R, Heinemann C, Neher E & Matthews G. (1994). Calcium dependence of the rate of exocytosis in a synaptic terminal. *Nature* **371,** 513-515.

Heinemann C, Chow RH, Neher E & Zucker RS. (1994). Kinetics of the secretory response in bovine chromaffin cells following flash photolysis of caged Ca2+. *Biophys J* **67,** 2546-2557.

Hellmich MR, Kennison JA, Hampton LL & Battey JF. (1994). Cloning and characterization of the Drosophila melanogaster CDK5 homolog. *FEBS Lett* **356,** 317-321.

Henkel AW & Almers W. (1996). Fast steps in exocytosis and endocytosis studied by capacitance measurements in endocrine cells. *Curr Opin Neurobiol* **6,** 350-357.

Henkel AW, Lubke J & Betz WJ. (1996). FM1-43 dye ultrastructural localization in and release from frog motor nerve terminals. *Proc Natl Acad Sci U S A* **93,** 1918-1923.

Hernandez-Guijo JM, Carabelli V, Gandia L, Garcia AG & Carbone E. (1999). Voltage-independent autocrine modulation of L-type channels mediated by ATP, opioids and catecholamines in rat chromaffin cells. *Eur J Neurosci* **11,** 3574-3584.

Hernandez-Guijo JM, de Pascual R, Garcia AG & Gandia L. (1998). Separation of calcium channel current components in mouse chromaffin cells superfused with low- and high-barium solutions. *Pflugers Arch* **436,** 75-82.

Hernandez-Guijo JM, Maneu-Flores VE, Ruiz-Nuno A, Villarroya M, Garcia AG & Gandia L. (2001). Calcium-dependent inhibition of L, N, and P/Q Ca^{2+} channels in chromaffin cells: role of mitochondria. *J Neurosci* **21,** 2553-2560.

Hess P, Lansman JB & Tsien RW. (1984). Different modes of Ca channel gating behaviour favoured by dihydropyridine Ca agonists and antagonists. *Nature* **311,** 538-544.

Heuser JE & Reese TS. (1973). Evidence for recycling of synaptic vesicle membrane during transmitter release at the frog neuromuscular junction. *J Cell Biol* **57,** 315-344.

Hillman D, Chen S, Aung TT, Cherksey B, Sugimori M & Llinas RR. (1991). Localization of P-type calcium channels in the central nervous system. *Proc Natl Acad Sci U S A* **88,** 7076-7080.

Hodgkin AL, Huxley AF & Katz B. (1952). Measurement of current-voltage relations in the membrane of the giant axon of Loligo. *J Physiol* **116,** 424-448.

Horrigan FT & Bookman RJ. (1994). Releasable pools and the kinetics of exocytosis in adrenal chromaffin cells. *Neuron* **13,** 1119-1129.

Hui A, Ellinor PT, Krizanova O, Wang JJ, Diebold RJ & Schwartz A. (1991). Molecular cloning of multiple subtypes of a novel rat brain isoform of the alpha 1 subunit of the voltage-dependent calcium channel. *Neuron* **7,** 35-44.

Ikeda SR. (1991). Double-pulse calcium channel current facilitation in adult rat sympathetic neurones. *J Physiol* **439,** 181-214.

Ikeda SR. (1996). Voltage-dependent modulation of N-type calcium channels by G-protein beta gamma subunits. *Nature* **380,** 255-258.

Ikeda SR & Dunlap K. (1999). Voltage-dependent modulation of N-type calcium channels: role of G protein subunits. *Adv Second Messenger Phosphoprotein Res* **33,** 131-151.

Jana A, Hogan EL & Pahan K. (2009). Ceramide and neurodegeneration: susceptibility of neurons and oligodendrocytes to cell damage and death. *J Neurol Sci* **278,** 5-15.

Jarvis SE, Barr W, Feng ZP, Hamid J & Zamponi GW. (2002). Molecular determinants of syntaxin 1 modulation of N-type calcium channels. *J Biol Chem* **277,** 44399-44407.

Jeon HJ, Lee DH, Kang MS, Lee MO, Jung KM, Jung SY & Kim DK. (2005). Dopamine release in PC12 cells is mediated by Ca^{2+}-dependent production of ceramide via sphingomyelin pathway. *J Neurochem* **95,** 811-820.

Jimenez RR, Lopez MG, Sancho C, Maroto R & Garcia AG. (1993). A component of the catecholamine secretory response in the bovine adrenal gland is resistant to dihydropyridines and omega-conotoxin. *Biochem Biophys Res Commun* **191,** 1278-1283.

Jones SW & Marks TN. (1989). Calcium currents in bullfrog sympathetic neurons. II. Inactivation. *J Gen Physiol* **94,** 169-182.

Kajimoto T, Okada T, Yu H, Goparaju SK, Jahangeer S & Nakamura S. (2007). Involvement of sphingosine-1-phosphate in glutamate secretion in hippocampal neurons. *Mol Cell Biol* **27,** 3429-3440.

Katz B & Miledi R. (1969). Spontaneous and evoked activity of motor nerve endings in calcium Ringer. *J Physiol* **203,** 689-706.

Kidokoro Y & Ritchie AK. (1980). Chromaffin cell action potentials and their possible role in adrenaline secretion from rat adrenal medulla. *J Physiol* **307,** 199-216.

Kitamura N, Ohta T, Ito S & Nakazato Y. (1998). Calcium channel current facilitation in porcine adrenal chromaffin cells. *Pflugers Arch* **435,** 781-788.

Kobayashi S. (1977). Adrenal medulla: chromaffin cells as paraneurons. *Arch Histol Jpn* **40 Suppl,** 61-79.

Kokubun S & Reuter H. (1984). Dihydropyridine derivatives prolong the open state of Ca channels in cultured cardiac cells. *Proc Natl Acad Sci U S A* **81,** 4824-4827.

Kongsamut S, Kamp TJ, Miller RJ & Sanguinetti MC. (1985). Calcium channel agonist and antagonist effects of the stereoisomers of the dihydropyridine 202-791. *Biochem Biophys Res Commun* **130,** 141-148.

Korn SJ & Horn R. (1989). Influence of sodium-calcium exchange on calcium current rundown and the duration of calcium-dependent chloride currents in pituitary cells, studied with whole cell and perforated patch recording. *J Gen Physiol* **94,** 789-812.

Kunze DL & Rampe D. (1992). Characterization of the effects of a new Ca^{2+} channel activator, FPL 64176, in GH3 cells. *Mol Pharmacol* **42,** 666-670.

Kuromi H, Ueno K & Kidokoro Y. (2010). Two types of Ca^{2+} channel linked to two endocytic pathways coordinately maintain synaptic transmission at the Drosophila synapse. *Eur J Neurosci* **32,** 335-346.

Lagnado L, Gomis A & Job C. (1996). Continuous vesicle cycling in the synaptic terminal of retinal bipolar cells. *Neuron* **17,** 957-967.

Lampe RA, Defeo PA, Davison MD, Young J, Herman JL, Spreen RC, Horn MB, Mangano TJ & Keith RA. (1993). Isolation and pharmacological characterization of omega-grammotoxin SIA, a novel peptide inhibitor of neuronal voltage-sensitive calcium channel responses. *Mol Pharmacol* **44,** 451-460.

Lara B, Gandia L, Martinez-Sierra R, Torres A & Garcia AG. (1998). Q-type Ca^{2+} channels are located closer to secretory sites than L-type channels: functional evidence in chromaffin cells. *Pflugers Arch* **435,** 472-478.

Lee A, Wong ST, Gallagher D, Li B, Storm DR, Scheuer T & Catterall WA. (1999). Ca^{2+}/calmodulin binds to and modulates P/Q-type calcium channels. *Nature* **399,** 155-159.

Lindau M & Neher E. (1988). Patch-clamp techniques for time-resolved capacitance measurements in single cells. *Pflugers Arch* **411,** 137-146.

Liu L, Gonzalez PK, Barrett CF & Rittenhouse AR. (2003). The calcium channel ligand FPL 64176 enhances L-type but inhibits N-type neuronal calcium currents. *Neuropharmacology* **45,** 281-292.

Livett BG. (1984). Adrenal medullary chromaffin cells in vitro. *Physiol Rev* **64,** 1103-1161.

Lopez MG, Villarroya M, Lara B, Martinez Sierra R, Albillos A, Garcia AG & Gandia L. (1994). Q- and L-type Ca^{2+} channels dominate the control of secretion in bovine chromaffin cells. *FEBS Lett* **349,** 331-337.

Lukyanetz EA & Neher E. (1999). Different types of calcium channels and secretion from bovine chromaffin cells. *Eur J Neurosci* **11,** 2865-2873.

Llinas R, Sugimori M, Lin JW & Cherksey B. (1989). Blocking and isolation of a calcium channel from neurons in mammals and cephalopods utilizing a toxin fraction (FTX) from funnel-web spider poison. *Proc Natl Acad Sci U S A* **86,** 1689-1693.

Marcantoni A, Carabelli V, Comunanza V, Hoddah H & Carbone E. (2008). Calcium channels in chromaffin cells: focus on L and T types. *Acta Physiol (Oxf)* **192,** 233-246.

Marchetti C, Carbone E & Lux HD. (1986). Effects of dopamine and noradrenaline on Ca channels of cultured sensory and sympathetic neurons of chick. *Pflugers Arch* **406,** 104-111.

Marks B & McMahon HT. (1998). Calcium triggers calcineurin-dependent synaptic vesicle recycling in mammalian nerve terminals. *Curr Biol* **8,** 740-749.

Marks DL & Pagano RE. (2002). Endocytosis and sorting of glycosphingolipids in sphingolipid storage disease. *Trends Cell Biol* **12,** 605-613.

Marmont G. (1949). Studies on the axon membrane; a new method. *J Cell Physiol* **34,** 351-382.

Mattson MP, Cheng B, Davis D, Bryant K, Lieberburg I & Rydel RE. (1992). beta-Amyloid peptides destabilize calcium homeostasis and render human cortical neurons vulnerable to excitotoxicity. *J Neurosci* **12,** 376-389.

McCleskey EW, Fox AP, Feldman DH, Cruz LJ, Olivera BM, Tsien RW & Yoshikami D. (1987). Omega-conotoxin: direct and persistent blockade of specific types of calcium channels in neurons but not muscle. *Proc Natl Acad Sci U S A* **84,** 4327-4331.

McEnery MW, Snowman AM, Sharp AH, Adams ME & Snyder SH. (1991). Purified omega-conotoxin GVIA receptor of rat brain resembles a dihydropyridine-sensitive L-type calcium channel. *Proc Natl Acad Sci U S A* **88,** 11095-11099.

Meir A, Ginsburg S, Butkevich A, Kachalsky SG, Kaiserman I, Ahdut R, Demirgoren S & Rahamimoff R. (1999). Ion channels in presynaptic nerve terminals and control of transmitter release. *Physiol Rev* **79,** 1019-1088.

Meuth S, Pape HC & Budde T. (2002). Modulation of Ca^{2+} currents in rat thalamocortical relay neurons by activity and phosphorylation. *Eur J Neurosci* **15,** 1603-1614.

Monje VD, Haack JA, Naisbitt SR, Miljanich G, Ramachandran J, Nasdasdi L, Olivera BM, Hillyard DR & Gray WR. (1993). A new Conus peptide ligand for Ca channel subtypes. *Neuropharmacology* **32,** 1141-1149.

Montero M, Alonso MT, Carnicero E, Cuchillo-Ibanez I, Albillos A, Garcia AG, Garcia-Sancho J & Alvarez J. (2000). Chromaffin-cell stimulation triggers fast millimolar mitochondrial Ca2+ transients that modulate secretion. *Nat Cell Biol* **2,** 57-61.

Moreno H, Rudy B & Llinas R. (1997). beta subunits influence the biophysical and pharmacological differences between P- and Q-type calcium currents expressed in a mammalian cell line. *Proc Natl Acad Sci U S A* **94,** 14042-14047.

Moro MA, Lopez MG, Gandia L, Michelena P & Garcia AG. (1990). Separation and culture of living adrenaline- and noradrenaline-containing cells from bovine adrenal medullae. *Anal Biochem* **185,** 243-248.

Murphy TH, Worley PF & Baraban JM. (1991). L-type voltage-sensitive calcium channels mediate synaptic activation of immediate early genes. *Neuron* **7,** 625-635.

Neher E. (1998). Vesicle pools and Ca^{2+} microdomains: new tools for understanding their roles in neurotransmitter release. *Neuron* **20,** 389-399.

Neher E. (2006). A comparison between exocytic control mechanisms in adrenal chromaffin cells and a glutamatergic synapse. *Pflugers Arch* **453,** 261-268.

Neher E & Zucker RS. (1993). Multiple calcium-dependent processes related to secretion in bovine chromaffin cells. *Neuron* **10,** 21-30.

Newcomb R, Palma A, Fox J, Gaur S, Lau K, Chung D, Cong R, Bell JR, Horne B, Nadasdi L & et al. (1995). SNX-325, a novel calcium antagonist from the spider Segestria florentina. *Biochemistry* **34,** 8341-8347.

Nordstedt C, Caporaso GL, Thyberg J, Gandy SE & Greengard P. (1993). Identification of the Alzheimer beta/A4 amyloid precursor protein in clathrin-coated vesicles purified from PC12 cells. *J Biol Chem* **268,** 608-612.

Nowycky MC, Fox AP & Tsien RW. (1985). Long-opening mode of gating of neuronal calcium channels and its promotion by the dihydropyridine calcium agonist Bay K 8644. *Proc Natl Acad Sci U S A* **82,** 2178-2182.

Nucifora PG & Fox AP. (1998). Barium triggers rapid endocytosis in calf adrenal chromaffin cells. *J Physiol* **508 (Pt 2),** 483-494.

Numakawa T, Nakayama H, Suzuki S, Kubo T, Nara F, Numakawa Y, Yokomaku D, Araki T, Ishimoto T, Ogura A & Taguchi T. (2003). Nerve growth factor-induced glutamate release is via p75 receptor, ceramide, and Ca^{2+} from ryanodine receptor in developing cerebellar neurons. *J Biol Chem* **278,** 41259-41269.

O'Farrell M, Ziogas J & Marley PD. (1997). Effects of N- and L-type calcium channel antagonists and (+/-)-Bay K8644 on nerve-induced catecholamine secretion from bovine perfused adrenal glands. *Br J Pharmacol* **121,** 381-388.

Olivera BM, McIntosh JM, Cruz LJ, Luque FA & Gray WR. (1984). Purification and sequence of a presynaptic peptide toxin from Conus geographus venom. *Biochemistry* **23,** 5087-5090.

Olivera BM, Miljanich GP, Ramachandran J & Adams ME. (1994). Calcium channel diversity and neurotransmitter release: the omega-conotoxins and omega-agatoxins. *Annu Rev Biochem* **63,** 823-867.

Paillart C, Li J, Matthews G & Sterling P. (2003). Endocytosis and vesicle recycling at a ribbon synapse. *J Neurosci* **23,** 4092-4099.

Pan CY, Wu AZ & Chen YT. (2007). Lysophospholipids regulate excitability and exocytosis in cultured bovine chromaffin cells. *J Neurochem* **102,** 944-956.

Pan S, Mi Y, Pally C, Beerli C, Chen A, Guerini D, Hinterding K, Nuesslein-Hildesheim B, Tuntland T, Lefebvre S, Liu Y, Gao W, Chu A, Brinkmann V, Bruns C, Streiff M, Cannet C, Cooke N & Gray N. (2006). A monoselective sphingosine-1-phosphate receptor-1 agonist prevents allograft rejection in a stringent rat heart transplantation model. *Chem Biol* **13,** 1227-1234.

Patil PG, Brody DL & Yue DT. (1998). Preferential closed-state inactivation of neuronal calcium channels. *Neuron* **20,** 1027-1038.

Pearson HA, Sutton KG, Scott RH & Dolphin AC. (1995). Characterization of Ca^{2+} channel currents in cultured rat cerebellar granule neurones. *J Physiol* **482 (Pt 3),** 493-509.

Perez Bay AE, Ibanez LI & Marengo FD. (2007). Rapid recovery of releasable vesicles and formation of nonreleasable endosomes follow intense exocytosis in chromaffin cells. *Am J Physiol Cell Physiol* **293,** C1509-1522.

Perissinotti PP, Giugovaz Tropper B & Uchitel OD. (2008). L-type calcium channels are involved in fast endocytosis at the mouse neuromuscular junction. *Eur J Neurosci* **27,** 1333-1344.

Plummer MR, Logothetis DE & Hess P. (1989). Elementary properties and pharmacological sensitivities of calcium channels in mammalian peripheral neurons. *Neuron* **2,** 1453-1463.

Pruett ST, Bushnev A, Hagedorn K, Adiga M, Haynes CA, Sullards MC, Liotta DC & Merrill AH, Jr. (2008). Biodiversity of sphingoid bases ("sphingosines") and related amino alcohols. *J Lipid Res* **49,** 1621-1639.

Qin J, Berdyshev E, Goya J, Natarajan V & Dawson G. (2010). Neurons and oligodendrocytes recycle sphingosine 1-phosphate to ceramide: significance for apoptosis and multiple sclerosis. *J Biol Chem* **285,** 14134-14143.

Richards DA, Guatimosim C & Betz WJ. (2000). Two endocytic recycling routes selectively fill two vesicle pools in frog motor nerve terminals. *Neuron* **27,** 551-559.

Robinson PJ, Sontag JM, Liu JP, Fykse EM, Slaughter C, McMahon H & Sudhof TC. (1993). Dynamin GTPase regulated by protein kinase C phosphorylation in nerve terminals. *Nature* **365,** 163-166.

Rosa JM, de Diego AM, Gandia L & Garcia AG. (2007). L-type calcium channels are preferentially coupled to endocytosis in bovine chromaffin cells. *Biochem Biophys Res Commun* **357,** 834-839.

Rosa JM, Gandia L & Garcia AG. (2009). Inhibition of N and PQ calcium channels by calcium entry through L channels in chromaffin cells. *Pflugers Arch* **458,** 795-807.

Roth D & Burgoyne RD. (1994). SNAP-25 is present in a SNARE complex in adrenal chromaffin cells. *FEBS Lett* **351,** 207-210.

Rouze NC & Schwartz EA. (1998). Continuous and transient vesicle cycling at a ribbon synapse. *J Neurosci* **18,** 8614-8624.

Royle SJ & Lagnado L. (2003). Endocytosis at the synaptic terminal. *J Physiol* **553,** 345-355.

Ryan TA, Smith SJ & Reuter H. (1996). The timing of synaptic vesicle endocytosis. *Proc Natl Acad Sci U S A* **93,** 5567-5571.

Sankaranarayanan S, De Angelis D, Rothman JE & Ryan TA. (2000). The use of pHluorins for optical measurements of presynaptic activity. *Biophys J* **79,** 2199-2208.

Sankaranarayanan S & Ryan TA. (2001). Calcium accelerates endocytosis of vSNAREs at hippocampal synapses. *Nat Neurosci* **4,** 129-136.

Santos SF, Pierrot N, Morel N, Gailly P, Sindic C & Octave JN. (2009). Expression of human amyloid precursor protein in rat cortical neurons inhibits calcium oscillations. *J Neurosci* **29,** 4708-4718.

Schramm M, Thomas G, Towart R & Franckowiak G. (1983). Novel dihydropyridines with positive inotropic action through activation of Ca^{2+} channels. *Nature* **303,** 535-537.

Shirokov R. (1999). Interaction between permeant ions and voltage sensor during inactivation of N-type Ca^{2+} channels. *J Physiol* **518 (Pt 3),** 697-703.

Smith C & Neher E. (1997). Multiple forms of endocytosis in bovine adrenal chromaffin cells. *J Cell Biol* **139,** 885-894.

Smith CB & Betz WJ. (1996). Simultaneous independent measurement of endocytosis and exocytosis. *Nature* **380,** 531-534.

Smith ER, Merrill AH, Obeid LM & Hannun YA. (2000). Effects of sphingosine and other sphingolipids on protein kinase C. *Methods Enzymol* **312,** 361-373.

Sobrado M, Lopez MG, Carceller F, Garcia AG & Roda JM. (2003). Combined nimodipine and citicoline reduce infarct size, attenuate apoptosis and increase bcl-2 expression after focal cerebral ischemia. *Neuroscience* **118,** 107-113.

Sollner T, Bennett MK, Whiteheart SW, Scheller RH & Rothman JE. (1993). A protein assembly-disassembly pathway in vitro that may correspond to sequential steps of synaptic vesicle docking, activation, and fusion. *Cell* **75,** 409-418.

Starr TV, Prystay W & Snutch TP. (1991). Primary structure of a calcium channel that is highly expressed in the rat cerebellum. *Proc Natl Acad Sci U S A* **88,** 5621-5625.

Stea A, Tomlinson WJ, Soong TW, Bourinet E, Dubel SJ, Vincent SR & Snutch TP. (1994). Localization and functional properties of a rat brain alpha 1A calcium channel reflect similarities to neuronal Q- and P-type channels. *Proc Natl Acad Sci U S A* **91,** 10576-10580.

Sudhof TC. (1995). The synaptic vesicle cycle: a cascade of protein-protein interactions. *Nature* **375,** 645-653.

Takei K & Haucke V. (2001). Clathrin-mediated endocytosis: membrane factors pull the trigger. *Trends Cell Biol* **11,** 385-391.

Takei K, Mundigl O, Daniell L & De Camilli P. (1996). The synaptic vesicle cycle: a single vesicle budding step involving clathrin and dynamin. *J Cell Biol* **133,** 1237-1250.

Tareilus E, Schoch J & Breer H. (1994). Ca^{2+}-dependent inactivation of P-type calcium channels in nerve terminals. *J Neurochem* **62,** 2283-2291.

Tavalin SJ, Shepherd D, Cloues RK, Bowden SE & Marrion NV. (2004). Modulation of single channels underlying hippocampal L-type current enhancement by agonists depends on the permeant ion. *J Neurophysiol* **92,** 824-837.

Teng H, Cole JC, Roberts RL & Wilkinson RS. (1999). Endocytic active zones: hot spots for endocytosis in vertebrate neuromuscular terminals. *J Neurosci* **19,** 4855-4866.

Teng H & Wilkinson RS. (2000). Clathrin-mediated endocytosis near active zones in snake motor boutons. *J Neurosci* **20,** 7986-7993.

Thomas P, Lee AK, Wong JG & Almers W. (1994). A triggered mechanism retrieves membrane in seconds after Ca^{2+}-stimulated exocytosis in single pituitary cells. *J Cell Biol* **124,** 667-675.

Tillotson D. (1979). Inactivation of Ca conductance dependent on entry of Ca ions in molluscan neurons. *Proc Natl Acad Sci U S A* **76,** 1497-1500.

Torri-Tarelli F, Villa A, Valtorta F, De Camilli P, Greengard P & Ceccarelli B. (1990). Redistribution of synaptophysin and synapsin I during alpha-latrotoxin-induced release of neurotransmitter at the neuromuscular junction. *J Cell Biol* **110,** 449-459.

Tsai LH, Delalle I, Caviness VS, Jr., Chae T & Harlow E. (1994). p35 is a neural-specific regulatory subunit of cyclin-dependent kinase 5. *Nature* **371,** 419-423.

Turner TJ, Lampe RA & Dunlap K. (1995). Characterization of presynaptic calcium channels with omega-conotoxin MVIIC and omega-grammotoxin SIA: role for a resistant calcium channel type in neurosecretion. *Mol Pharmacol* **47,** 348-353.

Uceda G, Garcia AG, Guantes JM, Michelena P & Montiel C. (1995). Effects of Ca^{2+} channel antagonist subtypes on mitochondrial Ca2+ transport. *Eur J Pharmacol* **289,** 73-80.

Ueda K, Shinohara S, Yagami T, Asakura K & Kawasaki K. (1997). Amyloid beta protein potentiates Ca^{2+} influx through L-type voltage-sensitive Ca^{2+} channels: a possible involvement of free radicals. *J Neurochem* **68,** 265-271.

Ulate G, Scott SR, Gonzalez J, Gilabert JA & Artalejo AR. (2000). Extracellular ATP regulates exocytosis in inhibiting multiple Ca^{2+} channel types in bovine chromaffin cells. *Pflugers Arch* **439,** 304-314.

Unsicker K, Griesser GH, Lindmar R, Loffelholz K & Wolf U. (1980). Establishment, characterization and fibre outgrowth of isolated bovine adrenal medullary cells in long-term cultures. *Neuroscience* **5,** 1445-1460.

Villarroya M, Olivares R, Ruiz A, Cano-Abad MF, de Pascual R, Lomax RB, Lopez MG, Mayorgas I, Gandia L & Garcia AG. (1999). Voltage inactivation of Ca^{2+} entry and secretion associated with N- and P/Q-type but not L-type Ca^{2+} channels of bovine chromaffin cells. *J Physiol* **516 (Pt 2),** 421-432.

Voets T, Toonen RF, Brian EC, de Wit H, Moser T, Rettig J, Sudhof TC, Neher E & Verhage M. (2001). Munc18-1 promotes large dense-core vesicle docking. *Neuron* **31,** 581-591.

von Gersdorff H & Matthews G. (1994). Inhibition of endocytosis by elevated internal calcium in a synaptic terminal. *Nature* **370,** 652-655.

von Gersdorff H & Matthews G. (1996). Calcium-dependent inactivation of calcium current in synaptic terminals of retinal bipolar neurons. *J Neurosci* **16,** 115-122.

Wahl-Schott C, Baumann L, Cuny H, Eckert C, Griessmeier K & Biel M. (2006). Switching off calcium-dependent inactivation in L-type calcium channels by an autoinhibitory domain. *Proc Natl Acad Sci U S A* **103,** 15657-15662.

Wang C & Zucker RS. (1998). Regulation of synaptic vesicle recycling by calcium and serotonin. *Neuron* **21,** 155-167.

Weber T, Zemelman BV, McNew JA, Westermann B, Gmachl M, Parlati F, Sollner TH & Rothman JE. (1998). SNAREpins: minimal machinery for membrane fusion. *Cell* **92,** 759-772.

Weiss JH, Pike CJ & Cotman CW. (1994). Ca^{2+} channel blockers attenuate beta-amyloid peptide toxicity to cortical neurons in culture. *J Neurochem* **62,** 372-375.

Westenbroek RE, Ahlijanian MK & Catterall WA. (1990). Clustering of L-type Ca^{2+} channels at the base of major dendrites in hippocampal pyramidal neurons. *Nature* **347,** 281-284.

Westenbroek RE, Hell JW, Warner C, Dubel SJ, Snutch TP & Catterall WA. (1992). Biochemical properties and subcellular distribution of an N-type calcium channel alpha 1 subunit. *Neuron* **9,** 1099-1115.

Westenbroek RE, Hoskins L & Catterall WA. (1998). Localization of Ca^{2+} channel subtypes on rat spinal motor neurons, interneurons, and nerve terminals. *J Neurosci* **18,** 6319-6330.

Wheeler DB, Randall A & Tsien RW. (1994). Roles of N-type and Q-type Ca^{2+} channels in supporting hippocampal synaptic transmission. *Science* **264,** 107-111.

Whitehouse PJ, Price DL, Struble RG, Clark AW, Coyle JT & Delon MR. (1982a). Alzheimer's disease and senile dementia: loss of neurons in the basal forebrain. *Science* **215,** 1237-1239.

Whitehouse PJ, Struble RG, Clark AW & Price DL. (1982b). Alzheimer disease: plaques, tangles, and the basal forebrain. *Ann Neurol* **12,** 494.

Wilson SM, Toth PT, Oh SB, Gillard SE, Volsen S, Ren D, Philipson LH, Lee EC, Fletcher CF, Tessarollo L, Copeland NG, Jenkins NA & Miller RJ. (2000). The status of voltage-dependent calcium channels in alpha 1E knock-out mice. *J Neurosci* **20,** 8566-8571.

Wilson SP & Kirshner N. (1977). Localization of adenylate cyclase in adrenal medulla. *Mol Pharmacol* **13,** 382-385.

Witcher DR, De Waard M, Sakamoto J, Franzini-Armstrong C, Pragnell M, Kahl SD & Campbell KP. (1993). Subunit identification and reconstitution of the N-type Ca2+ channel complex purified from brain. *Science* **261,** 486-489.

Wu F & Yao PJ. (2009). Clathrin-mediated endocytosis and Alzheimer's disease: an update. *Ageing Res Rev* **8,** 147-149.

Wu LG & Betz WJ. (1996). Nerve activity but not intracellular calcium determines the time course of endocytosis at the frog neuromuscular junction. *Neuron* **17,** 769-779.

Wu XS, McNeil BD, Xu J, Fan J, Xue L, Melicoff E, Adachi R, Bai L & Wu LG. (2009). Ca^{2+} and calmodulin initiate all forms of endocytosis during depolarization at a nerve terminal. *Nat Neurosci* **12,** 1003-1010.

Wykes RC, Bauer CS, Khan SU, Weiss JL & Seward EP. (2007). Differential regulation of endogenous N- and P/Q-type Ca^{2+} channel inactivation by Ca2+/calmodulin impacts on their ability to support exocytosis in chromaffin cells. *J Neurosci* **27,** 5236-5248.

Yan Z, Chi P, Bibb JA, Ryan TA & Greengard P. (2002). Roscovitine: a novel regulator of P/Q-type calcium channels and transmitter release in central neurons. *J Physiol* **540,** 761-770.

Yao PJ & Coleman PD. (1998). Reduced O-glycosylated clathrin assembly protein AP180: implication for synaptic vesicle recycling dysfunction in Alzheimer's disease. *Neurosci Lett* **252,** 33-36.

Yao PJ, O'Herron TM & Coleman PD. (2003). Immunohistochemical characterization of clathrin assembly protein AP180 and synaptophysin in human brain. *Neurobiol Aging* **24,** 173-178.

Yu HL, Li L, Zhang XH, Xiang L, Zhang J, Feng JF & Xiao R. (2009). Neuroprotective effects of genistein and folic acid on apoptosis of rat cultured cortical neurons induced by beta-amyloid 31-35. *Br J Nutr* **102,** 655-662.

Yue DT, Backx PH & Imredy JP. (1990). Calcium-sensitive inactivation in the gating of single calcium channels. *Science* **250,** 1735-1738.

Zha X, Pierini LM, Leopold PL, Skiba PJ, Tabas I & Maxfield FR. (1998). Sphingomyelinase treatment induces ATP-independent endocytosis. *J Cell Biol* **140,** 39-47.

Zheng W, Rampe D & Triggle DJ. (1991). Pharmacological, radioligand binding, and electrophysiological characteristics of FPL 64176, a novel nondihydropyridine Ca2+ channel activator, in cardiac and vascular preparations. *Mol Pharmacol* **40,** 734-741.

ANEXO 1

En estos experimentos, se han pré-tratado las células cromafines durante 24 horas con diferentes concentraciones del péptido Aβ 25-35 agregado y estudiado el efecto del péptido en las corrientes de calcio. Como podemos ver en la **Figura 1**, el péptido β-amiloide aumentó las corrientes de calcio que fueron bloqueadas en un 50% con nifedipino. Cabe destacar que la corriente control ha sido bloqueada en apenas un 20% con el bloqueante de canales L nifedipino. Así como, al bloquear los canales N y PQ con GVIA y AgaIVA, respectivamente, una corriente remaneciente de un aproximadamente 50% aún puede ser encontrada. Estos resultados corroboran los datos de la literatura donde la actividad del canal L se encuentra aumentada con la expresion de APP o incubación con Aβ.

Los datos presentados en esta Tesis Doctoral apuntan a un específico papel del calcio que entra por los canales L en la endocitosis. Ya que el canal L, en presencia de Aβ, presenta una mayor actividad hemos estudiado las repuestas exo-endocitóticas mediante la técnica de patch-clamp y medida de la capacidad de la membrana. En la **Figura 2** podemos ver el aumento de la endocitosis tras el pre-tratamiento de las células con el péptido β-amiloide, el cual ha sido inhibido por la aplicación del bloqueante de los canales L nifedipino. Aún nos cabe estudiar el efecto que tendría el bloqueo de los canales no-L en la endocitosis inducida por Aβ.

El péptido β-amiloide ha sido descrito por activar esfingomielinasas de membrana. La activación de las esfingomielinasas genera endógenamente e intracelularmente esfingosina, que como demostrado en el Artículo 5 de esta Tesis Doctoral es capaz de iniciar el proceso endocitótico. Hemos investigado si el bloqueo de las esfingomielinasas de membrana en presencia del péptico β-amilóide podría inhibir la endocitosis producida por Aβ (**Figura 3**). Amitriptilina es un fármaco utilizado en la clínica como antidepresivo tricíclico. Sin embargo, se ha descrito su acción como inhibidor de las esfingomielinasas de membrana. Al pretratar las células cromafines concomitantemente durante 24 horas con Aβ y amitriptilina, la endocitosis ha sido inhibida. Estos resultados sugieren la participación de la cascata esfingolípidos – endocitosis en nuestro modelo experimental utilizando el peptido β-amiloide.

Ceramida y esfingosina, productos de la activación de las esfingomielinasas, han sido descritas como pró-apoptóticas. Si el Aβ produce una activación de las esfingomielinasas, tanto la conseguinte síntesis de ceramida y esfingosina y activación de la endocitosis podrían tener una relación con la muerte celular producida por el Aβ. Hemos investigado, como la inhibición de las esfingomielinasas y endocitosis afectaban la muerte celular midiendo la viabilidad celular por MTT (**Figura 4**). Para eso, utilizamos amitriptilina y genisteína que inhibe la endocitosis vía caveolina y la formación de los endosomas. Ambos protocolos experimentales inhibieron la muerte celular producida por el péptido β-amiloide.

Figura 1

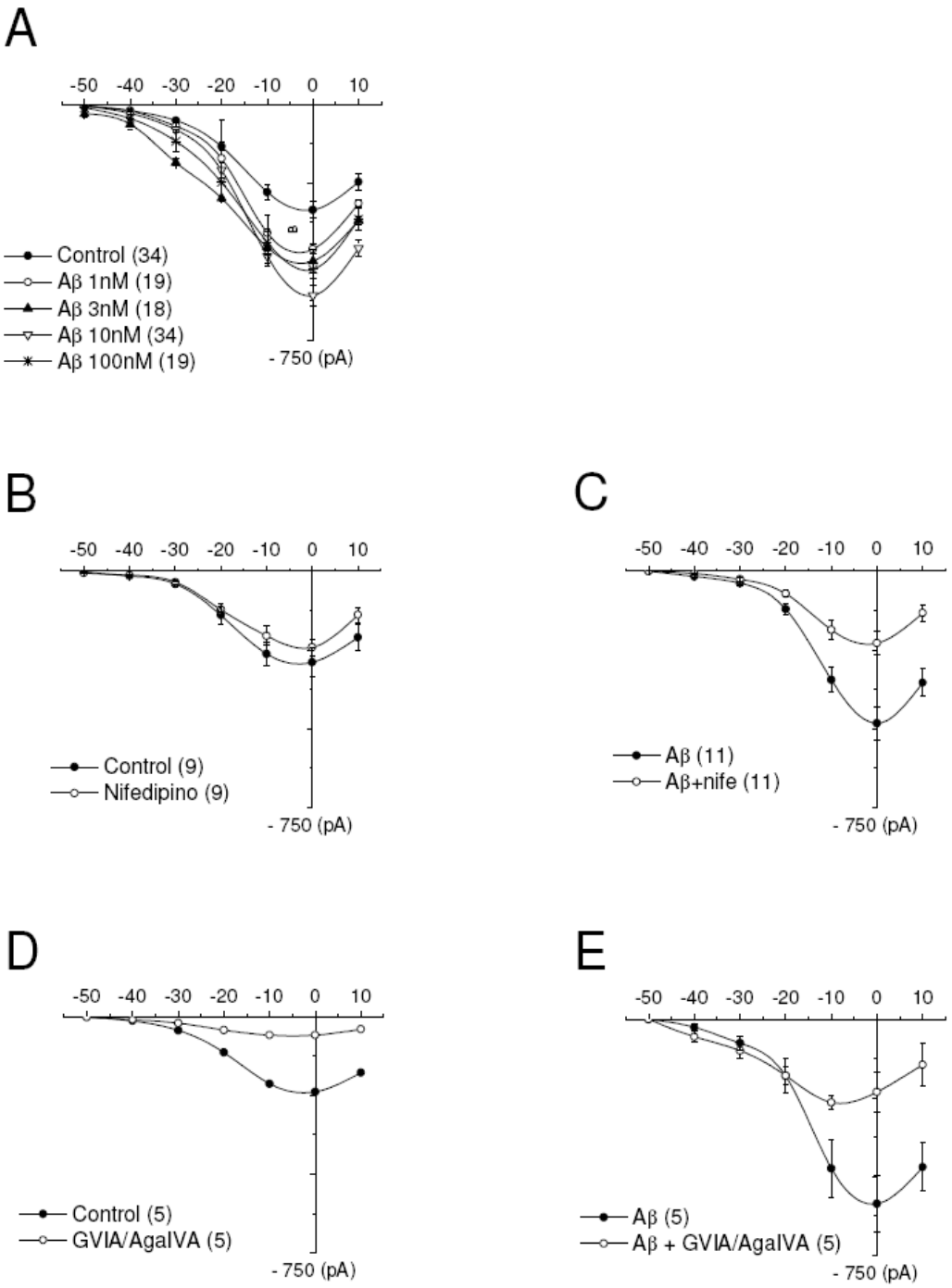

Figura 1: Aumento de la corriente L tras el pretratamiento con el péptido β-amiloide. Células cromafines bovinas fueron pretratadas durante 24 horas con diferentes concentraciones del péptido β-amiloide 25-35 agregado. Los experimentos se realizaron mediante la técnica de patch-clamp midiendo la entrada de Ca^{2+} por los CCDV. Se aplicaron pulsos despolarizantes de 50-ms de duración a diferentes voltajes (de -50 mV a +10 mV) en presencia de 2 mM Ca^{2+} en la solución extracelular. **A**, efecto de diferentes concentraciones de Aβ en la I_{Ca}. Los bloqueantes específicos se aplicaron mediante previa perfusion después del protocolo control. Se utilizó nifedipino (3 μM) para bloquear los canales L (**B**, control y **C**, células Aβ); ω-conotoxina GVIA (1 μM) para bloquear los canales N (**D**, control y **E**, células Aβ) y ω-conotoxina AgaIVA (1 μM) para los canales PQ (**F**, control y **G**, células Aβ).

Figura 2

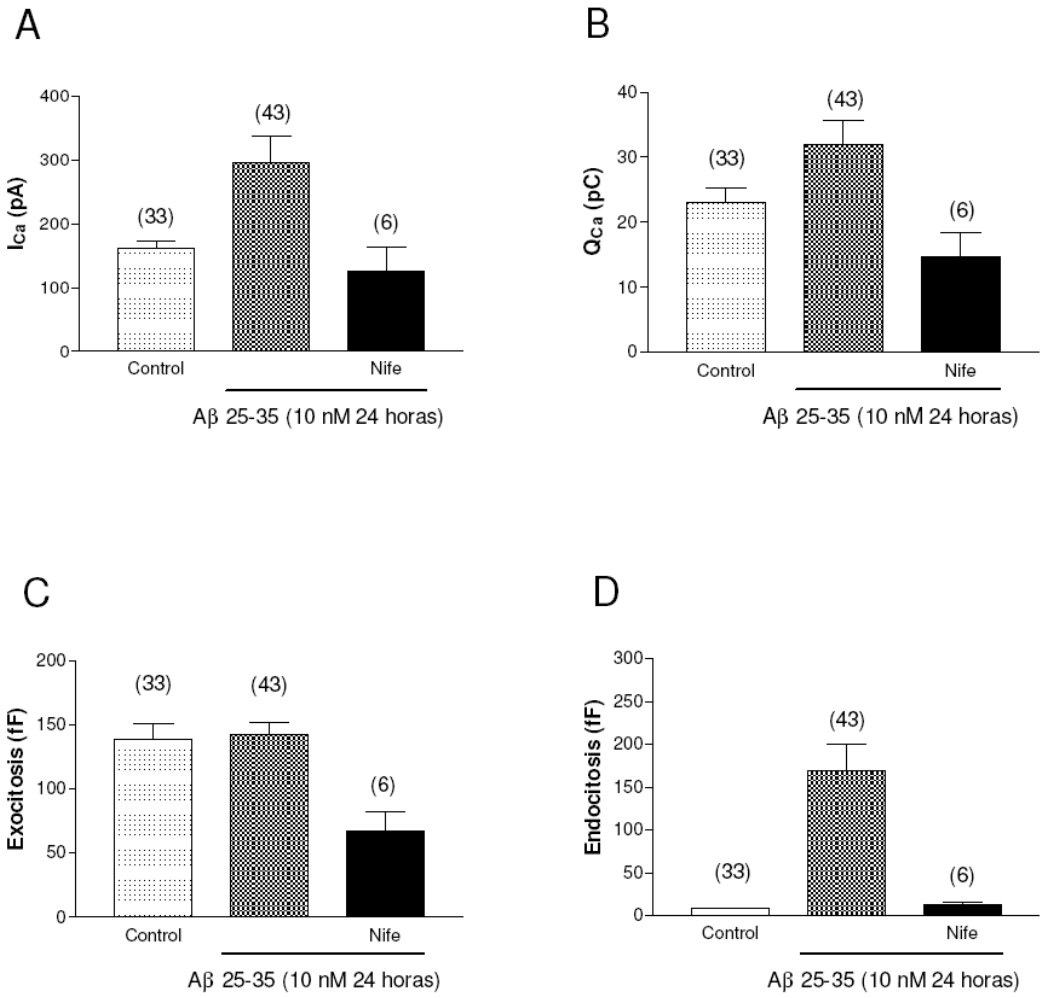

Figura 2: Aumento de la endocitosis por el péptido β-amiloide. Células cromafines bovinas fueron pretratadas durante 24 horas con 10 nM del péptido β-amiloide 25-35. Los experimentos se realizaron mediante la técnica de patch-clamp midiendo la entrada de Ca^{2+} por los CCDV (**A** y **B**) y la capacidad de la membrana (exo y endocitosis). Se aplicaron pulsos despolarizantes de 200-ms de duración en presencia de 2 mM Ca^{2+} en la solución extracelular. Se utilizó nifedipino (3 μM) para bloquear los canales L (**C** y **D**).

Figura 3

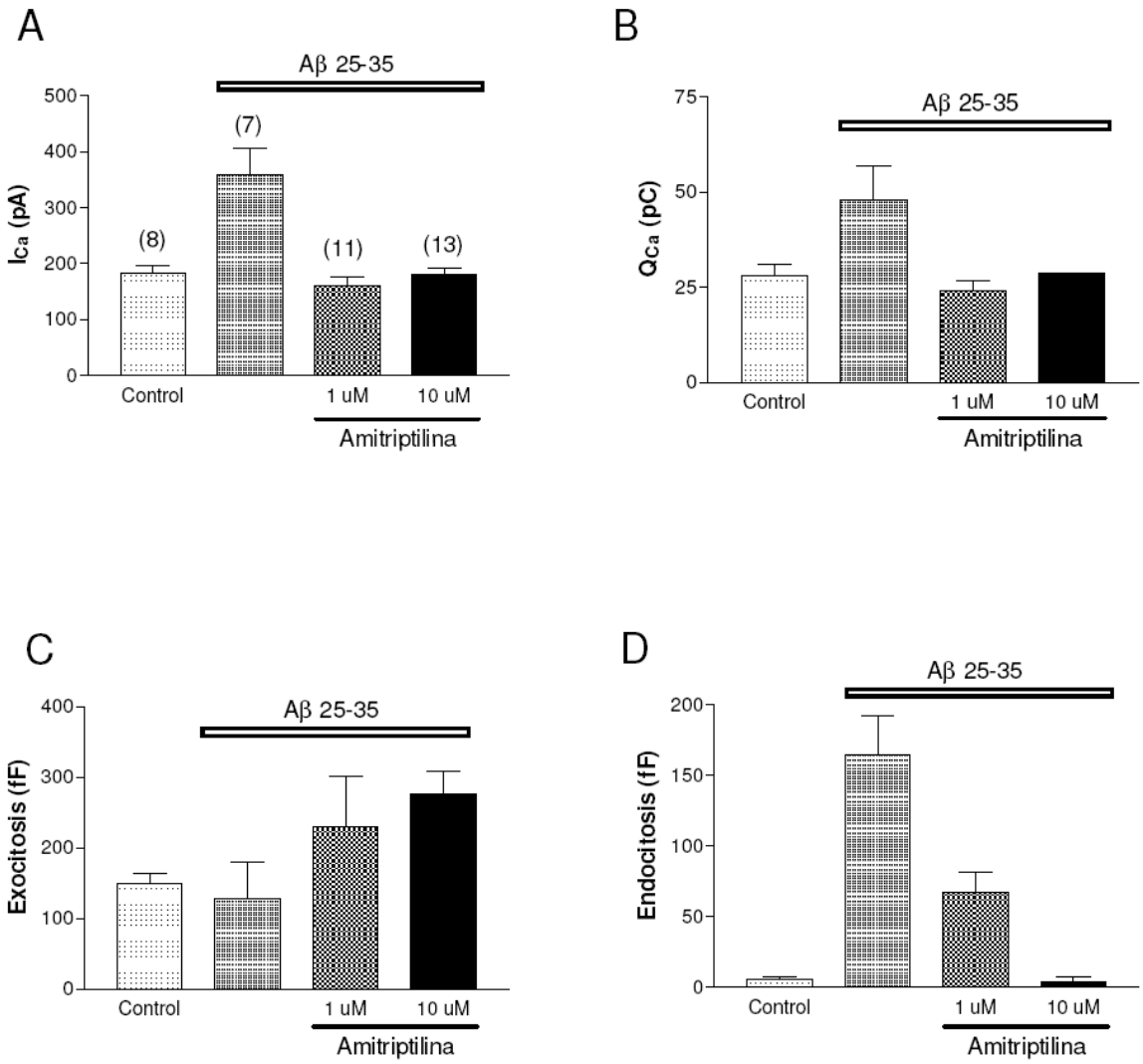

Figura 3: La inhibición de las esfingomielinasas de membrana por amitriptilina inhibe la endocitosis inducida por el péptido β-amiloide. Células cromafines bovinas fueron pretratadas durante 24 horas con 10 nM del péptido β-amiloide 25-35 en ausencia (control) o presencia de 1 o 10 μM de amitriptilina (amitriptilina). Los experimentos se realizaron mediante la técnica de patch-clamp midiendo la entrada de Ca^{2+} por los CCDV (**A** y **B**) y la capacidad de la membrana (exo y endocitosis). Se aplicaron pulsos despolarizantes de 200-ms de duración en presencia de 2 mM Ca^{2+} en la solución extracelular. Se utilizó nifedipino (3 μM) para bloquear los canales L (**C** y **D**).

Figura 4

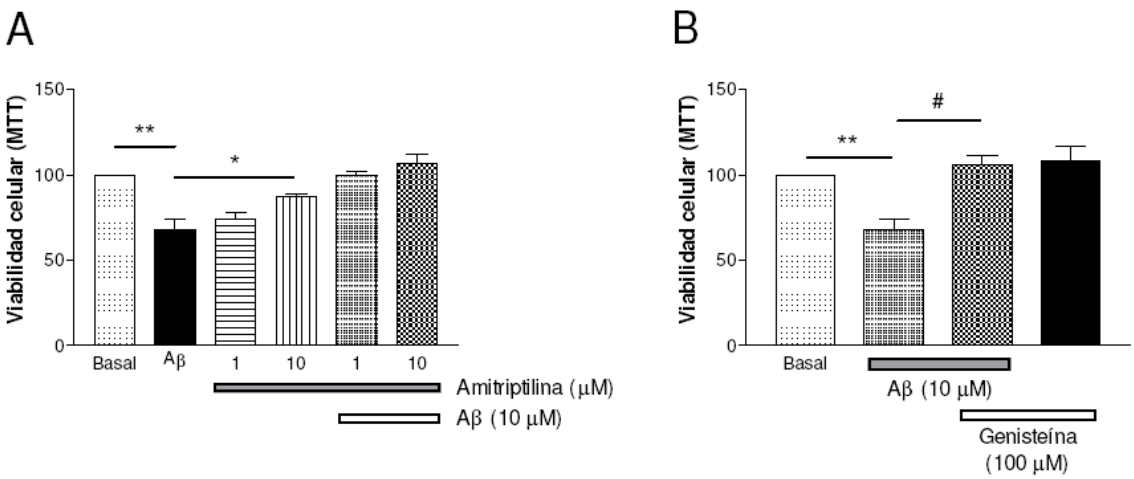

Figura 4: La inhibición de las esfingomielinasas de membrana por amitriptilina y de la endocitosis vía caveolina por genisteína inhibe la muerte celular inducida por el péptido β-amiloide. Células cromafines bovinas fueron pretratadas durante 24 horas con 10 μM del péptido β-amiloide 25-35. Los experimentos se realizaron mediante la técnica de medida de la viabilidad celular por MTT

Esquema

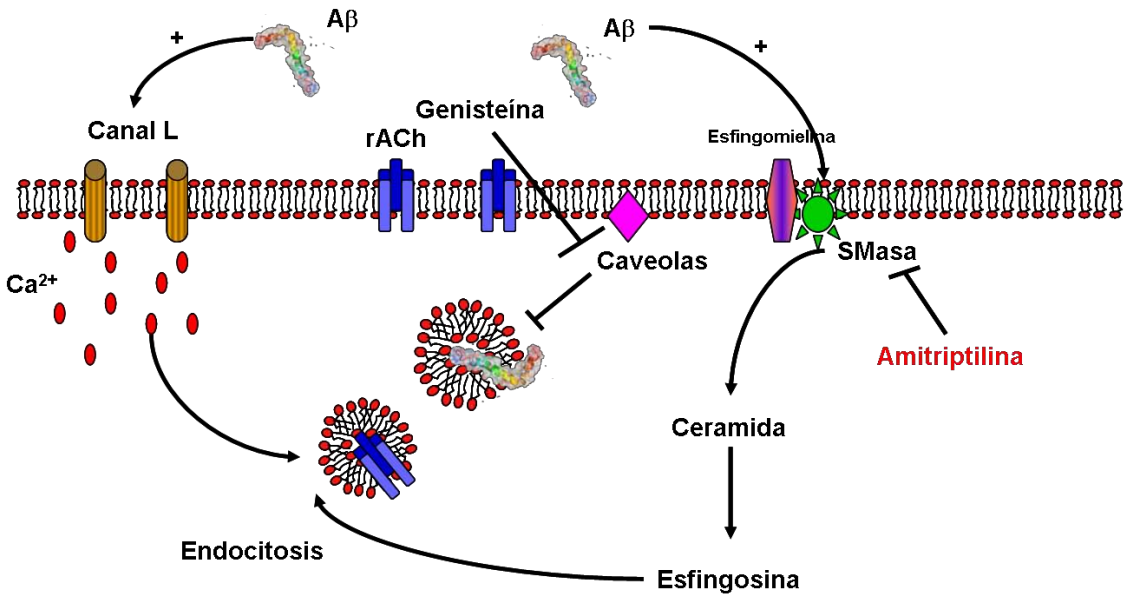

Esquema: Este esquema nos resume la hipótesis generada tras los resultados de este trabajo. En la Enfermedad de Alzheimer el aumento de la formación de los endosomas y la internalización del péptido β-amiloide podría darse mediante el mecanismo endocitótico inducido por la activación de las esfingomielinasas de membrana. La activación de las esfingomielinasas por Aβ induciría un aumento de la síntesis endógena de esfingosina que activaría el mecanismo endocitótico aumentando la internalización del Aβ y de receptores de superfície como los nicotínicos. Este mecanismo puede ser inhibido de dos modos distintos: (1) inhibiendo las esfingomielinasas, o (2) inhibiendo la endocitosis via caveolinas. El aumento de la entrada de Ca^{2+} por los canales L se puede deber a una activación de kinasas intracelulares por el Aβ. Desde que los canales de calcio tipo L participan en el proceso endocitótico, el bloqueo del calcio L sería otra posibilidad de inhibición de la endocitosis.